DETERMINING THE ROLE OF THE ERGIC-53 CARGO RECEPTOR COMPLEX IN ARENAVIRUS PROPAGATION

A Dissertation Presented

by

Joseph P. Klaus

to

The Faculty of the Graduate College

of

The University of Vermont

In Partial Fulfillment of the Requirements
for the Degree of Doctor of Philosophy
Specializing in Cell and Molecular Biology

October, 2014

Accepted by the Faculty of the Graduate College, The University of Vermont, in partial fulfillment of the requirements for the degree of Doctor of Philosophy, specializing in Cell and Molecular Biology.

Dissertation Examination Committee:

_____ Advisor
Jason W. Botten, Ph.D.

_____
Christopher Huston, M.D.

_____
Markus Thali, Ph.D.

_____ Chairperson
Douglas Taatajes, Ph.D.

_____ Dean, Graduate College
Cynthia J. Forehand, Ph.D.

Date: April 15, 2014

ABSTRACT

Arenaviruses and hantaviruses are human pathogens that cause significant morbidity and mortality. The current lack of vaccines and treatment options for these viruses is a global concern. Despite producing only 4 proteins, these viruses are able to maintain a persistent and asymptomatic infection in wild rodents while being continuously shed into the environment. In humans, these viruses cause a spectrum of diseases ranging from aseptic meningitis to severe hemorrhagic fever syndromes. Little is known about how arenavirus and hantavirus proteins engage and interact with the human proteome during the complex process of viral biogenesis, or how the interactions with human proteins contribute to viral propagation as well as the onset and progression of disease. This dissertation provides a road map of the protein interactions formed between a prototypic envelope glycoprotein encoded by either an arenavirus or hantavirus, and the human proteome.

The viral envelope glycoprotein (GP) decorates the surface of the virion. The primary function of the GP is to mediate attachment of the virus to specific cellular receptors, and after internalization of the virion, fuse the viral membrane with an internal endosomal membrane. In order to carry out these specific tasks, the viral GPs must first co-opt the extensive machinery found within the cellular secretory pathway to coordinate the proper glycosylation, folding, proteolytic maturation, and targeting of the GP during its biosynthesis. We identified a human protein with a conserved interaction amongst these two groups of viral GPs termed the Endoplasmic Reticulum (ER)-Golgi Intermediate Compartment Protein of 53 kiloDaltons (ERGIC-53). ERGIC-53 is an intracellular cargo receptor that normally cycles within the early secretory pathway of cells, where it is responsible for ferrying a small subset of cellular glycoproteins, most notably the coagulation factors FV and FVIII, from the ER to the Golgi apparatus.

Herein we describe a novel role for ERGIC-53 in the propagation of not only arenaviruses, but also coronaviruses and filoviruses. Following infection with an arenavirus, ERGIC-53 leaves the early secretory pathway and becomes incorporated into the virus as it pinches off from the cell surface. Newly formed viruses lacking ERGIC-53 are no longer infectious due, in part, to a defect in their ability to attach to host cells. We suggest that ERGIC-53 represents a promising broad-spectrum antiviral target because of its association with the GPs from many families of pathogenic viruses, as well as its ability to exert control over their infectivity; and finally, because ERGIC-53 itself is not required for human health. The discovery of ERGIC-53 outside of its normal location inside of cells suggests that it may have additional unknown functions. Lastly, by revealing the importance of the cellular protein in controlling viral infectivity, we provide insight into the ongoing co-evolution of virus and host.

CITATION

Material from this dissertation has been published in the following form:

Klaus, J.P.. (2013). The intracellular cargo receptor ERGIC-53 is required for the production of infectious arenavirus, coronavirus, and filovirus particles. Cell Host & Microbe, 14, 522-534.

DEDICATION

To the stones laid before me; heaved, hauled, and crafted, through years of dedication and perseverance, by the hardworking and oft underappreciated scientists; that allowed me to take a step, oh but a little step, and lay my own stones, so that another, after me, may do the same.

ACKNOWLEDGEMENTS

It does indeed take a village to raise, properly, a young scientist. By this notion, many warm-hearted thank-you's are needed for all the people who have helped to shape my career as well as to take on the task of completing a disseration. Specifically, first, and foremost, I must thank my wife. Her unquestioning loyalty, love, and support, warm meals, and comforting words, fed and nourished my heart, body, and mind. For this dedication, I am eternally grateful.

Throughout the course of my career I have had the distinct privilege to have several outstanding mentors from the onset of my career in science as a technician and throughout my graduate studies. To Jason Botten; a mentor, friend, and colleague, I am grateful for the gentle guidance and direction you gave me, both as a scientist, and as a person; the random meals (pizza of course) at odd hours of the night, and the interesting discussions in between. A properly controlled experiment will always be attributed to your tutelage.

I would also like to thank the Immunobiology group at large, for always providing critical, keen, and interesting insight into the science (whether I liked it or not). Within this group are a few people whom I also owe a proper thank-you. Jon Boyson introduced me to the delicate "art" of flow cytometry and always provided an interesting perspective. I would like to also thank Ralph Budd, who never failed to deliver on time, a well thought out, and eloquently stated question whenever I presented data during departmental meetings.

I was uniquely positioned, while producing the work for this dissertation, right next door to a very talented scientist who happened to study a receptor that several of the arenaviruses

use for entry. This simple fact became an introduction to Ann (Nan) Mason, who with a patience and surety showed me how to purify both protein and thought. Nan had an interesting story to go along with each experiment, and so taught me the history of science, while we tried to make some of it ourselves.

By studying the cellular biology of arenaviruses there was always a good reason to use a microscope. Because of this I very much made myself at home in the microscopy imaging center, where I could always count on a smile and a cookie from Janet Schwarz. Between Nicole Bishop, Michele von Turkovich, and Nicole Bouffard, as well as the guidance of Doug Taatjes, I was able to learn confocal, transmission electron, and super resolution microscopy. Both the people and the instrument helped to fuel a story that I have enjoyed both telling and showing.

Finally, to my parents, who instilled in me not only the need, but the willingness to continue on, no matter how difficult the day, or how challenging the circumstances; thank you for your love and support.

TABLE OF CONTENTS

LIST OF FIGURES

Figure Page

1 COMPREHENSIVE LITERATURE REVIEW

Overview of aims and significance

Arenaviruses are enveloped, negative sense, RNA viruses harbored in wild rodents in a variety of locales globally. Their natural history, genetic strategy, and cellular biology have provided a wealth of knowledge to researchers for nearly a century. In addition to providing scientists with an elaborate model to study virus-host interactions, these viruses are first and foremost, human pathogens that cause significant morbidity and mortality annually. Arenaviruses are known to cause a spectrum of disease ranging from aseptic meningitis to a severe hemorrhagic fever syndrome. The outcome of infection varies based on the route and amount of inoculation, as well as the genetics of the incoming virus. Additional clinical variation arises from differences in the age and immunological status of the infected person. With high mortality rates and a lack of preventative or therapeutic options available, arenaviruses represent an emerging and re-emerging zoonotic group of pathogens with a clear need of targeted antiviral development strategies. Herein, this dissertation presents the first systematic and comprehensive documentation of the interactome of the prototypic arenavirus glycoprotein (herein revised as GP) derived from lymphocytic choriomeningitis virus (LCMV), in addition to the interactome of the prototypic New World (NW) hantavirus glycoprotein derived from Andes virus (ANDV). The inclusion of a hantavirus glycoprotein is that of a natural control and companion to the arenavirus GP. Hantaviruses, similarly, are rodent-borne, negative sense, enveloped RNA viruses lacking

in not only vaccines, but treatment options. Hantaviruses, however, are genetically distinct and share few pathophysiological features. As members of the bunyavirus family, they are thus grouped alongside arenaviruses, filoviruses, and flaviviruses as agents causing viral hemorrhagic fevers.

The process of identifying and characterizing the interactome of the arenavirus and hantavirus GPs provided a platform for four distinct goals. First, by identifying the proteins in complex with these viral glycoproteins, a more detailed understanding of the basic cellular biology governing biogenesis and pathogenesis could be established at the resolution of protein-protein interactions. Secondly, by revealing which individual proteins, as well as protein networks, involved in biogenesis are biologically relevant to propagation and pathogenesis, a strategic approach to targeting crucial stages of the viral lifecycle could be implemented. Following bioinformatics comparisons, biochemical verification, and functional validation studies, characterization of a core suite of conserved cellular proteins that will serve as potential broad spectrum antiviral targets can occur. Next, mechanistic insight can be gained into the stage specific role of the virus-host interaction, through analyzing the organization and interaction of the protein or protein complexes, and their respective contributions to GP form and function. Lastly, by uncovering the protein determinants responsible for mediating the interaction, future studies can utilize this information to selectively disrupt the interactions therapeutically. The detailed investigation of the consequence and molecular mechanisms governing the arenavirus GP interactome revealed an interesting and unlikely candidate that coincided

with the four goals of this investigation; Endoplasmic Reticulum – Golgi intermediate compartment protein of 53 kilodaltons (kDa), hereafter referred to as ERGIC-53.

We demonstrate that ERGIC-53, a previously assumed intracellular cargo receptor required for trafficking of coagulation factors V and VIII (FV & FVIII), is part of a receptor complex with multiple coagulation factor deficiency protein 2 (MCFD2) that interacts with arenavirus and hantavirus glycoproteins. This interaction is shared, minimally, amongst coronavirus, filovirus, and orthomyxovirus envelope glycoproteins, and is required for the production of infectious viral particles. These dissertation studies revealed that during infection with an arenavirus, ERGIC-53 will traffic to the plasma membrane, and be incorporated into newly formed arenavirus particles. Depletion of ERGIC-53, or genetic ablation of its anterograde trafficking potential, severely impairs viral propagation. Depletion of MCFD2, inversely, bolsters viral replication. ERGIC-53 and MCFD2, despite representing halves of a single molecular complex, propagate opposing forces on the viral lifecycle. Interrogating the ERGIC-53:MCFD2 complex has revealed a rich and interesting molecular insight to the history of virus and host, and represents a novel molecular machine to interfere with therapeutically.

1.1. The Arenaviridae

Arenaviruses are zoonotic, enveloped, RNA viruses commonly associated with the Muridae family of rodents (Childs & Peters, 1993), with exceptions being Tacaribe virus (TACRV; *Artibeus*, fruit bat,) (Downs, Anderson, Spence, Aitken, & Greenhall,

1963), California academy of science virus (CASV, *Corallus annulatus*, the annulated tree boa), and, finally, Golden Gate virus and Collierville virus (GGV and CCV, *Boa constrictor*) (Stenglein et al., 2012). The majority of known arenavirus species are not associated with human disease and are thought to have co-evolved with their rodent hosts to cause little to no pathology. Lassa virus (LASV), Lujo virus (LUJV), and Lymphocytic choriomeningitis virus (LCMV) constitute the most widely recognized human pathogens in the Old World (Emonet, Lemasson, Gonzalez, de Lamballerie, & Charrel, 2006). Junín virus (JUNV), Machupo virus (MACV), Guanarito virus (GTOV), Sabia virus (SABV), Chapare virus (CHAPV), and White Water Arroyo virus (WWAV) are the predominant human pathogens in the NW grouping (Bowen, Peters, & Nichol, 1996).

The Arenaviridae consists of a single genus with approximately 25 species currently recognized by the international committee on the taxonomy of viruses (ICTV), and several new species are pending approval. The virus family is subdivided into Old and New world groups based on antigenic reactivity (serology) (Casals, Buckley, & Cedeno, 1975), geographic location, and genome similarity (Emonet et al., 2006). Old World (OW) viruses are predominantly found in Africa, as well as Asia and Europe. New World (NW) viruses are distributed in North and South America. The prototype of the Old World viruses, LCMV, is globally distributed and maintains a great deal of diversity with ~20 known strains (Albarino, 2010). Phylogenetic analyses of the OW grouping suggest up to four lineages of LCMV globally (Albarino, 2010), as well as four lineages of LASV within Western African countries (Bowen et al., 2000). Inter-species diversity is common among pathogenic New World arenaviruses (Bowen et al., 2000) and “non”-pathogenic

arenaviruses (Michael D. Bowen, Clarence J. Peters, & Stuart T. Nichol, 1997). The heterogeneity that is prevalent amongst both pathogenic and non-pathogenic arenaviruses, as well as intra-species genetic variation, may provide clues to mechanisms of pathogenesis. The New World arenavirus group is further subdivided into clades A, B, C, and more recently the Rec A/B sub-grouping (Charrel et al., 2003). Currently, pathogenic NW viruses all group into clade B (Charrel, de Lamballerie, & Emonet, 2008) with the exception being WWAV, which is found in the Rec A/B. The NW arenavirus group Rec A/B is posited to be the result of a recombination event from an ancestral North American arenavirus species (Charrel et al., 2002). As new arenaviruses are being identified and characterized, additional phylogenetic and evolutionary groupings may begin to appear. The current phylogenetic organization and diversity of the Arenaviridae is thought to have arisen from extensive co-evolution of viruses with their rodent hosts (Emonet, de la Torre, Domingo, & Sevilla, 2009). Accordingly, closely related arenavirus species (i.e. JUNV and MACV) are harbored in closely related rodent species (*C. musculinus and C. callosus*) (Michael D. Bowen et al., 1997), and WWAV and Catarina virus (CTNV) (*N. albigula* and *N. micropus*) (Cajimat et al., 2008; Cajimat, Milazzo, Bradley, & Fulhorst, 2007).

1.2. Arenavirus epidemiology: pathogenic Old World arenaviruses

1.2.1. Lassa virus

The predominant African arenavirus is LASV, the etiologic agent of Lassa Fever (LF) (Buckley & Casals, 1970; Frame, Baldwin, Gocke, & Troup, 1970; Leifer, Gocke, & Bourne, 1970; Speir, Wood, Liebhaber, & Buckley, 1970), and is endemic in countries along the Western coast of Africa (Sierra Leone, Nigeria, Liberia, and Guinea). It is estimated that 100,000 – 300,000 cases of LF occur annually (McCormick, Webb, Krebs, Johnson, & Smith, 1987; Monath, Maher, Casals, Kissling, & Cacciapuoti, 1974). Epidemiological studies suggest overall mortality rates of 1-2% (McCormick et al., 1987), however, fatalities in hospitalized patients are substantially higher (~15-20%) (Bausch et al., 2001) and can reach upwards of 80% during outbreaks (Günther & Lenz, 2004). LASV is particularly dangerous to both pregnant women (Monson, Frame, Jahrling, & Alexander, 1984; Price, Fisher-Hoch, Craven, & McCormick, 1988) and developing fetuses with mortality rates of 30-50% and 70-90%, respectively (Günther & Lenz, 2004). However, these numbers vary depending on the age of the mother and fetus (Monson et al., 1987; Webb et al., 1986). In endemic regions, upwards of 50% of the human population are seropositive for LASV antibodies, and the *Mastomys natalensis* reservoir seropositivity ranges from 8-80% demonstrating a large potential for continued transmission events (Frame et al., 1970; McCormick et al., 1987; Monath, Newhouse, Kemp, Setzer, & Cacciapuoti, 1974). Re-infection rates and underreporting may change the complete picture of the disease burden. Also, given the antigenic similarities of the African arenaviruses, the human seropositivity rates in the LASV endemic region may also represent pre-exposure to non-pathogenic species as well as exposure to strains of LASV that cause less severe disease (Günther & Lenz, 2004; McCormick et al., 1987; Thomas P. Monath et al., 1974).

The LASV rodent reservoir population covers a widespread geographic area that extends beyond the LASV endemic zone (Lalis et al., 2012). The rodents are commonly found amongst dwellings and are consumed as bushmeat, both of which contribute to the common occurrence and spread of LASV in the region (Keenlyside et al., 1983; Meulen et al., 1996). Multiple *Mastomys* species may be involved in the transmission of LASV, however, the exact phylogeny is still unclear for these rodents (Salazar-Bravo, Ruedas, & Yates, 2002). LASV also poses a new found risk as an imported pathogen, as several cases of imported LF have been documented globally (Amorosa et al., 2010; Haas et al., 2003; Hirabayashi et al., 1989).

1.2.2. Lujo virus

An unusually fatal outbreak of hemorrhagic fever in 2008 resulted in the identification of the most recent pathogenic Old World arenavirus, referred to as Lujo virus (LUJV) (Briese et al., 2009). Lujo virus was isolated and identified following the air-transfer of a patient from Zambia to South Africa. The nosocomial spread resulted in an 80% mortality rate and highlights the risk involved in hospital settings dealing with emergence/re-emergence of arenaviruses in a naïve community (Paweska et al., 2009). Lujo represents the first pathogenic arenavirus isolated in Africa in approximately four decades, and suggests a wider distribution of pathogenic species than has been previously documented. However, during the intervening years, a number of non-pathogenic viruses have been identified including: Ippy, Mobala, Mopia, and Luna viruses which overlap or are adjacent to LASV endemic areas. The vector responsible for transmitting LUJV has

yet to be identified. The index patient was reported to be near rodents in the week prior to the onset of symptoms, which is in accordance with most arenaviral transmission events.

1.2.3. Lymphocytic choriomeningitis virus

Lymphocytic choriomeningitis virus, the prototype virus of the family, has a global distribution which coincides with that of its reservoir, the common house mouse (*Mus musculus* or *Mus domesticus)* (Traub, 1936). The wide distribution of infected mice has been confirmed in several surveys within the United States and European countries which have demonstrated reservoir seroprevalence ranges of ~ 3-14% in urban settings (Childs, Glass, Korch, Ksiazek, & Leduc, 1992; Childs et al., 1991; Ledesma et al., 2009). The mortality rate for LCMV infection in an immunocompetent human host is < 1%. However, in the setting of solid organ transplantation, LCMV, or Dandenong virus (DANV), an LCMV-like virus (Palacios et al., 2008b), has recently been shown to be extraordinarily lethal (Staci A. Fischer et al., 2006; Macneil, Ströher, et al., 2012; Macneil, Stroher, et al., 2012; Palacios et al., 2008b). In addition to immunosuppressed transplant recipients, developing fetuses are also highly susceptible to disease (Daniel J. Bonthius, 2012; Bonthius et al., 2007). Congenital LCMV infections are thought be an underdiagnosed phenomena (D. J. Bonthius, 2012; Enders, Varho-Gobel, Lohler, Terletskaia-Ladwig, & Eggers, 1999). A number of outbreaks have also occurred in rodent breeding facilities (Centers for Disease & Prevention, 2012; Knust et al., 2014), as well as in research laboratories (Baum, Lewis, Rowe, & Huebner, 1966; Dykewicz, Dato, Fisher-Hoch, & et al., 1992; Knust et al., 2014), and from exposure to infected pet

rodents (Amman et al., 2007; Gregg, 1975; Rousseau, Saron, Brouqui, & Bourgeade, 1997), suggesting multiple routes and opportunities for human exposure to virus.

1.3. Arenavirus epidemiology: pathogenic New World arenaviruses

1.3.1. Junín virus

Junín virus, the etiological cause of Argentine hemorrhagic fever (AHF), was first reported in 1955 (Arribalzaga, 1955) as a febrile hemorrhagic disease of unknown origin, and was soon after isolated by Parodi et al. (Parodi et al., 1958). The virus is endemic amongst the rich agricultural land found in the pampas region and is responsible for approximately 100-3,000 cases annually in an area encompassing 150,000 km^2 (Maiztegui, 1975). The area of endemicity has increased from ~15,000 km since surveillance began, and now covers an area inhabited by ~ 1-5,000,000 people (Gómez et al., 2011). The principle host of JUNV is the vesper mouse (*Callomus musculinus*), however, some degree of spillover may be present in other closely related species (Mills et al., 1994; Salazar-Bravo et al., 2002). Approximately 10% of the vesper mice trapped in longitudinal studies have been reported as being seropositive (Mills et al., 1994; Mills et al., 1992), suggesting potential for widespread exposure.

The case fatality rate for Junín virus is approximately 20-30% when untreated, however administration of immune sera from convalescent patients reduces this to ~ 1%, albeit with a modest risk of late neurological complications (Maiztegui, Fernandez, & de Damilano, 1979; Ruggiero et al., 1986). The virus predominantly affects male agricultural workers in the endemic region (Maiztegui, 1975). Amongst the South

American arenaviruses, Junín is thought to be responsible for the majority of human arenavirus disease; however recent vaccination coverage with a live-attenuated vaccine (Candid1) has substantially reduced annual cases of severe human disease, and has been delivered to several hundred thousand people in at risk populations within Argentina (Enria, Ambrosio, Briggiler, Feuillade, & Crivelli, 2010; Maiztegui et al., 1998). The attenuated vaccine varies from the parental strain (XJ) by 13 amino acids (Goni et al., 2006), and has been given an investigational new drug status by the FDA. Concerns about the genetic stability of the vaccine, as well its passage history, have hampered its use outside of the endemic zone (Contigiani, Medeot, & Diaz, 1993). Despite the concerns, Candid1 has thus far provided roughly 90% protection against severe disease, and provides researchers a safe alternative (biosafety level 2 virus) to the BSL4 parental strain.

1.3.2. Machupo virus and Chapare virus

Machupo virus, the pathogen responsible for Bolivian hemorrhagic fever (BHF), carries with it a similar disease course and mortality rate as JUNV, but is more sporadic in incidence (Patterson, Grant, & Paessler, 2014). The virus became known to the western world in 1963 following a series of HF outbreaks in the village of San Joaquin (Johnson, 1965; Mackenzie, 1965). The virus reservoir, *Calomys callosus,* is commonly found amongst houses, unless preventative measures are set in place (Kuns, 1965; Salazar-Bravo et al., 2002). In addition to MACV, Chapare virus (CHAPV) was identified as an additional pathogenic arenavirus present in Bolivia. In December of 2003 and January 2004, Chapare virus was identified in an area outside of the MACV endemic

zone, following reports of several VHF cases. Sera was recovered and made available from the only known fatal case of which Chapare virus was later isolated and characterized (Delgado et al., 2008).

1.3.3. Guanarito virus and Sabia virus

Guanarito virus (GTOV), the agent responsible for Venezuelan hemorrhagic fever (VHF), was identified in the rural area of Portuguesa State in central Venezuela (Salas et al., 1991). Epidemiological studies suggest that the number of infected animal reservoirs (*Zygodontomys brevicuda*) (Fulhorst et al., 1999)) in the endemic area to range from 5-15% up to 48% and the human seroprevalence rates are approximated at 2.5% based on the limited serological surveillance to date (Milazzo, Cajimat, et al., 2011; Tesh et al., 1993). Sabia virus (SABV) was isolated from a fatal case of VHF in Sao Paolo, Brazil (Lisieux et al., 1994). During characterization and isolation of the virus, a laboratory worker became ill with the newly identified virus, but recovered successfully (Vasconcelos et al., 1993). The natural host of this virus has yet to be determined, however, given the history of rodents in arenavirus transmission, it is assumed to be an indigenous rodent species. These viruses (JUNV, MACV, GTOV, SABV, and CHAPV) constitute the known human pathogenic arenaviruses in South America able to cause viral hemorrhagic fever.

1.3.4. White water arroyo virus

White Water Arroyo virus (WWAV), identified in 2001, is associated with a brief outbreak of severe disease in California (Byrd et al., 2000), and is the only NW

pathogenic arenavirus currently recognized in North America. Its *Neotomys sp*., host covers a large area in the southwestern United States (Milazzo et al., 2010). In addition to WWAV, the other North American arenavirus suspected of being involved in human infection is Tamiami virus (TAMV). TAMV seropositivity exists minimally amongst a group of Seminole Indians, as well as the *Sigmodon hispidus* (TAMV) reservoir, which is geographically distinct from *Neotoma albigula* (WWAV) rodents (Fulhorst et al., 1996; Milazzo, Campbell, & Fulhorst, 2011). Despite the widespread prevalence of antibodies in North American rodents to arenaviruses, a limited number of bona-fide human pathogens have emerged (Milazzo et al., 2010; Salazar-Bravo et al., 2002). Additional epidemiological surveys and studies to identify molecular determinants of pathogenesis are required to ascertain the full risk involved with endogenous North American arenaviruses.

1.4. Reservoir biology

Arenaviruses, with the exception of tacaribe virus, and the newly identified grouping causing inclusion body disease (IBD) in related snake species, are each found within a discreet rodent species with minimal overlap and/or spillover. As such, their geographic distribution is restricted to the ecological range of the rodent hosts (Salazar-Bravo et al., 2002). Maintenance of arenaviruses within these reservoir species is more than simple tolerance, rather it is likely an intricate co-evolution of virus and host (M. D. Bowen, C. J. Peters, & S. T. Nichol, 1997; Charrel et al., 2003; Emonet et al., 2006; Hugot, Gonzalez, & Denys, 2001). A record of this is maintained not only in the arenavirus genome, but also in the rodent genomes (Choe, Jemielity, Abraham, Radoshitzky, &

Farzan, 2011; Demogines, Abraham, Choe, Farzan, & Sawyer, 2013; Tayeh, Tatard, Kako-Ouraga, Duplantier, & Dobigny, 2010; Zapata & Salvato, 2013). Along these lines, the most similarly related arenaviruses (e.g. JUNV and MACV, or LASV and MOBV) can be found in closely related rodents (e.g. *Calomus musculinus* and *Calomus callosus or Mastomys sp*). These relationships are not always obvious, however, as substantial heterogeneity also exists within the family and sub-species.

One of the distinguishing features of arenaviruses is the ability to establish a chronic infection in a host/cell whilst leaving the host/cell largely unharmed. This has been demonstrated both in vivo (Traub, 1936) in various rodent hosts, as well as in-vitro (Lehmann-Grube, Slenczka, & Tees, 1969) in laboratory settings. Rodent reservoirs, despite typically showing no overt signs of disease, are able to shed infectious virus into the environment via urine, saliva, and fecal leavings. The infectious fomites are thought to be the principal source for transmission of infectious matter into humans either through inhalation of aerosols, contaminated food sources, or through skin abrasions. Consumption of infected rodent meat may also play a role in rodent to human transmission. More recently, organ transplantations have produced a unique avenue for human to human transmission with exceptionally fatal outcomes (Botten, King, Klaus, & Zeigler, 2013).

The mechanisms of viral persistence have been examined from a molecular perspective (e.g. viral gene regulation and D.I. particle production) (Oldstone & Buchmeier, 1982; Rawls, Chan, & Gee, 1981; Welsh & Buchmeier, 1979), as well as from a systems - immunological perspective (Teijaro et al., 2013). Close examination of

both virus and host has provided ongoing clues to the amalgam of mechanisms at play in maintaining a persistent infection (Oldstone & Buchmeier, 1982; Valsamakis et al., 1986). Common themes include down-regulation of co-stimulatory molecules (e.g. MHC), avoiding and dampening type I interferon (IFN-I) production (Borrow, Martínez-Sobrido, & De la Torre, 2010; Teijaro et al., 2013), and promotion of T cell exhaustion (e.g. PD-1) (Wherry et al., 2007; Zajac et al., 1998; Zinselmeyer et al., 2013).

1.4.1. **Arenavirus transmission: rodent-rodent and rodent-human**

The principal route of maintenance for the prototype arenavirus, LCMV, relies upon transmission from infected mother to her dams. This LCMV-mouse model has been widely used as a surrogate to study arenavirus transmission amongst rodent reservoirs, due in part to the biosafety concerns with more pathogenic species, as well as the difficulties found in studying transmission in the endemic areas. These developing rodents are qualified as carriers and harbor virus systemically. As such, they can shed the virus via urine, feces, blood, and saliva. Evidence for horizontal transmission amongst some NW and OW rodents, particularly during aggressive encounters, suggests it may also play a substantial role. This is in contrast to LCMV in-uetero vertical models, as experimentally infected *C. musculinus* are reported to have reproductive consequences (Vitullo, Hodara, & Merani, 1987). However, this topic remains an issue of debate as additional studies suggest a prominent role also for vertical transmission (Vitullo & Merani, 1990).

The horizontal mechanism of transfer, though not key to maintenance is critical for zoonosis, and represents an additional ecological layer of complexity. Viral mutations acquired randomly can be selected via tissue-specific pressures which may assist in successful spillover into a naïve species (e.g. humans), as well as other closely related rodents depending on the fluctuations in rodent population numbers and behaviors (Gire et al., 2012; McCormick et al., 1987).

1.5. Pathophysiology of arenaviruses in humans and animal models.

Despite genetic dissimilarities, disparate vectors, and geographical separations, arenaviruses when transmitted to humans elicit some common symptoms. The common and unique aspects of arenavirus induced pathophysiology offers a challenge to both clinicians and researchers as they seek to understand the etiology of disease and to intervene in its progress. The onset of an infection by an arenavirus is widely considered insidious. Fever ensues, and is often relentless. The prevalence of the viruses geographically with other agents known to cause debilitating febrile illnesses often leads to complications in recognition and treatment (Daniel J. Bonthius, 2012; McLay, Liang, & Ly, 2014; Peters, 2002).

The prototype of the family, LCMV, generally, causes a subclinical disease that is self-limiting and often goes unreported (Buchmeier & Zajac, 1999). The primary LCMV case, reported in 1934 by Lillie and Armstrong, briefly described a middle aged woman complaining of general malaise, severe headache, and of being “very hot” (Armstrong & Lillie, 1934). The initial discovery was made during an outbreak of Saint Louis

encephalitis, and was typical of the disease occurring at the time, until passaging of the infectious agent through rhesus monkeys and white mice revealed the unique, and never before seen characteristics of the virus including its presence in the choroid plexus and meninges, of which it's named was garnered.

In certain conditions, LCMV, can cause a variety of severe diseases in humans including, but not limited to, aseptic meningitis and encephalitis (Buchmeier & Zajac, 1999). Sporadic reports of other manifestations (i.e. orchitis) in non-meningeal cases have also been documented (Baum et al., 1966). LCMV, though not frequently associated with hemorrhagic fevers, has also been documented as causing notable coagulopathy (Staci A. Fischer et al., 2006; Scott & Rivers, 1936). The disease in humans can manifest either systemically and/or neurologically and follows a biphasic course of development characterized by a febrile and late neurological episode that usually begins within 1-2 weeks after exposure (Botten et al., 2013; Lehmann-Grube, 1989). Non-meningeal forms that have been documented have similar general symptoms including a febrile illness with fever, loss of appetite, low back pain, general malaise, nausea, vomiting, retro-orbital headache, photophobia, maculopapular rash, occasional alopecia, with common lab findings leucopenia and occasional thrombocytopenia (Baum et al., 1966; Lewis & Utz, 1961; Strausbaugh, Barton, & Mets, 2001). LCMV acquired in-utero has been demonstrated to be highly teratogenic, can result in abortion of the fetus, and can cause severe developmental defects. Common signs in the fetus and surviving children are: hydrocephalus, microcephalus, chorioretinitis and retinal scarring, mental and psychomotor retardation, and cerebral palsy (Barton & Hyndman, 2000; Bonthius et al.,

2007; Enders et al., 1999; Wright et al., 1997). Prenatal LCMV infections are thought to be an underdiagnosed disease due to similar and overlapping symptoms of TORCH (toxoplasmosis, rubella, cytomegaoviurs, and herpes virus) (Daniel J. Bonthius, 2012; Bonthius, Mahoney, Buchmeier, Karacay, & Taggard, 2002; Bonthius et al., 2007; Wright et al., 1997).

African arenaviruses, in particular LASV, cause symptoms within 7-12 days post-exposure (Yun & Walker, 2012). Common symptoms include fever, severe headache, sore-throat, retro-sternal pain, myalgia, facial and neck swelling, and pharyngitis (Bausch et al., 2001; Buckley & Casals, 1970). An early leucopenia is often observed, followed by a late leukocytosis. LF, if fatal, occurs usually within 12 days, and follows a hypotensive, hypovolemic, and/or hypoxic shock syndrome (Edington & White, 1972; Fisher-Hoch, McCormick, Sasso, & Craven, 1988). Hemorrhaging, often gingival or more rarely gastrointestinal, is less common during LF and is an indicator of poor prognosis, along with neurological involvement (Bausch et al., 2001; Günther & Lenz, 2004; Gunther et al., 2001). An unusual sequala of LF is sensorineural hearing deficit, which is estimated to occur in up to 30% of LF patients. The etiology of the hearing loss is not well understood, and has been suggested to be an immunopathological development, as opposed to a direct result of virus infecting the cells involved (Cummins, McCormick, Bennett, & et al., 1990; Okokhere, Ibekwe, & Akpede, 2009). A more thorough description of the cellular and systemic features of this fatal disease course is lacking due to insufficient and infrequent post-mortem examinations.

An interesting feature of severe LASV disease is the insufficient immunological response early during infection (Mahanty et al., 2003). Antigen presenting cells (APCs) are thought to be a crucial early cell type infected with virus (macrophages and dendritic cells). Secondary dissemination occurs in most visceral tissue and virus can be found in hepatocytes, endothelial cells, epithelial cells, and fibroblasts. Immunosuppression is hypothesized to result from multiple dysfunctions within infected APCs, which could lead to a general repression of a functional antiviral CTL response thus facilitating uncontrolled viral replication (Günther & Lenz, 2004). Accordingly, uncontrolled viral replication and high titer are one of the few indicators of disease severity (Edington & White, 1972; Johnson et al., 1987). Several mechanisms have been proposed explaining, in part, how LASV deters activation of an immune response via nucleoprotein (NP) and matrix protein (Z) interactions involving cytosolic pattern sensors –RIG I and MDA5 and Caspase inhibition. These will be discussed below in the arenavirus protein sections. Also, the glycoprotein (GP) mediated tropism of the virus allows for direct infection of professional antigen presenting cells and is thought to interfere with sufficient antigen presentation and support the immunosuppressive state during the disease course (reviewed in (Russier, Pannetier, & Baize, 2012)).

The lack of extensive cytopathology by the virus has been a conundrum for clinicians and scientists. Disruption of the vascular endothelium, and its barrier function, is a feature thought to contribute to pathogenesis (Kunz, 2009; Peters & Zaki, 2002). The immunosuppressive phenotype observed during OW arenavirus infection, seems at odds with the disease course for NW arenaviruses, as will be discussed in the following

section. The paucity of neutralizing antibodies seen following infection, contrasts with NW arenavirus convalescence, where high nAbs are a common feature that protect against re-infection (Bausch et al., 2000; Bond, Schieffelin, Moses, Bennett, & Bausch, 2012).

South American pathogenic arenaviruses all generate a very similar clinical picture (Schattner, Rivadeneyra, Pozner, & Gómez, 2013). The clinical descriptions and pathophysiology of Junín virus are the most well-documented. Symptoms begin within 7-10 days post-infection and are highlighted by fever, malaise, macular popular rash, severe headache, photophobia, and petechial hemorrhaging (Grant et al., 2012; Molinas, Bracco, & Maiztegui, 1981). Neurological complications are common and include tongue tremor, hyporeflexia, confusion, ataxia, seizures, and coma in severe cases (Marta et al., 1999). As in severe LF, AHF cases have a terminal shock of unknown etiology. Autopsies from fatal cases report the involvement of lymphatic tissue as sites of replication with macrophages, dendritic cells, and monocytes being primary targets of replication (Pozner et al., 2010), as well as focal necrotic hepatic lesions (Gonzalez, Cossio, Arana, Maiztegui, & Laguens, 1980). In contrast to LASV infections, the South American arenaviruses elicit a potent inflammatory response in correlation with viral titer and disease severity, demonstrate high levels of proinflammatory cytokines -TNF alpha, IL-6, and have greater incidence of hemorrhaging (Heller, Saavedra, Falcoff, Maiztegui, & Molinas, 1992; Marta et al., 1999). Hemorrhaging caused by SA arenaviruses, in contrast to OW, does not correlate with disease severity or outcome (Heller et al., 1995; Molinas, de Bracco, & Maiztegui, 1981). In both OW and NW human disease, a consistent lack of

cytopathology exists which is insufficient to explain the severe disease and shock manifestations that people succumb to (Elsner, Schwarz, Mando, Maiztegui, & Vilches, 1973; Walker et al., 1982).

The exact alterations in the hematological system during arenavirus infections across New and Old World viruses that lead to bleeding abnormalities have been elusive, and multiple explanations have been proposed. Many explanations, however, are based on studies in animal models or tissue culture systems, such as the role of nitric oxide in endothelial cell permeability following PICV infection (Brocato & Voss, 2009). NO production during AHF has been noted in patients, confirmed in an endothelial cell culture systems, and is suggested to promote hemorrhage through barrier disruption (Gomez et al., 2003). Platelet dysfunction via IFN over-stimulation is another hypothesis, and accordingly, JUNV virus has been found to infect megakaryocytes, which can lead to deficits in pro-platelet production (Pozner et al., 2010). Specific deficiencies and alterations have also been observed in clotting factors, and their regulatory cofactors in animal models, and in patient serological examinations (Felisa C. Molinas et al., 1981; Molinas, Paz, Rimoldi, & de Bracco, 1978; Schwarz et al., 1972). Given the observation of infection of hepatocytes and megakaryocytes, and the synthesis of clotting factors within these sites (Lenting PJ, 1998), this hypothesis has gained interest. An additional possible contributor is an inhibitor of platelet aggregation, which has been suggested, but not identified, in both LASV and JUNV infections, and is thought to also contribute to platelet abnormalities during infection (Cummins et al., 1989; Cummins, Molinas, et al., 1990).

1.6. Animal models of arenavirus infection

Upon introduction of an arenavirus to a susceptible human, a variety of both sub-clinical and clinical features can present. Likewise, amongst rodent species, different routes of inoculation, as well different species and strains of virus, will cause a variety of outcomes both in the wild and in laboratory settings (Buchmeier & Zajac, 1999). Animal models have been established to recapitulate and investigate various aspects of human disease including the immunological responses of both rodents and non-human primates, vaccine efficacy, and antiviral screening. Many elegant studies have used LCMV infection of mice to characterize numerous aspects of virology, immunology, and modern medicine. The revelations, to name a few, include aspects of chronic viral infection, antigen presentation, and cytotoxic T cell responses (Buchmeier & Zajac, 1999), and have prompted the virus to be widely considered as the Rosetta stone of modern immunology.

Given the biosafety requirements for most pathogenic arenaviruses (BSL4), closely related arenaviruses (e.g. TCRV, Candid1, LCMV, PICV) have been used to understand the disease course from a micro and macroscopic perspective (Vela, 2012). Animal models include: inbred/outbred mice, Hartley guinea pigs, Strain 13 guinea pigs, Syrian hamsters, rhesus macaques, cynomolgus macaques, African green monkeys, and common marmosets. These animal models have been used to examine efficacy of vaccines, antiviral compounds, and neutralizing antibodies (Vela, 2012).

1.7. Arenavirus life cycle

The arenavirus lifecycle begins with an introduction of an infectious virus to a naïve host. The surface glycoprotein, embedded in the host-acquired viral envelope, interrogates the cell surface until a suitable receptor ligation event(s) can take place. Following sufficient attachment, virions are endocytosed, and need to be trafficked to a late endosome (LE). The acidic environment of the late endosome provides the cue for a molecular rearrangement of the glycoprotein complex. The receptor binding subunit (GP-1) is then shed from the complex, and a fusion peptide(s) is revealed on the transmembrane stalk (GP-2) that is able to insert into the LE membrane and initiate the fusion cascade. Successful viral to LE membrane fusion allows for the ejection of the viral genome, in the context of a ribonucleoprotein (RNP) complex, to be released into the cytoplasm. The RNP contains the minimal units required for transcription of genomic RNA, and replication of genome segments (genome, NP, L). Translation of viral proteins is proceeded by a highly dynamic assembly and staging event presumed to take place at the plasma membrane. Newly synthesized viral proteins and genomes are able to then passively bud from the plasma membrane, in the form of infectious viral particles, without destruction of the infected cell (Botten et al., 2013; Botten et al., 2007).

1.8. Arenavirus gene structure and replication

The arenavirus genome, though classified as negative sense (Leung, Ghosh, & Rawls, 1977), has both a negative (-) and positive (+) encoding polarity on each of the two genomic segments: the small (3 kb S segment) and large (~7 kb L segment). The S

segment contains the (+) GP coding region, the (-) NP coding region, and is separated by an intergenic region (IGR) that is thought to form a hairpin structure involved in transcriptional termination (Auperin, Romanowski, Galinski, & Bishop, 1984; Harnish, Dimock, Bishop, & Rawls, 1983; Riviere et al., 1985). The 3` and 5` untranslated region(s) (UTR) on each segment contains a 19 nt long, complementary termini that are proposed to form a pan-handle structure. The L segment encodes the matrix protein (Z) in the (+) and the L protein - RNA dependent RNA polymerase (RdRp) in the (-) with similar UTR and IGR features (Harnish et al., 1983) (see figure 1.2).

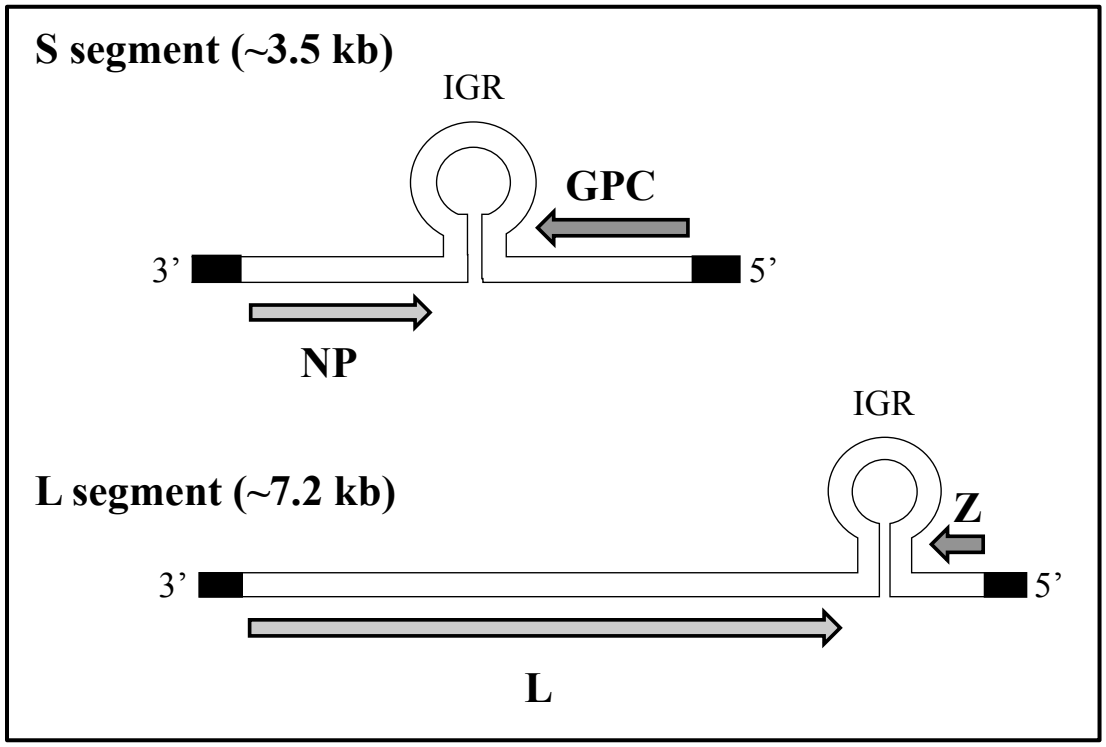

Figure 1.1 Arenavirus genome

Adapted from Botten et al., 2013. The arenavirus genome is bisegmented and ambisense. The protein coding regions (shaded arrows) within each RNA segment are separated by the noncoding IGR that forms a terminating hairpin structure. The termini of each segment contain untranslated regions UTRs involved in genome packaging

The arenavirus genome, upon entry into a host cell cytoplasm, is acted upon by the viral RdRp to facilitate the process of making sub-genomic viral mRNA, viral complementary (vc) RNA, as well as viral genomic sense RNA copies. This process requires first the translation of message sense NP and L, which after sufficient accumulation then support vcRNA synthesis from which GP and Z message can later be transcribed (Botten et al., 2013; Franze-Fernandez et al., 1987; Meyer, de la Torre, & Southern, 2002). Translation of NP is thought to facilitate a read-through of the polymerase along the viral RNA (i.e. transcriptional antiterminator) (Tortorici et al., 2001). Accumulation of Z has been shown, in-vitro, to inhibit the activity of the polymerase, and thus may play the role of transcriptional and replicative repressor (López, Jácamo, & Franze-Fernández, 2001). The dynamics of vRNA and viral antigen have been interrogated in-vivo using *in-situ* hybridization and immunocytochemistry techniques (Oldstone & Buchmeier, 1982; Valsamakis et al., 1986), which revealed the transient nature of glycoprotein expression, along with early and consistent maintenance of NP, and novel mechanisms of truncated interfering RNAs.

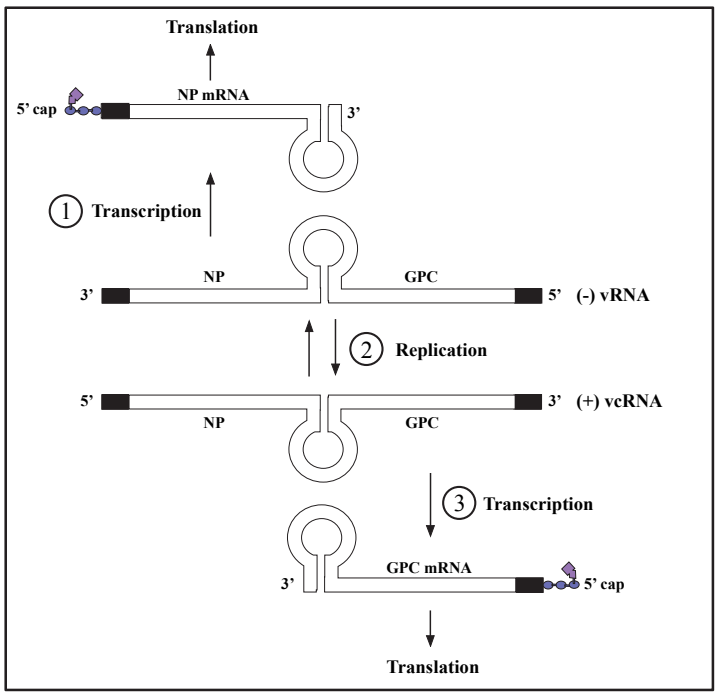

Figure 1.2 Arenavirus genome replication and transcription strategy

Adapted from Botten et al., 2013. This figure illustrates the steps carried out by the viral polymerase to carry out a successful round of replication, which begins with (1) synthesis of subgenomic RNAs needed for transcription of NP mRNA. (2) Newly translated NP facilitates the read-through of the IGR by the polymerase to generate a full length antigenomic RNA, and (3) which then serves as a template for transcription of GP mRNA.

1.9. Arenavirus anatomy

Arenaviruses are structurally simple viruses. Genetically, they maintain a bi-segmented, ambisense, single stranded RNA genome that codes for a total of four proteins. The most abundant viral protein, the nucleoprotein (NP), encapsidates the viral genome and is found clustered within the interior cavity of the virion. The viral

polymerase (L), also packaged within the virion, is responsible for all genomic transcription and replication events. The viruses are enveloped, which is derived from the plasma membrane of infected cells as they passively bud out into extracellular space in a process driven by the viral matrix protein, Z. The virions themselves are considered highly pleomorphic and range in size from ~ 90-300 nm in diameter. The membrane of the virions are decorated with the viral envelope glycoprotein (GP) which is derived from a cellular precursor, GPC, and is later processed into the multifunctional stable signal peptide (SSP), GP-1 receptor binding subunit, and the GP-2 transmembrane stalk. The name arenavirus, originally coined arenovirus, (latin *Arenosus,* meaning sandy) was agreed upon by Rowe et al. (1970) due to the unique granules observed within the cavity of budding virions when ultrathin sections of infected cells were viewed under a transmission election microscope. These granules were later defined as ribosomes, whose presence today remains an enigma. The incorporation of these cellular factories within the virions, however, is a harbinger of a far more elaborate and elusive network of cellular machinery involved in the biogenesis and transmission of this group of viruses (Murphy, Webb, Johnson, Whitfield, & Chappell, 1970; Rowe et al., 1970).

The limited arenaviral proteome (NP, L, Z, and GP) implies that these proteins must be: (i) highly multi-functional, and (ii) able to congregate and re-purpose a network of cellular proteins to carry out the obligatory steps in the viral lifecycle, without destroying integral and vital cellular functions. Much effort has gone into understanding the core function of each viral protein in replication of the virus (i.e genome packaging, receptor binding, budding etc) (Buchmeier, 2002; Buchmeier, Elder, & Oldstone, 1978; Burns &

Buchmeier, 1991; Pinschewer, Perez, & de la Torre, 2003). Scientists now are beginning to unravel the cellular synthetic machinery hijacked by the individual proteins as well as their mechanisms of action (Lucas T. Jae et al., 2013; Klaus et al., 2013; Madakasira Lavanya, Christian D. Cuevas, Monica Thomas, Sara Cherry, & Susan R. Ross, 2013; Debasis Panda et al., 2011).

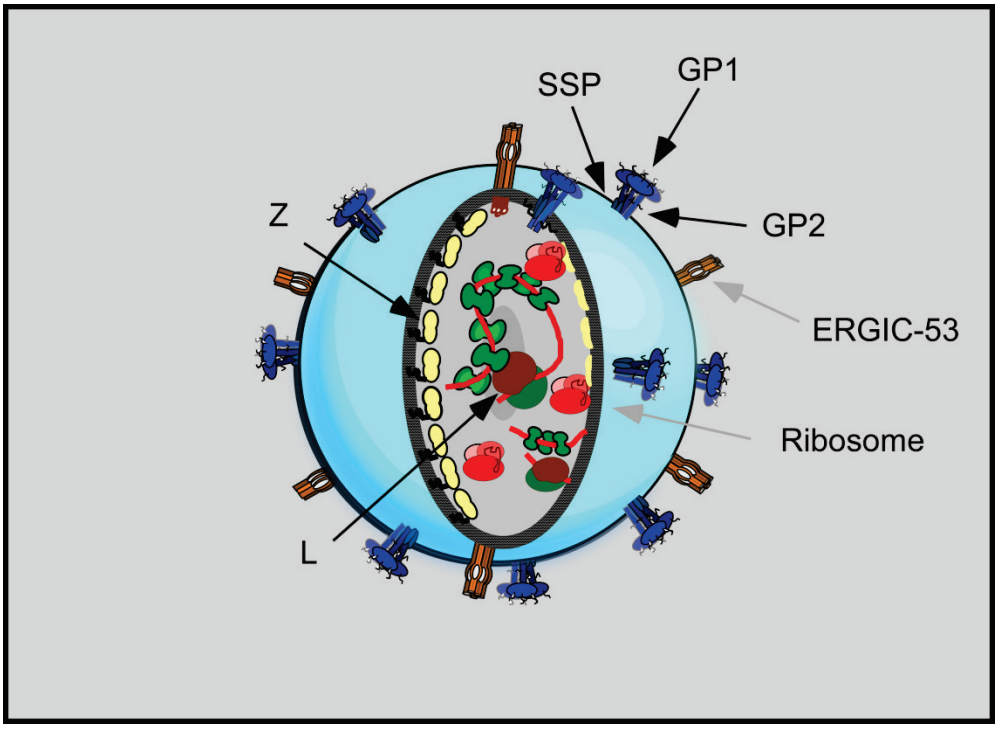

Figure 1.3 Arenavirus anatomy.

Mature arenavirus virions contain an envelope derived from the plasma membrane of an infected cell (blue shading) that is decorated by a tripartite glycoprotein complex consisting of the GP-1 ectodomain, the GP2 transmembrane domain, and the myristolated bitopic SSP. The inner leaflet of the plasma membrane is deformed into the curved shape via association of the myristolated matrix protein Z (yellow). The interior cavity of the virus contains the RNP consisting of the viral RNA genome (L and S segment- red loop) encapsulated by the NP (green). Each genome segment also contains the RdRp L (red and green). The virions also contain interior host derived ribosomes of unknown function (red and pink), as well as the intracellular cargo receptor ERGIC-53 (brown).

1.9.1. NP

The viral NP (ca~65 kDa), in addition to its canonical role of genome packaging and transcriptional regulation (Pinschewer et al., 2003), has been recently shown to play a role in subverting and manipulating innate immunological recognition. Structural studies of LASV NP revealed amino-terminal cap binding capabilities (*7-methyl guanosine triphosphate*) thought to be involved in cap snatching (Linda Brunotte et al., 2011; Qi et al., 2010) and carboxy terminal exonuclease activity that is specific for dsRNA (Hastie, Kimberlin, Zandonatti, MacRae, & Saphire, 2011; Hastie, King, Zandonatti, & Saphire, 2012; Jiang et al., 2013). The latter of which is important in restricting IFNβ production via recognition of dsRNA by cytosolic RNA sensors, retinoic acid-inducible gene 1, and melanoma differentiation-associated protein 5 (RIG I and MDA5), and inhibits the translocation of IFN regulatory factor 3 (IRF3). Interestingly, LCMV NP was found to directly complex with both RIG-I and MDA5 (Zhou et al., 2010). NP mediated inhibition of IFN activity has been shown for most arenaviruses (Martínez-Sobrido et al., 2009). TCRV NP IFN suppression is currently under debate (Jiang et al., 2013; Martínez-Sobrido, Giannakas, Cubitt, García-Sastre, & de la Torre, 2007), and likewise the residues involved in the active site of the DEDDh exonuclease domain are highly conserved. LCMV NP was also shown to associate with and inactivate IκB Kinase related Kinase IκKε, thereby preventing phosphorylation of its IRF3 substrate, a prequel to its nuclear translocation and IFN activation program (Pythoud et al., 2012). NFκB activation and transcriptional activity is likewise inhibited by NP (Rodrigo et al., 2012), further highlighting the multifactorial immune suppression ability of the NP molecule, and the

arenavirus limited proteome. An additional innate immune aversion tactic is postulated for Junín virus NP, which is hypothesized to act as an anti-apoptotic molecule, via inhibition of Caspase 3 activation (Wolff, Becker, & Groseth, 2013).

1.9.2. Z

Originally identified as an 11kDa really interesting new gene (RING) domain containing protein (Salvato, Schweighofer, Burns, & Shimomaye, 1992; Salvato & Shimomaye, 1989), Z has since been shown to be a core structural virion protein that is anchored to the viral membrane via a myristolation addition at the N-terminus (Perez, Greenwald, & de la Torre, 2004), GP (Capul et al., 2007), NP (Ortiz-Riano, Cheng, de la Torre, & Martinez-Sobrido, 2011), and L (Jacamo, Lopez, Wilda, & Franze-Fernandez, 2003; Kranzusch & Whelan, 2011). Z, the viral matrix protein, is minimally capable of forming virus-like particles (VLPs) that are morphologically identical to bona-fide virions (Eichler et al., 2004) and is also known to be curiously multifunctional despite its small size. Its primary function lies in orchestrating the deformation of the plasma membrane leading to the budding event, a process that involves recruitment of tumor susceptibility gene 101 (Tsg101) and members of the endosomal sorting complexes required for transport (ESCRT) pathway (Perez, Craven, & de la Torre, 2003). LCMV Z, along with NP, has been shown to be involved with recruiting ALG2-interacting protein X (ALIX/AIP1) during budding (Shtanko, Watanabe, Jasenosky, Watanabe, & Kawaoka, 2011). Interestingly, New World arenavirus Z proteins also have dedicated immune-modulatory features similar to NP, and act as IFN antagonists via RIG-I binding and sequestration from MAVS (Fan, Briese, & Lipkin, 2010). Association of Z with

translational machinery (e.g. EIF4E) is proposed to interfere with its 5' 7-methyl G cap binding potential (100-fold reduction), thereby repressing host cell protein synthesis (Kentsis et al., 2001; Volpon, Osborne, Capul, de la Torre, & Borden, 2010). Ribosomal protein P0 was also found to interact with Z in the nuclear compartment, and also gets packaged into virions (Borden, CampbellDwyer, Carlile, Djavani, & Salvato, 1998), however, the consequence of this interaction remains largely unknown. Z is also proposed to possess anti-apoptotic capabilities via cytoplasmic re-routing of Promyelocytic leukemia protein (PML) through a direct interaction (Borden, Campbell Dwyer, & Salvato, 1998). Curiously, PML null mice are more susceptible and generate higher titers earlier during the acute phase of replication, which suggested PML recruitment provides a means of delayed CTL response in PML $^{-/-}$ mice (Bonilla et al., 2002). Alternative proposals suggest it may also regulate the interferon sensitivity of virus, and or regulate the transcriptional activity of the polymerase via Z (Djavani et al., 2001).

1.9.3. L

The large arenavirus L protein (ca. 250kDa) contains an RdRp, the enzyme responsible for all RNA replication and transcription activity in the viral lifecycle (Buchmeier, de la Torre, & Peters, 2007; Lukashevich et al., 1997). Due to the large size of the protein, and difficulties procuring it, little is known about the cellular activities of L outside of genome maintenance and transcription. Within virions, it is the lowest copy-number protein amongst the viral proteome, and is found in complex with the RNPs. When present in virions, it is thought to be locked in a catalytically inert state via Z

mediated repression (Kranzusch & Whelan, 2011). Domain predictions segregate the protein into four domains (I-IV) (L. Brunotte et al., 2011). Synthesis of arenavirus mRNA is thought to occur via a small 5` cap of cellular origin, hypothesized to be "snatched" in a mechanism similar to other negative sense viruses (e.g. bunyavirus RdRp and influenza virus PA) (Morin et al., 2010). Accordingly, domain N1 of L contains a putative class II endonuclease implicated in the retrieval of caps via downstream liberation of RNA (Morin et al., 2010). Interestingly, mutations mapped to L provide a replicative benefit to LCMV in certain cell types (e.g. macrophages) (Bergthaler et al., 2010), however, the mechanism behind this replication enhancement remains obscure (Bergthaler, Merkler, Horvath, Bestmann, & Pinschewer, 2007). Genetic studies of virulent versus avirulent Pichinde virus have also revealed a number of pathogenic substitutions in the polymerase (Lan, McLay, Aronson, Ly, & Liang, 2008) indicating alternative functions may exist.

1.10. Arenavirus glycoproteins

Arenavirus glycoproteins (ca. 65-75 kDa) form ~ 10nm trimeric and tripartite (SSP-GP1-GP2) club-like projections on the surface of virions that facilitate the attachment of virus to cell surface receptors (e.g. α-DG (Cao et al., 1998), TfR1 (Radoshitzky et al., 2007), Axl, Tyro3, LseCTIn, DC-SIGN (Shimojima, Ströher, Ebihara, Feldmann, & Kawaoka, 2011), and L-SIGN (Martinez et al., 2013)). Arenavirus glycoproteins also enable the annealing of viral membrane to cellular membranes following endocytosis (Borrow & Oldstone, 1994; Fields, Knipe, & Howley, 2007). The primary GP role is that of viral sentinel protein which is able to interrogate and engage with the surface of

available cells, and thereby is the principle protein responsible for arenavirus tropism and downstream pathogenesis (Oldstone & Campbell, 2011). Its biogenesis requires an elaborate interplay with the synthetic machinery of host cells requiring sequential proteolysis, coordinated multimerization and folding, asparagine-linked glycosylation, myristolation, and targeted intracellular transport. There is limited information known about the cellular proteins orchestrating events involved in GP biogenesis, outside of the enzymes required for proteolysis, and the receptors involved in GP mediated viral entry. Our studies have illustrated the depth of cellular machinery involved in the intracellular biogenesis of viral glycoproteins, some of which have may have dual roles in intracellular vs extracellular processes (Klaus et al., 2013).

1.10.1. Glycoprotein biogenesis: formatting of the complex

The arenavirus glycoprotein complex is synthesized inside of cells as a single precursor polypeptide (Buchmeier & Oldstone, 1979; Clegg & Lloyd, 1983; Gangemi, Rosato, Connell, Johnson, & Eddy, 1978; Harnish, Leung, & Rawls, 1981). Following insertion into the ER by its signal peptide, two proteolytic maturation events are carried out by cellular proteases: (1) the signal peptidase (SP) cotranslationaly processes the growing peptide, and (2) the subtilisin kexin isozyme 1/ site-1 protease (SKI-1/S1P herein referred to as S1P) forms the GP-1/GP-2 functional subunits. The three part structure is strictly conserved across the arenaviridae. Additional domains lie within each subunit, of which a handful of known functions are currently attributed to. The glycoprotein ectodomain forms a globular structure capable of binding to receptors, the GP-2 stalk anchors the complex to the viral membrane and carries out fusion, and the

SSP is involved in intracellular trafficking and has multiple roles in viral infectivity (See figure 1.2).

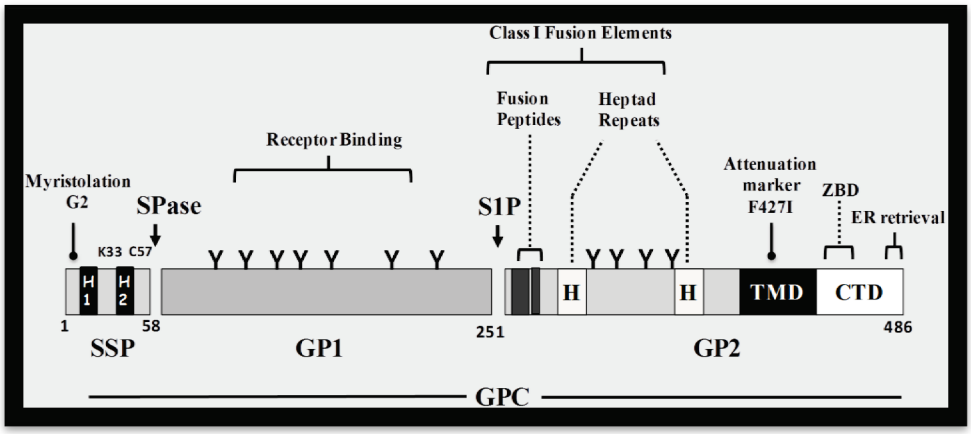

Figure 1.4 Arenavirus GP schematic.

Adapted from Botten et al., 2013. Proteolytic sites are indicated by black arrows. Specifically, the SSP is cleaved after AA 58 by the signal peptidase, and the GP1-GP2 consensus site is cleaved by site 1 protease after R[X]L[X] motif ending at aa ~251. The SSP contains a pan-arenaviral G2 myristol addition required for infectivity, two hydrophobic domains (H1 and H2) represented by black rectangles, which are each thought to span the membrane, residues K33 (critical for pH of fusion activation) as well as C57 (required for GP1-GP2 association). The GP-1 subunit contains the receptor binding domain and seven N-linked glycosylation additions indicated by (Y). GP-2 codes for the class I fusion structural elements including two sequential fusion peptides at the N terminus indicated by dark grey boxes, and two heptad repeats indicated by [H] . GP-2 also utilizes 4 N-linked sugars as indicated (Y) and are from LASV GPC consensus sites determined by Eichler et al. (2006). The GP-2 transmembrane (TMD) and C-teminal domains (CTD) include discontinous SSP binding sites which may overlap or include a Zinc-binding Domain (ZBD), which are hypothesized to contribute to folding, SSP interactions, and fusion of Junín virus GPC (York et al., 2007; Briknarova et al., 2010). F427I indicates a GP2 transmembrane domain (TMD) attenuation marker found in Junín virus by Albarino et al. (2011) also capable of attenuating LASV in-vitro.

1.10.2. GP post-translational modifications

Arenavirus glycoprotein structure and function has been shown to be critically dependent upon two known post translational modifications: asparagine linked glycosylation and myristolation. Myristolation of the SSP will be discussed in a later section. The presence and function of multiple mannose-rich N-linked sugars on GP (Buchmeier & Oldstone, 1979) have been studied using a variety of techniques including: chemical inhibitors of glycosylation, lectin binding, x-ray crystallography, site directed mutagenesis, analysis of proteolysis, intracellular processing, fusion, and release of infectious virus. Whilst a growing body of evidence supports the essential contribution of these modifications, the exact composition of the carbohydrates, the enzymes involved in their maturation, and the molecular mechanism by which they contribute to GPs functions remain largely unknown (Bonhomme et al., 2011; Bonhomme, Knopp, Bederka, Angelini, & Buchmeier, 2013; Bowden et al., 2009; Buchmeier & Oldstone, 1979; Burns & Buchmeier, 1993; Candurra & Damonte, 1997; Clegg, 1982; Damonte, Mersich, & Candurra, 1994; Eichler, Lenz, Garten, & Strecker, 2006; Lucas T. Jae et al., 2013; Mersich, Castilla, & Damonte, 1988; Parekh & Buchmeier, 1986; Parsy, Harlos, Huiskonen, & Bowden, 2013; Silber, Candurra, & Damonte, 1993; Wright, Salvato, & Buchmeier, 1989; Wright, Spiro, Burns, & Buchmeier, 1990b).

Investigations into the presence of carbohydrate additions to arenavirus glycoproteins via radiolabeling of viral and cellular derived LCMV GP (GP1/GP2 and GPC) performed by Buchmeier et al. identified a mannose-rich precursor GP molecule, which incorporated additional ^{3}H fucose and ^{3}H galactose during its secretion as

GP1/GP2 suggesting a degree of post-addition processing (Buchmeier et al., 1978; Buchmeier & Oldstone, 1979). The glycans on LCMV constitute approximately 35% of the molecular weight of the molecule (Wright et al., 1990b). Glycosidic mapping of JUNV GP-1 also suggests that the N-linked sugars contain terminal mannose and galactose, however, the level of fucose may have been substantially less using an alternatively less sensitive technique (Sergio Grutadauria a, 1999). Early studies on carbohydrate functions of LCMV GP maturation demonstrated tunicamycin addition, via inhibition of the *en bloc* addition of core oligosaccharides onto GPC, greatly diminished viral yield, and more specifically the cleavage of GPC into GP-1 and GP-2. This suggests that glycosylation was a precursor to proteolytic maturation (Wright et al., 1990b). Concomitant with the inhibition of cleavage following tunicamycin addition, there was no detectable GP at the surface of cells and no virus could be concentrated from conditioned cell medium, suggesting the addition of N-linked sugars affected an early step in the assembly and maturation of the glycoprotein (Wright et al., 1990b). In support of this, infectivity of the NW Junín virus was likewise substantially reduced, along with proteolytic maturation when cultured in the presence of tunicamycin. The authors however, in the latter study, presented data from concentrated radiolabeled virions that still contained viral structural proteins but lacked the normal amount of glycosylated GP-1. This indicates that some alterations in the requirements of N-linked sugars on GP may exist among arenaviruses (Padula & Segovia, 1984). This is in agreement with previous studies on the critical inclusion of glycosylation and its processing via demonstration of a high molar glucosamine block on JUNV replication (Martinez Peralta, Leon, Coto, & Laguens, 1979), as well as the role of terminal GP-1 sugars on adsorption (Raiger

Iustman, Castilla, Meich, & Mersich, 1998). Silber et al. demonstrated via use of a glucosidase I & II, as well as mannosidase I & II inhibitors that maturation of the GP glycans to a complex form was largely irrelevant for infectivity (Silber et al., 1993). Interestingly, in the same study, bromoconduritol, which inhibits the ER glucosidase II, was able to reduce infectivity. In accordance with those findings for JUNV, recent studies have shown that small molecules antagonizing glucosidases within the ER are promising antiviral agents against multiple VHFs (Chang et al., 2013).

Sequence comparisons across OW and NW GPs reveal four conserved sites within the GP-2 subunit, whereas GP-1 subunits maintain a degree of heterogeneity of N-linked glycosylation sites in placement, number, and utility (Bonhomme et al., 2011; Bonhomme et al., 2013; Briese et al., 2009). Genetic disruption of arenavirus N-linked glycosylation sites (NLS) has revealed the importance of individual NLS to specific features of glycoprotein maturation and glycoprotein specific functions within the viral lifecycle (Bonhomme et al., 2011; Bonhomme et al., 2013; Eichler et al., 2006). Bonhomme et al. (2011) identified in a prototypical LCMV GP the usage of eight of the nine consensus NLS, which is in accordance with previous data from Wright et al. (1990a) on LCMV NLS utilization (Bonhomme et al., 2011; Wright et al., 1990b). Interrupting glycosylation, at several sites in LCMV and LASV GP-1, interfered with the proteolytic maturation of the complex (Bonhomme et al., 2011; Eichler et al., 2006), whereas alterations to LCMV GP-2 sites enhanced cleavage (Bonhomme et al., 2011). Interestingly, disruption of several LCMV GP-1 glycosylation sites, interfered with the fusion activity of GP-2, yet trafficked normally to the plasma membrane. Ablation of

conserved N-terminal sites along with an N-terminal GP-2 site also restricted VLP infectivity (Bonhomme et al., 2011). Several NLS have also been demonstrated to be involved in cell-type specific fitness and tropism (e.g. primary macrophage versus neuron cells), as recombinant LCMV lacking specific GP NLS revealed altered expression, fusogenicity, and growth kinetics depending on the cell type (Bonhomme et al., 2013). Using the recombinant virus bearing individual NLS mutations, the first 2 N-terminal NLS, the most conserved of GP-1 sites, were found to be completely indispensable for virus recovery (Bonhomme et al., 2013). Structural studies of MACV GP-1 crystalized at 1.7Å (Bowden et al., 2009) and in a co-crystal with transferrin receptor 1 (Abraham, Corbett, Farzan, Choe, & Harrison, 2010) suggest that the NLS do not participate directly in receptor interactions, and instead help to solubilize the GP. Limited mass spec analysis of the glycopeptides did reveal substantial heterogeneity in the carbohydrate structures on GP-1 (Bowden et al., 2009), however a recent GTOV GP-2 structure suggests that given the packing and placement of GP-2 glycans, they are likely to be shielded from modification and remain in a homogeneous structure (Parsy et al., 2013). In the study by Parsy et al. the authors also suggest that the GP1-GP2 heterotrimer interface will require the structural influence of the N-linked sugars, which supports the infectivity data generated by Bonhomme et al. following NLS ablation.

Neutralizing epitopes on LCMV GP have been demonstrated to be structurally upheld by both intramolecular GP-1 disulfide bridges and N-linked glycosylation (Wright et al., 1989). LCMV GP-1 neutralizing epitope 1D requires minimally the core oligosaccharide added within the ER to maintain the folding required to present the

epitope properly. Interestingly, this same epitope is masked in other strains of LCMV by the addition of a GP-1 glycosylation site following a single point mutation; thereby extending the utility of N-linked glycosylation to not only assisting in folding, but in hiding neutralizing antibody epitopes (Bonhomme et al., 2011; Wright et al., 1989). Curiously, the immunosuppressive strain of LCMV (WE) lacks the GP1-D epitope, but the immunological extent of this observation was not clear as the site is reported to be genetically unstable (Parekh & Buchmeier, 1986).

1.10.3. Making the SSP

Following early GP mRNA translation, the arenavirus GP leader sequence, termed Stable Signal Peptide (SSP), directs the nascent peptide into the lumen of the rough Endoplasmic Reticulum (RER) presumably via the classical signal recognition particle and translocase (Eichler, Lenz, Strecker, Eickmann, et al., 2003; Eichler, Lenz, Strecker, & Garten, 2003; Froeschke, Basler, Groettrup, & Dobberstein, 2003). The SSP has several distinguishing and unusual characteristics which set it apart from conventional signal sequences. Signal Peptides are normally 18-30 residues long with an N terminal positive residue, a hydrophobic stretch, and a C-terminal signal peptidase cleavage site. The first glimpse of a potential nontraditional role for the arenavirus SSP came about during investigations that revealed a major histocompatibility complex (MHC) class I restricted immunodominant epitope present within the LCMV signal peptide, conserved across all arenavirus species (Burns, 1993), that was processed in a Transporter of Antigen Presentation (TAP) dependent process (Hombach, Pircher, Tonegawa, & Zinkernagel, 1995; Hudrisier, Oldstone, & Gairin, 1997; Pircher et al.,

1990). The amino acid sequence is curiously long (58 aa) (Eichler, Lenz, Strecker, & Garten, 2003) and has a half-life of > 6 hours (Froeschke et al., 2003). The enhanced stability and longevity can be ascribed directly to the SSP itself, rather than the remaining GPC molecule, as it is maintained when expressed in isolation (Froeschke et al., 2003).

The signal peptide, in addition to its greater than normal length (58 vs 18-25 AA), has an additional unusual molecular architecture, and rather than the prototypical single pass cellular signal peptides, potentially crosses the membrane twice, courtesy of its two hydrophobic domains. The bitopic peptide's N and C termini, for JUNV GP, are thought to lie within the cytoplasm (Agnihothram, York, Trahey, & Nunberg, 2007; Eichler et al., 2004), separated by a short lysine (K33) containing loop crucial for setting pH thresholding during activation of the fusion cascade (e.g. charge at position 33 determines what pH fusion occurs at) (Saunders et al., 2007; York & Nunberg, 2006). Some controversy remains as to the exact architecture of the SSP. Early studies with OW GPs suggested a class II transmembrane topology (N term anchored) (Eichler, Lenz, Strecker, Eickmann, et al., 2003; Froeschke et al., 2003), as well as two-pass with luminal termini (Schrempf, Froeschke, Giroglou, von Laer, & Dobberstein, 2007) versus the more recent bitopic –cytosolic termini arrangement (Agnihothram et al., 2007; Briknarova, Thomas, York, & Nunberg, 2011). Following liberation from the pre-GPC peptide via the cellular signal peptidase (Eichler, Lenz, Strecker, & Garten, 2003; York & Nunberg, 2007a), rather than being degraded, the SSP will maintain a non-covalent association with the arenavirus glycoprotein complex through the remainder of the viral life cycle (Froeschke et al., 2003; York, Romanowski, Lu, & Nunberg, 2004). The multiple membrane

spanning domains of the SSP are not each required for translocation of GPC, and each in isolation will suffice, in addition to alternative signal peptides (e.g CD4, CD8, or FLUAV HA) (Eichler, Lenz, Strecker, Eickmann, et al., 2003; Eichler et al., 2004; York et al., 2004). However, proper proteolytic maturation of the GPC into GP-1 and GP-2 subunits requires an intact arenavirus SSP, and, accordingly, can be segregated into proteolysis and fusion influencing regions (Messina, York, & Nunberg, 2012). Further, the SSP can, interestingly, be provided *in trans* to complement GPC translocated via an alternative signal and restore downstream maturation and function (Agnihothram, York, & Nunberg, 2006; Eichler et al., 2004; Eichler, Lenz, Strecker, & Garten, 2003; Saunders et al., 2007; York et al., 2004). Signal peptides from closely related arenavirus species (e.g. LASV and LCMV) can also complement the alternative species GP (Eichler, Lenz, Strecker, Eickmann, et al., 2003). However, more distantly related arenavirus SSPs (e.g. JUNV and LASV) fail to properly restore functionality to the GP molecule, presumably via specific signals in the GP2 transmembrane (TM) and C-terminal domain (CTD) (Agnihothram et al., 2006; Albarino, Bird, Chakrabarti, Dodd, White, et al., 2011). Association of the SSP with GP-2 is thought to facilitate the anterograde trafficking of GP-1/GP-2 via masking of a dibasic ER retention signal in the GP-2 CTD, and thus implements a quality control mechanism ensuring a properly assembled GP complex prior to anterograde movement (Agnihothram et al., 2006; Burri et al., 2013).

The SSP is also post-translationaly modified at a pan-arenavirus N-terminal GP-2 site via a myristolation addition (York et al., 2004). The myristolation addition appears to be irrelevant for assembly of the tripartite molecular arrangement, but is crucial for

enabling downstream contributions of the SSP in GP function, namely fusion and infectious particle formation (Saunders et al., 2007; Schrempf et al., 2007; York et al., 2004). It is hypothesized that the myristolation could also assist in proper targeting of the GP complex to sites of budding along with the myristolated Z molecule (Agnihothram et al., 2006). The SSP invariant C-terminal C57 residue has also recently been shown to be involved in the formation of a zinc finger domain in collaboration with GP-2 (Briknarova et al., 2011; York & Nunberg, 2007b). This zinc-finger moiety is considered to play a stabilizing role with the GP-2 CTD (Briknarova et al., 2011; York & Nunberg, 2007b), which, in addition to interactions between the SSP K33 loop-GP2 ectodomain (York & Nunberg, 2006, 2009) and first SSP hydrophobic region- GP2 TM domain, may become active during the fusion cascade; however, the exact molecular mechanism and chronology remains to be fully elucidated (Messina et al., 2012). *In toto* several lines of evidence support the role of the SSP in the anterograde transport, proteolytic maturation, fusion, and infectivity activities of the arenavirus GP (Nunberg & York, 2012). The role of SSP in orchestrating the mature trimeric assembly of SSP-GP1-GP2, and its functionality, is yet to be completely understood. However, elucidating SSP interactions and functions provides fertile ground for therapeutic intervention. As such, several small molecules have been identified that interfere with SSP-GP-2 based fusion activity (Bolken et al., 2006; A. M. Lee et al., 2008; Thomas et al., 2011; York, Dai, Amberg, & Nunberg, 2008).

1.10.4. SKI-1/S1P cleavage: creating the GP-1 ectodomain and GP-2 stalk

Arenavirus GPs require sequential proteolysis in order to generate a functional tripartite complex. The second proteolytic maturation event, the cleavage of GPC into GP-1 and GP-2 subunits, is an absolute requirement for the activation of the metastable fusion elements entrenched in GP-2 and the formation of the globular GP-1 ectodomain containing the receptor binding determinants. GP-1 is formed from GPC by the proteolytic cleavage of site 1 protease (S1P) (Lenz, 2001), a calcium-dependent cellular endoprotease involved in sterol metabolism and the ER stress response (Seidah et al., 1999). After separation from the parental precursor , mature GP-1 maintains a non-covalent association with GP-2 on virions until acid induced ejection begins inside of endosomes (Burns & Buchmeier, 1991; Di Simone, Zandonatti, & Buchmeier, 1994). Properly processed GP-1/GP-2 molecules are incorporated into arenavirus particles and appear as evenly spaced club-like projections embedded in the membrane of virions, extending ~ 5-10nm from their surface (Burns & Buchmeier, 1993; Kunz, Edelmann, de la Torre, Gorney, & Oldstone, 2003; Neuman et al., 2005).

The timing and molecular mechanism involved in S1P proteolytic maturation of arenavirus GPs has garnered much attention. The site for the cleavage event was initially mapped to a nine amino acid peptide in LCMV GP and was determined to have a conserved, but slightly degenerate sequence, amongst the Arenaviridae involving a dibasic cluster (Buchmeier, Southern, Parekh, Wooddell, & Oldstone, 1987). Studies examining post-translational processing of LCMV GP determined a cleavage event, approximately in or transiting from, the late Golgi (Wright et al., 1990b). This was in agreement with studies on JUNV GP processing, which demonstrated that cleavage

could be inhibited via disruption of ER to Golgi trafficking through the use of monensin, BFA, and temperature shifts (Candurra & Damonte, 1997; Damonte et al., 1994). The GPC cleavage site was further narrowed to a four amino acid motif in LASV GP (RRLL), spanning residues 256-260 (Lenz, ter Meulen, Feldmann, Klenk, & Garten, 2000). An investigation of LASV GP also first revealed the enzyme S1P was responsible for the maturation cleavage of GPC into GP-1 and GP-2. Cleavage could be specifically blocked via calcium ionophores (S1P requires Ca^{2+} for proteolysis), but was insensitive to BFA (Lenz, 2001). This suggested the location of maturation cleavage was either ER or cis-Golgi, in contrast to the findings for LCMV GP (Beyer, Popplau, Garten, von Laer, & Lenz, 2003; Wright et al., 1990b) and JUNV GPs. These were thought to occur later in transit through the Golgi/trans Golgi after the glycan additions became complex (Damonte et al., 1994). LCMV was subsequently and quizzically also found to be a substrate for S1P (Beyer et al., 2003), along with the NW HF arenavirus GPs (Rojek, Lee, Nguyen, Spiropoulou, & Kunz, 2008). The differences in subcellular locations of cleavage were attributed to subtle changes in the cleavage consensus site. LASV GP contains a tetra peptide (RRLL) that resembles the autocatalytic site C embedded within the protease, which is acted on early in the secretory pathway (e.g. ER), whereas the JUNV GP site RSLK more closely resembles the autoprocessing site B (Pasquato et al., 2011). Given the conservation of arenavirus GPC usage of S1P, mechanistic insight into the substrate selection may be gleaned from the evolutionary history of S1P and rodent maintenance of arenaviruses. Accordingly, a recent study demonstrated that a wood rat allele of S1P with reduced activity provided a means of protection against persistent, but not acute infection with LCMV in a tissue specific fashion, in bone marrow derived

dendritic cells (Popkin et al., 2011), which are known to be dysregulated during persistence (Borrow, Evans, & Oldstone, 1995; Popkin et al., 2011; Sevilla, Kunz, McGavern, & Oldstone, 2003). The extent of S1P function in the arenavirus lifecycle will require further studies, but has been greatly hampered by the lack of a tractable animal model due to embryonic lethality following gene deletion (Mitchell et al., 2001).

Maturation cleavage has been proposed to be an absolute requirement for incorporation of glycoprotein species into arenavirus particles (Stefan Kunz et al., 2003; Lenz, 2001), and for cell-to-cell spread of virus (Rojek, Lee, et al., 2008). Interestingly, unprocessed GPC has been shown to traffic to the plasma membrane in certain circumstances: following production in S1P-deficient Chinese Hamster Ovary (CHO) cells, during expression of cleavage defective GP mutants, following exposure of cells to calcium ionophore additions (Beyer et al., 2003; Stefan Kunz et al., 2003; Rojek, Lee, et al., 2008). However, GP produced in these environments, is not efficiently incorporated into virions, which still bud with normal quantities of viral structural proteins. Thus, cleavage and plasma membrane trafficking are not predicated upon each other, *per se*, as it has also been shown that removal of the GP-2 CTD dibasic cluster, reported in JUNV to mediate anterograde trafficking via SSP masking, will negate cleavage of LCMV and LASV GP (Agnihothram et al., 2006; Stefan Kunz et al., 2003; Schlie et al., 2009; Schlie, Strecker, & Garten, 2010). The role of cleavage has been ascribed to activation of the fusion machinery in the GP-2 subunit (Klewitz, Klenk, & ter Meulen, 2007). However, its role in targeting and packaging of GP into virions remains under investigation (Beyer et al., 2003). Inhibiting the cleavage event has, however, through

the use of reverse genetic systems and small molecules, shown promise as an anti-viral tactic (Maisa, Stroher, Klenk, Garten, & Strecker, 2009; Pasquato, 2006; Rojek et al., 2010).

The association of arenavirus GP's with S1P has additional implications with regard to the role of S1P in the ER stress response, or the unfolded protein response (UPR). Synthetic peptides corresponding to the LASV GP recognition site (RRLL) are able to inhibit S1P-based cleavage of pro-activating transcription factor 6 pro-(ATF6) in CHO cells (Pasquato, 2006). Following the accumulation of unfolded proteins in the ER, ATF6 dissociates from BiP/GRP78 (both ER-resident chaperones capable of sensing folding capacity), undergoes sequential proteolysis by S1P and S2P, and becomes nATF6, which translocates to the nucleus and initiates a branch of the UPR (Pasquato, 2006; Pasquato et al., 2011) (reviewed in (Chakrabarti, Chen, & Varner, 2011)). Moreover, the LCMV GP has been shown to be a selective inducer of the ATF6-mediated UPR, independent of the other viral structural proteins. This response occurs during the acute phase of infection, when GP expression is highest. The response is thought to enhance the folding capacity within the ER which may be required for efficient viral replication (Pasqual, Burri, Pasquato, de la Torre, & Kunz, 2011b). An additional hypothesis is that the selective induction of the ATF6-mediated UPR facilitates the upregulation of ERGIC-53 (Nyfeler, Nufer, Matsui, Mori, & Hauri, 2003b), which which we show in Chapter 2 to enhance arenavirus replication in a GP-specific fashion (Klaus et al., 2013).

1.10.5. GP assembly and virion release

Assembly of arenavirus particles has been observed, via thin sectioning of infected cells, to take place at the plasma membrane, and in some instances, at intracellular locations (Murphy et al., 1970). Electron dense club-like projections have been shown to protrude from an engorged plasma membrane laden on the inner leaflet with matrix protein. The RNPs are shepherded into particles via an ill-described mechanism along with host ribosomes. Limited information exists as to the cellular factors involved in the assembly and release of particles; however, the viral matrix protein is widely accepted as the driving force of arenavirus budding (Fehling, Lennartz, & Strecker, 2012). The role of GP in polarized budding will be discussed more in detail in the following section (1.11).

Given the myristolation requirement for proper function of both the glycoprotein and matrix protein of arenaviruses, several investigations have followed lipid requirements for arenavirus assembly. Junín virus GP was observed to cluster in discrete sections at the surface of cells when expressed in isolation, a feature commonly associated with lipid microdomains (Agnihothram et al., 2009). Through the use of non-ionic detergents, which are commonly used to identify cholesterol rich lipid rafts, it was demonstrated that Junín virus GP is located in detergent soluble fractions of cell membranes, indicating no association with the detergent resistant membrane (DRM) fractions (Agnihothram et al., 2009). These findings, however, were contested in later studies that demonstrated cholesterol depleting drugs led to a substantial reduction in surface presentation and solubility of JUNV GP, as well as release of NP-containing

particles (Cordo, Valko, Martinez, & Candurra, 2013). Further studies of LASV GP using similar DRM extraction methods demonstrated a lack of association with DRMs indicating both Old and New world arenaviruses assemble in detergent soluble fractions (Schlie et al., 2009). Furthermore, the clustering of GP at the membrane was found to occur independent of the G2A myristolation addition in Junín virus SSP (Agnihothram et al., 2009). Immunogold labeling of GP-1 at the cell surface, which was visualized by transmission electron microscopy, confirmed discrete clustering of GPC into microdomains of approximately 120-160nM (Agnihothram et al., 2009). Interestingly, GPC, when expressed in isolation, was found in areas containing localized membrane curvature reminiscent of budding sites, thereby suggesting matrix-independent budding (Agnihothram et al., 2009) which has also been observed for LASV GP (Schlie, Maisa, et al., 2010). Curiously, in this same study, the authors were unable to demonstrate colocalization of the matrix protein with the glycoprotein at the surface, which does not support evidence provided by a number of studies which have demonstrated the interactions of GP and Z (Luis M. Branco et al., 2010; Capul et al., 2007; Casabona, Levingston Macleod, Loureiro, Gomez, & Lopez, 2009; Neuman et al., 2005; Schlie, Strecker, et al., 2010). Treatment of purified LASV virions, or VSV psuedovirus particles decorated with LASV GP, with cholesterol sequestering drugs, causes a profound reduction in infectivity that can be restored via exogenous cholesterol (Schlie et al., 2009). This finding suggests that budding, though not from cholesterol rich DRMs, occurs in non-raft cholesterol containing microdomains.

1.10.6. GP-1 form and function

The arenavirus GP-1 subunit contains the majority of neutralizing antibody epitopes as well as the sequence controlling receptor binding for arenaviruses (Cresta, Padula, & de Martinez Segovia, 1980; Oldstone, 1992; Parekh & Buchmeier, 1986; Sanchez et al., 1989; Wright et al., 1989). Therefore GP-1 largely controls the initial cellular tropism and downstream pathology of arenaviruses (Oldstone & Campbell, 2011). Several studies have shown the importance of this decision making capabilities inherent in GP-1. In particular, studies of LCMV infection of inbred mice have illustrated how a single amino acid substitution in GP-1 can alter the tropism of the virus, and elicit strikingly different outcomes (e.g. persistence vs acute vs death of animal) (Ahmed, Salmi, Butler, Chiller, & Oldstone, 1984; Kunz, Sevilla, McGavern, Campbell, & Oldstone, 2001; Salvato, Borrow, Shimomaye, & Oldstone, 1991; Sevilla et al., 2003; Sullivan et al., 2011; Teng, Borrow, Oldstone, & de la Torre, 1996). A substitution found at position 260 (F→L) changes the tropism (LCMV Arm to clone 13 transition) from red to white splenic pulp areas (macrophage-tropic to dendritic cell - tropic). In accordance with this, an acutely cleared virus becomes immunosuppressive and establishes persistence (Ahmed & Oldstone, 1988; Borrow et al., 1995; Sevilla et al., 2000). Interestingly, these changes (F260L) also follow the affinity of the GP for α-DG, a surface molecule highly expressed on dendritic cells (Sevilla et al., 2003; Smelt et al., 2001). Further, LCMV WE GP-1 mutation S153→F enables the virus to replicate within the growth hormone (GH) producing cells of the anterior pituitary (Oldstone et al., 1982), resulting in GH deficiency and hypoglycemia (Teng et al., 1996). A number of point mutations have been identified in variants of LCMV, yet most seem to alter the nature of the residue at position 260. Heterogeneity in NW arenavirus GP-1 molecules

have also been implicated in disease alterations (i.e. Junín attenuation) in both rodents and humans (Flanagan et al., 2008; Scolaro, Mersich, & Damonte, 1990; Zhang, Marriott, & Aronson, 1999). Studies mapping the determinants of NW arenavirus GP-1 molecules with the transferrin receptor 1 (TfR1) have demonstrated how limited alterations to the GP or the receptor can change the tropism of the virus for cells bearing TfR1 (Abraham et al., 2010; Abraham et al., 2009; Martin et al., 2009; Oldenburg, Reignier, Flanagan, Hamilton, & Cannon, 2007; Radoshitzky et al., 2008; Reignier et al., 2008).

In addition to its well supported role in receptor binding, additional alternative functions for LASV GP-1 have been suggested following plasmid driven expression in HEK293T cells. A series of truncations and deletions of GP-1 and GP-2 revealed alterations in the kinetics of GP-1 release, as well as a potential GP-1 chaperone function for GP-2. This model suggests that the proteolytic maturation and glycosylation profile of GP-2 are contingent upon association with GP-1 through the latter half of the secretory pathway, as expression of GP-2 alone resulted in a protein that was inefficiently expressed, had a heterogeneous glycosylation pattern, and was transported poorly (Luis M. Branco et al., 2010; Illick et al., 2008). Further, the shed GP-1 (sGP) was shown to move independently of the GP2-SSP complex after cleavage (Burri et al., 2013). Contradictory studies examining JUNV entry found GP-1 to retain the GP complex in a mechanism involving stabilization by SSP of the intact GP1-GP2 complex (York et al., 2008). As such, alternative functions may be different between OW and NW GP-1 subunits. Interestingly, secreted or shed LASV GP-1 has been reported to

contain distinct glycosylation patterns (Branco & Garry, 2009) based on binding to the mannose specific lectin *Galanthus nivalis agglutinin* (Van Damme, Allen, & Peumans, 1987). Whether or not LASV GP-1 shedding outside of the late endosome has a functional role *in vivo* is yet to be determined. Analysis of serum from very early time points of suspected LF patients did, interestingly, provide initial evidence for the presence of sGP prior to synthesis of whole virus in-vivo (L. M. Branco et al., 2010).

A recent study also suggested that LASV GP is capable of forming virus like particles (VLPs) independent of the matrix protein. Further, the GP in these studies, when co-expressed with the remaining structural proteins, directed the assembly and release of VLPs from the apical surface of a polarized epithelial cell line (Schlie, Maisa, et al., 2010). The solitary expression of Z exhibited a bipolar release of VLPs, suggesting that GP may play a crucial role in setting the appropriate time and place for budding of infectious virus to occur (Schlie, Maisa, et al., 2010).

1.10.6.1. GP-1 receptor binding domain

Arenavirus GP-1 structural features have been characterized both by electron microscopy (Burns & Buchmeier, 1993; Neuman et al., 2005) and more recently by x-ray crystallography either in isolation (Bowden et al., 2009) or with one of its cognate surface receptors (TfR1) (Abraham et al., 2010). Despite the sequence heterogeneity amongst GP-1 subunits, inherent in the receptor binding differences, the core architecture is thought to remain similar (Bonhomme et al., 2013). The globular domain, seen by EM in a cup-like arrangement in both OW and NW GPs, has a similar concave

arrangement made up of a series of beta-sheets stretching 6-7 nm across. The entire spike is thought to be composed of three GP1/GP2 heterodimers (Neuman et al., 2005).

1.10.6.2. OW arenavirus receptor interactions

The receptor utilized by OW arenaviruses, in particular LASV and LCMV, was of great interest to virologists, yet its identification remained elusive for a number of years. Borrow et al., using an enzymatic process of surface molecule elimination (e.g. protease, lipase, glycosylase), narrowed the search down to a glycosylated proteinaceous surface molecule (Oldstone, 1992). In a seminal study by Cao et al. using the virus overlay protein blot Assay (VOPBA), the alpha-dystroglycan molecule was found to be an obligate receptor for several species of OW arenaviruses including several strains of LCMV, as well as LASV, and MOBV, and surprisingly, the NW clade C arenavirus OLIV (Cao et al., 1998). The additional NW arenavirus LATV from clade C was also found to use α-DG using a similar VOPBA approach (Spiropoulou, Kunz, Rollin, Campbell, & Oldstone, 2002).

The dystroglycan complex is synthesized as a precursor molecule that is processed into mature α and β proteins. The complex is involved in connecting extracellular matrix proteins (laminin, agrin, perlecan, and neurexins) to the actin cytoskeletal elements within cells. α-DG is the soluble extracellular protein of the complex that is non-covalently associated with the transmembrane β-DG protein (Barresi & Campbell, 2006). The β-DG molecule was found to be dispensable for arenavirus binding and entry, as replacement of the β-DG protein via fusion of α-DG to the TM domain of PDGF receptor still facilitated entry (Kunz, Campbell, & Oldstone, 2003).

Interestingly, the region of α-DG that binds arenavirus glycoproteins overlaps with that of its cellular ligands (Kunz et al., 2001). As such, it has been demonstrated that arenavirus binding can displace the cellular ligands (e.g. laminin). This phenomenon is hypothesized to dysregulate cellular junctions, which could contribute to viral pathogenesis, particularly of the endothelium (Oldstone & Campbell, 2011).

In follow-up studies, strains of LCMV were identified with little or no binding activity to α-DG. These strain-specific GP alterations were found to have implications in the tropism and disease outcome when introduced to mice. The GP changes have been minimally mapped to the F260L mutation (Kunz et al., 2001; Smelt et al., 2001; Sullivan et al., 2011) and S153F (Sevilla et al., 2000; Teng et al., 1996). These findings were further corroborated by another study characterizing α-DG-independent entry of different strains of LCMV which strongly suggested the use of alternate receptors (Kunz, Sevilla, Rojek, & Oldstone, 2004). It is likely that additional viral and host factors contribute to both tropism and pathogenesis as viruses with markedly different disease potential in humans have been demonstrated to utilize α-DG.

In support of the notion that arenaviruses can utilize alternative receptors or co-receptors to gain access to cells (Reignier et al., 2006), in a recent study utilizing cDNA libraries derived from Vero, *Cercopithecus aethiops,* and human liver cells were transduced into immortalized T lymphocytes, which are refractory to infection under normal conditions, and were later screened for entry of LASV and LCMV GP psuedotypes (Shimojima & Kawaoka, 2012; Shimojima et al., 2011). The authors identified four additional proteins that could facilitate α-DG independent entry of authentic LASV including liver and lymph node sinusoidal endothelial calcium

dependent lectin (LSECtin), Axl, Dendritic cell-specific intercellular adhesion molecule-3-grabbing non-integrin (DC-SIGN), and Tyro3 (Shimojima et al., 2011). In contrast to the *in vitro* demonstration of enhanced entry of LCMV GP psuedovirus, another study found that the TAM receptor Axl failed to influence LCMV infection in Axl-deficient mice (Sullivan, Welch, Lemke, & Oldstone, 2013). LASV usage of DC-SIGN was confirmed in an additional study using chimeric LCMV bearing LASV GP and authentic LASV virions. In these studies entry was found to be critically dependent upon the mannose rich GP1 ectodomain. Accordingly, use of free mannan or chelators could specifically block binding to DC-SIGN, but not α-DG (Goncalves et al., 2013). Interestingly, DC-SIGN-mediated entry was found to be dependent upon the actin cytoskeleton, which contrasts with α-DG mediated entry (Goncalves et al., 2013).

The biosynthesis of α-DG itself is dysregulated during infection via a mechanism proposed to prevent super-infection (Rojek, Campbell, Oldstone, & Kunz, 2007). Key O-mannosylation events taking place within the Golgi involving the (LARGE) molecule, a putative glycosyltransferase involved in the O-mannosylation of the receptor, lead to a GP-dependent inhibition of this post-translational modification (PTM) event. This in turn disrupts the biological activity of α-DG without interfering with its surface presentation. The PTM of the receptor is required for both virus and ECM ligands to bind (Hara et al., 2011; Imperiali, Spörri, Hewitt, & Oxenius, 2008; Imperiali et al., 2005; Kunz et al., 2005; Rojek, Spiropoulou, Campbell, & Kunz, 2007). Interestingly, recent genomic surveys in Africa have identified SNPs within the LARGE gene [and also dystrophin (DMD), a β-DG interacting molecule] demonstrating evidence for positive selection

(Sabeti et al., 2007). It has been hypothesized that these polymorphisms may protect against LASV infection (Oldstone & Campbell, 2011).

1.10.6.3. NW arenavirus receptor interactions

The identity of a high affinity surface receptor for NW arenaviruses, like that of their OW counterparts, was of great interest to the arenavirus feild. Early attempts at deducing the nature of the receptor relied upon enzymatic digests of cell surface molecules and yielded a proteinaceus molecule that required glycosylation. However, studies by Rojek et al. using a broader range of glycosidases and mutant CHO cells deficient in GalNac and Gal, contested glycosylation requirements - albeit on a different cell type (Raiger Iustman, Candurra, & Mersich, 1995; Raiger Iustman et al., 1998; Rojek, Spiropoulou, & Kunz, 2006). In an elegant series of experiments by Rojek and colleagues, they determined that a common receptor was utilized by the South American HF arenaviruses, and that inactivated heterologous clade B virus competition was possible, albeit at high PFU/cell ratios. These data also suggested that the common receptor was also highly expressed and abundant on numerous cell types (Rojek et al., 2006). The human transferrin receptor 1 (hTfR1) was identified in 2007 by Radoshitzky and colleagues, using a recombinant MACV GP1 molecule fused to an immunoglobulin Fc probe, as being the cellular receptor for several pathogenic NW clade B arenaviruses (e.g. MACV, JUNV, GTOV, and SABV) (Radoshitzky et al., 2007). TfR1 is a receptor ubiquitously expressed across most tissues. It ferries transferrin bound in its holo (Fe^{3+}) bound form into cells via clathrin-dependent endocytosis, and has been suggested to deliver this cargo ultimately to the mitochondria, or to unload TF-Fe^{3+} in the acidic

environment while traversing late endosomes (Eckenroth, Steere, Chasteen, Everse, & Mason, 2011). Later genetic studies mapping the binding sites revealed an apical portion of the receptor that was distinct from its TF binding pocket. The ligation of TfR1 by arenavirus GPs, therefore, does not interfere with the normal function of this otherwise critical receptor involved in iron homeostasis (Demogines et al., 2013; Radoshitzky et al., 2007; Sheftel, Mason, & Ponka). The relationship between TfR1 and zoonotic viruses has, however, left its mark on the genome of not only the rodent reservoirs, but also the human genome. A seminal study published by Demogines et al. revealed ongoing positive codon selection in TfR1 genes across multiple mammals that correspond to sites of arenavirus GP contact (Demogines et al., 2013). Importantly, the authors also identified positive selection specifically within areas of GP1 that faced the receptor, rather than GP2, thereby, providing additional support to receptor-mediated, evolutionarily-induced, selective pressure (Demogines et al., 2013).

A number of studies have investigated non-TfR1 based entry in NW pathogenic arenaviruses (e.g. JUNV) (Cuevas, Lavanya, Wang, & Ross, 2011; Flanagan et al., 2008). Similar to OW arenavirus GPs, it was recently shown that both DC-SIGN and L-SIGN could facilitate the entry of JUNV pseudoparticles (Martinez et al., 2013). The authors propose that both DC-SIGN and L-SIGN are capable of binding to a terminal mannose residue on GP-1 (Martinez et al., 2013) (likewise in support of the data provided by Goncalves et al.). Accordingly, increasing concentrations of mannan were able to block entry of virus into cells. A growing number of viral envelope glycoproteins (e.g. human immunodeficiency virus (HIV), Dengue virus (DENV), severe acute respiratory

syndrome coronavirus (SARS CoV), influenza A viruses (FLUAV) and ebola virus (EBOV)) have been identified that are able to use these C-type lectins as attachment factors suggesting a common underlying mechanism of carbohydrate dependent capture (Han, Lohani, & Cho, 2007; Lin et al., 2003; Tassaneetrithep et al., 2003). This mechanism is dependent upon maintenance of a high mannose structure, as a complex N-linked structure is not recognized by these lectins.

Attachment to host cells by NW arenaviruses has also been demonstrated to occur via T-cell Immunoglobulin and Mucin-domain containing proteins (TIM1, 3, and 4) in a mechanism involving phosphatidyl serine (PS) present on the viral envelope (Jemielity et al., 2013). In support of this mechanism, studies have visualized the presence of PS on PICV infected cells as well as on the outer leaflet of virions (Soares, King, & Thorpe, 2008). Interestingly, a chimeric mouse/human monoclonal antibody recognizing PS via its high affinity binding plasma protein β2GP1 was demonstrated to have a protective effect in a guinea pig model of PICV infection.

1.10.7. GP-2

Synthesis of the arenavirus GP-2 subunit, as in GP-1 biogenesis, requires proteolysis via SP and S1P. GP-2 anchors the maturing glycoprotein complex to the host membrane via its transmembrane domain and maintains a non-covalent interaction with the peripheral GP-1 and SSP subunits, as it traverses the exocytic pathway to the plasma membrane and, ultimately, to the extracellular space in the context of mature virions. Targeting, folding determinants, and pathogenicity factors have been genetically mapped

to the GP-2 subunit and to its core fusion machinery (Agnihothram et al., 2006; Eschli et al., 2006; Gallaher, DiSimone, & Buchmeier, 2001; York, Agnihothram, Romanowski, & Nunberg, 2005). As such, the arenavirus GP-2 subunit is a class I viral fusion protein, based on homology prediction to other class I viral fusion proteins (Gallaher et al., 2001), which are responsible for acid-induced annealing of viral to endosomal membranes (Castilla, 1996; Castilla, Mersich, & Damonte, 1991; Di Simone & Buchmeier, 1995; Di Simone et al., 1994) that facilitate the injection of the viral genome into the cytoplasmic space (Borrow & Oldstone, 1994; Disimone & Buchmeier, 1993; Quirin et al., 2008).

1.10.7.1. GP-2 ectodomain (fusion domain)

The GP-2 subunit is arguably the most dynamic of the viral proteome. Its maturation and function requires a profound molecular arrangement beginning with an SSP-primed metastable arrangement and ending in the classical type I fusion protein 6 helix coiled-coil in the post-fusion state. Gallaher et al. using a bioinformatics approach, assigned LCMV and LASV GP to the family of class I fusion proteins based on heptad repeat regions predicted to form characteristic 6-helix bundles found in GP-2, similar to Ebola and influenza fusion proteins (Gallaher et al., 2001). The authors in the same study were able to generate peptides from the 2nd hydrophobic heptad region (aa 326-355) that were able to form helices in solution in support of the notion. Genetic studies of the fusion machinery within GP-2 of LASV, LCMV, and JUNV also identified the two adjacent N-terminal heptad repeats and their ability to form distinctive trimers (Eschli et al., 2006; Klewitz et al., 2007; York et al., 2005). A 4.1 Å crystal structure of GTOV

GP2 (Parsy et al., 2013) and a 1.8 Å structure of LCMV GP2 (Igonet et al., 2011) (aa312-438) have confirmed the presence of trimeric protomers which formed the post-fusion hairpin structure typical of the class. A unique feature of the arenavirus GP-2 fusion architecture is the presence of 2 N-terminal GP-2 fusion peptides (Glushakova, Lukashevich, & Baratova, 1990; Glushakova et al., 1992) that are normally covered by the globular GP1 head of the spike in a prefusion metastable state. The arenavirus fusion machinery is also unique in its requirement of the SSP to maintain the metastable form (described in 1.10.3). The fusion peptides lie at the N-terminus and are followed by the two antiparallel helices which fold together to form the coiled-coil hairpin structure, a thermodynamically favorable arrangement that is thought to facilitate the removal of water molecules between membrane leaflets prior to fusion pore formation (Nunberg & York, 2012; York et al., 2010).

1.10.7.2. GP-2 transmembrane domain (TMD)

A recent investigation of the attenuation process in a vaccine strain of Junín Virus, Candid1, (Albarino et al., 1997; Ghiringhelli, Riverapomar, Lozano, Grau, & Romanowski, 1991; Pablo Daniel Ghiringhelli, 1997; Scolaro et al., 1990) which varies from its parental virulent strain by a total of 13 residues, revealed a single substitution in the transmembrane domain (F427I) of GP-2 to be responsible for the severely attenuated phenotype of the vaccine in mice (Albarino, Bird, Chakrabarti, Dodd, Flint, et al., 2011). The authors utilized a reverse genetics strategy to generate viruses representing the unique attenuation mutations and found the F426I mutation to be solely responsible for the decreased virulence. The same mutation when placed in the LASV GPC utilizing an

HIV psuedotyping system, displayed reduced infectivity *in vitro*, supporting a novel and critical role of the arenavirus GP-2 TMD in the viral lifecycle.

In a recent report the I427 residue of Candid1 GP-2 was also demonstrated to confer the ability of neutral pH-induced cell-cell fusion (Droniou-Bonzom et al., 2011).The authors proposed a model by which this change from the parental virulent virus alters the metastable arrangement of the prefusion complex, allowing for premature conformational rearrangement required for fusion, and thereby contributing to the decreased infectivity in their assays (Droniou-Bonzom et al., 2011).

1.10.7.3. GP-2 carboxy-terminal domain (CTD)

The carboxy terminal domain (CTD) of Junín Virus GP-2 was recently reported to contain a series of 6 cysteine and histidine residues conserved across both Old and New world Arenaviruses (York & Nunberg, 2007b). Residues H447, H449, C455, H459, C467, and C469 similar to those required to form zinc fingers were found to bind Zn^{2+} with a kD of 1nM. Mutation of these residues abolished the interaction of the SSP with the GP1/GP2 complex in *trans*-complementation assays and inhibited the proteolytic maturation of the complex as well as the membrane fusion activity of GPC (York & Nunberg, 2007b). A structure of the ZBD was recently determined using NMR spectroscopy of residues 445-485 of the Junín Virus GP-2 CTD which confirmed the presence of the ZBD and highlighted the necessity of the conserved H and C residues in coordinating 2 Zn^{2+} ions within a novel fold (Briknarova, Thomas, York, & Nunberg, 2010). The authors propose a model where the 2 Zn^{2+} molecules are responsible for bridging with the conserved C57 residue on the SSP thereby stabilizing the complex. It

remains to be determined if this structure is indeed a requisite of GP-2 SSP association across other Old and New World arenaviruses.

Involvement of the GP-2 CTD of both LASV (Schlie, Strecker, et al., 2010) and LCMV (Stefan Kunz et al., 2003), however, have been demonstrated to be involved in determining the cleavage state of the GPC. The studies support a model where specific residues located within the CTD of GP-2 are responsible for stabilizing the conformation of the glycoprotein in a permissive state for cleavage by SKI/S1P. Differences have been demonstrated in the utility of the CTD between OW and NW arenaviruses. Specifically, mutations of conserved residues spanning 463-491 were shown to inhibit cleavage of LASV (Schlie, Strecker, et al., 2010) and LCMV GPC (Stefan Kunz et al., 2003), whereas mutations in the JUNV GP-2 CTD (Agnihothram et al., 2006) were permissive for cleavage. Several explanations may account for these differences. The use of a C-terminal epitope tag may have altered the native ultrastructural conformation of the recombinant JUNV GP-2 used, or the sensitivity at which the protein could be detected in the assays used. Alternatively NW arenaviruses may have evolved independent functions for the CTD in maintaining the stability of the glycoprotein complex. The inability of the CTD mutants to facilitate fusion, however, supports the hypothesis that cytoplasmic residues can signal through the transmembrane domain and modulate features of the viral life cycle.

1.11. Determinants of entry

Entry of arenaviruses involves a growing number of recognized receptors and surface molecules mentioned in the previous sections (hTfR1, α-DG, Axl, Tyro3, DC-SIGN, L-SIGN, LsECTIN, and TIM family proteins) and their ability to interact with the virion embedded glycoproteins. A number of other protein and lipid cellular factors have also been described that contribute to the entry events. Early work to describe arenavirus entry featuring the prototype LCMV observed its uptake into cells, by EM, via smooth-walled and clathrin independent vesicles that were internalized via a process insensitive to cytochalasin disrupted actin filaments (Borrow & Oldstone, 1994). These entities have been described more thoroughly in the intervening years through use of specific endosomal markers. The fusion cascade for both OW and NW arenaviruses is known to be inhibited via the addition of lysomotropic agents such as ammonium chloride, which prevents the acidification of the maturing endosomes (Castilla et al., 1991; Lukashevich, 1989). The ammonium chloride block for JUNV could be overcome if the media was buffered to low pH, suggesting that under these circumstances fusion could take place at the plasma membrane (Castilla, Mersich, Candurra, & Damonte, 1994).

1.11.1. Clathrin, caveolin, and cholesterol

The entry mechanisms between OW and NW arenaviruses are divergent, which is consistent with the biological properties of their cognate receptors. The high affinity receptor for most OW arenaviruses, α-DG, currently has no known endocytic mechanism. JUNV and consequently TfR1 enter into cells via clathrin mediated endocytosis (CME) (Martinez, Cordo, & Candurra, 2007). Accordingly, drugs that inhibit clathrin coated pit (CCP) formation on the plasma membrane inhibited JUNV and TCRV particle entry into

clathrin coated vesicles. The authors did note, however, that at high MOI an alternate route of entry occurred that was sensitive to nystatin, a cholesterol sequestering drug (Martinez et al., 2007). A similar finding was observed in studies of α-DG-dependent LCMV entry using MOIs ranging from 10-100 (Shah, Peng, & Carbonetto, 2006). The authors also concluded that α-DG is not associated with DRMs, but remained sensitive to agents capable of perturbing cholesterol at the plasma membrane (Shah et al., 2006). Shah et al. also demonstrated that movement of the DG complex to cholesterol rich fractions was not observed following DG ligation by LCMV, indicating that post-receptor ligation trafficking to DRMs was likely not taking place. The authors posited that cholesterol could be involved in coordinating signaling events proceeding ligation, prior to entry (Shah et al., 2006).

Vela et al. provided additional data supporting the role of cholesterol in arenavirus entry by demonstrating that both PICV and LASV entry was diminished in the presence of MβCD pretreatment (Vela, Zhang, Colpitts, Davey, & Aronson, 2007). Interestingly, the authors also observed an effect when MβCD was added to cells 10 minutes after addition of virus, suggesting the defect, though occurring early, may also occur post-attachment. The exact influence of non-raft cholesterol in arenavirus entry remains unknown. Vela et al. also demonstrated that entry of both LASV and PICV pseudoviruses occurred independent of caveolae, highlighting independence from the endocytic route involving lipid rafts. Following expression of a dominant negative EGFR pathway substrate clone 15 (Eps15) GFP fusion protein, a critical component involved in clathrin-coated pit assembly, the authors observed a defect in entry of both PICV and LASV

pseudovirus, suggesting use of a clathrin-dependent endocytic route (Vela et al., 2007). These data also suggest that entry pathways may differ greatly between LCMV and LASV (i.e. clathrin-independent vs clathrin-dependent endocytosis). Rojek et al. refined the entry model for LCMV to include one that utilized non-raft cholesterol, specifically not for attachment, but rather for the internalization of virus using a thiol-sensitive biotinylated virus uptake assay (Rojek, Perez, & Kunz, 2008). The authors also tested the cellular requirements of LCMV entry pathways: caveolae-dependent via expression of a caveolin-1 dominant negative mutant cav-1Y14F, siRNA against CAV1, and cell lines naturally lacking cav1 and 2, the GTPase dynamin I and II dominant negative mutants (blocks both clathrin and caveolin-mediated entry), and the DN Eps15Δ95/295 (able to block CCP formation), and found entry of LCMV to be independent of both caveolae and clathrin-dependent entry pathways (Rojek, Perez, et al., 2008).

Several studies have thus demonstrated a discreet role for cholesterol in the internalization and assembly of arenaviruses. In addition to the entry event it was recently determined that treatment of purified virions (native LASV particles or LASV GP pseudotyped VSV) with cholesterol also greatly restricted infectivity in a reversible manner (Schlie et al., 2009). The role of virion contained-cholesterol can be restricted, in part, to the incorporation of the glycoprotein into the envelope. The contribution of cholesterol in the post attachment of arenaviruses remains to be fully described.

1.11.2. Other factors

JUNV entry has been shown to require clathrin-mediated endocytosis (Martinez et al., 2007), in a process that also requires actin polymerization and microtubule dynamics. The OW pathogenic arenaviruses LCMV and LASV have been reported to use both clathrin-dependent (Vela et al., 2007) as well as clathrin-, caveolin-, dynamin-, and macropinocytosis/actin-independent pathways (Quirin et al., 2008; Rojek & Kunz, 2008). Differences in cell type and virus likely play a role in the emphasis of entry routes. To date, little information is known regarding the endocytic machinery and trafficking determinants. A study using rLCMV bearing the LASV GP (rLCMV-LASV GP) entry routes identified some influence of Rab5 but not Rab7 (following expression of DN mutants) suggesting an unusual mechanism of delivery to a late endosomal compartment that may bypass early endosomes (Rojek, Sanchez, Nguyen, de la Torre, & Kunz, 2008). This entry route is also independent of actin, but requires an intact microtubule network up to and including entry and post-fusion steps (Rojek, Sanchez, et al., 2008). Interestingly, the kinetics of entry for both LASV pseudovirus as well as authentic Candid1virions are very similar despite the differences in trafficking patterns and optimal fusion pH (4.5 vs 5.5) (Klewitz et al., 2007; York & Nunberg, 2006). Quirin et al. while monitoring Rab5- and Rab7-GFP fusion proteins during LCMV entry observed some colocalization of virus with both Rab5-positive and Rab7-positive (early and late) endosomes. However, expression of DN mutants of Rab5 and Rab7 caused little (20% Rab5) to no defect in replication. Following additional imaging of early and late endosomal markers in tandem with CME directed siRNA knockdown, the authors concluded that LCMV can use a CME dependent entry route through both early and late endosomes, however, the majority of incoming virus enters in a CME-independent route

that circumvents the early endosome (Quirin et al., 2008). This unusual route of entry was expanded upon by Pasqual et al., who demonstrated LCMV and rLCMV-LASVGP entry occurs through the multivesicular body (MVB) compartment en-route to late endosomes (Pasqual, Rojek, Masin, Chatton, & Kunz, 2011). Further, the authors demonstrated the activity of PI3K, involved in generating the PI3P lipid requirements of MVB, along with LBPA, a lipid concentrated during ILV morphogenesis, are critical factors in OW arenavirus entry, suggesting a crucial role for MVBs. RNAi knockdown of ESCRT complex 0- III proteins (e.g. Hrs, Tsg101 which is also involved in budding, Vps 22 & 24, and Alix) all restricted, in part, entry as well. The authors propose a model whereby incoming LCMV bypasses early endosomes, and transiently passes through the MVB utilizing the ESCRT network en-route to late endosomes; a process dependent upon the microtubule transport (Pasqual, Rojek, et al., 2011). The authors also posit a very clear and plausible benefit to this unusual route of entry where the incoming virus circumvents detection by Toll-like receptors found within early endosomes, which would coincide with the lacking early immune response to LCMV and LASV.

1.11.3. Polarization

The use of cell lines to study entry, however, often fails to take into account the 3-dimensional architecture and polarization requirements of the complex tissue that virus comes into contact with *in vivo*. As such, the distribution of OW and NW arenavirus receptors and their usage in terms of polarity have been a topic of debate. Functional studies of α-DG suggest a preferential accumulation of α-DG at the basolateral surface of cells, consistent with its role in organizing basement membranes. In contrast, other

studies have described a bipolar distribution of the OW receptor (Dylla, Michele, Campbell, & McCray, 2008). A recent study demonstrated that basolateral infection by LASV resulted in a substantial increase of virus uptake compared to apical infection in polarized Madine-Derby canine kidney (MDCK) cells (Schlie, Maisa, et al., 2010). This finding was confirmed using LCMV and JUNV applied to primary human epithelial cells (Dylla et al., 2008). This contradicts an earlier report for apically-dependent binding of JUNV by Cordo and colleagues (Cordo, Cesio y Acuna, & Candurra, 2005). The authors, however, noted that entry could occur in a non-polarized fashion suggesting perhaps diffusion of virus-receptor complexes following binding.

Despite discrepancies in the route of entry and release current models agree on a polarized entry and release of both OW and NW arenaviruses. Further investigation of the requirements for polarization *in vivo* will be required to substantiate these contradictory findings and reconcile them with observations of primary cellular targets initiating human infection including macrophages and dendritic cells.

1.12. Overview of endomembrane protein trafficking

Arenavirus glycoproteins need to traverse the highly dynamic endomembrane system present in eukaryotic cells. Our understanding of the processive maturation is limited to a few key parts. In order to discuss the proteomics blue-print laid out in this dissertation, and the influence of the ERGIC-53 cargo receptor complex, we must first discuss in more detail some of the basic and more elaborate factors governing protein folding, modification, and trafficking within the confines of the cell. The ability to selectively identify and traffic cargo within a cell, facilitates and underlies a dynamic necessity for

protein concentration within the membranous systems of eukaryotic cells. Specialized transport systems have facilitated the growth and divestment of compartmentalized faculties within cells that require a multitude of growth and survival signals as well as the ability to ascertain and respond to the repertoire of extracellular stimuli. Selectively transporting and maintaining proteins within the endomembrane system also allows for a dynamic and well-coordinated (usually) maturation of cargo destined for sites containing machinery involved in post-translational modifications that ensure the timing, folding, and function of the target molecules.

Protein folding and trafficking within the endomembrane system begins within the Endoplasmic Reticulum (ER) where both co- and post-translational modifications arise. In many cases asparagine-linked glycosylation consensus sites (NLS) (NxS/T) receive a covalent en-bloc addition of a 14 piece high-mannose oligosaccharide unit. This glycan moiety enters the molecule into the calreticulin-calnexin cycle, to ensure proper folding via recognition of hydrophobic patches, which are characteristic of misfolded proteins, utilizing a repeated addition and removal of a terminal glucose residue (Hammond, Braakman, & Helenius, 1994). Following correct folding and disulfide linkage, proteins are either transported further through the secretory pathway, retained within the ER or retrieved soon after exit (e.g. KDEL receptor retrieval) (Munro & Pelham, 1987; Pelham, 1988), or are shunted into an ER-assisted degradation pathway (ERAD) whereby proteins are reverse translocated and targeted for destruction via the proteasome (Wiertz et al., 1996). Approximately one-third of all mammalian proteins are synthesized into the ER and become glycosylated. Therefore, the complex interplay of chaperones, isomerases,

lectins, and glycosyltransferases ensures not only the primary folding, but the functional retention versus degradation or passage of massively complex molecules destined either for an intracellular membranous compartment, the plasma membrane, or the extracellular space (Fiedler & Simons, 1995).

Forward trafficking of proteins has been proposed to occur either via a non-specific bulk flow mechanism (Pfeffer & Rothman, 1987; Wieland, Gleason, Serafini, & Rothman, 1987) or one that requires specific intramolecular signals selectively recognized by transport receptors (Kelly, 1985; Palade, 1975). Transport receptors can assist in concentrating soluble cargo proteins within specialized exit domains of the ER termed ER exit sites (ERES) (Palade, 1975). Glycoproteins, if selected for anterograde movement, maintain a limited amount of primary information in the carbohydrate structure whilst in the ER. However, additional enzymes, concentrated within the Golgi cisterna, chemically and functionally elaborate the signature entrenched within the glycan structure (Helenius & Aebi, 2001; Reuter & Gabius, 1999). An outstanding question of cellular biologists' remains unanswered in regard to the glycosylation pathway: why does the cell build up a carbohydrate modification in the ER, only to tear it down and build anew later in the pathway (Hammond et al., 1994; Helenius & Aebi, 2001)? The energy devoted to creating and maintaining the glycosylome suggests a key and fundamental purpose that remains to be fully described.

1.12.1. Lectins

A key group of molecules involved in the biogenesis of cellular glycoproteins are the lectin family of proteins. Originally identified by plant biologists as early as 1888 (Lis & Sharon, 2007), this diverse class of typically non-enzymatic, carbohydrate binding molecules have provided cellular biologists, immunologists, and biochemists with powerful tools to purify, biochemically examine, and track the glycosylation profile of proteins inside and outside of the secretory pathway (Lis & Sharon, 2007). The abundance of cellular glycoproteins, as such, requires a complex array of lectins, and their specific activities. Intracellular lectins are thought to be intimately involved in decoding the glycosylated messages embedded within the changing structure of glycans within each membranous compartment. This class of proteins is evolutionarily conserved from archaea to mammals. Thus, the study of lectins has also facilitated the study of the co-evolution of carbohydrate structure and function (Reuter & Gabius, 1999).

1.12.1.1. Common structural features, nomenclature, and function

Lectins can be complex multi-domain proteins that function within a variety of environments including the secretory pathway, at the surface of cells, or in the extracellular space. Despite substantial heterogeneity via their modular domain structures, a single domain, the carbohydrate recognition domain (CRD) facilitates that sugar binding activity on most lectins. Accordingly, lectins can be characterized by the structural features of the CRD into a more discreet grouping (Varki, Etzler, Cummings, & Esko, 2009). Animal lectins are primarily segregated into C-type, Galectins, I-type, L-type, P-type, and R-type (Dodd & Drickamer, 2001). For the purposes of the dissertation C-type, Galectins, and L-type lectins will be briefly discussed. C-type lectins are a broad

superfamily of proteins, characterized initially by their requirement for calcium ions for binding to sugars. Functions of this superfamily include pathogen clearance, endocytosis, and cell adhesion. This superfamily includes collectins, endocytic receptors, selectins, as well as lymphocyte lectins (Varki et al., 2009). The first animal lectin discovered, hepatic asialoglycoprotein receptor, belongs to this grouping. C-type lectins have been increasingly demonstrated to be involved in host-pathogen interactions (i.e. DC-SIGN has been shown to facilitate entry of a number of enveloped RNA viruses). Galectins are commonly found to bind to beta galactosides, but have other known high and low affinity interactions. Though the most widely expressed group of lectins across organisms, very few Galectins have been found in humans with examples being Galectins 1 and 3. Their physiological roles are not well described, but are thought to be involved in basement membrane interactions (Cummings & Liu, 2009; Tellez-Sanz, Garcia-Fuentes, & Vargas-Berenguel, 2013). L-type, or leguminous, lectins were originally isolated from leguminous plant seeds, and were known for their hemagglutinating abilities via binding to cell surface glycans. Many lectins in this family contain a "jelly-roll" fold, however, this fold has been found across disparate primary sequences (e.g. Galectin-3) and species (e.g. the Rotavirus spike protein VP4) (Etzler, Surolia, & Cummings, 2009).

1.13. ERGIC-53 and the intermediate compartment

Outside of CRT and CNX, arguably the most well studied mammalian lectin is the Endoplasmic Reticulum Intermediate Compartment Protein of 53 kilo Daltons (ERGIC-53). The uninspiring name harbors a wealth of knowledge acquired by multiple generations of scientists probing the inner coming and goings of the secretory pathway. The protein is hypothesized to be an intracellular cargo receptor that facilitates the anterograde movement of a select subset of glycosylated cellular glycoproteins by binding to them via its, calcium-sensitive lectin function and coat protein interactions (see Figure 1.5). The protein is highly conserved across species from humans to yeast, and yet is paradoxically unessential (its loss in humans, though tolerated, is not without consequence). By studying its trafficking patterns and ligand selections, scientists have been able to synthesize a more comprehensive model of selective/receptor mediated protein trafficking within the early secretory pathway. Further, the loss of ERGIC-53 or its cofactor, multiple coagulation factor deficiency protein 2 (MCFD2), result in the Combined Deficiency of Factor V and Factor VIII (F5F8D), yet this happens without gross alteration of the machinery in the early secretory pathway. The majority of cellular glycoproteins cycle and are secreted normally, and other than the bleeding abnormalities, F5F8D patients live normal lives. Through the study of this biological conundrum,

Science has thus been advanced.

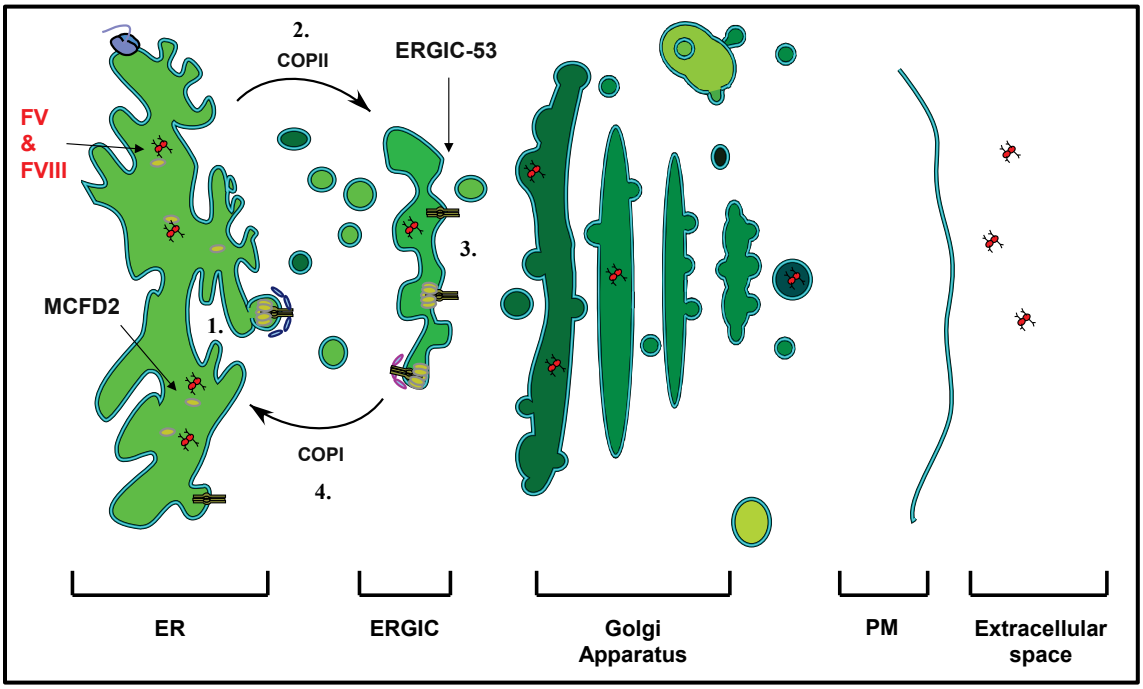

Figure 1.5 Recycling of ERGIC-53 in the early secretory pathway.

The early secretory pathway, comprised of the ER, ERGIC, and Golgi network provides the structural and biochemical cues for the cycling of ERGIC-53. Cargoes (depicted as FV & FVIII (red lumenal molecules)) are concentrated within specialized ER exit site (ERES) domains **(1)** with the help of the soluble, calcium-binding, cofactor MCFD2 (yellow lumenal molecule). Hexameric, cargo loaded ERGIC-53 (bown transmembrane molecule), via c-terminal FF – COPII (blue) interactions, and with the help of the sub-optimal TM length, is able to overcome the ER retention signal strength and traffic forward to the ERGIC (2). Fusion of ERGIC-53 positive carrier vesicles introduces the cargo receptor to an environment that is substantially lower in calcium concentrations, and subtly lower in pH (the green gradient represents changing chemical composition of the pathway). The composition of the ERGIC is hypothesized to act as the cue to dislodge calcium from the ERGIC-53 receptor complex, which reversibly attenuates its lectin activity and causes cargo release (3). COPI (purple) complexes assemble onto new ERGIC-53 sites via the dilysine (KK) c-terminal retrieval signal, and facilitate the Golgi-independent retrograde trafficking of the cargo receptor (4).

ERGIC-53 was identified by several independent groups via complimentary approaches. Schweizer and colleagues, following immunization of mice with material from enriched Golgi fractions of human Caco-2 cells, proceeded with the immunologic identification of an ~ 53 kDa protein and thus preceded its provenance as marker to a network of vesicular tubular clusters at the cis-face of the Golgi, to be later termed the ERGIC (Schweizer, Fransen, Bachi, Ginsel, & Hauri, 1988). The protein was biochemically characterized as a non-glycosylated integral membrane protein containing a short cytoplasmic tail, and found capable of forming long lasting dimers and hexamers (a half-life of several days is suggested). Saraste et al., using a similar approach in rat pancreatic cells, identified a protein of a similar nature dubbed p58 (Saraste, Palade, & Farquhar, 1987). Following its further genetic characterization, p58 was identified as the rat homologue of ERGIC-53 (Lahtinen, Hellman, Wernstedt, Saraste, & Pettersson, 1996). A third group identified a protein termed MR60 from a human promyelocytic cell line that bound a mannose column in a divalent cation-dependent fashion (Pimpaneau, Midoux, Monsigny, & Roche, 1991) that was also determined to be ERGIC-53 (Arar et al., 1995). In the intervening years, ERGIC-53 orthologues have been identified from a variety of species covering the spectrum from C. elegans to humans, suggesting a highly evolutionarily conserved protein (C. Appenzeller, H. Andersson, F. Kappeler, & H. P. Hauri, 1999a).

The ability to reproducibly isolate and identify this intermediate compartment via ERGIC-53 has since facilitated the biochemical investigation of its purpose (Schweizer, Matter, Ketcham, & Hauri, 1991). The identity of the intermediate compartment is

biochemically unique relative to the ER, ERES, and Golgi stacks. Alterations not only in protein content (Breuza et al., 2004; Klumperman et al., 1998a; Schweizer et al., 1991), but in lipid content (Ben-Tekaya, Kahn, & Hauri, 2010), and tonic qualities (e.g. ion concentrations and pH) have been identified (Paroutis, Touret, & Grinstein, 2004; Pezzati, Bossi, Podini, Meldolesi, & Grohovaz, 1997). Several hypotheses regarding the genesis and function of the compartment have been tested experimentally *in vivo*, as well as *in vitro* (e.g. maturation model versus stationary model) (Zeuschner et al., 2006). Schweizer and colleagues, using Vesicular stomatitis virus G (VSV G) as a marker along with a temperature shift characterized the ERGIC-53 compartment as an intracellular site where anterograde trafficking halts at 15° (e.g.15° compartment) (Schweizer et al., 1991). Upon rewarming, Klumperman and colleagues demonstrated that the ERGIC-53 positive structure was also involved in a Golgi-independent retrograde trafficking process to the ER (Klumperman et al., 1998a). The compartment has also been demonstrated to be a site of coat protein sorting. COPII anterograde moving vesicles ferrying cargo from ERES fuse with the adjacent ERGIC (Aridor, Bannykh, Rowe, & Balch, 1995), while COP I vesicles exit towards either ER (retrieval carrier vesicles) or towards the Golgi (Nickel & Brügger, 1999; Scales, Pepperkok, & Kreis, 1997). Live cell imaging studies using an ERGIC-53 GFP fusion protein highlighted the active qualities of the compartment. The GFP-ERGIC-53 positive structure, though highly dynamic, was indeed a stationary compartment (Ben-Tekaya, Miura, Pepperkok, & Hauri, 2005a) rather than one rapidly formed and decomposed, as had been formerly proposed (Scales et al., 1997). The localized movement of ERGIC-53 positive net-stationary (mobile-yet permanent) clusters and the anterograde and retrograde transporting vesicles were shown to be dependent

upon microtubules (Ben-Tekaya et al., 2005a) and (Cole, Sciaky, Marotta, Song, & Lippincott-Schwartz, 1996; Lippincott-Schwartz et al., 1990). The majority of ERGIC-53 is localized to the intermediate compartment. When it does escape the ER-ERGIC cycling, it is generally limited to the first cisterna of the Golgi (Klumperman et al., 1998a). The cycling of ERGIC-53 will be discussed more in detail in a later section (section 1.13.1.3).

1.13.1. ERGIC-53 the lectin: structural and biochemical features

ERGIC-53, along with its closely related resident Golgi homologues vesicular integral membrane protein of 36 kDa (VIP36), ERGIC-53-like (ERGL), and VIP-36-like (VIPL), is categorized as an L-type lectin based on homology of its CRD to leguminous lectins and to some extent mammalian galectins (Arar et al., 1995; Fiedler & Simons, 1994). The protein consists of approximately 510 amino acids in humans and consists of a signal sequence, a large lumenal segment subdivided into a CRD and helical region, a transmembrane domain, and a cytoplasmic tail (see figure 1.6).

1.13.1.1. ERGIC-53 CRD

ERGIC-53 contains a large, ER-lumenal CRD encompassing ~240 amino acids (31-285) which contain all the information necessary for, minimally, *in vitro* carbohydrate binding. Extensive structural and biochemical studies have determined: the residues involved in binding to carbohydrate ligands (Zheng et al., 2013), separate structures with (Velloso, Svensson, Pettersson, & Lindqvist, 2003b) and without (Velloso et al., 2003b) Ca^{2+}, and residues binding to the soluble EF-hand protein MCFD2 (Nishio et al., 2010;

Wigren, Bourhis, Kursula, Guy, & Lindqvist, 2010) . The CRD folds into a β-sandwhich, compromised of a concave and convex β-sheet (Velloso et al., 2003b). Removal of specific amino acids from β-peptides (e.g.Δβ2-4) (Zheng, Liu, Yuan, Zhou, & Zhang, 2010) or structurally distant Ca^{2+} binding residues (N156A and D181) (Zheng et al., 2013) are thought to create structural reformations causing collapse of the ligand binding site.

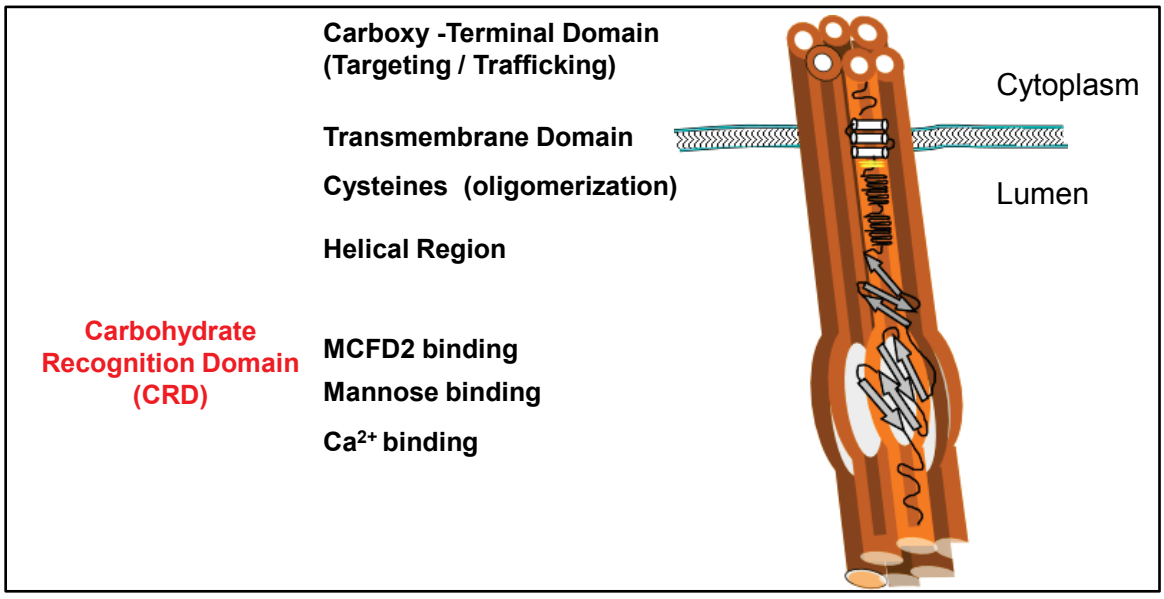

Figure 1.6 ERGIC-53 structural features.

This schematic depicts a hexameric ERGIC-53 molecule inserted into a membrane. The known functional regions are listed in the approximate areas (not drawn to scale). The N-terminus lies within the lumen of the ER/ERGIC and the C-terminus is exposed to the cytoplasm. The carbohydrate recognition domain (bulbous white central region) contains residues controlling binding to calcium, carbohydrates, and MCFD2. The helical stem is thought to be involved in oligomerization and peptide binding. Two oligomerization critical cysteins are depicted as yellow ovals. The transmembrane domain has also been suggested to be involved in trafficking via a mechanism involving a sub-optimal length.

Following extensive examinations of its sugar binding capabilities, it was determined to be a mannose specific lectin (*in vitro* binding) in the presence of calcium and at the

approximate pH of the ER (Itin, Roche, Monsigny, & Hauri, 1996), and was able to recognize the man8/9 structures when bound to calcium *in vivo* and *in vitro* (Itin et al., 1996; Kamiya et al., 2008; Moussalli et al., 1999a; Zheng et al., 2013). This feature is one that separates ERGIC-53 biochemically from VIP-36, which has been proposed to bind to mannose in a calcium-independent fashion (Hara-Kuge, Ohkura, Seko, & Yamashita, 1999; Kamiya et al., 2008), and from the yeast orthologues, of ERGIC-53, Emp46p, which utilizes K^+, and Emp47p binds carbohydrate independent of metal ion cofactors (Satoh et al., 2007). ERGIC-53's N-terminal (ER-lumenal) carbohydrate recognition domain contains conserved residues involved in sugar binding amongst other L- lectins. When these restudies are disrupted (e.g. N156A and D121 mutations) the sugar binding features are lost (Itin et al., 1996; Nyfeler, Michnick, & Hauri, 2005; Nyfeler, Reiterer, et al., 2008a; Zheng, Liu, Yuan, et al., 2010). Another feature of the unique CRD of ERGIC-53 is its broader specificity for high mannose carbohydrate structures relative to other L-type lectins, and its inability able to discriminate between glucosylated and deglucosylated forms of high-mannose *in vitro* (Kamiya et al., 2008).

The mannose binding capabilities (and structure) of ERGIC-53 were determined to be sensitive to not only calcium (Velloso et al., 2003b), but also to the pH of the environment (Appenzeller-Herzog, 2003). Binding of ERGIC-53 to mannose on a column was found to drop precipitously below the ER pH range (7-7.4). Further, by neutralizing the acidification of the ERGIC using chlorquine (albeit nonspecifically), the authors demonstrated impairment in the release of ERGIC-53 specific cargo in cells. The authors proposed a model by which ERGIC-53's lectin activity reversibly facilitates

cargo loading and unloading based on pH - potentiated calcium binding. Within the ER, at a neutral pH, the lectin activity is optimal and glycoprotein binding can occur. As ERGIC-53 reaches the ERGIC, a subtle drop in pH was proposed to cause a critical pH sensing histidine (His178) to become protonated and dislodge calcium from the lectin (Appenzeller-Herzog, 2003). Contradictory evidence has also been provided as to the role of pH in cargo loading and unloading. Zheng et al., via a crystallographic analysis of the CRD in complex with terminal high-mannose type mannans, proposed that His178, rather than functioning as a pH switch, directly engaged in polar interactions with the hydroxyls present on the carbohydrate (Zheng et al., 2013). Further, the authors could not find any evidence of pH regulation in binding of ERGIC-53's CRD to mannose, however, in contradiction to the studies by Appenzeller et al., who used a full length ERGIC-53, the latter study by Zheng and colleagues examined the CRD independently (Zheng et al., 2013).

ERGIC-53's method of recognizing cargo proteins was later extended when evidence was provided that illustrated that, in addition to the mannose requirement for binding cargo, a beta-hairpin peptide structure also contributed to ligand selection (Appenzeller-Herzog, Roche, Nufer, & Hauri, 2004). This composite glycan-peptide recognition motif suggested that ERGIC-53 was capable of adding an additional layer of selectivity in cargo transported from the ER that had not only been successfully trimmed by the CRT-CNX cycle, but also correctly folded such that its peptide conformation matches that of the ERGIC-53 pocket (Appenzeller-Herzog et al., 2004). However, the glucose trimming requirement for selection of cargo contradicts studies done on purified

CRD (Kamiya et al., 2008) and suggests that additional signals may be involved in binding.

1.13.1.2. ERGIC-53 stalk

The CRD is followed by a 210 residue helical-rich stalk that separates its lectin activity from the membrane and is able to form disulfide linked dimers and hexamers (Hauri, Kappeler, Andersson, & Appenzeller, 2000a; Schweizer et al., 1988). The stalk contains four predicted alpha-helices thought to form a coiled-coil (Lahtinen, Svensson, & Pettersson, 1999). Embedded within this helical region are four cysteine residues, two of which are critical (aa 466 and 475) in the formation of dimers and hexamers (C. Appenzeller et al., 1999a; Lahtinen et al., 1999; Zheng, Liu, Yuan, et al., 2010). Interestingly, in order to form a completely monomeric ERGIC-53 the two cysteines must be removed along with the helix region, suggesting some intramolecular peptide interactions also facilitate oligomerization (E. P. A. Neve, U. Lahtinen, & R. F. Pettersson, 2005; Zheng, Liu, Yuan, et al., 2010). Oligomerization has been proposed to be a requisite for anterograde trafficking (C. Appenzeller et al., 1999a; Lahtinen et al., 1999), and for binding to specific ligands (Carrière, Piller, Legrand, Monsigny, & Roche, 1999; Nufer, Kappeler, Guldbrandsen, & Hauri, 2003). A membrane proximal glutamine residue has also been proposed to play a role in ER-retention, although the exact mechanism by which it contributes has remained obscure (Kappeler, Klopfenstein, Foguet, Paccaud, & Hauri, 1997).

1.13.1.3. ERGIC-53 transmembrane domain, carboxy terminus, and transport

ERGIC-53, a type I transmembrane protein, encodes a short 18 residue membrane spanning domain (TM), that in cooperation with the short 12 amino acid C-terminal tail (CT), largely determines the subcellular trafficking of the protein . However, some lumenal residues have also been shown to contribute as well (Kappeler et al., 1997b) (Itin, Foguet, Kappeler, Klumperman, & Hauri, 1995; Itin, Schindler, & Hauri, 1995a). These features control ER retention, retrieval, as well as anterograde trafficking with the assistance of two coatomer proteins (COP I and COPII), as well as a network of microtubules, motor proteins (presumably), and a network of regulatory molecules that are still largely unknown (Haines et al., 2012; Itin, Schindler, et al., 1995a; Kappeler, Itin, Schindler, & Hauri, 1994a; Nufer et al., 2003; Schindler, Itin, Zerial, Lottspeich, & Hauri, 1993; E. J. Tisdale, H. Plutner, J. Matteson, & W. E. Balch, 1997). The length of the transmembrane domain, rather than its specific chemical identity, has been proposed to augment the efficiency of ER exit via a suboptimal-length based mechanism, and swapping of the TM with that of CD4 removes the retention signal completely (Felix Kappeler & Hauri, 1997; Itin, Foguet, et al., 1995).

The C-terminal tail of ERGIC-53 ends with a KKFF tetrapeptide that contains anterograde (FF) and retrograde (KK) signals (Andersson, Kappeler, & Hauri, 1999; E. J. Tisdale et al., 1997). The dilysine motif has been recognized as an ER-retention signal (Andersson et al., 1999) and interacts with COPI (Kappeler et al., 1997b; E. J. Tisdale et al., 1997). However, retention can be separated from binding to COPI (Andersson et al.,

1999). Mutating ERGIC-53's dilysine signal to SS, or removing the cytoplasmic tail completely, resulted in the exposure of the molecule on the surface of cells. Surprisingly, overexpression of the WT protein also resulted in surface exposure in a population of ~25% of the cells (Itin, Kappeler, Linstedt, & Hauri, 1995; Kappeler et al., 1994a). This was proposed to occur via saturation of the ER retention system (Kappeler et al., 1994a), but may also involve additional targeting mechanisms (Itin, Schindler, et al., 1995a). Surprisingly, the protein at the surface, when labeled with antibodies, was efficiently endocytosed in a process that utilized the C-terminal KKFF motif (Itin, Kappeler, et al., 1995; Kappeler et al., 1994a). Transfer of the KKFF containing C-terminal sequence to CD4 also facilitated its trafficking to the surface, whereas the dilysine motif followed by di-alanine (KKAA) is restricted to the ER, confirming that the dilysine motif acts not only in COPI-retrieval (Itin, Schindler, et al., 1995a), but also is involved in ER retention (Andersson et al., 1999). The retention was not a side effect *per se* of lacking an exit signal (FF), but rather, it is a bona-fide retention signal as proteins given a poly A tail were able to traffic forward, and cells making a temperature sensitive ε-COP also retained molecules bearing the KKAA signal (Andersson et al., 1999). A more recently proposed mechanism for ER-retention of ERGIC-53 involves its interaction with VIPL, which contains a double arginine retention signal (Nufer et al., 2003; Qin et al., 2012). Interestingly, an antibody against the C-terminus of ERGIC-53 was found to block coatomer exchange at the level of the ERGIC, concentrating the protein there via COPI retrieval blocking (E. J. Tisdale et al., 1997). A recent proteomics based study identified a number of cellular proteins bound specifically to the tail of ERGIC-53. The authors noted that UBDX, a p97 adaptor protein, formed a complex with p97/VCP (vasolin containing

protein), that they propose regulates tail binding proteins, and thus, recycling potential of the protein. Accordingly, they discovered that this complex was able to influence the post-ERGIC movement of ERGIC-53 to an area near the cell periphery (Haines et al., 2012) suggesting a complex and regulated post-ERGIC trafficking mechanism may exist.

The two C-terminal phenylalanines have been demonstrated to facilitate anterograde trafficking of ERGIC-53. *In vitro* binding studies demonstrated selective binding of these peptides to the Sec23p subunit of the COPII complex (Kappeler et al., 1997b), and that lack of this binding due to a KKAA mutation results in a blockage of anterograde movement of ERGIC-53. Expression of the KKAA construct restricted movement of the recombinant protein and the endogenous pool, and so acts in a dominant negative fashion. Accordingly, immunoprecipitation of recombinant KKAA ERGIC-53 via its myc tag enabled purification of endogenous ERGIC-53 and recombinant protein, suggesting heterodimer/heterohexamer complexes form (Kappeler et al., 1997b; Vollenweider, Kappeler, Itin, & Hauri, 1998a). Interestingly, during *in vitro* binding assays, the KKAA peptide bound more efficiently to coatomer proteins, which could provide an additional mechanism whereby it's trafficking is restricted to the ER (Kappeler et al., 1997b). It should be noted that restriction of ERGIC-53 to the ER did not disrupt the architecture or function of the secretory pathway, based on maintenance and location of fiducial protein markers of ER, and Golgi apparatus, and via analysis of glycoprotein secretion.

Given the connection between ERGIC-53 protein levels and its intracellular localization, a number of studies were focused on determining its genetic regulatory

mechanisms. Several ER stressors have been shown to upregulate ERGIC-53 either from a transcriptional level (e.g. induction of the ATF6 branch of the unfolded protein response via transcription factor binding to an ER stress response element (ERSRE)) (Nyfeler et al., 2003b; Renna, Caporaso, Bonatti, Kaufman, & Remondelli, 2007) or from a translational level (e.g. heat shock induction via a ribosomal shunting mechanism) (Spatuzza et al., 2004). Raising the temperature to 42° C redistributes ERGIC-53 to a more peripheral site (along with MCFD2). These latter studies failed to examine potential surface decoration of ERGIC-53 though, as was reported earlier following its enhanced expression. A phenotypic alteration has yet to be established under these circumstances of increased transcription or translation, outside of increases to the folding capacity of the ER during stress. Further, two proteomic reports have also identified ERGIC-53 within purified preparations of exosomes via a highly sensitive mass spectroscopy approach (Conde-Vancells et al., 2008; Gonzalez-Begne et al., 2009). The presence of the protein within extracellular vesicles has no currently ascribed function, and no current mechanism has been proposed to explain how ERGIC-53 is trafficked or targeted to sites of exosome formation.

1.13.2. ERGIC-53 the cargo receptor

The structural and biological features of ERGIC-53 led researchers initially to predict its role as a cargo receptor (Schweizer et al., 1988). The lumenal CRD, type I transmembrane feature of the protein, and the ability of its C-terminus to interact both with COPII and COPI proteins, fit the criteria for selection criteria for a cargo receptor. This class of proteins is able to connect soluble cargo proteins to COPI/II molecules and

to selectively move their cargo in the early secretory pathway (Hauri et al., 2000a; Mitrovic, Ben-Tekaya, Koegler, Gruenberg, & Hauri, 2008; Nyfeler et al., 2003b; Nyfeler, Reiterer, et al., 2008a; B. Nyfeler, B. Zhang, D. Ginsburg, R. J. Kaufman, & H. P. Hauri, 2006). Evidence to support this claim was substantiated by Vollenweider et al. when they noticed a specific deficiency of a 57 kDa secreted protein following the expression of ER-restricted ERIGC-53 mutant (KKAA). Isolation of the protein with the mannose-specific lectin ConA and tryptic sequencing led to the identification of the first soluble glycosylated ligand, cathepsin (CTSC), a lysosomal targeted protease, that required ERGIC-53 for its efficient export (Vollenweider et al., 1998a). In a related study Appenzeller and colleagues identified an additional cathepsin, Z, (CTSZ), that was also found to require the cargo receptor for its efficient transport (Appenzeller-Herzog, 2003; C. Appenzeller, H. Andersson, F. Kappeler, & H.-P. Hauri, 1999). Analysis of these cargoes illuminated the additional requirement for cargo containing a β-peptide along with the high-mannose glycan previously mentioned (Appenzeller-Herzog et al., 2004; C. Appenzeller et al., 1999a; Vollenweider et al., 1998a). Using a protein complementation assay (PCA) featuring a split YFP molecule, Nyfeler and colleagues identified an additional ligand alpha-1 antitrypsin (Nyfeler, Reiterer, et al., 2008a). Also using a similar PCA approach, Chen et al., identified Mac-2BP as another glycosylation-dependent ERGIC-53 cargo (Chen, Hojo, Matsumoto, & Yamamoto, 2013).

1.13.3. ERGIC-53 and F5F8D

Originally described in 1954 (Oeri, Matter, Isenschmid, Hauser, & Koller, 1954), Combined Factors V and VIII Deficiency is a type of mild hemophilia with specific

deficiencies in both antigen and activity of these two clotting factors. The disease manifests as deficits in the serum levels of coagulation factor V (FV) and VIII (FVIII) at approximately 5-30% of normal values. Inefficient secretion of these two protease cofactors causes a notable impairment in the activation of both thrombin and coagulation factor Xa (Camire & Bos, 2009; Spreafico & Peyvandi, 2008). The mild bleeding abnormalities can present as easy bruising, epistaxis, menorrhea, and gingival bleeding. Treatments are encouraged only as needed, and include fresh frozen plasma (FFP) and/or recombinant factor. Treatments are common following trauma such as dental extraction, child birth, and circumcision (Zhang, 2009).

The underlying genetic cause for this type of rare hemophilia remained a mystery for nearly five decades. Using a homozygosity mapping technique developed by Lander and Botsein to study genetic disorders in children born of consanguinity (Lander & Botstein, 1987), a flurry of rapid publications first by Nichols and colleagues, and later by Neerman-Abez and colleagues, narrowed the loci responsible for the disease to a region on chromosome 18 (Neerman-Arbez et al., 1997; Nichols et al., 1997). In a seminal study, Nichols et al., through the use of positional cloning, identified the locus responsible for causing the rare hemophilia (F5F8D omim 227300) to a region on the long arm of chromosome 18 containing the gene lectin mannose binding protein 1 (LMAN1), the gene encoding ERGIC-53 (Nichols et al., 1998).

The homozygous recessive syndrome was identified amongst Jews of Middle Eastern decent, and soon after additional affected families were identified in northern regions of Italy, Iran, and Pakistan (Neerman-Arbez et al., 1999). The disease is considered

extremely rare in the general population with incidence of ~ 1:1,000,000. Interestingly, in areas where consanguinity is commonplace, the incidence is approximately 1:100,000. In the intervening years since its initial discovery, multiple founder mutations have arisen suggesting a more widespread basis than was originally hypothesized (Sirachainan et al., 2005; Zhang, 2009; Zhang et al., 2006; Zhang et al., 2008; Zhang, Zhou, Yang, & Xiong, 2009). ERGIC-53 null populations have since been documented on most continents (Antarctica has thus far been excluded) (Spreafico & Peyvandi, 2008), and instances of compound heterozygousity leading to a clinical cases have also emerged (Farah et al., 2006; Ge et al., 2010; Patel, Liu, Lager, Malkovska, & Zhang, 2013). To date there are nearly 50 known disease causing mutations in the ERGIC-53 gene and over 500 polymorphisms have been recorded in NCBI.

Biochemical and cellular studies have focused on identifying the mechanism by which lack of ERGIC-53 contributes to F5F8D. In an elegant series of experiments, Mousalli and colleagues demonstrated that ERGIC-53 was acting as a cargo receptor required for the ER to Golgi trafficking of the clotting factors (Moussalli et al., 1999a). The authors provided evidence that the ER-ERGIC recycling of ERGIC-53, as well as the FV/FVIII N-linked glycans, were necessary for efficient secretion of the clotting factors (Moussalli et al., 1999a). Biochemical evidence supports a direct binding of ERGIC-53 to FVIII; however, FV binding has not been demonstrated in vitro (Cunningham MA, 2003). Zheng and colleagues recently described specific residues of ERGIC-53 (e.g. His178 and Gly 241/252) crucial for binding to FVIII (Zheng et al., 2013). The exact mechanism by which the ERGIC-53 cargo receptor complex facilitates the secretion of

FV and FVIII is currently unknown. The phenotypic impairment of FV/VIII secretion is not absolute following its loss, suggesting that either a redundant pathway exists, or that FV/FVIII may leak out via bulk flow (Moussalli et al., 1999a).

1.13.4. MCFD2 and F5F8D

Nearly five years after the discovery of the genetic basis for F5F8D, clinicians and scientists remained intrigued about the remaining 30% of F5F8D patients, whose ERGIC-53 gene remained normal. In 2003, a study by Zhang and colleagues brought to light the nature of the disease in the remaining population of F5F8D patients. The genetic abnormalities pointed to a gene on chromosome 2, and subsequently became known as multiple coagulation factor deficiency protein 2 (MCFD2) (Bin Zhang et al., 2003). MCFD2 encodes for a soluble 16 kDa protein found in the lumen of the ER that contains a disordered N terminal region, followed by 2 C-terminal EF-hands separated by a short linker region. These EF hands become ordered when calcium is bound, and subsequently disorder without the metal cation (Nishio et al., 2010).

MCFD2 forms a 1:1 calcium-dependent stoichiometric cargo receptor complex with ERGIC-53 (Bin Zhang et al., 2003; Zhang, Kaufman, & Ginsburg, 2005b). In addition to the biochemical interaction, interestingly, the genetic regulation of MCFD2 has been demonstrated to follow closely that of ERGIC-53 (e.g. both proteins are upregulated during stress) (Spatuzza et al., 2004). Genetic and structural studies have mapped the residues responsible for mediating the interaction to the first beta sheet in ERGIC-53 (residues 47-60), as well as multiple regions in MCFD2 (e.g. both EF-hands) (Wigren et

al., 2010; Zheng, Liu, Zhou, & Zhang, 2010), in addition to the C-terminal 3 residues (Nyfeler, Kamiya, et al., 2008). Missense mutations in MCFD2 causing F5F8D have been demonstrated to abolish its interaction specifically with ERGIC-53, a result that has been proposed to occur via gross alterations in the tertiary structure of the protein (Hamza et al., 2012). The interaction of MCFD2 and FV/FVIII occurs independently of ERGIC-53, as such, mutations affecting its binding to ERGIC-53 do not ablate its interaction with clotting factors (Zheng, Liu, Zhou, et al., 2010). The cargo receptor complex formed by MCFD2 and ERGIC-53 has thus far been demonstrated to be important only in the trafficking of FV and FVIII, as well as the more recently described Mac-2BP (Chen et al., 2013). Both cathepsins (C & Z) and α-1 antityrpsin are able to be ferried forward without the need for MCFD2 (B. Nyfeler et al., 2006).

1.13.4.1. MCFD2 outside of F5F8D

MCFD2 has recently been demonstrated by several groups to be a secretory protein (Liu et al., 2013; Toda et al., 2003). In addition to its role in recruiting and binding coagulation factors with ERGIC-53, it has been demonstrated to become O-glycosylated and secreted into the extracellular space (B. Nyfeler et al., 2006). The secreted protein has been found to have a phenotypic influence on the maintenance and differentiation of neuronal stem cells. It is currently unknown how MCFD2 is exerting this influence, and if sMCFD2 is indeed a physiological phenomenon, or an artefactual event resulting from overexpression in a tissue culture system. Nyfeler et al., following knockdown of ERGIC-53 noticed that the MCFD2 molecule was secreted, suggesting an ERGIC-53 retention of MCFD2 (B. Nyfeler et al., 2006). An outstanding question left

unanswered hinges upon this predicament. The answer will be of great interest to not only the study of receptor mediated transport (e.g. ERGIC-53:MCFD2 receptor biology), but also to elucidating signal transduction involved in maintenance of adult stem cells, and lastly, its potential role as a therapeutic agent for a variety of maladies (to be discussed within the confines of chapter 3).

1.13.5. Final remarks on the ERGIC-53 cargo receptor complex

The ERGIC-53 MCFD2 cargo receptor complex has been studied extensively *in vitro*, in cells, but to only a limited extent within a complex organism. A mouse LMAN1 knockout model yielded a partial recapitulation of human disease with plasma levels of FV and FVIII at approximately 50% of wt (Zhang et al., 2011). The authors of the study also noted alterations in liver accumulation of alpha-1 antitrypsin. Of the proteins found to bind to either ERGIC-53, MCFD2, or the ERGIC-53-MCFD2 complex, only the clotting factors have been demonstrated to be disrupted in people lacking either of these two functional proteins. A recent series of studies demonstrated that ERGIC-53 is involved in the efficient polymerization and secretion of IgM in concert with Erp44. However, the authors noted no overt immunological defects in F5F8D patients could be detected in their limited study. An additional manuscript by these authors on the topic is pending and will be of great interest to the community at large (Anelli et al., 2007; M. Cortini & R. Sitia, 2010).

2. THE INTRACELLULAR CARGO RECEPTOR ERGIC-53 IS REQUIRED FOR THE PRODUCTION OF INFECTIOUS ARENAVIRUS, CORNAVIRUS, AND FILOVIRUS PARTICLES

THE INTRACELLULAR CARGO RECEPTOR ERGIC-53 IS REQUIRED FOR THE PRODUCTION OF INFECTIOUS ARENAVIRUS, CORONAVIRUS, AND FILOVIRUS PARTICLES

Joseph Klaus[1,7], Philip Eisenhauer[1], Joanne Russo[1], Anne Mason[2], Danh Do[1], Benjamin King[1,7], Douglas Taatjes[3], Cromwell Cornillez-Ty[9], Jonathan E. Boyson[4], Markus Thali[6], Chunlei Zheng[10], Lujian Liao[8], John R. Yates III[9], Bin Zhang[10], Bryan A. Ballif[5] and Jason Botten[1,6,*]

[1]Department of Medicine, Division of Immunobiology

[2]Department of Biochemistry

[3]Department of Pathology

[4]Department of Surgery

[5]Department of Biology

[6]Department of Microbiology and Molecular Genetics

[7]Cellular and Molecular Biology Graduate Program

University of Vermont, Burlington, VT 05405, USA

[8]Shanghai Key Laboratory of Regulatory Biology, Institute of Biomedical Sciences and School of Life Sciences, East China Normal University, Shanghai 200241, China

[9]The Scripps Research Institute, La Jolla, CA 92037, USA

[10]Genomic Medicine Institute, Lerner Research Institute of Cleveland Clinic, Cleveland, OH 44195, USA

*Correspondence: jbotten@uvm.edu

Running Title: ERGIC-53 IS REQUIRED FOR VIRION INFECTIVITY

2.1. SUMMARY

Arenaviruses and hantaviruses cause severe and often fatal diseases in humans. Little is known regarding host proteins required for their propagation. We identified human proteins that interact with the glycoproteins (GPs) of a prototypic arenavirus and hantavirus and show that the lectin ERGIC-53 - a cargo receptor required for cellular glycoprotein trafficking within the early exocytic pathway - associates with arenavirus, hantavirus, coronavirus, orthomyxovirus, and filovirus GPs. ERGIC-53 binds to arenavirus GPs through a lectin-independent mechanism, traffics to arenavirus budding sites, and is incorporated into arenavirus particles. ERGIC-53 is required for arenavirus, coronavirus, and filovirus propagation; in its absence, GP-containing virus particles form, but are noninfectious due, in part, to their inability to attach to host cells. Thus, we have identified a class of pathogen-derived ERGIC-53 ligands, a lectin-independent basis for their association with ERGIC-53, and a role for ERGIC-53 in the propagation of several highly pathogenic RNA virus families.

2.2. HIGHLIGHTS

- Identification of host protein partners of arenavirus and hantavirus glycoproteins (GPs)
- ERGIC-53 associates with viral GPs via a lectin-independent mechanism
- ERGIC-53 is critical for arenavirus, coronavirus, and filovirus propagation
- ERGIC-53 is a virion component; in its absence virions form, but are noninfectious

2.3. INTRODUCTION

Arenaviruses and hantaviruses are rodent-borne, negative-sense RNA viruses that cause significant morbidity and mortality in humans (Buchmeier et al., 2007; Schmaljohn and Nichol, 2007). Most pathogenic arenaviruses are associated with severe hemorrhagic fever syndromes in humans. Examples include the New World arenaviruses Junin virus (JUNV), Machupo virus (MACV), and Guanarito virus (GTOV), which are the etiologic agents of Argentine, Bolivian, and Venezuelan hemorrhagic fevers, respectively, as well as Lassa virus (LASV), an Old World arenavirus that causes Lassa Fever along the coast of West Africa (Buchmeier et al., 2007). Additionally, lymphocytic choriomeningitis virus (LCMV) can cause aseptic meningitis in immunocompetent individuals and is a potent teratogen (Buchmeier et al., 2007). LCMV and Dandenong virus (DANV), an LCMV-like virus, are also responsible for a nearly uniform lethality in immunosuppressed recipients of virus-infected tissues (Fischer et al., 2006; Palacios et al., 2008). Hantaviruses cause two human illnesses: hemorrhagic fever with renal syndrome in the Old World and hantavirus cardiopulmonary syndrome (HCPS) in the New World (Schmaljohn and Nichol, 2007). Sin Nombre virus (SNV) and Andes virus (ANDV) are the primary etiologic agents of HCPS in North and South America, respectively, and are associated with a fatality rate of 35 - 39% (da Rosa Elkhoury et al., 2012; MacNeil et al., 2011). U.S. Food and Drug Administration (FDA)-approved vaccines or effective antivirals do not currently exist for the prevention and/or therapeutic treatment of arenavirus or hantavirus disease.

Arenaviruses and hantaviruses each encode an envelope glycoprotein (GP) that decorates the surface of the virion and functions to mediate attachment and entry of virions into permissive host cells. Each GP is encoded as a precursor (GPC) that is proteolytically processed into mature subunits. The arenavirus GPC is post-translationally modified to yield a stable signal peptide (SSP) as well as GP1 and GP2 subunits (Lenz et al., 2001), whereas the hantavirus GPC is co-translationally processed into G1 and G2 subunits (Lober et al., 2001). In each case, the GP subunits form a mature GP complex (SSP-GP1-GP2 for arenaviruses; G1-G2 for hantaviruses) that facilitates receptor binding and entry (Buchmeier et al., 2007; Schmaljohn and Nichol, 2007).

Relatively little is known regarding interactions that arenavirus or hantavirus GPs have with host proteins or the importance of such interactions for viral replication and disease pathogenesis. Herein, we utilized a proteomics approach to comprehensively identify human proteins that interact with GPs encoded by a prototypic arenavirus or hantavirus. We show that the ER-Golgi intermediate compartment 53 kDa protein (ERGIC-53) - an intracellular cargo receptor that facilitates the anterograde transport of a limited number of glycoprotein ligands in the early exocytic pathway (Appenzeller et al., 1999) - has a conserved interaction with GPs encoded by multiple families of RNA viruses and is essential for the formation of infectious arenavirus, coronavirus, and filoviruses in a GP-specific manner. Our results suggest that loss of ERGIC-53 or its functionality leads to the formation of GP-containing virions that are defective in their ability to attach to permissive host cells.

2.4. RESULTS

2.4.1. Identification of Cellular Proteins that Associate with Arenavirus and Hantavirus GPs and Choice of ERGIC-53

To identify human proteins that associate with arenavirus and hantavirus GPs we used an approach that featured affinity purification (AP) of biotinylated viral proteins (LCMV GP to represent arenaviruses or ANDV GP for hantaviruses) in complex with host proteins followed by mass spectrometry to identify host protein partners as described in Figure S1A and the Extended Experimental Procedures. We identified a number of host proteins that associated with LCMV GP (n = 309), ANDV GP (n = 134), or both GPs (n = 51) (Figures 1A-C, S1B, and S1C; Tables S1A-C). As shown in Figure S1D and Table S1D, host proteins that associated with both GPs were enriched for processes involving the ER, protein folding, and vesicular transport. The LCMV GP-only partners were enriched for processes that included the ER, the proteosome, and nuclear import while the ANDV GP-only partners were enriched for protein translation and ribosome biogenesis. We were particularly interested in the subset of proteins that interacted with both GPs as they could serve as broad-spectrum antiviral targets. Of these, we chose ERGIC-53 for further study based upon several criteria. First, the ERGIC-53 - viral GP interaction is physiologically plausible (e.g. each protein traffics within the exocytic pathway; ERGIC-53 is a mannose-specific lectin (Itin et al., 1996) and the viral GPs are mannosylated (Schmaljohn et al., 1986; Wright et al., 1990). Second, based on its identification as a cargo receptor within the exocytic pathway (Appenzeller et al., 1999), we hypothesized

that ERGIC-53 could be required for GP maturation and therefore might be critical for viral propagation. Finally, ERGIC-53 is an attractive target because loss of this protein or its normal function is well tolerated both *in vitro* (Mitrovic et al., 2008; Nyfeler et al., 2006; Vollenweider et al., 1998) and *in vivo* (Khoriaty et al., 2012).

2.4.2. Confirmation that ERGIC-53 Has a Conserved Association with GPs Encoded by Multiple Pathogenic Arenaviruses and Hantaviruses

We next wished to determine whether ERGIC-53 could associate with additional GPs encoded by arenaviruses (LASV, MACV, JUNV strain XJ, JUNV strain Candid #1 (C#1), and Whitewater Arroyo virus (WWAV)) or hantaviruses (SNV). Each viral GP tested, when serving as bait, was able to co-precipitate ERGIC-53 (Figure 1D, 1F-H, S1E, and data not shown). Likewise, ERGIC-53 was able to co-precipitate each GP screened (Figures 1E, 1I-K, S1F-I, and data not shown). For the arenavirus GPs, only the full length GPC was co-precipitated as prey. A full length hantavirus GPC cannot be recovered as this protein is co-translationally cleaved into G1 and G2 subunits prior to synthesis of a full length GPC species (Lober et al., 2001). As shown in Figure 1L, we further verified the specificity of the ERGIC-53 - JUNV C#1 GP interaction by showing both proteins strongly colocalize within a structure that we putatively identify as the ERGIC; both proteins also preferentially concentrate in this structure.

2.4.3. ERGIC-53 Is Required for Arenavirus Propagation

We conducted a series of viral challenge studies to determine how various manipulations of ERGIC-53 might impact the ability of arenaviruses (JUNV C#1 or DANV) to release infectious progeny. Partial silencing of ERGIC-53 expression via siRNA transfection led to a considerable reduction in the release of infectious JUNV C#1 (24 hr pi, 39.6% decrease, $p = 0.03$; 48 hr pi, 64% decrease, $p = 0.02$; 72 hr, 51% decrease, $p = 0.01$) (Figures 2A and S2A) whereas increased expression of WT ERGIC-53 enhanced release of infectious JUNV C#1 (24 hr pi, 48% increase, $p = 0.025$; 48 hr pi, 68% increase, $p = 0.004$) (Figures 2B and S2B). Expression of an ER-restricted, dominant negative (DN) mutant of ERGIC-53 (Vollenweider et al., 1998) resulted in a pronounced reduction in the release of infectious JUNV C#1 (48 hr pi, 90.5% decrease, $p = 1.4 \times 10^{-8}$; 72 hr pi, 99.8% decrease, $p = 3.2 \times 10^{-4}$) (Figures 2C and S2C), DANV (95% reduction, $p = 0.003$) (Figures 2D and S2D), and LCMV strain Armstrong 53b (data not shown). These experiments clearly demonstrate that ERGIC-53 is required for the propagation of New World and Old World arenaviruses.

2.4.4. The Release of Infectious JUNV C#1 Is Restricted in Cell Lines Derived from ERGIC-53 Null Individuals

Humans with homozygous null mutations in *LMAN1* (lectin, mannose binding 1), the gene encoding ERGIC-53, have combined deficiency of factor (F)V and FVIII (F5F8D, OMIM 227300), a mild bleeding disorder characterized by reduced levels of circulating FV and FVIII (Nichols et al., 1998). We therefore conducted challenge studies featuring

B cells derived from *LMAN1*$^{+/+}$ (2829-D) and *LMAN1*$^{-/-}$ (CRC-78 and CRC-79) individuals. The two *LMAN1*$^{-/-}$ individuals, despite being from separate families (A2 and A12 in (Neerman-Arbez et al., 1999), encode an identical null mutation (c.822-1G>A splice site mutation) that abrogates expression of ERGIC-53. Significantly less infectious virus was released from each of the *LMAN1*$^{-/-}$ cell lines when compared to the *LMAN1*$^{+/+}$ control cells (96% and 97% decrease for CRC-78 and CRC-79, respectively; $p < 0.0001$ for each) (Figures 2E and S2E).

2.4.5. ERGIC-53's Influence on JUNV Replication Is Specific and Can Be Minimally Mapped to the JUNV GP

To determine the specificity of ERGIC-53's impact on arenavirus replication we employed a pseudotyping approach featuring vesicular stomatitis virus (VSV) strain ΔG, a recombinant VSV that does not encode its native glycoprotein (G) and accordingly cannot form infectious particles unless a suitable viral glycoprotein (e.g. VSV G or JUNV GP) is provided in *trans* (Whitt, 2010). There was no difference in the formation of infectious VSVΔG particles decorated with native VSV G between the WT and DN ERGIC-53 backgrounds (Figures 3A and S3A). This may be due to the fact that VSV G does not associate with ERGIC-53 in co-immunoprecipitation assays (Figures 3E and 3F). The formation of infectious VSVΔG decorated with JUNV XJ GP was significantly impaired in cells expressing DN ERGIC-53 compared to the WT ERGIC-53 cells (80% reduction; $p = 0.001$) (Figures 3B and S3B). These experiments demonstrate that ERGIC-53's impact on arenavirus propagation is specific and can be minimally restricted to the

GP itself. Importantly, the fact that ERGIC-53 does not associate with VSV G demonstrates the specificity of its interaction with arenavirus and hantavirus GPs.

2.4.6. ERGIC-53 Broadly Associates with Viral Class I Fusion Proteins and Is Required for the Propagation of Coronaviruses and Filoviruses.

We next screened for an association between ERGIC-53 and class I fusion GPs encoded by coronaviruses (the severe acute respiratory syndrome coronavirus (SARS CoV) spike protein (S)), orthomyxoviruses (the H1N1 influenza virus A/WSN/33 hemagglutinin protein (HA)), and filoviruses (the Ebola (EBOV) and Marburg virus (MARV) GPs). Each GP, when used as bait, was able co-precipitate ERGIC-53 (Figures 3G and 3I). Reciprocally, ERGIC-53 was able to co-precipitate the uncleaved, precursor GP from each virus (Figures 3H and 3J). The formation of infectious VSVΔG particles decorated with either the SARS CoV S or EBOV GP was significantly impaired in cells expressing DN ERGIC-53 compared to the WT ERGIC-53 cells (81% reduction, $p = 0.03$ for SARS CoV; 70% reduction, $p = 0.0002$ for EBOV) (Figures 3C, 3D, S3C, and S3D). In summary, ERGIC-53 has a conserved interaction with class I fusion GPs and is required for the propagation of coronaviruses and filoviruses in a GP-specific manner.

2.4.7. Trafficking of JUNV C#1 GP or hTfR1 to the Plasma Membrane Is Not Influenced by ERGIC-53

To determine how the loss of ERGIC-53 function impaired the formation of infectious arenavirus particles we first tested whether ERGIC-53 could be a *bona fide* cargo receptor required for the proper anterograde trafficking of JUNV GP (Appenzeller et al.,

1999). Cells expressing WT or DN ERGIC-53 were infected with JUNV C#1 and screened for surface expression of JUNV C#1 GP. Interestingly, GP surface staining was equivalent in both the WT and DN ERGIC-53 transfected cells in terms of the frequency of cells with GP expression (46% WT versus 47% DN) as well as the intensity of GP staining (median fluorescence intensity (MFI) 348 WT versus 363 DN) (Figure 4B). Confocal microscopy analysis revealed a similar result (Figure 4A). The DN ERGIC-53 had no impact on the ability of hTfR1 - the surface receptor required for GP-mediated JUNV entry into host cells (Radoshitzky et al., 2007) - to traffic to the cell surface (Figure S4). In summary, cells expressing DN ERGIC-53 have normal surface expression of hTfR1, manifest no defect in viral entry of WT JUNV C#1 particles, and display no defect for GP synthesis or its trafficking to the plasma membrane.

2.4.8. The DN ERGIC-53 Mutant Does Not Impair Proteolytic Processing of JUNV GPC or the Incorporation of GP Species into Virus-Like Particles (VLPs)

Cells expressing WT or DN ERGIC-53 were transfected with plasmids encoding the JUNV matrix protein, Z, and JUNV XJ GP to allow for VLP formation and release. Expression of DN ERGIC-53 did not impair the generation of GP2 from GPC in cells or the incorporation of GP2 into VLPs (Figure 4C).

2.4.9. Loss of ERGIC-53 Leads to the Formation of Virus Particles that Are Noninfectious

In Figures 2E and S2E we show that JUNV C#1 is impaired in its ability to release infectious progeny from *LMAN1*$^{-/-}$ cells. To determine whether this was due to i) a

general deficiency in JUNV particle release or ii) the release of defective particles, we concentrated virions from the supernatants of *LMAN1*$^{+/+}$ (2829-D) or *LMAN1*$^{-/-}$ (CRC-78) cells and screened them for infectious virus, viral genome, and viral structural proteins. We found no discernible difference in the quantity of viral proteins (GP1, nucleoprotein (NP), or Z) released from *LMAN1*$^{+/+}$ or *LMAN1*$^{-/-}$ cells (Figure 4D) despite a nearly 10-fold reduction in infectious virus titer from *LMAN1*$^{-/-}$ cells (Figure 4E). Additionally, the *LMAN1*$^{-/-}$-derived particles contained viral genomic RNA with a 6.4-fold higher ratio of genome to infectious virus compared to *LMAN1*$^{+/+}$ particles (Figure 4F). Lastly, the *LMAN1*$^{-/-}$ particles also exhibited a specific defect in attachment to host cells (52% reduction compared to *LMAN1*$^{+/+}$ particles) (Figure 4G). In summary, loss of ERGIC-53 expression does not impact the ability of JUNV to generate particles containing viral structural proteins or genome, but rather renders the particles themselves noninfectious due, in part, to a defect in their ability to attach to permissive host cells.

2.4.10. ERGIC-53 Traffics to Sites of JUNV Assembly and Is Incorporated into Virions

Based on our finding that ERGIC-53 was detectable in concentrated supernatant preparations from JUNV C#1-infected cells (Figure 4D) we hypothesized that ERGIC-53 might be packaged into viral particles. We first addressed whether ERGIC-53 trafficking was altered during infection by surface labeling cells with antibodies specific for JUNV C#1 GP and ERGIC-53. We observed discrete JUNV C#1 GP puncta of ~200 to 400 nm at the plasma membrane that we suggest are putative sites of viral assembly and budding

(Figure 5B). Strikingly, ERGIC-53 formed puncta of the same size, shape, and position as GP (Figure 5B). In contrast, ERGIC-53 was not detectable at the plasma membrane of uninfected cells (Figure 5B). This altered trafficking is specific as calreticulin (CRT), another Ca^{2+}-binding lectin of the exocytic pathway, did not similarly redistribute to the plasma membrane following infection (Figure 5C). The intracellular distribution of ERGIC-53 did not change between mock- or JUNV C#1-infected cells (Figure 5A). We next captured JUNV particles using an anti-GPC/GP1 antibody and found that ERGIC-53 was detectable in JUNV particles via Western blot (Figure 5D). ERGIC-53 also colocalized with JUNV NP in viral particles adhered onto cover slips (Figure S5). Thus, during arenavirus infection, ERGIC-53 traffics to sites of viral assembly and budding and is incorporated into virions.

2.4.11. The JUNV GP - ERGIC-53 Interaction Requires a Unique Region of ERGIC-53's Carbohydrate Recognition Domain (CRD) and Occurs Independently of ERGIC-53's Ability to Oligomerize, Traffic, or Bind Mannose, MCFD2, or Ca^{2+}

To determine the molecular basis for ERGIC-53's association with viral GPs, we screened a panel of ERGIC-53 mutants (described in detail in Figure S6 and in (Zheng et al., 2010)), for their ability to associate with the JUNV C#1 GP. As shown in Figure 6, of the 11 mutants screened, only the ΔCRD mutant displayed a defect in binding to JUNV C#1 GP. Interestingly, despite the requirement of the CRD for binding, the association of ERGIC-53 with JUNV C#1 GP does not appear to be lectin-mediated as mutations that disrupt ERGIC-53's ability to bind mannose (N156A, D181A, Δβ2, Δβ3, and Δβ4) do not

disrupt its interaction with JUNV C#1 GP. Likewise, the association does not appear to require Ca^{2+}-binding (N156A and D181A), oligomerization (ΔHM), the helix domain (ΔHelix) or the association of MCFD2 (Δβ1, Δβ2, Δβ3, Δβ4, and ΔHM). The ΔHM and DN ERGIC-53 (KKAA) results also suggest that trafficking beyond the ER is not required for the interaction. Finally, the ΔCRD, Δβ4, and ΔHelix results indicate that the GP-interacting domain on ERGIC-53 lies within the C-terminal 185 amino acids of the CRD (residues 84 - 269).

2.5. DISCUSSION

Arenaviruses and hantaviruses are significant human pathogens for which FDA-approved vaccines or effective antivirals do not exist. Their proteomes consist of only four proteins. While functional roles have been defined for each viral protein, their interactions with host proteins, and the importance of these interactions for viral replication and disease pathogenesis, remain largely unknown. In the current study we addressed this deficiency by providing a comprehensive viral GP - human protein interactome map using GPs encoded by a representative arenavirus and hantavirus. We identified ERGIC-53 as a potential antiviral target based upon its ability to associate with GPs encoded by several families of pathogenic RNA viruses and its clear role in the propagation of arenaviruses, coronaviruses, and filoviruses. We demonstrate that ERGIC-53 is not required for the formation of GP-containing arenavirus particles, but rather their infectiousness. We also show that ERGIC-53 traffics to sites of arenavirus

budding and is incorporated into virions. Finally, we provide insight into the molecular basis for the GP - ERGIC-53 interaction by showing that the C-terminal region of ERGIC-53's CRD is required for the interaction independent of ERGIC's ability to oligomerize, traffic, or bind mannose, MCFD2, or Ca^{2+}.

ERGIC-53 is a nonglycosylated, hexameric type I integral membrane protein that functions as a cargo receptor for soluble glycoproteins within the early exocytic pathway. Its lumenal domain contains a CRD with homology to leguminous lectins and mammalian galectins; it selectively binds to high mannose glycans in a pH- and Ca^{2+}-dependent manner (Appenzeller-Herzog et al., 2004; Appenzeller et al., 1999; Itin et al., 1996). Only five glycoproteins - FV and FVIII (Moussalli et al., 1999; Nichols et al., 1998), the cathepsins C and Z (Appenzeller et al., 1999; Vollenweider et al., 1998), and alpha-1 antitrypsin (Nyfeler et al., 2008) - have been shown to require ERGIC-53 for their efficient anterograde trafficking. Typically ERGIC-53 captures its cargo proteins in the ER via its lectin activity and releases them in the ERGIC, presumably due to the lower pH of this compartment (Appenzeller-Herzog et al., 2004; Appenzeller et al., 1999). In the case of FV and FVIII, MCFD2 is also required for trafficking of these proteins independent of ERGIC-53 (Zhang et al., 2003). Because ERGIC-53 and MCFD2 directly interact, it has been suggested that they form a mature cargo receptor required for efficient FV/FVIII trafficking (Nyfeler et al., 2006; Zhang et al., 2005). Importantly, while loss of ERGIC-53 expression or function impairs movement of its specific ligands, the overall architecture of the exocytic pathway is maintained and major glycoproteins still traffic normally (Mitrovic et al., 2008; Nyfeler et al., 2006; Vollenweider et al.,

1998). Indeed, humans with homozygous null mutations in ERGIC-53 or MCFD2, despite having F5F8D - a condition that features mild to moderate bleeding symptoms due to reduced levels of circulating FV/FVIII (~5 to 30% of normal) - are generally healthy and lead normal lives provided they receive FV/FVIII supplementation following trauma (Khoriaty et al., 2012). These observations clearly suggest that ERGIC-53 is dispensable in humans and therefore represents a viable antiviral target.

Our studies demonstrate that ERGIC-53 associates with a class of pathogen-derived ligands, specifically GPs encoded by arenaviruses, hantaviruses, coronaviruses, orthomyxoviruses, and filoviruses (Figures 1, 3G-J, S1E-I, and data not shown). We show that, with the exception of the hantavirus GPs, ERGIC-53 preferentially interacts with the uncleaved, precursor GP, but not the proteolytically processed GP subunits (Figures 1I-K, 3H, 3J, S1F-H, and data not shown). In the case of the arenaviruses, this finding strongly suggests that the interaction takes place in the ER and/or ERGIC, prior to proteolytic cleavage of GPC into GP1/GP2 by the SKI-1/SP1 protease, which is thought to occur in the Golgi (Lenz et al., 2001; Wright et al., 1990). Indeed, imaging of JUNV C#1-infected cells revealed that GP and ERGIC-53 both concentrate in the ERGIC (Figure 1L and 5A). It was recently reported that the HIV glycoprotein Env can also associate with ERGIC-53 (Jager et al., 2012).

Based on previous studies we initially hypothesized that the ERGIC-53 - GP interaction would be mediated by ERGIC-53's CRD binding to one or more high mannose glycans on the viral GPs. Our results demonstrate that while ERGIC-53's CRD is indeed critical for the interaction, its lectin- and Ca^{2+}-binding functions are completely

dispensable (Figures 6 and S6). Consistent with this claim, we also found the interaction to be unaffected by competition with free mannose, manipulation of Ca^{2+}, changes in pH (as low as 5.0), or deglycosylation of the JUNV or ANDV GP (data not shown). In summary, our studies reveal that the molecular basis for ERGIC-53's interaction with JUNV GP is different from any of its previously characterized partners; only the C-terminal region of ERGIC-53's CRD (residues 84 to 269) is critical for the interaction whereas ERGIC-53's ability to oligomerize, traffic, or bind mannose, Ca^{2+}, or MCFD2 are not.

Movement of ERGIC-53 within the exocytic pathway is controlled by at least three targeting determinants that work in concert with two types of vesicular coats (COPII and COPI) to mediate ER retention, ER exit, and retrieval from post-ER compartments (Hauri et al., 2000; Nufer et al., 2003). ERGIC-53 preferentially accumulates in the ERGIC and recycles between this compartment and the ER (Ben-Tekaya et al., 2005; Klumperman et al., 1998). Under normal conditions, ERGIC-53 does not appear to traffic beyond the *cis*-Golgi. However, following its overexpression via plasmid, ERGIC-53 can traffic to the plasma membrane, presumably due to saturation of COPI (Kappeler et al., 1994). JUNV C#1 infection induces a striking redistribution of a portion of the intracellular pool of ERGIC-53 to the plasma membrane, where it strongly colocalizes with GP at putative sites of viral assembly and budding (Figure 5B). Furthermore, ERGIC-53 is packaged into arenavirus particles (Figures 5D and S5), which may indicate that it is required for virion structure/function.

The mechanism by which ERGIC-53 traffics to the plasma membrane during JUNV C#1 infection is unclear, but one possibility is that ERGIC-53 expression increases during JUNV infection and that saturation of COPI allows ERGIC-53 to traffic, perhaps independent of its interaction with JUNV GP, beyond the ERGIC/*cis*-Golgi area to reach the plasma membrane. In support of this idea, infection with the related arenavirus LCMV triggers the activating transcription factor 6 (ATF6)-arm of the unfolded protein response (UPR) (Pasqual et al., 2011), which is known to increase ERGIC-53 expression (Nyfeler et al., 2003). Indeed, LCMV infection of nonhuman primates results in increased transcription of ERGIC-53 (Djavani et al., 2009). Alternatively, it is also possible that JUNV GP functions as a cargo receptor to facilitate the movement of ERGIC-53 beyond the ERGIC/*cis*-Golgi to sites of viral assembly and budding.

How does ERGIC-53 impact arenavirus replication? We initially hypothesized that ERGIC-53 was acting as a *bona fide* cargo receptor required for the anterograde movement of GP out of the ER and ultimately to the plasma membrane. This idea proved incorrect as expression of the ER-restricted, DN ERGIC-53 mutant had no impact on the ability of GP to reach the plasma membrane (Figures 4A and 4B). Likewise, there was no disruption of either the proteolytic processing of GPC into GP1/GP2 or ability of these GP species to be incorporated into VLPs (Figure 4C). Additionally, the DN ERGIC-53 mutant had no impact on the ability of WT JUNV C#1 particles to enter cells (Figures 4A and 4B) or on the level of expression of hTfR1 at the plasma membrane (Figure S4). To formally test whether ERGIC-53 is required for the release of viral particles, we challenged normal or ERGIC-53 null cell lines with JUNV C#1 and found similar

quantities of viral particles in the supernatants from each cell line (Figure 4D). However, despite equivalent particle release, the null cell-derived particles were ~10-fold less infectious (Figure 4E), demonstrating that ERGIC-53 is essential for the infectivity of JUNV C#1 particles. Therefore, in the absence of ERGIC-53, arenavirus particles are produced in normal quantities, but are defective in the early phase of replication. Our results suggest that this defect minimally exists at the level of virus attachment to the host cell (Figure 4G). It is possible that this defect may also impair other steps of viral entry such as endocytic uptake of particles into host cells and/or fusion and release of genome into the cytoplasm (see Figure 7 for our proposed model).

How does ERGIC-53 mechanistically impact the infectiousness of arenavirus particles? ERGIC-53 itself may be a critical structural component of the virion, perhaps by acting as a co-receptor required for virion attachment to host cells. Direct support for this idea is our finding that ERGIC-53 is a component of virions (Figures 5D and S5) and that virions lacking ERGIC-53 are defective (Figures 4D-G). Additionally, less infectious virus was produced in our challenge studies featuring the ER-restricted, DN ERGIC-53 mutant (Figures 2C, 2D, 3B, S2C, S2D, and S3B) or ERGIC-53 siRNA (Figures 2A and S2A). Conversely, overexpression of WT ERGIC-53 leads to increased trafficking of ERGIC-53 to the plasma membrane (Kappeler et al., 1994), which could lead to more ERGIC-53 being incorporated into particles and explain the increased release of infectious virus seen under these conditions (Figures 2B and S2B). Alternatively, ERGIC-53 could be required to traffic and/or recruit cellular proteins that are critically

required for virion structure and function or for the proper maturation of the arenavirus GP (e. g. glycan maturation or other posttranslational modifications).

The protein partners of arenavirus and hantavirus GPs identified in this study help advance our understanding of how these viruses interact with host cell machinery to facilitate GP biogenesis and other aspects of the viral lifecycle. As the GPs themselves are likely to be highly multifunctional due to the small size of their respective proteomes, the identified partners may also help elucidate additional functions for each GP. Each partner represents a candidate target for future antiviral screening. Indeed, four additional proteins identified in our study - stromal cell derived factor 4 (SDF4), archain 1 (ARCN1), coatomer protein complex, subunit alpha (COPA), and renin receptor (ATP6AP2) - were recently shown to be required for LCMV and VSV replication (Panda et al., 2011). These examples clearly highlight the feasibility and utility of using a proteomics-based approach to identify candidate antiviral targets.

In conclusion, ERGIC-53 represents a potential antiviral target because of its clearly demonstrated importance for the replication of pathogenic arenaviruses, coronaviruses, and filoviruses and the fact that loss of this protein or its function is well tolerated in humans (Khoriaty et al., 2012). Furthermore, in the case of the arenaviruses, targeting ERGIC-53 function with an antiviral could be expected to set up an ongoing immunizing therapy as defective, but presumably immunogenic, viral particles would be released during the course of treatment. While ERGIC-53 represents a potential broad-spectrum antiviral target for arenaviruses, coronaviruses, and filoviruses, it may also be required for additional human pathogens such as the New World hantaviruses,

orthomyxoviruses, or retroviruses based upon its conserved interaction with their GPs (Figures 1D, 1E, 3I, 3J, and S1I) (Jager et al., 2012) or for DNA viruses based on the finding that a murine gamma herpes virus was negatively impacted by silencing of ERGIC-53 (Mages et al., 2008). Based on our finding that JUNV propagation is impaired in cells from ERGIC-53 null individuals, future studies should also address whether exposure to rodent-borne viruses such as the arenaviruses has exerted a selective pressure to maintain ERGIC-53 mutations within the human population as a means to confer resistance to infection. Additionally, while bleeding is not a major cause of morbidity or mortality during arenavirus or hantavirus infection, it is also interesting to consider that viral GPs, by interacting with ERGIC-53, may disrupt ERGIC-53's normal cargo receptor function for FV and FVIII, contributing to some of the hemorrhagic manifestations seen following infection with these viruses, which can include deficiencies in the levels and/or activity of circulating FV or FVIII (Lee, 1987; Lee et al., 1989; Schwarz et al., 1972). The interaction of ERGIC-53 with the filovirus GPs is particularly intriguing considering the prominent coagulation abnormalities observed during human infection (Feldmann and Geisbert, 2011). Finally, our studies and others (Gonzalez-Begne et al., 2009) have shown that ERGIC-53 is actively secreted from cells in viral particles and/or cellular exosomes and strongly suggest that it has important roles outside of its normal distribution within the exocytic pathway, perhaps outside of the cell where, in the case of arenaviruses, coronaviruses, and filoviruses, it may influence the endocytic pathway-driven process of viral entry.

2.6. EXPERIMENTAL PROCEDURES

Cells, Viruses, Antibodies, Plasmids, siRNAs, and Transfections

A full description of the cells (HEK 293T cells, Vero E6 cells, and B lymphoblastoid cells from either normal or ERGIC-53 null individuals), viruses (DANV, JUNV C#1, and VSVΔG), antibodies, siRNAs, plasmids, and transfection procedures used can be found in the Extended Experimental Procedures.

Affinity Purification, Immunoprecipitation, Mass Spectrometry, Virus/VLP Concentration, and Western Blot

To affinity purify viral GPs for the identification of human protein partners via mass spectrometry or validation of protein partners via Western blot, HEK 293T cells were co-transfected with a plasmid that encodes each respective viral GP with a C-terminal HA epitope tag and a biotin acceptor peptide (BAP), and a second plasmid that encodes the bacterial biotin ligase BirA to facilitate biotinylation of the viral GPs. Two days later, biotinylated GPs and associated host proteins were affinity purified from whole cell lysates using magnetic streptavidin beads and separated on polyacrylamide gels for either Western blot analysis to confirm bait/prey purification or Coomassie staining for mass spectrometry analysis. To determine the identity of cellular proteins captured, each Coomassie-stained gel lane was cut into sections for in-gel, trypic digestion and mass spectrometry analysis.

Immunoprecipitation of viral GPs or ERGIC-53 was accomplished by incubating clarified whole cell protein lysates with antibodies specific for each respective protein followed by magnetic Protein G beads. To purify intact JUNV C#1 particles, supernatants were collected at 72 hr post-inoculation, clarified, and incubated with either an anti-GP antibody or an isotype control antibody followed by magnetic protein G beads. Immunopurified proteins or viral particles were then washed, eluted from beads, and electrophoresed on polyacrylamide gels for Western blot analysis.

JUNV C#1 virions and VLPs were concentrated via ultracentrifugation through a 20% layer of sucrose.

For Western blot analysis, protein lysates were separated by SDS-PAGE using Novex 4-20% Tris-Glycine polyacrylamide gels. Protein transfer to nitrocellulose membranes was accomplished using the iBlot Gel Transfer Device and iBlot Transfer Stack nitrocellulose membranes from Invitrogen (Carlsbad, CA). Proteins were detected using either chemiluminescence or an Odyssey Infrared Imaging System (LI-COR Biosciences, Lincoln, NE).

Full details of these approaches are described in the Extended Experimental Procedures.

Confocal Immunofluorescence Microscopy

A Zeiss LSM 510 Laser Scanning Confocal Microscope was used to visualize internal or surface expression of ERGIC-53, CRT, JUNV NP and/or JUNV GP in cells or virions. Colocalization analysis was done using the Zeiss AIM software package as described in the Extended Experimental Procedures.

Flow Cytometry

An LSRII (BD Biosciences, San Jose, CA) was used to enumerate the frequency and intensity of JUNV GP or hTfR1 staining at the plasma membrane or Myc-tagged WT and/or DN ERGIC-53 internally in HEK 293T cells as described in the Extended Experimental Procedures.

Viral Challenge Assays

Viral challenge assays were performed to evaluate how various manipulations of ERGIC-53 (siRNA silencing of ERGIC-53, overexpression of WT ERGIC-53, expression of DN ERGIC-53, or loss of ERGIC-53 expression due to null mutation of *LMAN1*) would influence the release of infectious JUNV C#1, DANV, or VSVΔG (pseudotyped with VSV G, JUNV XJ GP, SARS CoV S, or EBOV GP). At each time point examined in the various assays, supernatants and cells were collected (from each replicate well) to measure infectious virus or protein expression levels, respectively. Infectious virus load was determined via plaque assay for JUNV C#1 and DANV while GFP-positive foci

were enumerated via focus assay for VSVΔG; differences were determined using the unpaired Student's *t* test. Quantitative RT-PCR was used to determine copy number of JUNV C#1 S segment genomic viral RNAs. Virus attachment to cells was determined through a virus-cell binding assay. A full description of each challenge assay can be found in the Extended Experimental Procedures.

2.7. ACKNOWLEDGMENTS

We thank Ralph Budd, Sean Diehl, Chris Huston, Janet Lindow, Gary Ward, J. Lindsay Whitton, and the UVM Immunobiology group for insightful discussions and Jonathan Aiwazian, Nicole Bishop, Nicole Bouffard, Marie Lambelé, Nathan Roy, and Gian Samaritoni for technical assistance. We are grateful to Michael Buchmeier, Paula Cannon, James Cook, Juan Carlos de la Torre, Adolfo Garcia-Sastre, Sandra Goñi, Hans-Peter Hauri, Ian Lipkin, Megan Shaw, Robert Tesh, Michael Whitt, and BEI Resources for providing critical reagents as described in the Extended Experimental Procedures. We acknowledge NIH grants R21 AI088059 (JB), AI065359 (JB), P41 GM103533 (JRY), 1S10RR019246 (DT), T32 AI055402 (JK), 8P20GM103449 (BAB), and P20RR021905 (JB).

2.8. REFERENCES

Appenzeller-Herzog, C., Roche, A.C., Nufer, O., and Hauri, H.P. (2004). pH-induced conversion of the transport lectin ERGIC-53 triggers glycoprotein release. Journal of Biological Chemistry *279*, 12943-12950.

Appenzeller, C., Andersson, H., Kappeler, F., and Hauri, H.P. (1999). The lectin ERGIC-53 is a cargo transport receptor for glycoproteins. Nat Cell Biol *1*, 330-334.

Ben-Tekaya, H., Miura, K., Pepperkok, R., and Hauri, H.P. (2005). Live imaging of bidirectional traffic from the ERGIC. Journal of Cell Science *118*, 357-367.

Buchmeier, M.J., de la Torre, J.C., and Peters, C.J. (2007). *Arenaviridae*: The Viruses and Their Replication. In Fields Virology, D.M. Knipe, P.M. Howley, D.E. Griffin, R.A. Lamb, M.A. Martin, B. Roizman, and S.E. Straus, eds. (Philadelphia: Wolters Kluwer Health/Lippincott Williams & Wilkins), pp. 1791-1827.

da Rosa Elkhoury, M., da Silva Mendes, W., Waldman, E.A., Dias, J.P., Carmo, E.H., and Fernando da Costa Vasconcelos, P. (2012). Hantavirus pulmonary syndrome: prognostic factors for death in reported cases in Brazil. Transactions of the Royal Society of Tropical Medicine and Hygiene *106*, 298-302.

Djavani, M., Crasta, O.R., Zhang, Y., Zapata, J.C., Sobral, B., Lechner, M.G., Bryant, J., Davis, H., and Salvato, M.S. (2009). Gene expression in primate liver during viral hemorrhagic fever. Virol J *6*, 20.

Feldmann, H., and Geisbert, T.W. (2011). Ebola haemorrhagic fever. Lancet *377*, 849-862.

Fischer, S.A., Graham, M.B., Kuehnert, M.J., Kotton, C.N., Srinivasan, A., Marty, F.M., Comer, J.A., Guarner, J., Paddock, C.D., DeMeo, D.L.*, et al.* (2006). Transmission of lymphocytic choriomeningitis virus by organ transplantation. The New England journal of medicine *354*, 2235-2249.

Gonzalez-Begne, M., Lu, B., Han, X., Hagen, F.K., Hand, A.R., Melvin, J.E., and Yates, J.R. (2009). Proteomic analysis of human parotid gland exosomes by multidimensional protein identification technology (MudPIT). Journal of proteome research *8*, 1304-1314.

Hauri, H.P., Kappeler, F., Andersson, H., and Appenzeller, C. (2000). ERGIC-53 and traffic in the secretory pathway. Journal of Cell Science *113 (Pt 4)*, 587-596.

Itin, C., Roche, A.C., Monsigny, M., and Hauri, H.P. (1996). ERGIC-53 is a functional mannose-selective and calcium-dependent human homologue of leguminous lectins. Molecular Biology of the Cell *7*, 483-493.

Jager, S., Cimermancic, P., Gulbahce, N., Johnson, J.R., McGovern, K.E., Clarke, S.C., Shales, M., Mercenne, G., Pache, L., Li, K.*, et al.* (2012). Global landscape of HIV-human protein complexes. Nature *481*, 365-370.

Kappeler, F., Itin, C., Schindler, R., and Hauri, H.P. (1994). A dual role for COOH-terminal lysine residues in pre-Golgi retention and endocytosis of ERGIC-53. Journal of Biological Chemistry *269*, 6279-6281.

Khoriaty, R., Vasievich, M.P., and Ginsburg, D. (2012). The COPII pathway and hematologic disease. Blood *120*, 31-38.

Klumperman, J., Schweizer, A., Clausen, H., Tang, B.L., Hong, W., Oorschot, V., and Hauri, H.P. (1998). The recycling pathway of protein ERGIC-53 and dynamics of the ER-Golgi intermediate compartment. Journal of Cell Science *111 (Pt 22)*, 3411-3425.
Lee, M. (1987). Coagulopathy in patients with hemorrhagic fever with renal syndrome. JKorean MedSci *2*, 201-211.
Lee, M., Kim, B.K., Kim, S., Park, S., Han, J.S., Kim, S.T., and Lee, J.S. (1989). Coagulopathy in hemorrhagic fever with renal syndrome (Korean hemorrhagic fever). Reviews of Infectious Diseases *11 Suppl 4*, S877-883.
Lenz, O., ter Meulen, J., Klenk, H.D., Seidah, N.G., and Garten, W. (2001). The Lassa virus glycoprotein precursor GP-C is proteolytically processed by subtilase SKI-1/S1P. Proc Natl Acad Sci U S A *98*, 12701-12705.
Lober, C., Anheier, B., Lindow, S., Klenk, H.D., and Feldmann, H. (2001). The Hantaan virus glycoprotein precursor is cleaved at the conserved pentapeptide WAASA. Virology *289*, 224-229.
MacNeil, A., Ksiazek, T.G., and Rollin, P.E. (2011). Hantavirus pulmonary syndrome, United States, 1993-2009. Emerging Infectious Diseases *17*, 1195-1201.
Mages, J., Freimuller, K., Lang, R., Hatzopoulos, A.K., Guggemoos, S., Koszinowski, U.H., and Adler, H. (2008). Proteins of the secretory pathway govern virus productivity during lytic gammaherpesvirus infection. Journal of cellular and molecular medicine *12*, 1974-1989.
Mitrovic, S., Ben-Tekaya, H., Koegler, E., Gruenberg, J., and Hauri, H.P. (2008). The cargo receptors Surf4, endoplasmic reticulum-Golgi intermediate compartment (ERGIC)-53, and p25 are required to maintain the architecture of ERGIC and Golgi. Molecular Biology of the Cell *19*, 1976-1990.
Moussalli, M., Pipe, S.W., Hauri, H.P., Nichols, W.C., Ginsburg, D., and Kaufman, R.J. (1999). Mannose-dependent endoplasmic reticulum (ER)-Golgi intermediate compartment-53-mediated ER to Golgi trafficking of coagulation factors V and VIII. Journal of Biological Chemistry *274*, 32539-32542.
Neerman-Arbez, M., Johnson, K.M., Morris, M.A., McVey, J.H., Peyvandi, F., Nichols, W.C., Ginsburg, D., Rossier, C., Antonarakis, S.E., and Tuddenham, E.G. (1999). Molecular analysis of the ERGIC-53 gene in 35 families with combined factor V-factor VIII deficiency. Blood *93*, 2253-2260.
Nichols, W.C., Seligsohn, U., Zivelin, A., Terry, V.H., Hertel, C.E., Wheatley, M.A., Moussalli, M.J., Hauri, H.P., Ciavarella, N., Kaufman, R.J*., et al.* (1998). Mutations in the ER-Golgi intermediate compartment protein ERGIC-53 cause combined deficiency of coagulation factors V and VIII. Cell *93*, 61-70.
Nufer, O., Kappeler, F., Guldbrandsen, S., and Hauri, H.P. (2003). ER export of ERGIC-53 is controlled by cooperation of targeting determinants in all three of its domains. Journal of Cell Science *116*, 4429-4440.
Nyfeler, B., Nufer, O., Matsui, T., Mori, K., and Hauri, H.P. (2003). The cargo receptor ERGIC-53 is a target of the unfolded protein response. Biochem Bioph Res Co *304*, 599-604.
Nyfeler, B., Reiterer, V., Wendeler, M.W., Stefan, E., Zhang, B., Michnick, S.W., and Hauri, H.P. (2008). Identification of ERGIC-53 as an intracellular transport receptor of alpha1-antitrypsin. Journal of Cell Biology *180*, 705-712.

Nyfeler, B., Zhang, B., Ginsburg, D., Kaufman, R.J., and Hauri, H.P. (2006). Cargo selectivity of the ERGIC-53/MCFD2 transport receptor complex. Traffic *7*, 1473-1481.
Palacios, G., Druce, J., Du, L., Tran, T., Birch, C., Briese, T., Conlan, S., Quan, P.L., Hui, J., Marshall, J.*, et al.* (2008). A new arenavirus in a cluster of fatal transplant-associated diseases. New England Journal of Medicine *358*, 991-998.
Panda, D., Das, A., Dinh, P.X., Subramaniam, S., Nayak, D., Barrows, N.J., Pearson, J.L., Thompson, J., Kelly, D.L., Ladunga, I.*, et al.* (2011). RNAi screening reveals requirement for host cell secretory pathway in infection by diverse families of negative-strand RNA viruses. Proceedings of the National Academy of Sciences of the United States of America *108*, 19036-19041.
Pasqual, G., Burri, D.J., Pasquato, A., de la Torre, J.C., and Kunz, S. (2011). Role of the host cell's unfolded protein response in arenavirus infection. Journal of Virology *85*, 1662-1670.
Radoshitzky, S.R., Abraham, J., Spiropoulou, C.F., Kuhn, J.H., Nguyen, D., Li, W., Nagel, J., Schmidt, P.J., Nunberg, J.H., Andrews, N.C.*, et al.* (2007). Transferrin receptor 1 is a cellular receptor for New World haemorrhagic fever arenaviruses. Nature *446*, 92-96.
Schmaljohn, C.S., Hasty, S.E., Rasmussen, L., and Dalrymple, J.M. (1986). Hantaan virus replication: effects of monensin, tunicamycin and endoglycosidases on the structural glycoproteins. JGenVirol *67 (Pt 4)*, 707-717.
Schmaljohn, C.S., and Nichol, S.T. (2007). Bunyaviridae. In Field's Virology, D.M. Knipe, P.M. Howley, D.E. Griffin, R.A. Lamb, M.A. Martin, B. Roizman, and S.E. Straus, eds. (Philadelphia: Wolters Kluwer Health/Lippincott Williams & Wilkins), pp. 1741-1789.
Schwarz, E.R., Mando, O.G., Maiztegui, J.I., Vilches, A.M., Otero, E.R., and Berrutti, Z.C. (1972). [Coagulation changes in Argentine hemorrhagic fever]. Medicina *32*, 247-259.
Vollenweider, F., Kappeler, F., Itin, C., and Hauri, H.P. (1998). Mistargeting of the lectin ERGIC-53 to the endoplasmic reticulum of HeLa cells impairs the secretion of a lysosomal enzyme. Journal of Cell Biology *142*, 377-389.
Whitt, M.A. (2010). Generation of VSV pseudotypes using recombinant DeltaG-VSV for studies on virus entry, identification of entry inhibitors, and immune responses to vaccines. Journal of Virological Methods *169*, 365-374.
Wright, K.E., Spiro, R.C., Burns, J.W., and Buchmeier, M.J. (1990). Post-translational processing of the glycoproteins of lymphocytic choriomeningitis virus. Virol *177*, 175-183.
Zhang, B., Cunningham, M.A., Nichols, W.C., Bernat, J.A., Seligsohn, U., Pipe, S.W., McVey, J.H., Schulte-Overberg, U., de Bosch, N.B., Ruiz-Saez, A.*, et al.* (2003). Bleeding due to disruption of a cargo-specific ER-to-Golgi transport complex. Nature genetics *34*, 220-225.
Zhang, B., Kaufman, R.J., and Ginsburg, D. (2005). LMAN1 and MCFD2 form a cargo receptor complex and interact with coagulation factor VIII in the early secretory pathway. Journal of Biological Chemistry *280*, 25881-25886.

Zheng, C., Liu, H.H., Yuan, S., Zhou, J., and Zhang, B. (2010). Molecular basis of LMAN1 in coordinating LMAN1-MCFD2 cargo receptor formation and ER-to-Golgi transport of FV/FVIII. Blood *116*, 5698-5706.

2.9. FIGURE LEGENDS

Figure 2.1 Identification of Human Proteins that Associate with Arenavirus and Hantavirus GPs

(A and B) HEK 293T cells were co-transfected with a pCAGGS plasmid encoding each respective viral GP with a C-terminal HA epitope tag and a biotin acceptor peptide (BAP), along with a second plasmid that encodes BirA, a bacterial biotin ligase, to ensure biotinylation of the viral GPs. As a control, cells were co-transfected with the BirA plasmid and an empty vector. Biotinylated GPs and associated host proteins were affinity purified (AP) from cell lysates (input) using magnetic streptavidin beads and separated on polyacrylamide gels for Western blot analysis to verify purification of the various GP species (GPC, GP1, and GP2 for LCMV; G1 and G2 for ANDV) and Coomassie staining for mass spectrometry analysis. Each Coomassie-stained gel lane was cut into sections for in-gel, trypic digestion and mass spectrometry analysis as described in the Extended Experimental Procedures (See Figure S1A for the proteomics workflow, Figures S1B and S1C for cut maps, Tables S1A-C for a list of the proteins, and Table S1D and Figure S1D for results of a functional clustering analysis).

(C) Venn diagram representing the number of identified host proteins associated with LCMV GP, ANDV GP, or both GPs.

(D-G, I, and J) ERGIC-53 has a conserved association with arenavirus and hantavirus GPs**.** HEK 293T cells were transfected with a pCAGGS plasmid encoding the indicated viral GPs with a C-terminal HA epitope tag and a BAP or, as a control, an empty pCAGGs plasmid. In panels D, F, and G, cells were also transfected with the BirA

plasmid to ensure biotinylation of each GP. Viral GPs (D, F, and G) or ERGIC-53 (E, I, and J) were AP or immunoprecipitated, respectively, as bait from cell lysates. Input lysates and purified bead fractions were screened for ERGIC-53 (D, F, and G) or viral GP species (G2 for hantaviruses; GPC and GP2 for arenaviruses) (E, I, and J) as prey via Western blot. See Figures S1E-I for screening of additional GPs.

(H and K) HEK 293T or Vero E6 cells were infected with JUNV C#1 and JUNV GP (H) or ERGIC-53 (K) was immunoprecipitated from cell lysates. Input lysates and purified bead fractions were screened for ERGIC-53 (H) or JUNV C#1 GP species (GPC and GP1) (K) as prey via Western blot.

(L) ERGIC-53 and JUNV C#1 GP concentrate in the same intracellular structure. JUNV C#1-infected HEK 293T cells were fixed, permeabilized, and stained for JUNV C#1 GP (green) and ERGIC-53 (red). Colocalization between GP and ERGIC-53 is displayed as white pixels in the colocalization mask. The histogram shows background gating (white lines) and specific immunofluorescence signal for JUNV GP (region 1), ERGIC-53 (region 2) or colocalized GP and ERGIC-53 (region 3) (78.6% of ERGIC-53 signal colocalized with GP signal; 52.2% of GP signal colocalized with ERGIC-53 signal). Scale bar, 20 μm.

Figure 2.2 ERGIC-53 is Required for Arenavirus Propagation

(A) Silencing ERGIC-53 expression impairs the release of infectious JUNV C#1. HEK 293T cells were transfected with an ERGIC-53-specific siRNA or a scrambled, negative control siRNA and challenged 72 hr later with JUNV C#1. Supernatants and cell protein

lysates were screened for JUNV C#1 plaque forming units (PFU) via plaque assay and ERGIC-53 or calreticultin (CRT) via Western blot. Data are presented as mean PFU ± SEM relative to the empty vector transfected wells and are the summation of 2 independent experiments (24 & 48 hr pi n = 5, 72 hr n = 6).

(B) Overexpression of WT ERGIC-53 enhances infectious JUNV release. HEK 293T cells were transfected with a plasmid encoding Myc-tagged, WT ERGIC-53 or, as a control, an empty plasmid; 48 hr following transfection these cells were challenged with JUNV C#1. Supernatants and cell protein lysates were screened for JUNV C#1 PFU via plaque assay and Myc-ERGIC-53 or CRT via Western blot. Data are presented as mean PFU ± SEM relative to the empty vector transfected wells and are the summation of 2 independent experiments (n = 6 at each time point).

(C and D) Restriction of ERGIC-53 to the ER impairs the release of infectious JUNV C#1 and DANV. HEK 293T cells were transfected with a plasmid encoding Myc-tagged DN ERGIC-53 or, as a control, an empty plasmid; 24 hr later cells were challenged with JUNV C#1 (C) or DANV (D). Supernatants and cell protein lysates were screened for PFU via plaque assay and Myc-DN ERGIC-53 or CRT via Western blot. Data are presented as mean PFU ± SEM relative to the empty vector transfected wells and are representative of 2 independent experiments (n = 12 or n = 6 per experiment for JUNV C#1 or DANV, respectively).

(E) Release of infectious JUNV C#1 is impaired in ERGIC-53 (*LMAN1*$^{-/-}$) null cells. EBV-transformed B cells from *LMAN1*$^{+/+}$ (2829-D) and *LMAN1*$^{-/-}$ (CRC-78 and CRC-79)

individuals were challenged with JUNV C#1. Supernatants and cell protein lysates were screened for JUNV C#1 PFU via plaque assay and ERGIC-53 or actin via Western blot. Data are presented as mean PFU ± SEM relative to the *LMAN1*$^{+/+}$ cells and are representative of 2 independent experiments (n = 3 per condition per experiment).

(A - E) *p < 0.05, **p < 0.01, ***p < 0.001, determined using the unpaired Student's *t* test. Note that Western blot results from representative lysates are shown; the full panel of lysates is displayed in Figure S2.

Figure 2.3 ERGIC-53 Broadly Associates with Class I Viral Fusion GPs and Influences the Propagation of JUNV, SARS CoV, and EBOV in a GP-Specific Manner

(A - D) ERGIC-53 is required for the production of infectious viral particles in a GP-specific manner. HEK 293T cells were initially transfected with a plasmid encoding Myc-tagged WT or DN ERGIC-53, then 24 hr later with a plasmid encoding VSV G, JUNV XJ GP, SARS CoV S, or EBOV GP. Twenty-four hr following the final transfection, cells were challenged with VSVΔG. Supernatants and cell protein lysates were screened for infectious VSVΔG particles pseudotyped with the indicated viral GP via focus assay and Myc-ERGIC-53 (WT or DN) or CRT via Western blot (see Figure S3 for blots), respectively. Data are presented as mean infectious units ± SEM relative to the WT ERGIC-53 vector transfected wells and are representative of 2 independent experiments (n = 3 wells per condition per experiment). *p < 0.05, **p < 0.01, ***p < 0.001, determined using the unpaired Student's *t* test.

(E and F) ERGIC-53 does not associate with VSV G. HEK 293T cells were transfected with a plasmid encoding VSV G or an empty plasmid and either VSV G (E) or ERGIC-53 (F) was immunoprecipitated as bait from cell lysates (input). Immunoprecipitated bead fractions were screened for ERGIC-53 (E) or VSV G (F) as prey via Western blot.

(G-J) ERGIC-53 has a conserved association with class I viral fusion GPs**.** HEK 293T cells were transfected with a plasmid encoding WT ERGIC-53 and a pCAGGS plasmid encoding the indicated viral GPs with a C-terminal HA epitope tag and BAP or an empty pCAGGs plasmid. In panels G and I, cells were also transfected with the Bir A plasmid to ensure biotinylation of each GP. Viral GPs (G and I) or ERGIC-53 (H and J) were AP or immunoprecipitated, respectively, as bait from cell lysates. Input lysates and purified bead fractions were screened for ERGIC-53 (G and I) or viral GP species (full length S and the processed S2 subunit for SARS CoV; full length HA0 and the processed subunit HA2 for influenza virus A/WSN/33; and full length GP0 and the processed GP2 subunit for EBOV and MARV) (H and J) as prey via Western blot. Data are representative of 2 independent experiments.

Figure 2.4 Loss of ERGIC-53 Function Does Not Inhibit the Formation of GP-Containing Arenavirus Particles but Instead Renders Them Noninfectious

(A and B) The ER-restricted, DN ERGIC-53 does not impair trafficking of JUNV C#1 GP to the plasma membrane. HEK 293T cells were transfected with a plasmid expressing WT or DN ERGIC-53, then inoculated 24 hr later with JUNV Candid #1 or not (mock), and collected 72 hr later to visualize internal rERGIC-53 and surface JUNV GP staining

via confocal immunofluorescence microscopy (GP, red; Myc-ERGIC-53, green) (A) or FACS (B). In B, the histograms are gated on Myc-positive cells and show the percentage of transfected cells with GP staining (grey = mock infected; white = JUNV C#1 infected). The median fluorescence intensity (MFI) is reported. Scale bars, 20 μm. Surface expression of hTfR1 is not altered by DN ERGIC-53 (Figure S4).

(C) The DN ERGIC-53 mutant does not impair proteolytic processing of JUNV GPC or the incorporation of GP species into virus-like particles (VLPs). HEK 293T cells were transfected with a plasmid expressing WT or DN ERGIC-53, then 24 hr later with plasmids encoding the JUNV Z and XJ GPC proteins, respectively, to permit the formation of VLPs. Cells and supernatants (concentrated via ultracentrifugation through sucrose) were screened for the presence of various GP species (the C-terminally FLAG-tagged precursor GPC or proteolytically processed GP2) or actin via Western blot. The data are representative of 2 independent experiments.

(D - G) JUNV C#1 generates GP-containing virus particles that are noninfectious in ERGIC-53 null cell lines. B cells derived from *LMAN1*$^{+/+}$ (2829-D) and *LMAN1*$^{-/-}$ (CRC-78) individuals were challenged with JUNV C#1 or not and supernatants from these cells were concentrated through sucrose and screened for viral proteins (GP1, NP, and Z), ERGIC-53, or actin via Western blot (D), JUNV C#1 plaque forming units (PFU) via plaque assay (E), the ratio of S segment genomic RNA copies, as measured by quantitative RT-PCR, to PFU (F), or attachment to host cells (G). All values are reported relative to the *LMAN1*$^{+/+}$ particles. Statistics are not shown because the values in panels D-G were derived from the same individual preparation of either *LMAN1*$^{+/+}$- or *LMAN1*$^{-/-}$

-derived viral particles. For the attachment assay, virions were allowed to bind to cells at 4°C for 1.5 hr. Following washes to remove unbound particles, bound virus was enumerated on the basis of viral S segment genomic RNA copies detected via quantitative RT-PCR. The data in panels D-F are representative of 2 independent experiments.

Figure 2.5 ERGIC-53 Traffics to Sites of Arenavirus Budding and Is Incorporated into Virions

(A-C) ERGIC-53 traffics to sites of arenavirus budding. JUNV C#1- or mock-infected HEK 293T cells were screened for either internal (A) or surface (B and C) expression of JUNV GPC/GP1 and ERGIC-53 (A and B) or JUNV GPC/GP1 and CRT (C) via confocal microscopy. Scale bars, 10 μm (white), 20 μm (red), and 300 nm (yellow).

(D) ERGIC-53 is a component of arenavirus particles. An anti-GP1 antibody was used to immunoprecipitate viral particles from supernatants of JUNV-infected or mock-infected Vero E6 cells. An irrelevant, species-matched antibody was also used for immunoprecipitation from the JUNV-infected supernatants. Cell lysates and immunoprecipitated protein fractions were screened for viral proteins (GP1, NP, and Z) and ERGIC-53 via Western blot under non-reducing conditions. Data are representative of 2 independent experiments. ERGIC-53 was also detectable in JUNV C#1 particles via confocal microscopy (Figure S5).

Figure 2.6 The C-Terminal Region of ERGIC-53's CRD Is Required for the ERGIC-53 - JUNV GP Interaction

(A) Depiction of ERGIC-53 mutants used in this study. SS, signal sequence; F, Flag epitope tag; TM, transmembrane. See Figure S6 for a detailed description of each mutant.

(B) HEK 293T cells were co-transfected with the BirA plasmid, a plasmid encoding JUNV C#1 GP with a C terminal HA tag and BAP, and a plasmid encoding the indicated ERGIC-53 mutants with an N-terminal FLAG tag. JUNV GP species (GPC and GP2) were AP as bait from cell lysates. Input lysates and captured bead fractions were screened for ERGIC-53 (prey) and, as a control, CRT (prey) via Western blot. The data are representative of 2 independent experiments.

Figure 2.7 Proposed Model Depicting the Role of ERGIC-53 in JUNV Propagation

Under WT conditions (top half of left cell), the arenavirus GP undergoes a series of maturation steps within the early exocytic pathway (1), including proteolytic cleavage and trafficking to the plasma membrane where it is incorporated into newly forming viral particles (2) that bud out of the cell (3). The GP on newly formed particles then attaches to its cellular receptor (4), which permits endocytic uptake of particles into endosomes (5) where low pH leads to GP2-mediated fusion of the viral and endosomal membranes and, ultimately, release of viral genome into the cytoplasm (6). In the absence of ERGIC-53 (null) or in the presence of the ER-restricted, DN ERGIC-53 (DN) (bottom half of left cell), GP is still proteolytically processed, trafficked to the plasma membrane, and incorporated, along with other viral structural proteins and viral genome, into budding particles (1-3). These particles, however, lack ERGIC-53 and are defective in their ability to attach to host cells (4). They may have deficiencies in other early replication events (5 and 6) as well.

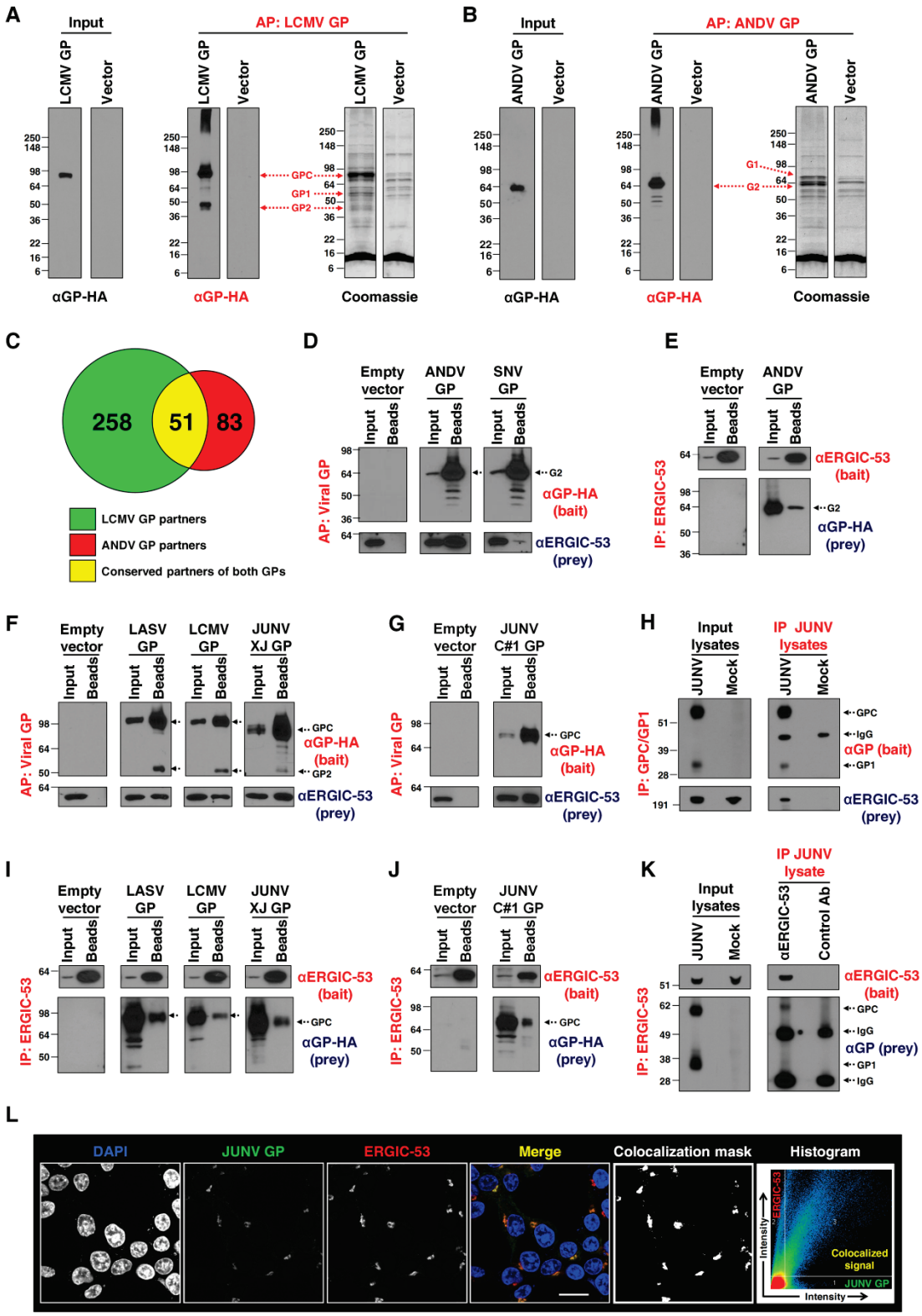
A
Input
AP: LCMV GP
LCMV GP
Vector
αGP-HA
Coomassie
GPC
GP1
GP2
B
Input
AP: ANDV GP
ANDV GP
Vector
G1
G2
C
258
51
83
LCMV GP partners
ANDV GP partners
Conserved partners of both GPs
D
Empty vector
ANDV GP
SNV GP
Input
Beads
AP: Viral GP
αGP-HA (bait)
αERGIC-53 (prey)
E
IP: ERGIC-53
αERGIC-53 (bait)
αGP-HA (prey)
F
LASV GP
LCMV GP
JUNV XJ GP
G
JUNV C#1 GP
H
Input lysates
IP JUNV lysates
JUNV
Mock
IP: GPC/GP1
αGP (bait)
IgG
I
J
K
IP JUNV lysate
αERGIC-53
Control Ab
αGP (prey)
L
DAPI
JUNV GP
ERGIC-53
Merge
Colocalization mask
Histogram
Colocalized signal
Intensity

Figure 2.1 Identification of Human Proteins that Associate with Arenavirus and Hantavirus GPs

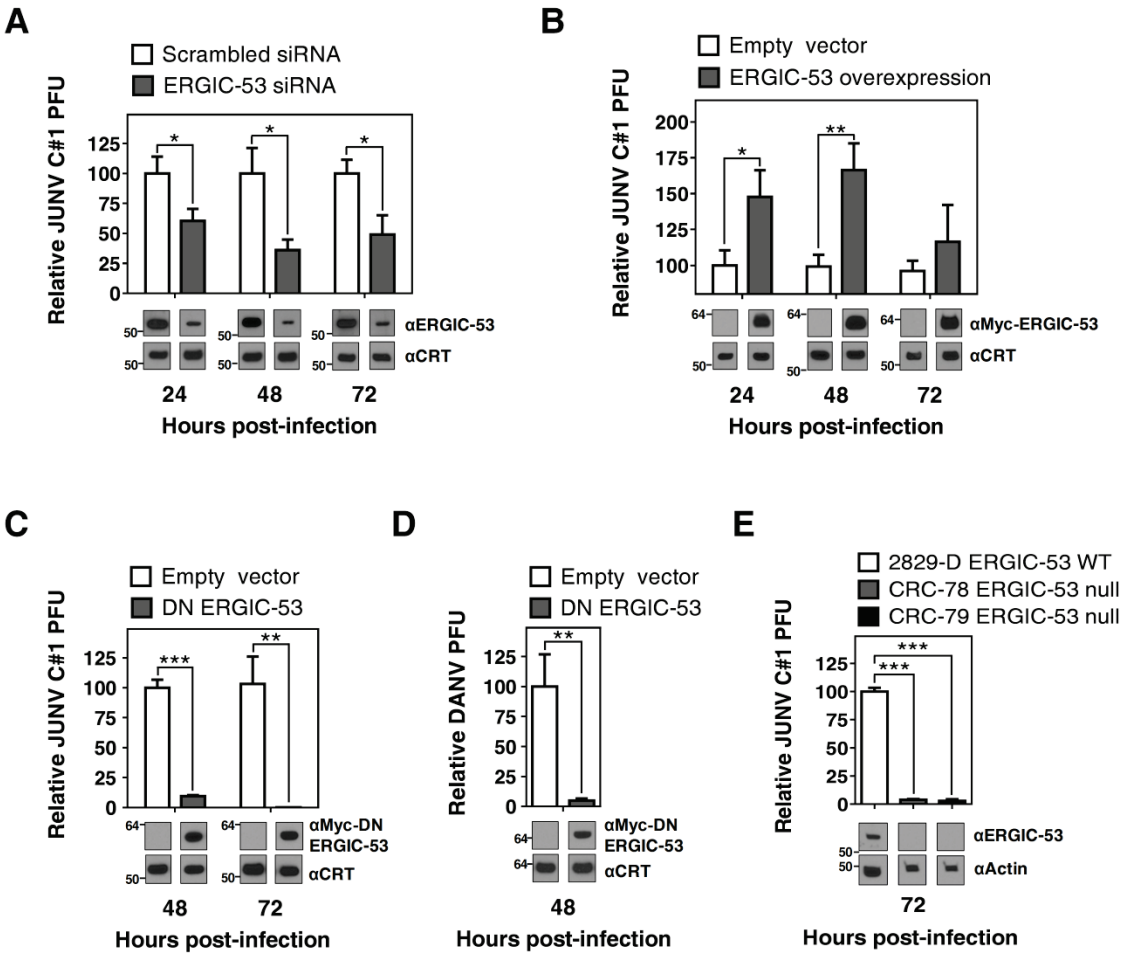

Figure 2.2 ERIGC-53 is Required for Arenavirus Propagation.

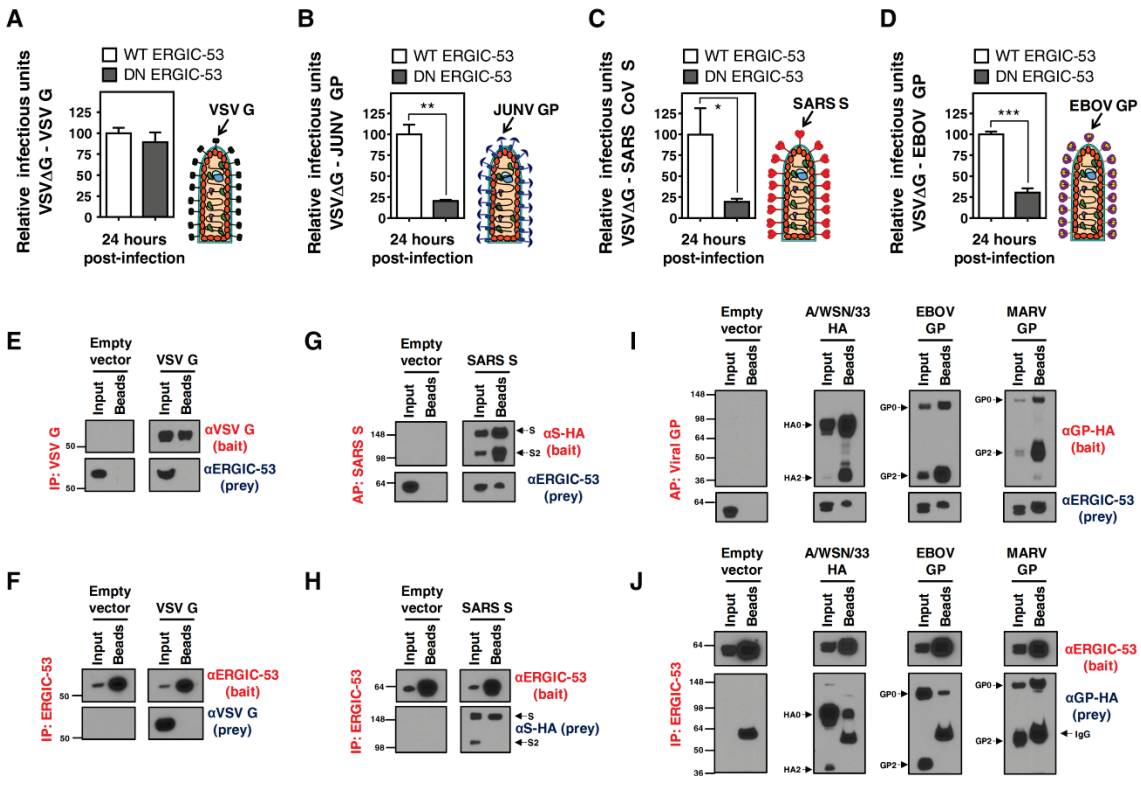

Figure 2.3 ERGIC-53 Broadly Associates with Class I Viral Fusion GPs and Influences the Propagation of JUNV, SARS CoV, and EBOV in a GP-Specific Manner

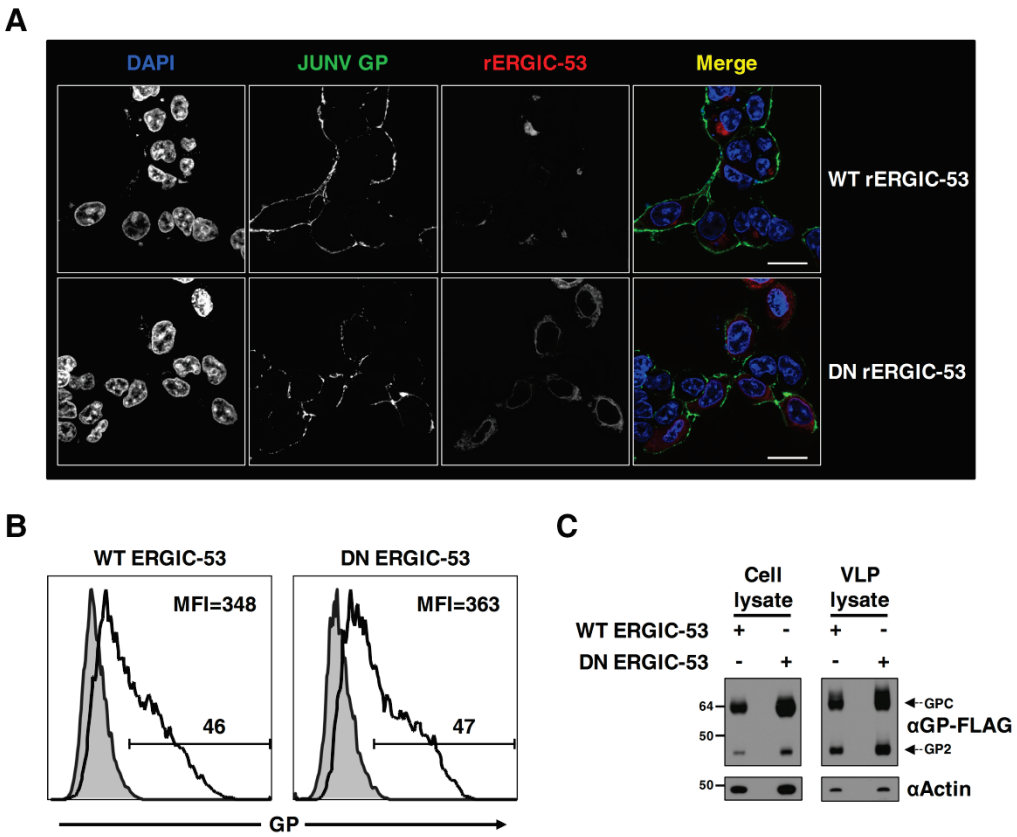
A
DAPI
JUNV GP
rERGIC-53
Merge
WT rERGIC-53
DN rERGIC-53
B
WT ERGIC-53
DN ERGIC-53
MFI=348
MFI=363
46
47
GP
C
Cell lysate
VLP lysate
WT ERGIC-53 + - + -
DN ERGIC-53 - + - +
64
50
GPC
αGP-FLAG
GP2
50
αActin
D
Supernatant
JUNV
Mock
WT ERGIC-53 + - + -
ERGIC-53 null - + - +
50
αGP1
64
αNP
16
αZ
64
αERGIC-53
50
αActin
E
WT ERGIC-53
ERGIC-53 null
Relative JUNV C#1 PFU
125
100
75
50
25
0
F
WT ERGIC-53
ERGIC-53 null
Relative JUNV C#1 S segment vRNA copies/PFU
700
500
300
100
G
WT ERGIC-53
ERGIC-53 null
Relative JUNV C#1 particle binding to cells
125
100
75
50
25
0

Figure 2.4 Loss of ERGIC-53 Function Does Not Inhibit the Formation of GP-Containing Arenavirus Particles but Instead Renders Them Noninfectious

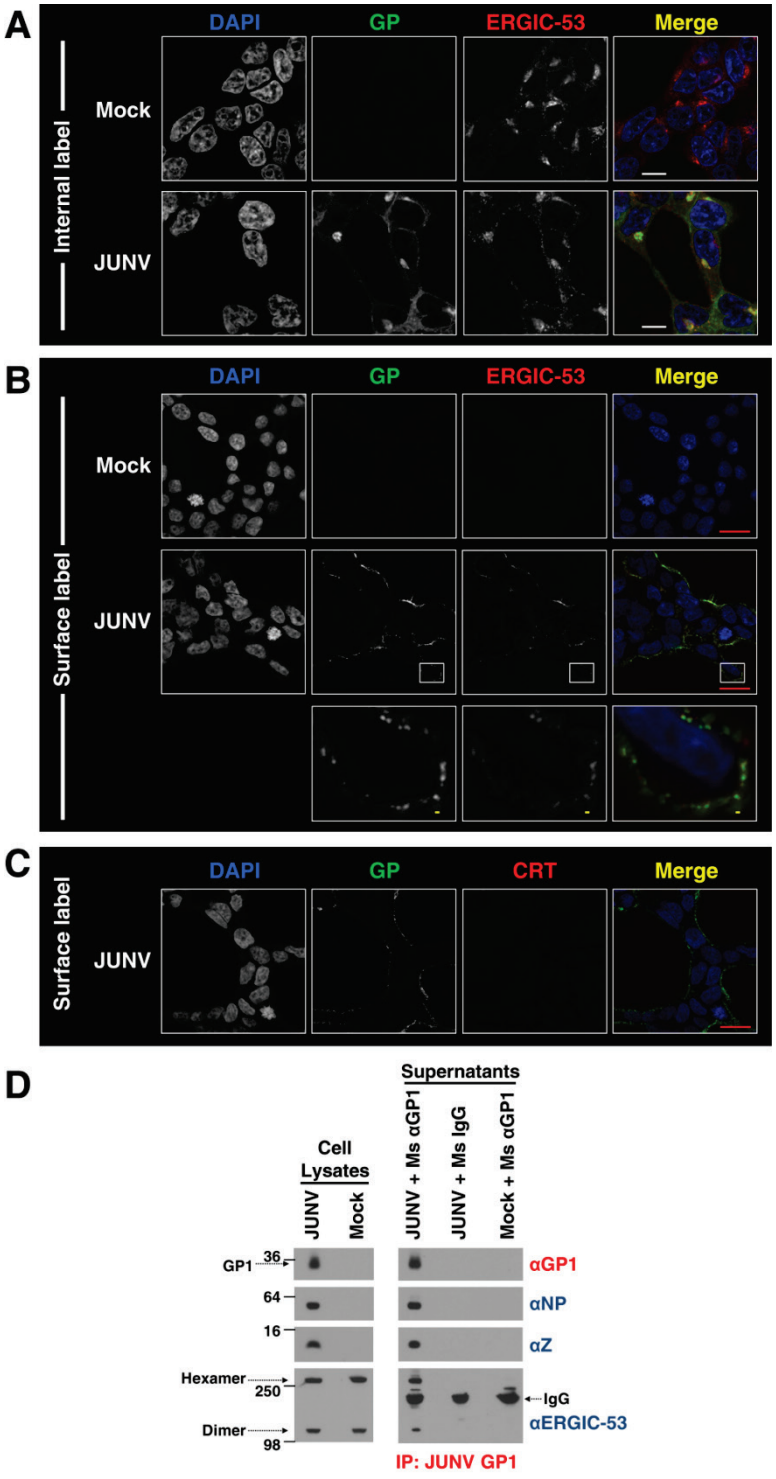

Figure 2.5 ERGIC-53 Traffics to Sites of Arenavirus Budding and is Incorporated into Virions

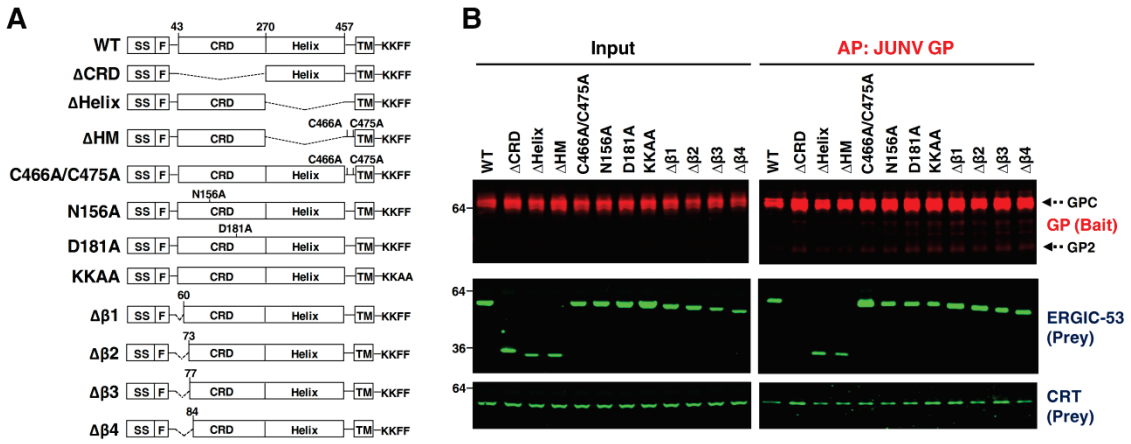

Figure 2.6 The C-Terminal Region of ERGIC-53's CRD is Required for the ERGIC-53 –JUNV GP interaction

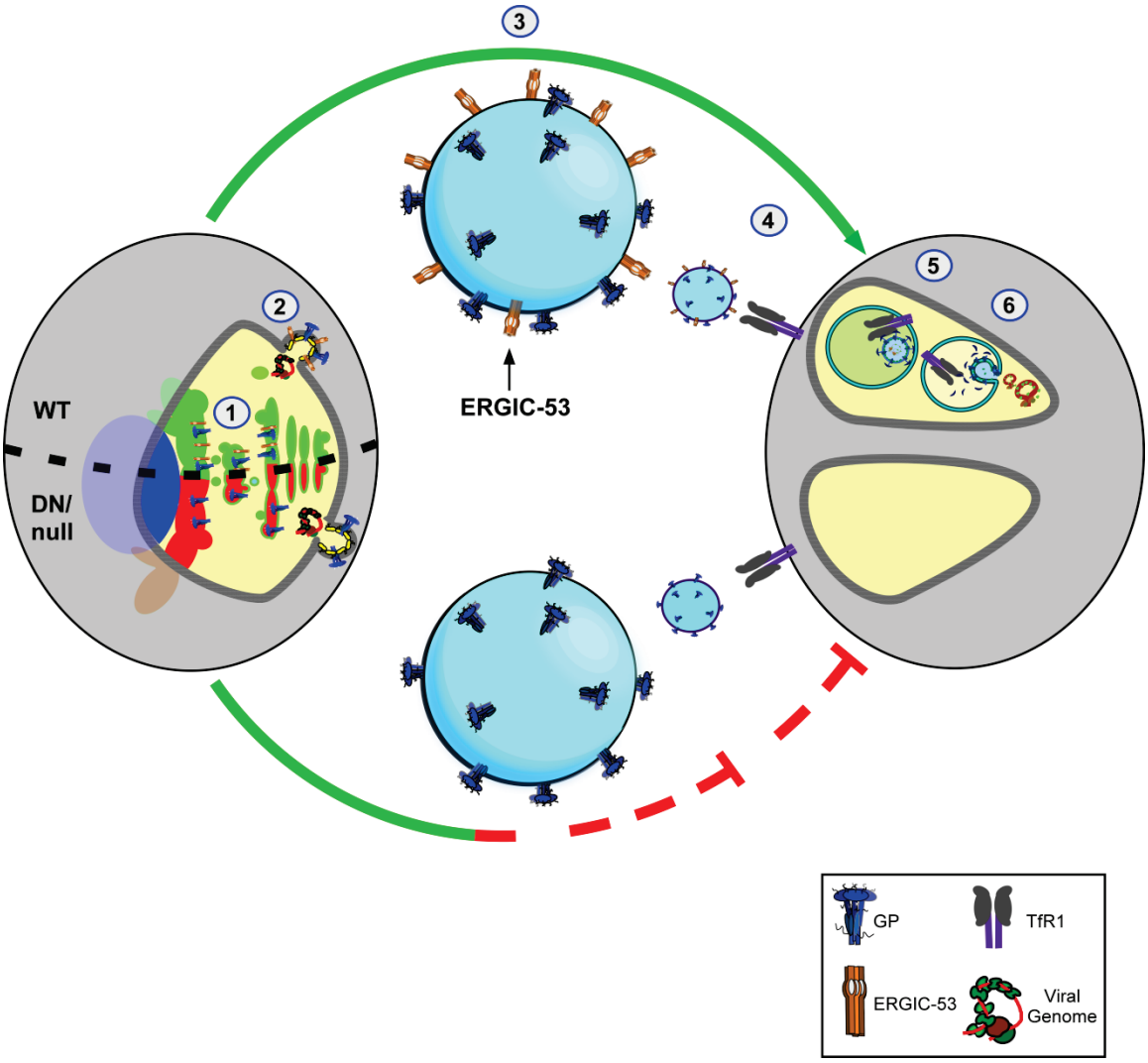

Figure 2.7 Proposed Model Depicting the Role of ERGIC-53 in JUNV Propagation

Cell Host & Microbe, Volume *14*

2.10. Supplemental Information

The Intracellular Cargo Receptor ERGIC-53 Is Required for the Production of Infectious Arenavirus, Coronavirus, and Filovirus Particles

Joseph Klaus, Philip Eisenhauer, Joanne Russo, Anne Mason, Danh Do, Benjamin King, Douglas Taatjes, Cromwell Cornillez-Ty, Jonathan E. Boyson, Markus Thali, Chunlei Zheng, Lujian Liao, John R. Yates III, Bin Zhang, Bryan A. Ballif, and Jason Botten

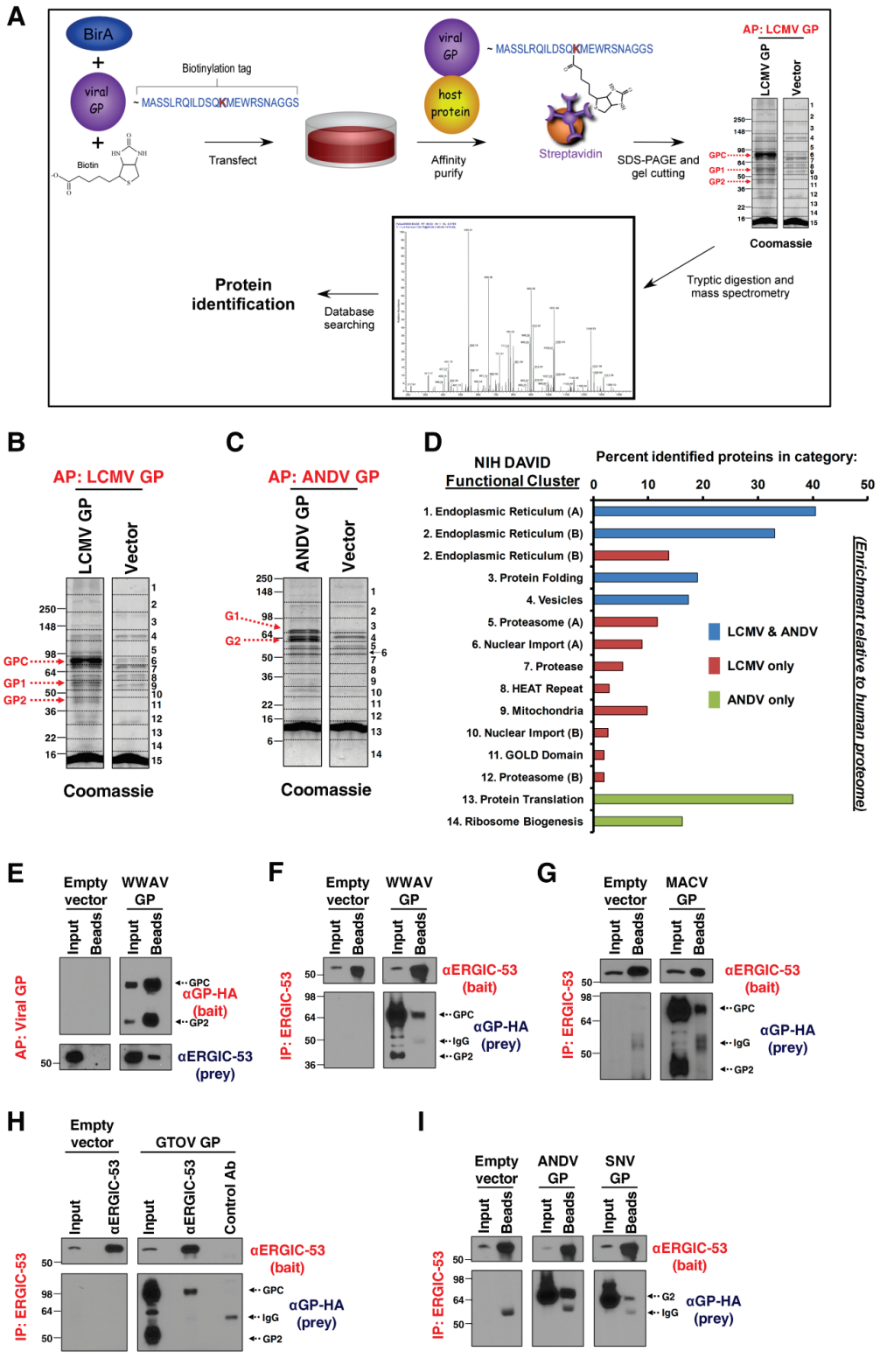
A
BirA
viral GP
Biotin
Biotinylation tag
~ MASSLRQILDSQKMEWRSNAGGS
Transfect
viral GP
host protein
Affinity purify
Streptavidin
SDS-PAGE and gel cutting
AP: LCMV GP
LCMV GP
Vector
GPC
GP1
GP2
Coomassie
Tryptic digestion and mass spectrometry
Database searching
Protein identification
B
AP: LCMV GP
LCMV GP
Vector
Coomassie
C
AP: ANDV GP
ANDV GP
Vector
G1
G2
Coomassie
D
NIH DAVID Functional Cluster
Percent identified proteins in category:
1. Endoplasmic Reticulum (A)
2. Endoplasmic Reticulum (B)
2. Endoplasmic Reticulum (B)
3. Protein Folding
4. Vesicles
5. Proteasome (A)
6. Nuclear Import (A)
7. Protease
8. HEAT Repeat
9. Mitochondria
10. Nuclear Import (B)
11. GOLD Domain
12. Proteasome (B)
13. Protein Translation
14. Ribosome Biogenesis
LCMV & ANDV
LCMV only
ANDV only
(Enrichment relative to human proteome)
E
Empty vector
WWAV GP
Input
Beads
AP: Viral GP
αGP-HA (bait)
αERGIC-53 (prey)
F
IP: ERGIC-53
αERGIC-53 (bait)
αGP-HA (prey)
IgG
G
MACV GP
H
GTOV GP
αERGIC-53
Control Ab
I
ANDV GP
SNV GP
G2

Figure S1. Proteomics Workflow, Cut Map of Coomassie-Stained Gels Containing Human Proteins Purified in Complex with LCMV GP or ANDV GP, Functional Clustering Analysis of Host Protein Partners, and Additional Viral GPs that Associate with ERGIC-53, Related to Figure 1

(A) Workflow for identification of human proteins that associate with the GPs encoded by LCMV and ANDV. HEK 293T cells were co-transfected with a plasmid encoding each respective viral GP with a C-terminal HA epitope tag and a biotin acceptor peptide (BAP), along with a second plasmid that encodes BirA, a bacterial biotin ligase, to ensure biotinylation of the viral GPs. As a control, cells were co-transfected with the BirA plasmid and an empty vector. Two days later, biotinylated GPs and associated host proteins were affinity purified (AP) from whole cell lysates using magnetic streptavidin beads and separated on 4-20% polyacrylamide gels for Coomassie staining. To determine the identity of cellular proteins captured, each Coomassie-stained gel lane was cut into sections (see dashed lines) for in-gel, tryptic digestion and mass spectrometry analysis as described in the Extended Experimental Procedures.

(B and C) Cut maps of the affinity purified LCMV GP (B) and ANDV GP (C) samples following SDS-PAGE and Coomassie staining.

(D) NIH DAVID functional clustering identifies enriched protein functional categories from proteomic datasets representing proteins identified binding to both LCMV and ANDV GP proteins, LCMV GP alone, or ANDV GP alone. Official gene symbols (see Tables S1A-S1C) of these data sets were entered into NIH DAVID, searched under

medium stringency choosing *Homo sapiens* as background. Functional clusters showing four-fold or more increases were chosen for display here. Functional clusters were simplified by providing labels 1-14 above (see Table S1D for details). The percent of proteins (average of functional cluster subsets) in each data set in each of these categories is provided as well as the relative enrichment of a given cluster relative to the human proteome. Note that one protein may be found in more than one category. Also note that because the size of each dataset is different a category may show a higher percentage, but a lower enrichment when compared to the same category in a different data set.

(E) HEK 293T cells were transfected with the BirA plasmid and a modified pCAGGS plasmid encoding WWAV GP with a C-terminal HA epitope tag and BAP or, as a control, an empty pCAGGS plasmid. Whole cell lysates (input) were collected 2 days later and incubated with streptavidin beads to isolate each biotinylated GP species (GPC and GP2). Input lysates and captured bead fractions were screened for GP species (GPC and GP2) (bait) and ERGIC-53 (prey) via Western blot.

(F - I) HEK 293T cells were transfected with a plasmid encoding the indicated viral GPs with a C-terminal HA epitope tag or an empty plasmid. Two days later ERGIC-53 was immunoprecipitated from whole cell lysates (input). Inputs and immunoprecipitated bead fractions were screened for ERGIC-53 (bait) and the various GP species (GPC and GP2 for arenaviruses; G2 for hantaviruses) (prey) via Western blot.

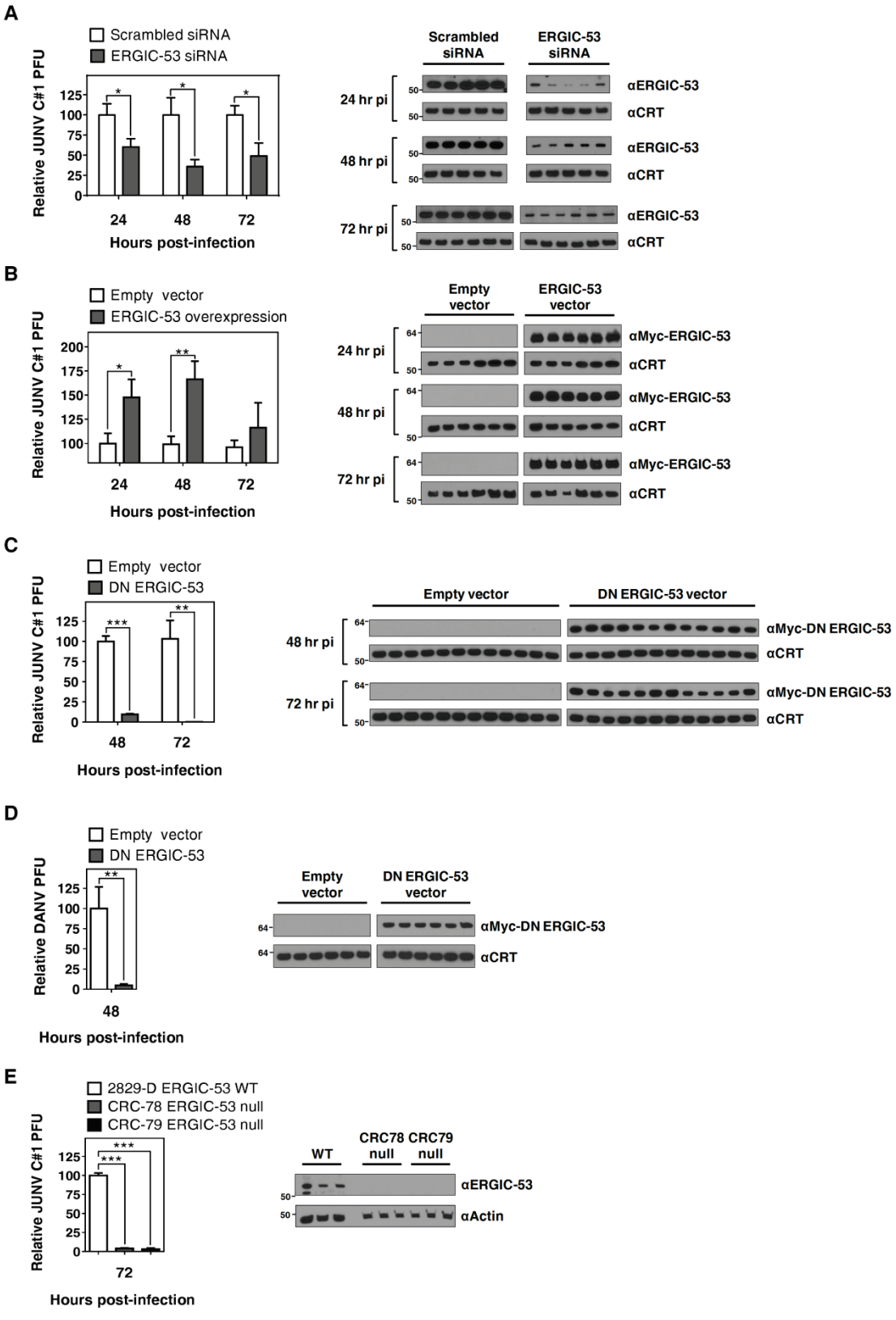
A
Scrambled siRNA
ERGIC-53 siRNA
Relative JUNV C#1 PFU
125
100
75
50
25
0
*
*
*
24
48
72
Hours post-infection
Scrambled siRNA
ERGIC-53 siRNA
24 hr pi
48 hr pi
72 hr pi
50
αERGIC-53
αCRT
B
Empty vector
ERGIC-53 overexpression
Relative JUNV C#1 PFU
200
175
150
125
100
*
**
24
48
72
Hours post-infection
Empty vector
ERGIC-53 vector
64
50
αMyc-ERGIC-53
αCRT
C
Empty vector
DN ERGIC-53
Relative JUNV C#1 PFU
***
**
48
72
Hours post-infection
Empty vector
DN ERGIC-53 vector
48 hr pi
72 hr pi
αMyc-DN ERGIC-53
αCRT
D
Empty vector
DN ERGIC-53
Relative DANV PFU
**
48
Hours post-infection
Empty vector
DN ERGIC-53 vector
αMyc-DN ERGIC-53
αCRT
E
2829-D ERGIC-53 WT
CRC-78 ERGIC-53 null
CRC-79 ERGIC-53 null
Relative JUNV C#1 PFU
***
***
72
Hours post-infection
WT
CRC78 null
CRC79 null
αERGIC-53
αActin

Figure S2. ERGIC-53 is Required for Arenavirus Propagation, Related to Figure 2

(A) Silencing ERGIC-53 expression impairs the release of infectious JUNV C#1 (related to Figure 2A). HEK 293T cells were transfected with an ERGIC-53-specific siRNA or a scrambled, negative control siRNA and challenged 72 hr later with JUNV C#1 at an MOI of 0.1. Supernatants and cell protein lysates were collected at 24, 48, and 72 hr post-inoculation (pi) and screened for JUNV C#1 plaque forming units (PFU) via plaque assay and ERGIC-53 or CRT (loading control) via Western blot (each lane represents an individual well). Data are presented as mean PFU ± SEM relative to the empty vector transfected wells and are the summation of 2 independent experiments (24 & 48 hr pi n = 5, 72 hr n = 6).

(B) Overexpression of WT ERGIC-53 enhances infectious JUNV release (related to Figure 2B). HEK 293T cells were transfected with a plasmid encoding Myc-tagged, WT ERGIC-53 or, as a control, an empty plasmid; 48 hr following transfection these cells were challenged with JUNV C#1 at an MOI of 0.1. Supernatants and cell protein lysates were collected at 24, 48, and 72 hr pi and screened for JUNV C#1 PFU via plaque assay and Myc-ERGIC-53 or CRT (loading control) via Western blot (each lane represents an individual well). Data are presented as mean PFU ± SEM relative to the empty vector transfected wells and are the summation of 2 independent experiments (n = 6 per time point).

(C and D) Restriction of ERGIC-53 to the ER impairs the release of infectious JUNV C#1 and DANV (related to Figures 2C and 2D, respectively). HEK 293T cells were transfected with a plasmid encoding Myc-tagged DN ERGIC-53 or, as a control, an empty plasmid; 24 hr later cells were challenged with JUNV C#1 (C) or DANV (D) at an MOI of 0.1 or 0.001, respectively. Supernatants and cell protein lysates were collected at the indicated times pi and screened for PFU via plaque assay and Myc-DN ERGIC-53 or CRT (loading control) via Western blot (each lane represents an individual well). Data are presented as mean PFU ± SEM relative to the empty vector transfected wells and are representative of 2 independent experiments (n = 12 or n = 6 per experiment for JUNV C#1 or DANV, respectively).

(E) Release of infectious JUNV C#1 is impaired in ERGIC-53 (*LMAN1*$^{-/-}$) null cells (related to Figure 2E). B cells from *LMAN1*$^{+/+}$ (2829-D) and *LMAN1*$^{-/-}$ (CRC-78 and CRC-79) individuals were challenged with JUNV C#1 at an MOI of 1. Supernatants and cell protein lysates were collected at 48 and 72 hr pi and screened for JUNV C#1 PFU via plaque assay and ERGIC-53 or actin (loading control) via Western blot (each lane represents an individual well). Data are presented as mean PFU ± SEM relative to the *LMAN1*$^{+/+}$ cells and are representative of 2 independent experiments (n = 3 per condition per experiment).

(A - E) *$p < 0.05$, **$p < 0.01$, ***$p < 0.001$, determined using the unpaired Student's *t* test.

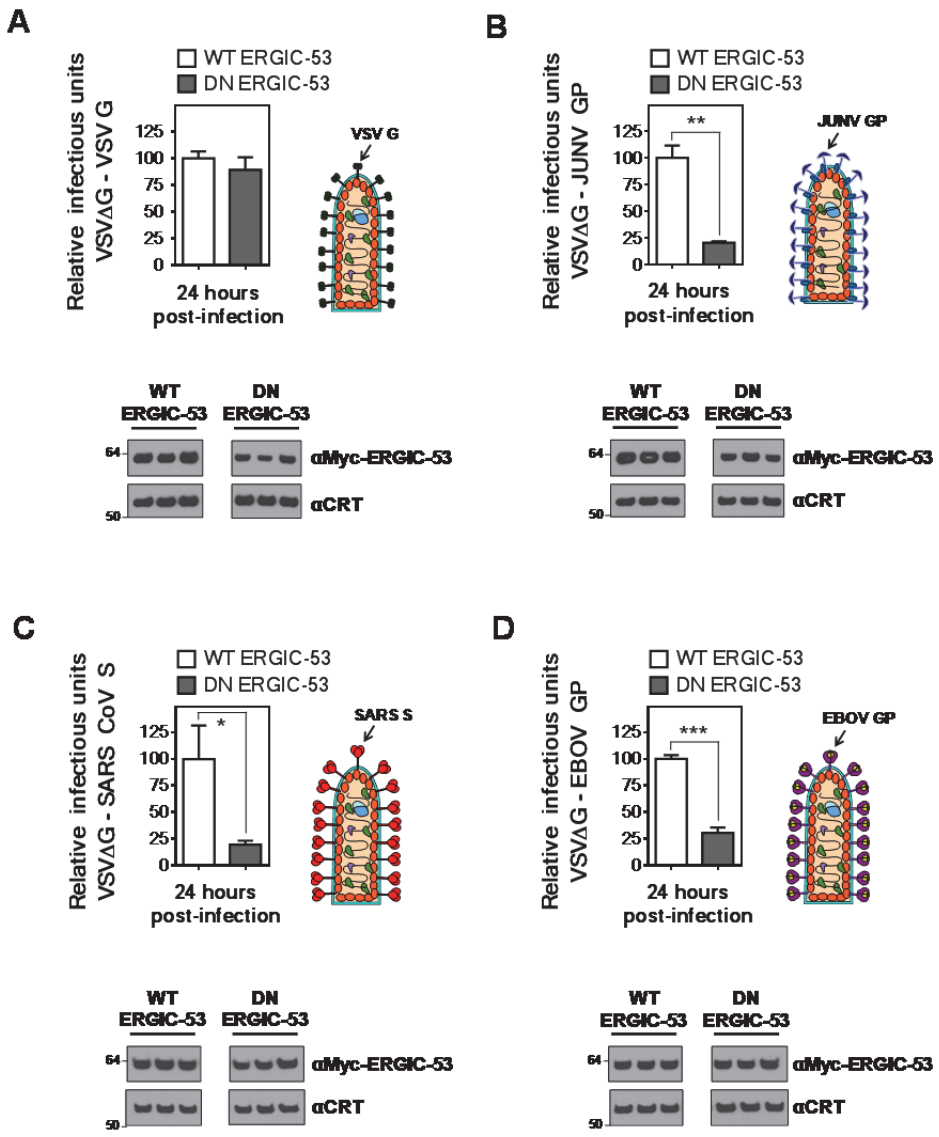

Figure S3. ERGIC-53's Influence on JUNV, SARS CoV, and EBOV Propagation is Specific and Can Be Minimally Mapped to the viral GP, Related to Figure 3

(A - D) HEK 293T cells were initially transfected with a plasmid encoding Myc-tagged WT or DN ERGIC-53, then 24 hr later the WT and DN ERGIC-53 cells were transfected with a plasmid encoding VSV G (A), JUNV XJ GP (B), SARS CoV S (C), or EBOV GP (D). Twenty-four hr following the final transfection, cells were challenged with VSVΔG at an MOI of 2. Supernatants and cell protein lysates were collected 24 hr later and

screened for infectious VSVΔG particles pseudotyped with VSV G, JUNV XJ GP, SARS CoV S, or EBOV GP via focus assay and Myc-ERGIC-53 (WT or DN) or CRT (loading control) via Western blot (each lane represents an individual well), respectively. Data are presented as mean infectious units ± SEM relative to the WT ERGIC-53 vector transfected wells and are representative of 2 independent experiments (n = 3 wells per condition per experiment). *p < 0.05, **p < 0.01, ***p < 0.001, determined using the unpaired Student's *t* test.

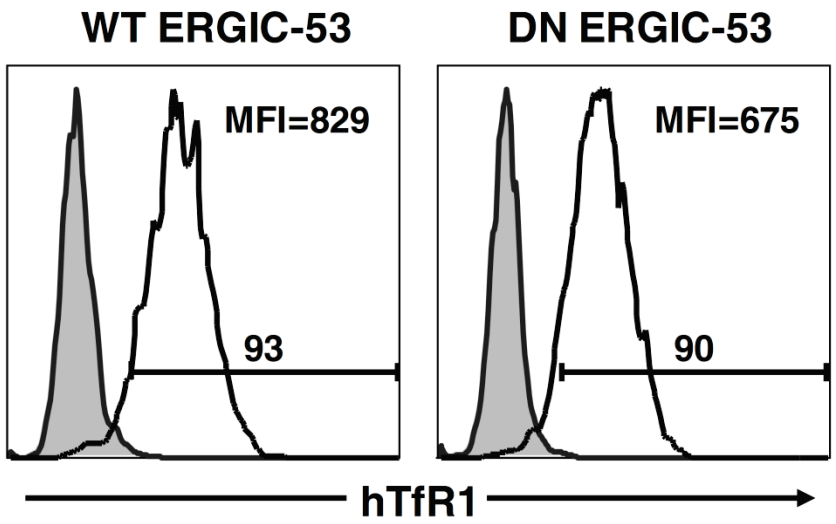

Figure S4. The ER-Restricted, DN ERGIC-53 Does Not Impair Trafficking of hTfR1 to the Plasma Membrane, Related to Figure 4

HEK 293T cells were transfected with a plasmid expressing WT ERGIC-53 or the DN ERGIC-53 mutant and 72 hr later incubated at 4^{o}C with an anti-hTfR1 antibody to stain

for surface expression of hTfR1 and then fixed, permeabilized, and incubated with an anti-Myc antibody to stain for internal Myc-ERGIC (WT or DN). The histograms are gated on Myc-positive cells and show the percentage of transfected cells with hTfR1 staining (grey shaded = isotype-matched IgG control antibody signal; white = hTfR1 signal). The median fluorescence intensity (MFI) is reported for each condition.

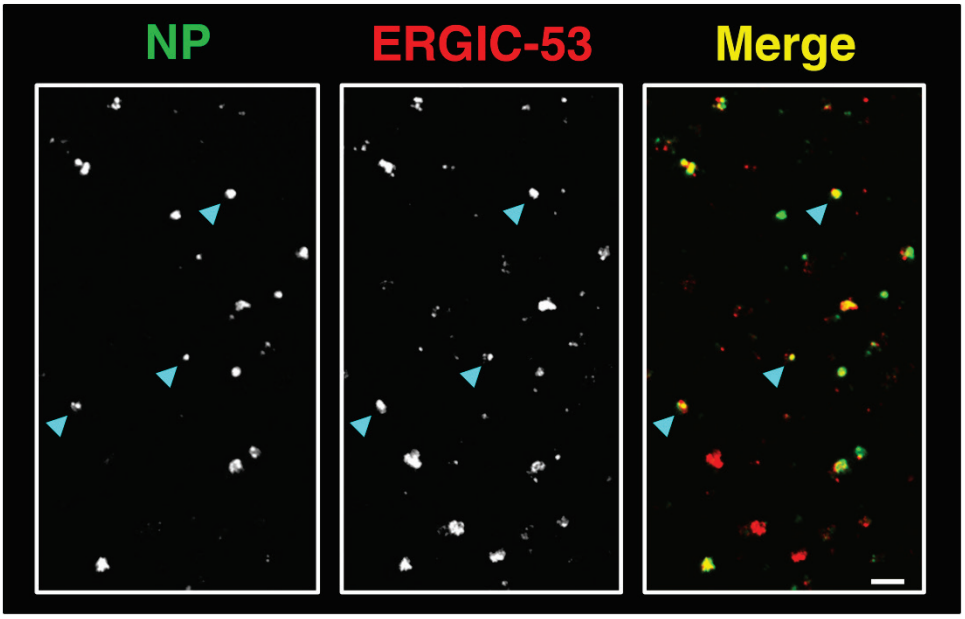

Figure S5. ERGIC-53 is Incorporated into Arenavirus Particles, Related to Figure 5D

JUNV C#1 particles generated in Vero E6 cells were adhered onto glass cover slips, permeabilized, and screened for JUNV NP (green) and ERGIC-53 (red) via confocal microscopy as described in the Extended Experimental Procedures. The data presented

are representative of 2 independent experiments. The arrowheads highlight JUNV particles that contain ERGIC-53. Scale bar, 5 µm.

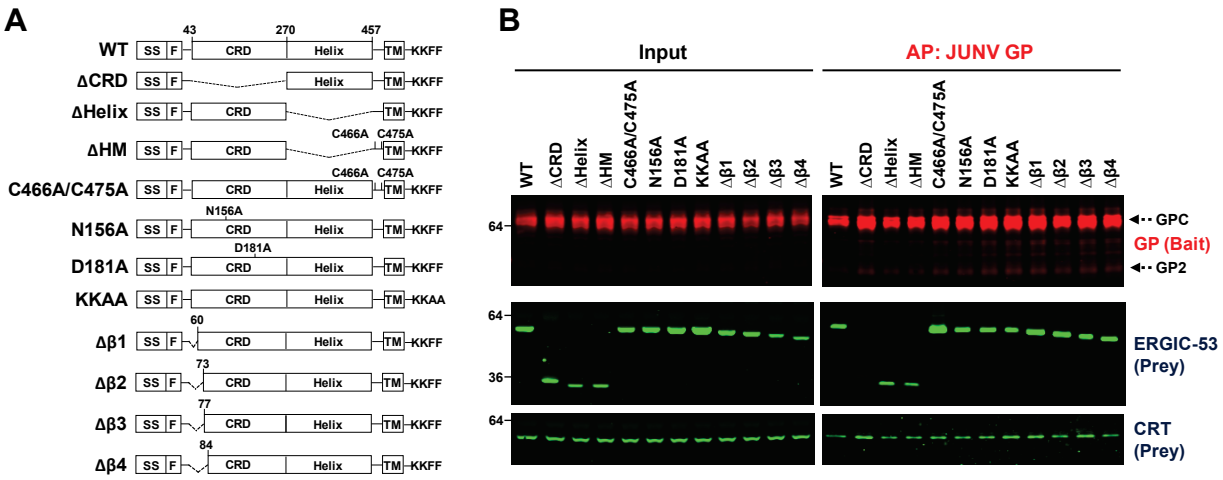

Figure S6. The C-Terminal Region of ERGIC-53's CRD Is Required for the ERGIC-53 - JUNV GP Interaction, Related to Figure 6

(A) Depiction of ERGIC-53 mutants used in this study. ERGIC-53 is a nonglycosylated, type I transmembrane protein that forms homohexamers and consists of an ER-lumenal domain, a transmembrane domain, and a cytoplasmic domain (for review see (Hauri et al., 2000b)). The ER-lumenal portion of the protein contains a carbohydrate recognition domain (CRD) that selectively binds high mannose glycans in a Ca^{2+}- and pH-dependent manner (Appenzeller-Herzog et al., 2004; C. Appenzeller et al., 1999b; Itin et al., 1996). Lectin binding can be disrupted by deletion of the entire CRD (ΔCRD) (residues 44 -

269) or specific β-strands within the CRD (e.g. strands 1 & 2 (Δβ2) (residues 43-72), 1 through 3 (Δβ3) (residues 43 - 76), or 1 through 4 (Δβ4) (residues 43-83)) (Zheng, Liu, Yuan, et al., 2010), or through mutation of individual amino acids (N156A or D181A) (Itin et al., 1996; Velloso, Svensson, Pettersson, & Lindqvist, 2003a; Zheng, Liu, Yuan, et al., 2010) within the CRD that are critically required for coordinating Ca^{2+}-binding. The ER-lumenal region of ERGIC-53 also encodes an alpha helical domain and two cysteine residues (C466 & C475) that are all required for the formation of ERGIC-53 homohexamers. Deletion of the helical domain (ΔHelix) (residues 271 - 457) (E. P. Neve, U. Lahtinen, & R. F. Pettersson, 2005) or mutation of the cysteine residues to alanine (C466A/C475A) (Nufer et al., 2003) results in the loss of noncovalently-associated or disulfide-linked homohexamers, respectively. Deletion of the helical domain combined with mutation of C466 and C475 to alanine (Δhelix monomer (ΔHM)) (Zheng, Liu, Yuan, et al., 2010) completely abolishes ERGIC-53 oligomerization and yields monomeric ERGIC-53, which, like the DN mutant (KKAA) (Kappeler, Klopfenstein, Foguet, Paccaud, & Hauri, 1997a), cannot traffic beyond the ER. Additionally, several of these constructs (ΔCRD, Δβ1, Δβ2, Δβ3, Δβ4, and ΔHM) abolish ERGIC-53's ability to interact with MCFD2 (Zheng, Liu, Yuan, et al., 2010). SS, signal sequence; F, Flag epitope tag; TM, transmembrane.

(B) HEK 293T cells were co-transfected with the BirA plasmid, a plasmid encoding JUNV C#1 GP with a C terminal HA tag and BAP, and a plasmid encoding the indicated ERGIC-53 mutants with an N-terminal FLAG epitope tag. JUNV GP species (GPC and GP2) were AP as bait from cell lysates. Input lysates and captured bead fractions were

screened for ERGIC-53 (prey) and, as a control, CRT (prey) via Western blot. The data are representative of 2 independent experiments.

Supplemental Experimental Procedures

Cells and Viruses

HEK 293T/17 cells (CRL-11268, American Type Culture Collection, Manassas, VA) (referred to as HEK 293T cells in the manuscript) were grown in Dulbecco's Modified Eagle Medium (DMEM) (11965-118) supplemented with 10% fetal bovine serum, 1% Penicillin-Streptomycin (15140-163), 1% MEM Non-Essential Amino Acids Solution (11140-050), 1% HEPES Buffer Solution (15630-130), and 1% GlutaMAX (35050-061) purchased from Invitrogen (Carlsbad, CA). Vero E6 cells were provided by J. L. Whitton (The Scripps Research Institute, La Jolla) and grown in DMEM supplemented with 10% FBS, 1% Penicillin-Streptomycin, and 1% HEPES Buffer Solution. The EBV-immortalized B lymphoblastoid cell lines derived from normal (*LMAN1*$^{+/+}$; 2829-D) or ERGIC-53 null (*LMAN1*$^{-/-}$; CRC-78 and CRC-79) individuals have been described previously (the null lines are described as A2 and A12, respectively, in (Neerman-Arbez et al., 1999)) and were maintained in RPMI 1640 Medium (22400-105, Invitrogen)

containing 10% FBS and 1% Penicillin-Streptomycin. The two *LMAN1*$^{-/-}$ individuals are from different families but encode an identical null mutation (c.822-1G>A splice site mutation) that completely abrogates expression of ERGIC-53. All cell lines were cultured at 37°C in a humidified incubator containing 5% CO_2. JUNV C#1 was provided by R. Tesh (The University of Texas Medical Branch at Galveston) and M. J. Buchmeier (University of California, Irvine) and DANV by W. I. Lipkin (Columbia University). JUNV C#1, which is an attenuated vaccine strain, was originally derived from WT JUNV strain XJ and differs by 12 amino acids (Chosewood, Wilson, Centers for Disease Control and Prevention (U.S.), & National Institutes of Health (U.S.), 2009; Goni et al., 2006). Working stocks of infectious JUNV C#1 and DANV were generated in Vero E6 cells. Infectious titers of these viruses were determined via plaque assay on Vero E6 cells. VSVΔG encoding a GFP reporter has been described elsewhere (Takada et al., 1997) and was provided by M. Whitt (The University of Tennessee Health Science Center, Memphis, TN). An infectious stock of VSVΔG pseudotyped with VSV G was generated by first transfecting HEK 293T cells with a pCAGGS plasmid encoding VSV G and then 24 hr later inoculating these cells with infectious VSVΔG (which had previously been pseudotyped with VSV G) at a multiplicity of infection (MOI) of 3. Supernatants were collected 24 hr following inoculation and infectious titer was determined by enumerating green foci via focus assay in Vero E6 cells.

Plasmids and Transfections

To identify and/or validate the interaction of human proteins, including ERGIC-53, with various viral GPs in Figures 1, 3, 6, S1, and S6, we subcloned each respective viral GP into our previously described pCAGGS expression vector (C. T. Cornillez-Ty, L. Liao, J. R. Yates, 3rd, P. Kuhn, & M. J. Buchmeier, 2009). This vector expresses each GP as a fusion protein containing 3 C-terminal elements: a hemaglutinin (HA) epitope tag (YPYDVPDYA) followed by the tobacco etch virus (TEV) cleavage site (ENLYFQG) followed by a 23 amino acid biotin acceptor peptide (BAP) (MASSLRQILDSQKMEWRSNAGGS). When co-transfected with a second plasmid that encodes the bacterial biotin ligase BirA, the BAP can be biotinylated for affinity purification with streptavidin beads. GPs were subcloned into this vector using Gateway Technology (Invitrogen) following the manufacturer's instructions. Briefly, each GP was first amplified via PCR using forward and reverse primers containing *att*B1 and *att*B2 sequences, respectively. In each case, the stop codon was excluded. PCR products were subcloned into pDONR221 via a BP recombination reaction. GP genes were then subcloned from pDONR221 into the modified pCAGGS vector via an LR recombination reaction. The nucleotide sequence of each GP clone was verified by DNA sequencing. GPs were subcloned from the following viral strains (for each GP, an NCBI Gene Identifier number and a Protein Locus number are listed to provide a link to the actual nucleotide sequence cloned for that particular GP and the corresponding translated amino acid sequence, respectively): ANDV strain CHI-7913 (30313864, AAO86638), SNV NMR11 (999407 (note that there are two silent mutations in our clone: G changed to T and A changed to C at positions 60 and 843, respectively, of referenced sequence), AAC42202), LASV strain Josiah (23343509, NP_694870), LCMV strain Armstrong 53b

(61655715, AAX49341), JUNV strain XJ (also referred to as Parodi) (see (Reignier et al., 2006) for description of the nucleotide sequence; the amino acid sequence of the cloned gene matches JVU70799), JUNV strain C#1 (52222815, AAU34180), MACV strain Carvallo (see (Reignier et al., 2006) for description of nucleotide sequence, the amino acid sequence of the cloned gene matches AAN09942); GTOV strain INH-95551 (22901284, AAN09938), WWAV strain AV 9310135 (14333982, AAK60497), SARS CoV S from strain Tor2 (JX163924, AFR58686), influenza HA from strain A/WSN/33 (CY010788, ABF47955), EBOV strain Zaire (EBORNA, AAB81004), and MARV strain Musoke (DQ217792, ABA87127). Each of these GPs, with the exception of LCMV GP, JUNV XJ GP, MACV GP, SARS CoV S, influenza virus A/WSN/33 HA, EBOV GP, and MARV GP was synthesized by Bio Basic Inc. (Markhamm, ON). The LCMV strain Armstrong GP gene was provided by J. C. de la Torre (The Scripps Research Institute, La Jolla) while the JUNV strain XJ GP and MACV strain Carvallo GP were provided by P. Cannon (University of Southern California, Los Angeles). The MARV GP in pCAGGS and EBOV GP in pcDNA3.1 were obtained through BEI Resources, NIAID, NIH, Manassas, VA (NR-19815 and NR-19814, respectively). The SARS CoV S was provided by M. J. Buchmeier (University of California, Irvine) while the influenza virus A/WSN/33 HA in pCAGGS was provided by M. Shaw and A. Garcia-Sastre (Mount Sinai School of Medicine, New York). For the VSV pseudotyping experiments in Figures 3 and S3, we utilized standard pCAGGS vectors encoding VSV G (provided by J. C. de la Torre (Lee, Perez, Pinschewer, & de la Torre, 2002)) or EBOV GP (NR-19814, BEI Resources), our modified pCAGGS vector encoding SARS CoV S, and a pSA90 vector encoding JUNV XJ GP provided by P. Cannon (Reignier et al., 2006). The pCAGGS

VSV G plasmid was also used for the immunoprecipitation experiments to screen for an interaction between VSV G and ERGIC-53 in Figures 3E and 3F. For the viral challenges (Figures 2, 3, S2, and S3), GP interaction (Figures 3G-3J), GP trafficking (Figures 4A and 4B), hTfR1 trafficking (Figure S4), and VLP experiments (Figure 4C) we utilized pCDNA3 GM (which encodes WT ERGIC-53 with an N-terminal c-Myc tag) and/or pECE KKAA (which encodes the DN ERGIC-53 with an N-terminal c-Myc tag; the 2 C-terminal phenylalanines of this ERGIC-53 gene have been replaced with alanines) plasmids that were provided by H. P. Hauri (University of Basel, Basel, Switzerland) (Itin, Schindler, & Hauri, 1995b). For the VLP experiments, we also utilized our modified pCAGGS vector encoding JUNV strain XJ13 Z (this gene was synthesize by Bio Basic Inc. and subcloned via Gateway Technology) (33868610, AAQ55249 as well as JUNV XJ GP with a modified series of C-terminal epitope tags (HA followed by FLAG). We have previously described the panel of ERGIC-53 plasmids that were utilized to determine the molecular basis for the JUNV GP - ERGIC-53 association in Figures 6 and S6 (Zheng, Liu, Yuan, et al., 2010). Briefly, the WT and ERGIC-53 mutants were cloned into the pED plasmid by replacing the ERGIC-53 signal sequence with that of calreticulin (CRT) and introducing a FLAG epitope directly after the signal sequence. The mutant plasmids used were ΔCRD (R44-E269), ΔHelix (G271-N457), ΔHM (G271-N457 and C466A/C475A), C466A/C475A, N156A, D181A, KKAA (the 2 C-terminal phenylalanines were replaced with alanines), Δβ1 (H43-Q59), Δβ2 (H43-N72), Δβ3 (H43-S76), and Δβ4 (H43-A83) (a schematic of each mutant is shown in Figures 6A and S6A; a detailed description of each mutant is provided in the Figure S6A legend). All transfections were done using either Fugene HD (4709713001, Roche

Applied Science, Indianapolis, IN) (3 µl Fugene HD per 1 µg DNA) or Polyethylenimine (PEI) (23966, Polysciences, Inc., Warrington, PA) (5 µl PEI (from a 1 mg/ml solution in PBS (10010049, Invitrogen)) per 1 µg DNA).

Affinity Purification of Viral GPs

To capture biotinylated viral GPs for the identification of human protein partners via mass spectrometry (Figures 1A, 1B, S1B, and S1C) or validation of protein partners via Western blot (Figures 1D, 1F, 1G, and S1E), HEK 293T cells were co-transfected with our modified pCAGGS plasmid that encodes each respective viral GP with a C-terminal HA epitope tag and a BAP, and a second plasmid that encodes BirA to facilitate biotinylation of the viral GPs. As a control for the mass spectrometry studies and APs done to validate an interaction between a given viral GP and endogenous ERGIC-53, cells were co-transfected with the BirA plasmid and an empty pCAGGS plasmid. For the experiments to screen for an association between ERGIC-53 and coronavirus, orthomyxovirus, or filovirus GPs in Figures 3G and 3I, in addition to receiving the GP and BirA plasmids, cells were also transfected with pCDNA3 GM plasmid encoding WT ERGIC-53. For the experiments to map the molecular basis for the interaction between JUNV GP and ERGIC-53 in Figures 6 and S6, in addition to receiving the GP and BirA plasmids, cells were also transfected with a third plasmid encoding either the WT or one of mutant FLAG-tagged, ERGIC-53 proteins. In each case, cells were scraped into the media 48 hr following transfection, pelleted, washed with cold PBS, and then gently lysed on ice in 25 mM Tris-HCL, pH 7.6 containing 1% Triton X-100 (T9284, Sigma-

Aldrich, St. Louis, MO), 0.5% Nonidet P-40 IGEPAL CA-630 (198596, MP Biomedicals, Solon, OH), 140mM NaCl, 1 mM calcium chloride (21115, Sigma-Aldrich), and a Complete Mini EDTA-Free Protease Inhibitor Cocktail tablet (04693159001, Roche Applied Science). Cell lysates were clarified of insoluble material by centrifugation at 10,000 rpm at 4°C followed by incubation with magnetic streptavidin beads (Dynabeads MyOne Streptavidin T1, 65602, Invitrogen) on a rotating platform for 2.5 hours at 4°C. Following 4 washes in ice cold lysis buffer to remove nonspecific proteins, each captured viral GP and its associated cellular protein partners were stripped from the streptavidin beads by boiling the beads in Laemmli buffer containing 5% β-mercaptoethanol and separated by size and charge on Novex 4-20% Tris-Glycine polyacrylamide gels (EC60285BOX, Invitrogen) for either Western blot analysis to confirm bait/prey purification or Coomassie staining for mass spectrometry analysis (described in next section).

Mass Spectrometry

To identify human protein partners of LCMV GP or ANDV GP in Figures 1A, 1B, S1B, and S1C, HEK 293T cells were co-transfected with our modified pCAGGS plasmid encoding each respective viral GP with a C-terminal HA epitope tag and a biotin acceptor peptide (BAP) and a second plasmid encoding BirA to ensure biotinylation of the viral GPs. As a control, cells were co-transfected with the BirA plasmid and an empty vector. Two days later, biotinylated GPs and associated host proteins were affinity purified (AP)

from whole cell lysates as described above, run out on a Novex 4-20% Tris-Glycine polyacrylamide gel, stained with Coomassie stain (0.1% Brilliant Blue R (B7920, Sigma-Aldrich) in 40% methanol with 20% acetic acid) diluted in 30% methanol with 10% acetic acid solution to 20% v/v overnight at room temperature, and then destained for 4 to 6 hr in 30% methanol with 10% acetic acid solution. Each gel lane was cut into 15 (LCMV GP) or 14 (ANDV GP) sections (see Figures S1B and S1C for cut maps) for in-gel digestion of captured proteins using Sequencing Grade Modified Trypsin (V5111, Promega, Madison, WI 6 ng/μL) in 50 mM ammonium bicarbonate overnight at 37°C as previously described (Ballif, Cao, Schwartz, Carraway, & Gygi, 2006). Peptides were extracted from gel sections with 50% acetonitrile (MeCN) and 2.5% formic acid (FA) and then dried. Peptides were then resuspended in 2.5% MeCN and 2.5% FA and loaded onto a microcapillary column packed with 12 cm of reversed-phase Magic C18 material (5 μm, 200 Å, Michrom Bioresources, Inc., Auburn, CA) using a MicroAS autosampler (Thermo Scientific, Pittsburgh, PA). Elution was performed with a 5−35% MeCN (0.15% FA) gradient using a Surveyor Pump Plus HPLC (Thermo Scientific) over 40 min, after a 15 min isocratic loading at 2.5% MeCN and 0.15% FA. Mass spectra were acquired in an LTQ-XL linear ion trap mass spectrometer (Thermo Scientific) over the entire run using 10 MS/MS scans following each survey scan. Raw data were searched against the human IPI forward and reverse concatenated databases using SEQUEST software requiring tryptic peptide matches with a 2 Da mass tolerance. Cysteine residues were required to have a static increase in 71.0 Da for acrylamide adduction, and differential modification of 16.0 Da on methionine residues was permitted. Host proteins were considered legitimate GP protein partners if 2 or more unique tryptic peptides were detected from a

host protein in samples transfected with a given GP plasmid but not the empty vector or, alternatively, if there was a 5-fold higher quantity of total tryptic peptides detectable from a given human protein in a GP sample compared to the empty vector sample. These filters resulted in a false discovery peptide rate of less than 1%.

Immunoprecipitations

Whole cell protein lysates used for immunoprecipitation studies were generated as described above in the "Affinity Purification of Viral GPs" section. Following centrifugation at 10,000 rpm at 4°C to remove insoluble material, protein lysates were pre-cleared by incubating them with magnetic Protein G beads (Dynabeads Protein G beads, 10004D, Invitrogen) on a rotating platform for 15 minutes at 4°C. Each cleared lysate was then incubated (on a rotating platform) with its respective antibody for 2 hr followed by magnetic Protein G beads for 1 hr. The beads were then washed 4 times with ice cold lysis buffer to remove nonspecific proteins and excess antibody. Captured bait proteins and their associated protein partners (prey) were stripped from the beads by boiling them in Laemmli buffer (with or without 5% β-mercaptoethanol) and separated by size and charge on gradient Novex 4-20% Tris-Glycine polyacrylamide gels for Western blot analysis to confirm bait/prey purification. Immunoprecipitations from cellular protein lysates were carried out using the following antibodies: ERGIC-53 was immunoprecipated with either the mouse anti-ERGIC-53 G1/93 antibody (ALX-804-602-C100, Enzo Life Sciences Farmingdale, NY) (Figures 1E, 1I-1K, 3F, 3H, 3J, S1G and S1H) or a rabbit anti-ERGIC-53 antibody (sc-66880, Santa Cruz, Dallas, TX) (Figure S1F and S1I); VSV G with the mouse anti-VSV G antibody (11 667 351 001, Roche

Applied Science) (Figure 3E); JUNV GP with the mouse anti-GP1/GPC antibody GB03-BE08 (NR-2564, BEI Resources) (Figure 1H); or, as a control, a species matched, non-immune Mouse IgG1 Isotype (MAB002, R&D Systems Minneapolis, MN) (Figures 1K and S1H).

To purify intact JUNV C#1 particles in Figure 5D, supernatant from JUNV C#1-infected Vero E6 cells was collected 72 hr post-inoculation, cleared of cells by centrifugation at 1400 RPM, then pre-cleared with magnetic Protein G beads, incubated with the GP1-specific mouse monoclonal antibody QC03-BF11 (NR-2566, BEI Resources) for 2 hr followed by magnetic Protein G beads for 1 hr. The beads were washed 4 times with PBS containing 0.1% BSA and 1 mM calcium chloride and then boiled in Laemmli buffer to elute/lyse the captured viral particles. The collected lysate was then electrophoresed on a Novex 4-20% Tris-Glycine polyacrylamide gel for Western blot analysis. Controls for this experiment included the use of the GP1-specific antibody with supernatants from mock-infected cells as well as using the MAB002 Mouse IgG1 Isotype Control antibody for immunoprecipitation from the JUNV C#1-infected supernatants.

SDS-PAGE and Western Blot

Protein lysates were separated by SDS-PAGE using Novex 4-20% Tris-Glycine polyacrylamide gels. Protein transfer to nitrocellulose membranes was accomplished using the iBlot Gel Transfer Device and iBlot Transfer Stack nitrocellulose membranes (IB3010-01) from Invitrogen according to the manufacturer's instructions. Following

transfer, membranes were blocked by rocking in a solution of 5% milk in PBS for 1 hour at room temperature followed by 3 washes with Western wash solution (PBS with 0.5% Nonidet P-40 IGEPAL CA-630). Primary antibodies were diluted in antibody diluent (PBS containing 5% milk, 3% FBS, and 0.05% Nonidet P-40 IGEPAL CA-630) and incubated overnight at room temperature. Following 3 washes in Western wash, membranes were incubated with secondary antibodies diluted in antibody diluent for 2 hr at room temperature, followed by 3 final washes in Western wash. Membranes were then developed using chemiluminescence (SuperSignal West Pico (34080) or Femto (34096) Chemiluminescent Substrate, Thermo Scientific). The membranes that were visualized via an Odyssey Infrared Imaging System (LI-COR Biosciences, Lincoln, NE) in Figures 6 and S6 were treated as described above with the following changes: the antibody diluent for the primary antibodies was PBS containing 5% milk and 0.05% Nonidet P-40 IGEPAL CA-630, the antibody diluent for the secondary antibodies was PBS containing 5% milk, 0.02% SDS, and 0.05% Nonidet P-40 IGEPAL CA-630, while the final wash was done using PBS.

Primary antibodies (and the dilutions they were used at) were: G1/93 mouse anti-ERGIC-53 (1:500), sc-66880 rabbit anti-ERGIC-53 (1:4,000), QC03-BF11 mouse anti-JUNV GPC/GP1 (1:5,000), GB03-BE08 mouse anti-JUNV GPC/GP1 (1:500), 11 667 351 001 mouse anti-VSV G antibody (1:1,000), 9B11 mouse anti-Myc (2276, Cell Signaling, Danvers, MA) (1:3,000), 71D10 rabbit anti-Myc (2278, Cell Signaling) (1:4,000), NA05-AG12 mouse anti-JUNV NP (NR-2582, BEI Resources) (1:200), clone M2 mouse anti-FLAG (F1804, Sigma-Aldrich) (1:3,000), SPA-600 rabbit anti-CRT

(Stressgen, Ann Arbor, MI) (1:4,000), Clone AC-15 mouse anti-β-Actin (A5441, Sigma-Aldrich) (1:5,000), HA.11 Clone 16B12 mouse anti-HA (MMS-101P, Covance Emeryville, CA) (1:4,000), and rabbit anti-JUNV Z (1:2,000) (provided by Sandra Goñi and described in (Goni et al., 2010)). Detection of native JUNV C#1 GPC/GP1 using GB03-BE08 or QC03-BF11 was done under non-reducing conditions.

Secondary antibodies used for chemiluminescence were: goat anti-mouse IgG HRP conjugate (H+L) (71045, EMD Millipore, Billerica, MA) (1:10,000), goat anti-mouse light chain IgG HRP conjugate light chain specific (AP200P, EMD Millipore) (1:50,000), Peroxidase-AffiniPure Goat Anti-Rabbit IgG (H+L) (111035045, Jackson, West Grove, PA) (1:10,000), mouse anti-rabbit light chain IgG HRP (211032171, Jackson) (1:50,000).

Secondary antibodies used for LI-COR were: IRDye 800CW Goat Anti-Rabbit IgG (H+L) (926-32211, LI-COR) (1:20,000), IRDye 800CW Goat Anti-Rabbit IgG (H+L) (926-32210, LI-COR) (1:20,000), and IRDye 680CW Goat Anti-Rabbit IgG (H+L) (926-68070, LI-COR) (1:20,000).

Viral Challenge Assays

A series of viral challenge assays were conducted to determine how various manipulations of ERGIC-53 (siRNA silencing of ERGIC-53, overexpression of WT ERGIC-53, expression of DN ERGIC-53, or loss of ERGIC-53 expression due to null mutation of *LMAN1*) would impact the ability of viruses (JUNV C#1, DANV, or VSVΔG pseudotyped with VSV G, SARS CoV S, EBOV GP or JUNV XJ GP) to release

infectious progeny. At each time point examined in the various assays, supernatants and cells were collected (from each replicate well) to measure infectious virus or protein expression levels, respectively. Supernatants were clarified via centrifugation at 2000 RPM for 5 minutes and then screened for infectious virus via plaque assay (JUNV C#1 and DANV) or focus forming assay (pseudotyped VSVΔG). To generate protein lysates, cells were scraped into PBS, combined with any cells that pelleted while clarifying the supernatants, pelleted by centrifugation at 2000 RPM, and then lysed on ice in 25 mM Tris-HCL, pH 7.6 containing 1% Triton X-100, 0.5% Nonidet P-40 IGEPAL CA-630, 140 mM NaCl, and a Complete Mini EDTA-Free Protease Inhibitor Cocktail tablet. Lysates were clarified of insoluble material by centrifugation at 10,000 rpm at 4°C and run on Novex 4-20% Tris-Glycine polyacrylamide gels for Western blot analysis. For selected challenge assays described below, we utilized the unpaired Student's *t* test to determine whether statistically significant differences existed between the quantities of infectious virus released from control versus experimental groups as indicated in the Figure legends.

For the siRNA challenge experiments shown in Figures 2A and S2A, HEK 293T cells were plated in 6-well plates, reverse transfected with 25 nM of either an ERGIC-53-specific siRNA (5'-GGACAGAAUCGUAUUCAUCdTdT-3' as sense and 5'-AUGAAUACGAUUCUGUCCdTdT-3' as antisense) (B. Nyfeler et al., 2006) or a scrambled, negative control siRNA (Allstars Negative Control siRNA, 1027280, Qiagen, Valencia,

CA) using HiPerFect Transfection Reagent (301705, Qiagen) according to the

manufacturer's instructions. Cells were challenged 72 hr later with JUNV C#1 at an MOI of 0.1. Supernatants and cell protein lysates were collected at 24, 48, and 72 hr post-inoculation (96, 120, and 144 hr post-transfection with siRNA, respectively) and screened for JUNV C#1 plaque forming units (PFU) via plaque assay or ERGIC-53 and CRT (loading control) expression via Western blot. Prior to carrying out the viral challenge, we determined, using the ERGIC-53-specific siRNA, the timeframe post-transfection that would yield optimal ERGIC-53 knock-down. Using Western blot as a read out, we observed silencing of ERGIC-53 in HEK 293T cells from 48 to 144 hr post-transfection (data not shown).

For the overexpression challenge experiments shown in Figures 2B and S2B, HEK 293T cells were plated in 6-well plates, transfected the next day with a plasmid encoding Myc-tagged, WT ERGIC-53 or an empty vector, and challenged 1 day later with JUNV C#1 at an MOI of 0.1. Supernatants and cell protein lysates were collected at 24, 48, and 72 hr post-inoculation and screened for JUNV C#1 PFU via plaque assay or Myc-WT ERGIC-53 and CRT (loading control) expression via Western blot.

For the DN ERGIC-53 challenge assays shown in Figures 2C, 2D, S2C, and S2D, HEK 293T cells were plated in 24-well plates, transfected the next day with a plasmid encoding Myc-tagged, DN ERGIC-53 or an empty vector, and challenged 1 day later with JUNV C#1 or DANV at an MOI of 0.1 or 0.001, respectively. Supernatants and cell protein lysates were collected at 48 and 72 hr post-inoculation for JUNV C#1 or 48 hr post-inoculation for DANV and screened for PFU via plaque assay or Myc-DN ERGIC-53 and CRT (loading control) expression via Western blot.

For the ERGIC-53 null cell line challenge assays shown in Figures 2E and S2E, EBV-immortalized B lymphoblastoid cell lines derived from 1 normal (*LMAN1*$^{+/+}$; 2829-D) or 2 ERGIC-53 null (*LMAN1*$^{-/-}$; CRC-78 and CRC-79) individuals were seeded in a 24-well plate and challenged with JUNV C#1 at an MOI of 1. Supernatants and cell protein lysates were collected 72 hr post-inoculation and screened for PFU via plaque assay or ERGIC-53 and actin (loading control) expression via Western blot.

For the VSVΔG pseudotyping challenge assays shown in Figures 3A-3D and S3, HEK 293T cells were initially transfected with a plasmid encoding Myc-tagged WT or DN ERGIC-53, then 24 hr later the WT and DN ERGIC-53 cells were transfected with a plasmid encoding VSV G, JUNV XJ GP, SARS CoV S, or EBOV GP. Twenty-four hr following the final transfection, cells were challenged with VSVΔG (that had been previously pseudotyped with VSV G) at an MOI of 2. Supernatants and cell protein lysates were collected 24 hr later and screened for infectious VSVΔG particles pseudotyped with VSV G, JUNV XJ GP, SARS CoV S, or EBOV GP via focus assay and Myc-ERGIC-53 (WT or DN) or CRT (loading control) via Western blot, respectively.

For the ERGIC-53 null cell line challenge assays shown in Figures 4D-4G, EBV-immortalized B lymphoblastoid cell lines derived from a normal (*LMAN1*$^{+/+}$; 2829-D) or ERGIC-53 null (*LMAN1*$^{-/-}$; CRC-78) individual were seeded in T-75 flasks and challenged or not (mock) with JUNV C#1 at an MOI of 0.1. Supernatants were collected 96 hr post-inoculation, concentrated via ultracentrifugation as described below, and screened for PFU via plaque assay, JUNV proteins (GP1, NP, and Z) or cellular proteins (ERGIC-53 and actin (loading control)) via Western blot, and viral S segment genomic

RNA via quantitative RT-PCR (as described below). RNA was extracted from each viral preparation using the QIAamp Viral RNA Mini Kit (52906, Qiagen) according to the manufacturer instructions. Virion preparations were also screened for their ability to bind host cells in a virus-cell binding assay (described below).

Virus-Cell Binding Assay

To determine whether the viral particles produced in EBV-immortalized B lymphoblastoid cell lines derived from a normal (*LMAN1*$^{+/+}$; 2829-D) or ERGIC-53 null (*LMAN1*$^{-/-}$; CRC-78) individual had differing capacities to bind host cells in Figure 4G, we chilled Vero E6 cells grown in 48-well plates to 4°C, washed them twice with PBS, and then incubated duplicate wells with each viral preparation for 1.5 hrs at 4°C. Unbound virus was then aspirated and each well was washed 3 times in PBS. Following the final wash, total RNA was extracted from each monolayer using the RNeasy Mini Kit (74106, Qiagen) according to the manufacturer instructions. RNA samples were then subjected to quantitative RT-PCR, as described below, to determine the copies of JUNV C#1 S segment genomic RNA.

Quantitative RT-PCR

To enumerate quantities of JUNV C#1 viral S segment genomic RNA, cDNA was generated using 200 nM of primer 5'-AAGGGTTTAAAAATGGTAGCAGAC-3', which is specific for the NP region of the S segment genomic (negative-sense) RNA, with Multiscribe-RT (4311235, Life Technologies, Carlsbad, CA). Reaction conditions were 25^{o}C for 10 min, 48^{o}C for 30 min, and 95^{o}C for 5 min. Quantitative PCR was then

performed using a primer-probe set originally described in (Trombley et al., 2010). Specifically, we used forward primer (900 nM) 5'-CATGGAGGTCAAACAACTTCCT-3', reverse primer (900 nM) 5'-GCCTCCAGACATGGTTGTGA-3', and probe (200 nM) 5'-6FAM-ATGTCATCGGATCCTT-MGBNFQ-3'. Note that the forward primer differs by 1 nt from the originally reported sequence. Reactions were carried out using Taqman Universal PCR Master Mix (4326614, Life Technologies). Reaction conditions were 95^{o}C for 10 min and 45 cycles of 95^{o}C for 15 sec and 60^{o}C for 1 min. Absolute copy numbers of JUNV C#1 S segment genomic RNA were determined by comparison with a series of standard dilutions of the our modified pCAGGS plasmid encoding the JUNV C#1 NP gene. Data was acquired using an Applied Biosystems StepOnePlus Real-Time PCR System and analyzed with the provided StepOne software.

Virus-Like Particle (VLP) Assay

For the VLP assays shown in Figure 4C, HEK 293T cells were initially transfected with a plasmid expressing Myc-tagged WT or DN ERGIC-53, then 24 hr later with a cocktail of 2 plasmids encoding the JUNV Z and XJ GPC proteins, respectively, to permit the formation and release of VLPs. Cells and supernatants were collected 72 hr later and screened for the presence of various GP species (the C-terminally FLAG-tagged precursor GPC or proteolytically processed GP2) or actin (to serve as a loading control) via Western blot. Cells were collected as described above in the "Viral Challenge Assay" section. VLPs were concentrated from supernatants via ultracentrifugation through sucrose (as described below) prior to Western blot analysis.

Ultracentrifugation of VLPs and Authentic JUNV C#1 Particles

The JUNV VLPs in Figure 4C and JUNV C#1 particles in Figure 4D were concentrated via ultracentrifugation through sucrose as previously described (Neuman, Adair, Yeager, & Buchmeier, 2008). Briefly, supernatants were clarified of cellular debris via 2 rounds of centrifugation at 1500 rpm and 2500 rpm, respectively. VLPs/particles were then precipitated by dissolving polyethylene glycol MW 8,000 (81268, Sigma-Aldrich) into clarified supernatants (10% weight/volume) at 4^{o}C. Supernatants were then centrifuged at 10,000 RPM for 30 minutes at 4^{o}C to pellet VLPs/particles. Pellets were gently resuspended in HEPES buffered saline, pH 7.4, layered onto 20% sucrose, and centrifuged at 100,000 x g in a T-865 Rotor (Thermo Scientific) for 2.5 hr at 4^{o}C. Pelleted virus was gently resuspended in HEPES buffered saline, pH 7.4 for use in plaque and/or Western blot assays.

Confocal Microscopy

Confocal microscopy was used to visualize the localization of JUNV C#1 GP and ERGIC-53 in HEK 293T cells (either internally, at the plasma membrane, or a combination of internal/surface staining) or JUNV C#1 NP and ERGIC-53 in virions. For the internal staining of JUNV C#1 GP and endogenous ERGIC-53 shown in Figure 1L, HEK 293T cells were seeded onto 22 mm glass cover slips (12-541-B, Thermo Scientific) within 6-well dishes, inoculated or not (mock) the next day with JUNV C#1 at an MOI of 0.1, then 72 hr later washed with PBS, fixed with Z-FIX (174, ANATECH,

Battle Creek, MI), permeabilized in PBS with 0.1% Triton X-100 and 1% BSA, then blocked in PBS containing 3% FBS and 10% normal goat serum (005-000-121, Jackson) for 30 minutes at room temperature. Cells were then incubated with a 1:500 dilution of the G1/93 mouse anti-ERGIC-53 antibody in PBS containing 1% BSA and 0.1% Triton X-100 overnight at 4^{o}C. Cells were then washed 3 times with PBS containing 0.1% BSA and incubated with Alexa Fluor 647-conjugated goat anti-mouse IgG (H+L) (A-21236, Invitrogen). After 3 washes in PBS containing 0.1% BSA, cells were incubated with a 1:50 dilution of the GB03-BE08 mouse anti-JUNV GP1/GPC antibody that had been directly conjugated to Alexa Fluor 488. Cover slips were washed 3 times with PBS, stained with 4', 6-diamidino-2-phenylindole hydrochloride (DAPI) (D9542, Sigma Aldrich), washed 3 times with PBS, and then mounted onto glass slides using ProLong Gold Antifade Reagent (P36934, Invitrogen).

The intracellular and surface staining of JUNV C#1 GP and endogenous ERGIC-53 shown in Figures 5A and 5B, respectively, was accomplished by seeding HEK 293T cells in T-75 flasks and then inoculating them or not (mock) the next day with JUNV C#1 at an MOI of 0.1. Cells were trypsinized 2 days later (at 48 hr post-inoculation), reseeded onto 22 mm glass cover slips within 6-well dishes, and at 72 hr post-inoculation either a) fixed, permeabilized, and blocked in an identical manner described above for internal staining or b) incubated at 4^{o}C for surface staining. Following blocking, internal staining was done by incubating cells with a 1:500 dilution of the GB03-BE08 mouse anti-JUNV GP1/GPC antibody and a 1:200 dilution of the sc-66880 rabbit anti-ERGIC-53 antibody in PBS with 1% BSA overnight at 4^{o}C. After 3 washes in PBS with 0.1% BSA, cells

were incubated with a 1:800 dilution of both the Alexa Fluor 488-conjugated Goat Anti-Mouse IgG (H+L) (A-11029, Invitrogen) and Alexa Fluor 647-conjugated Goat Anti-Rabbit IgG (H+L) (A-21245, Invitrogen) antibodies. For the live-cell surface staining, cells were incubated with a 1:50 dilution of the GB03-BE08 mouse anti-JUNV GP1/GPC antibody and a 1:50 dilution of the sc-66880 rabbit anti-ERGIC-53 antibody in PBS with 3% FBS and 10% normal goat serum for 20 minutes at 4^{o}C. After 3 washes in PBS with 3% FBS, cells were incubated with a 1:200 dilution of both the Alexa Fluor 488-conjugated Goat Anti-Mouse IgG (H+L) and Alexa Fluor 647-conjugated Goat Anti-Rabbit IgG (H+L) antibodies. In both staining protocols, cells were washed 3 times following incubation with the secondary antibodies, stained with DAPI, washed 3 times with PBS, and then mounted onto glass slides using ProLong Gold Antifade Reagent. As a control, cells were surface stained for JUNV C#1 GP and CRT using a 1:50 dilution of the SPA-600 rabbit anti-CRT antibody (Figure 5C). The protocol was the same with the exception of replacing the ERGIC-53-specific antibody with the CRT-specific antibody.

The surface staining of JUNV C#1 GP and intracellular staining of either Myc-tagged WT or DN ERGIC-53 shown in Figure 4A was accomplished by seeding HEK 293T cells in T-75 flasks, transfecting them with plasmids encoding either Myc-tagged WT or DN ERGIC-53, then 1 day later inoculating them with JUNV C#1 at an MOI of 0.1. Cells were trypsinized 2 days later (at 48 hr post-inoculation) and reseeded onto 22 mm glass cover slips within 6-well dishes. At 72 hr post-inoculation cells were washed in PBS and then surface stained for JUNV GP1/GPC via incubation with a 1:50 dilution of the GB03-BE08 mouse anti-JUNV GP1/GPC antibody directly conjugated to Alexa

Fluor 488 in PBS containing 3% FBS for 20 minutes at 4°C. Cells were then washed 3 times in PBS and fixed using Z-FIX. Following fixation, cells were washed 2 times with PBS, permeabilized via incubation with PBS containing 0.1% Triton X-100 and 1% BSA for 10 minutes, washed 3 times with PBS containing 0.1% BSA, blocked for 30 minutes at room temperature with PBS containing 1% BSA and 10% normal goat serum, then stained for Myc-tagged WT or DN ERGIC-53 via overnight incubation at 4°C with a 1:200 dilution of the 71D10 rabbit anti-Myc antibody in PBS containing 0.1% BSA. Cells were washed 3 times in PBS containing 0.1% BSA, then incubated with a 1:800 dilution of the Alexa Fluor 647-conjugated goat anti-rabbit antibody in PBS containing 0.1% BSA for 2 hr, washed 3 times in PBS, stained with DAPI, washed 3 times in PBS, then mounted on glass slides using ProLong Gold Antifade Reagent.

Detection of ERGIC-53 in JUNV C#1 particles shown in Figure S5 was accomplished by incubating clarified media from either mock- or JUNV C#1-infected cells for 2 hr at 37°C in 35 mm glass bottom culture dishes (P356-1.5-10-C, MatTek Corporation, Ashland, MA) that had been coated with 0.01% Poly-L-Lysine (3438-100-01, Trevigen, Gaithersburg, MD). The JUNV C#1-containing media had a titer of ~1 x 10^7 PFU/ml. Viral particles were subsequently fixed by incubation in 4% paraformaldehyde for 30 minutes at room temperature, washed three times with 1X PBS, permeabilized in PBS containing 1% BSA and 0.1% Triton X-100 for 10 minutes at room temperature, and then blocked in PBS containing 1% BSA and 10% normal goat serum for 30 minutes at room temperature. Staining for JUNV NP and ERGIC-53 was done via incubation with a 1:200 dilution of the mouse anti-JUNV NP antibody NA05-AG12 (NR-

2582, BEI Resources) and a 1:100 dilution of a rabbit anti-ERGIC-53 antibody (raised by B.Z.) in PBS containing 1% BSA for 2 hours at room temperature. Following 3 washes in PBS with 0.1% BSA, the dishes were incubated with a 1:200 dilution of both the Alexa Fluor 488-conjugated Goat Anti-Mouse IgG (H+L) and Alexa Fluor 647-conjugated Goat Anti-Rabbit IgG (H+L) antibodies. The stained dishes were then washed 3 times in PBS and stored at 4°C prior to imaging in PBS.

Images for all confocal experiments were obtained using a Zeiss LSM 510 Laser Scanning Confocal Microscope. Images were captured using either a 63X or 100X objective lens with a numerical aperture of 1.4. Optical zoom was set to 1.5X and images were obtained at 1.0 Airy unit. The colocalization analysis shown in Figure 1L was performed with the colocalization analysis module contained in the Zeiss Aim software on images that were captured using the 63X objective lens. To determine background gating thresholds for colocalization analysis, we averaged the background signal from triplicate images of either mock-infected cells stained using the GB03-BE08 mouse anti-JUNV GP1/GPC antibody directly conjugated to Alexa Fluor 488 or JUNV C#1-infected cells stained with the Alexa Fluor 647-conjugated goat anti-mouse secondary antibody (gates are shown as white lines in the histogram in Figure 1L).

Flow Cytometry

Flow cytometry was utilized to screen, in cells expressing either WT or DN ERGIC-53, whether JUNV C#1 GP (Figure 4B) or hTfR1 (Figure S4) was detectable at the plasma

membrane and, if so, the median fluorescence intensity (MFI) of these respective signals. In both cases, HEK 293T cells were seeded in 6-well dishes and transfected the next day with plasmids encoding either Myc-tagged WT or DN ERGIC-53. To screen for surface expression of JUNV C#1 GP, cells were inoculated the next day with JUNV C#1 at an MOI of 1.0. At 72 hr post-inoculation the media was aspirated and cells detached from the plates by incubating them with Versene (2 mM EDTA in PBS) for 15 minutes at 37^{o}C. Cell pellets were washed 2 times with PBS and then surface stained for JUNV GP1/GPC via incubation with a 1:100 dilution of the GB03-BE08 mouse anti-JUNV GP1/GPC antibody directly conjugated to Alexa Fluor 488 in FACS buffer (PBS containing 2% fetal bovine serum and 0.2% sodium azide) for 20 minutes at 4^{o}C. Cells were then washed 3 times in FACS buffer, fixed/permeabilized in BD Cytofix/Cytoperm solution (554722, BD Biosciences, San Jose, CA) for 20 minutes at room temperature, washed 2 times in BD Perm/Wash buffer (554723, BD Biosciences), then stained for Myc-tagged WT or DN ERGIC-53 via a 20 minute incubation at 4^{o}C with a mouse anti-Myc antibody directly conjugated to Alexa Fluor 647 (2233, Cell Signaling) diluted 1:100 in Perm/Wash buffer. For the experiments looking at surface expression of hTfR1, 72 hr following transfection of the WT or DN ERGIC-53 plasmids, cells were collected and stained as described for JUNV C#1 GP with the exception of replacing the mouse-anti JUNV C#1 GP Alexa Fluor 488 antibody with a primary/secondary antibody combination consisting of a 1:100 dilution of an unlabeled A4A6 mouse monoclonal anti-hTfR1antibody provided by J. Cook (University of Kansas Medical Center, Kansas City, KS) and a 1:200 dilution of a goat anti-mouse antibody directly conjugated to R-

Phycoerythrin (P852, Invitrogen). Data was acquired on an LSR II (BD Biosciences) and analysis was done using FlowJo software (v9.6.2, TreeStar, Inc., Ashland, OR).

Supplemental References

Appenzeller-Herzog, C., Roche, A.C., Nufer, O., and Hauri, H.P. (2004). pH-induced conversion of the transport lectin ERGIC-53 triggers glycoprotein release. J Biol Chem 279, 12943-12950.

Appenzeller, C., Andersson, H., Kappeler, F., and Hauri, H.P. (1999). The lectin ERGIC-53 is a cargo transport receptor for glycoproteins. Nat Cell Biol 1, 330-334.

Ballif, B.A., Cao, Z., Schwartz, D., Carraway, K.L., 3rd, and Gygi, S.P. (2006). Identification of 14-3-3epsilon substrates from embryonic murine brain. J Proteome Res 5, 2372-2379.

Chosewood, L.C., Wilson, D.E., Centers for Disease Control and Prevention (U.S.), and National Institutes of Health (U.S.) (2009). Biosafety in microbiological and biomedical laboratories, 5th edn (Washington, D.C., U.S. Dept. of Health and Human Services, Public Health Service, Centers for Disease Control and Prevention, National Institutes of Health).

Cornillez-Ty, C.T., Liao, L., Yates, J.R., 3rd, Kuhn, P., and Buchmeier, M.J. (2009). Severe acute respiratory syndrome coronavirus nonstructural protein 2 interacts with a host protein complex involved in mitochondrial biogenesis and intracellular signaling. J Virol 83, 10314-10318.

Goni, S.E., Borio, C.S., Romano, F.B., Rota, R.P., Pilloff, M.G., Iserte, J.A., Tortorici, M.A., Stephan, B.I., Bilen, M.F., Ghiringhelli, P.D., et al. (2010). Expression and purification of Z protein from Junin virus. J Biomed Biotechnol 2010, 970491.

Goni, S.E., Iserte, J.A., Ambrosio, A.M., Romanowski, V., Ghiringhelli, P.D., and Lozano, M.E. (2006). Genomic features of attenuated Junin virus vaccine strain candidate. Virus Genes 32, 37-41.

Hauri, H.P., Kappeler, F., Andersson, H., and Appenzeller, C. (2000). ERGIC-53 and traffic in the secretory pathway. J Cell Sci 113 (Pt 4), 587-596.

Itin, C., Roche, A.C., Monsigny, M., and Hauri, H.P. (1996). ERGIC-53 is a functional mannose-selective and calcium-dependent human homologue of leguminous lectins. Mol Biol Cell 7, 483-493.

Itin, C., Schindler, R., and Hauri, H.P. (1995). Targeting of protein ERGIC-53 to the ER/ERGIC/cis-Golgi recycling pathway. J Cell Biol 131, 57-67.

Kappeler, F., Klopfenstein, D.R., Foguet, M., Paccaud, J.P., and Hauri, H.P. (1997). The recycling of ERGIC-53 in the early secretory pathway. ERGIC-53 carries a cytosolic endoplasmic reticulum-exit determinant interacting with COPII. J Biol Chem 272, 31801-31808.

Lee, K.J., Perez, M., Pinschewer, D.D., and de la Torre, J.C. (2002). Identification of the lymphocytic choriomeningitis virus (LCMV) proteins required to rescue LCMV RNA analogs into LCMV-like particles. J Virol 76, 6393-6397.

Neerman-Arbez, M., Johnson, K.M., Morris, M.A., McVey, J.H., Peyvandi, F., Nichols, W.C., Ginsburg, D., Rossier, C., Antonarakis, S.E., and Tuddenham, E.G. (1999). Molecular analysis of the ERGIC-53 gene in 35 families with combined factor V-factor VIII deficiency. Blood 93, 2253-2260.

Neuman, B.W., Adair, B.D., Yeager, M., and Buchmeier, M.J. (2008). Purification and electron cryomicroscopy of coronavirus particles. Methods Mol Biol 454, 129-136.

Neve, E.P., Lahtinen, U., and Pettersson, R.F. (2005). Oligomerization and interacellular localization of the glycoprotein receptor ERGIC-53 is independent of disulfide bonds. J Mol Biol 354, 556-568.

Nufer, O., Kappeler, F., Guldbrandsen, S., and Hauri, H.P. (2003). ER export of ERGIC-53 is controlled by cooperation of targeting determinants in all three of its domains. J Cell Sci 116, 4429-4440.

Nyfeler, B., Zhang, B., Ginsburg, D., Kaufman, R.J., and Hauri, H.P. (2006). Cargo selectivity of the ERGIC-53/MCFD2 transport receptor complex. Traffic 7, 1473-1481.

Reignier, T., Oldenburg, J., Noble, B., Lamb, E., Romanowski, V., Buchmeier, M.J., and Cannon, P.M. (2006). Receptor use by pathogenic arenaviruses. Virology 353, 111-120.

Takada, A., Robison, C., Goto, H., Sanchez, A., Murti, K.G., Whitt, M.A., and Kawaoka, Y. (1997). A system for functional analysis of Ebola virus glycoprotein. Proc Natl Acad Sci U S A 94, 14764-14769.

Trombley, A.R., Wachter, L., Garrison, J., Buckley-Beason, V.A., Jahrling, J., Hensley, L.E., Schoepp, R.J., Norwood, D.A., Goba, A., Fair, J.N., et al. (2010). Comprehensive panel of real-time TaqMan polymerase chain reaction assays for detection and absolute quantification of filoviruses, arenaviruses, and New World hantaviruses. Am J Trop Med Hyg 82, 954-960.

Velloso, L.M., Svensson, K., Pettersson, R.F., and Lindqvist, Y. (2003). The crystal structure of the carbohydrate-recognition domain of the glycoprotein sorting receptor p58/ERGIC-53 reveals an unpredicted metal-binding site and conformational changes associated with calcium ion binding. J Mol Biol 334, 845-851.

Zheng, C., Liu, H.H., Yuan, S., Zhou, J., and Zhang, B. (2010). Molecular basis of LMAN1 in coordinating LMAN1-MCFD2 cargo receptor formation and ER-to-Golgi transport of FV/FVIII. Blood 116, 5698-5706.

3. MOLECULAR DISSECTION OF THE ERGIC-53 CARGO RECEPTOR COMPLEX: IMPLICATIONS FOR THE ROLE OF MCFD2 IN VIRAL REPLICATION

Molecular dissection of the ERGIC-53 cargo receptor complex: implications for the role of MCFD2 in viral replication

Joseph P. Klaus[1], Nicole Bouffard[2], Philip Eisenhauer[1], Douglas Taatajes[2], Anne B. Mason[3], and Jason W. Botten[1]

Vermont Center for Immunology & Infectious Diseases, The University of Vermont College of Medicine, Burlington, VT 05405[1]

Corresponding author: Jason W. Botten

Vermont Center for Immunology & Infectious Diseases

The University of Vermont College of Medicine

Given Medical Building, D-405

Burlington, VT 05405-0068

Phone: 802-656-

Fax: 802-656-

Email: bottenj@uvm.edu

3.1. Abstract

The Arenaviridae are a family of zoonotic viruses able to cause a severe and often fatal disease in humans. Despite the morbidity and mortality caused by these pathogens, no FDA approved vaccines or effective antivirals exist. The simplicity of the viral proteome (4 ORFs from 2 RNA segments) suggests an extensive interplay between the viral and host proteomes. Identifying these host proteins and understanding their roles in viral replication and disease progression is a promising strategy to develop therapeutic interventions for arenavirus disease. Accordingly, we demonstrate a three-part macromolecular complex is formed by arenavirus envelope glycoproteins (GPs) and the Endoplasmic Reticulum (ER)- Golgi Intermediate Compartment 53 kilo-Dalton protein/ Multiple Coagulation Factor Deficiency Protein 2 (ERGIC-53/MCFD2) intracellular cargo receptor complex, which is involved in trafficking of a restricted number of cellular glycoproteins in the early secretory pathway, including coagulation factors V and VIII. Loss of MCFD2, or changing of its protein levels, though not affecting GP binding, potently regulates the ERGIC-53-dependent function of the intracellular cargo receptor in the production of infectious arenavirus, coronavirus, filovirus, and hantavirus particles. We show that MCFD2 expression is upregulated during arenavirus infection; addition of an O-glycosylated purified MCFD2 restricts virus propagation, and thereby represents a novel candidate for antiviral development. Collectively, these findings provide insight

into the biology of the ERGIC-53/MCFD2 axis in the extracellular space, and provide additional functionality to the cargo receptor complex.

3.2. Introduction

The Arenaviridae are a family of enveloped RNA viruses comprised of a number of human pathogens found within rodent populations in a variety of global settings (1). The zoonotic nature of the viruses, and the biology of their reservoir rodents (2, 3), has resulted in the emergence of new and re-emergence of existing human pathogens (4). Increased surveillance and detection capabilities have facilitated the detection of new arenavirus species approximately every 2-3 years (5). As such, there is a clear need to develop antiviral treatments for this family of viruses that cause significant morbidity and mortality annually (6). The Arenaviridae is comprised of a single genus that is subdivided into Old and New World groupings based on location, serological reactivity, and genome similarity (7). Pathogens in the Old World arenavirus grouping include Lassa virus (LASV), which is the predominant cause of human disease in the family (8, 9), and Lymphocytic choriomeningitis virus (LCMV), an under-reported pathogen able to cause aseptic meningitis as well as severe neurological abnormalities in a developing fetus (10, 11). Dandenong virus (DANV), an LCMV-like virus, along with LCMV, has been associated with severe and highly fatal outcomes in cases of organ transplantation (12-14). Pathogenic arenaviruses in the New World grouping include Junín, Chapare, Guanarito, Machupo, and White Water Arroyo viruses, which cause a severe hemorrhagic fever syndrome (1). Junín virus is unique amongst the Arenaviridae in that an attenuated vaccine strain has been developed, JUNV Candid1 (15), which currently has FDA investigational new drug (IND) status (16).

The limited arenavirus proteome consists of: an RNA-dependent RNA polymerase (L polymerase) responsible for viral genome transcription and replication, a viral nucleoprotein (NP) which encapsidates the RNA genome, a small zinc-binding matrix protein (Z) that drives budding and, along with NP, has been proposed to interfere with cellular immune responses (17-19), and lastly a tripartite envelope glycoprotein complex (SSP-GP1-GP2) formed from a precursor molecule (GPC) that is proteolyzed by the host signal peptidase (SPase) (20, 21), and site-1 protease (S1P) (22) to form the functional spike complex required for attachment and entry (17, 23). The simplicity of the arenavirus proteome suggests that these viruses have evolved highly multifunctional proteins that are able to effectively utilize a network of host-derived macromolecular complexes to accomplish their entry (24-26), biosynthesis (21, 22), and exit strategies (27) encoded for in such limited viral genomic space. We have recently utilized a proteomics screen to identify human proteins in complex with a prototypic arenavirus GP molecule. In doing so we uncovered a novel role for ERGIC-53 in the production of infectious arenaviruses, coronaviruses, and filoviruses. We found that ERGIC-53, during infection with an arenavirus, is relieved of its normal ER-ERGIC recycling program and gets packaged into arenavirus particles. Viral particles lacking ERGIC-53 were found to be non-infectious, in part, because of their inability to attach to host cells (28).

Given the importance of these findings for ERGIC-53 in viral propagation, and knowing that the protein forms a receptor complex, we wished to further investigate the function of the primary macromolecular complex formed by ERGIC-53 and MCFD2. ERGIC-53 is a type 1 transmembrane protein that cycles continuously between the ER

and ERGIC (29-31), under normal conditions, where it functions as an intracellular cargo receptor. ERGIC-53 can require a soluble cofactor, MCFD2, for binding to and moving a discreet subset of cellular glycoproteins via its calcium-sensitive lectin activity (32, 33). The cellular ligands dependent upon the complete complex are the coagulation factors V and VIII. Loss of ERGIC-53 in humans results in combined deficiencies of factor V and VIII (OMIM 2273000), a rare and often mild hemophilia which results in low serum concentration and activity of FV and FVIII (34, 35). A second genetic impairment causing F5F8D has been identified in the MCFD2 locus (36). The resulting genetic lesions result in either a loss of protein, or code for a protein no longer able to interact with ERGIC-53 (37). The ERGIC-53 cargo receptor complex is maintained in a calcium-dependent fashion via several intramolecular contact sites, and both Ca^{2+} and ligand binding cause conformational changes in its structure (38, 39). ERGIC-53 is able to bind to high mannose N-linked glycans in the absence of MCFD2 (40-42), however upon MCFD2 binding, it has been reported that ERGIC-53 has a higher affinity for its cognate glycans (43).

The precise molecular mechanisms involved in ERGIC-53's role in arenavirus attachment and entry are currently unknown. In the current study we have extended our analysis of ERGIC-53's function in arenavirus propagation to include the soluble cofactor MCFD2, and show that a three-part complex is formed between the GP, ERGIC-53 and MCFD2, that only occurs in the presence of ERGIC-53. We show that binding of MCFD2, minimally, to ERGIC-53 regulates the function of the complex in arenavirus propagation, and that MCFD2's antiviral function is conserved across not only

arenaviruses, but also coronavirus, filovirus, and hantavirus particles in a GP restricted fashion. We demonstrate that the addition of exogenous MCFD2 neutralizes cell-free arenaviruses, and also provide mechanistic insight into the orientation of the cargo receptor complex on arenavirus particles through the use of super resolution imaging.

3.3. Methods

3.3.1. Antibodies, Cells, Viruses and Plasmids

The following antibodies were used: HA.11 Clone 16B12 mouse anti-HA (MMS-101P, Covance Emeryville, CA) (1:4,000) was used to detect recombinant viral glycoproteins in Western Blot assays. Mouse anti MCFD2 and rabbit anti ERGIC-53, used in microscopic examination of endogenous MCFD2 and ERGIC-53 by confocal and STORM applications respectively, were the generous gift of Bin Zhang and have been previously described (28, 44). 9B11 mouse anti-Myc (2276, Cell Signaling, Danvers, MA) (1:3000) was used to detect myc-MCFD2 in Western Blot assays. Calreticulin was used as a calcium-sensitive lectin prey-control in Western blots and was detected using rabbit anti (CRT) SPA-600 (Stressgen, Ann Arbor, MI) at 1:4,000. Mouse monoclonal anti JUNV GP-1 QC03-BF11 and NP NA05-AG12 (NR-2566 and NR-2582, BEI resources) were used to detect intracellular GP (confocal analysis) and C#1 particles (NP dSTORM analysis). Recombinant ERGIC-53 was detected in Western blots using clone M2 mouse anti-FLAG (1:3,000) (F1804, Sigma-Aldrich), and rabbit anti-ERGIC-53 antibody (sc-66880, Santa Cruz, Dallas, TX) (1:4,000) was used to detect endogenous ERGIC-53 in Western blot assays. For a thorough description of each viral GP used :

JUNV XJ GP, JUNV C#1 GP, LASV GP, SARS S, ANDV GP, EBOV GP, MARV GP, FLUAV WSN33A HA, and VN HA, see the extended supplemental section of ref (28).

JUNV C#1, DANV, and recombinant VSVΔG have been previously described (28). JUNV C#1 was provided by R. Tesh (The University of Texas Medical Branch at Galveston) and M. J. Buchmeier (University of California, Irvine) and DANV by W. I. Lipkin (Columbia University). VSVΔG engineered to express a Green Fluorescent Protein (GFP) in lieu of its own native G protein was provided by M. Whitt (The University of Tennessee Health Science Center, Memphis TN).

All transfections were carried out using low-passage HEK293T/17 cells (CRL-11268, American Type Culture Collection, Manassas, VA). HEK293T cells were maintained in Dulbecco's Modified Eagle Medium (DMEM) supplemented with 10% fetal bovine serum, 1% Penicillin-Streptomycin, 1% MEM Non-Essential Amino Acids solution, 1% GlutaMax, and buffered with 1% Hepes. All cell culture reagents were purchased from Invitrogen (Carlsbad, CA). Vero cells were provided by J. Lindsay Whitton (The Scripps Research Institute, La Jolla, CA) were cultivated in DMEM supplemented with 10% FBS, 1% Penicillin-Streptomycin, and 1% Hepes. B-cells from either a healthy donor (MCFD2 $^{+/+}$) (2829D) or from F5F8D patients with MCFD2 mutations CRC80 (c.149+5G>A (family A32)) and 1258 (c.103delC (family A21)) have been previously described (36) and were cultured in RPMI 1640 containing 10% FBS, 1% Penicillin-Streptomycin, and 1% Hepes.

3.3.2. Transfections

All transfections were carried out using Polyethylenimine (PEI) (23966, Polysciences, Inc., Warrington, PA) using a ratio of 5μL PEI (1mg/mL stock brought up in PBS) to 1μg plasmid DNA.

3.3.3. Affinity Purifications

To determine the molecular basis for arenavirus glycoproteins binding to ERGIC-53 and MCFD2 we transfected into sub-confluent HEK293T/17 cells a PCAGGS expression plasmid previously described by Cornillez-Ty et al., into which we subcloned JUNV C#1 GP [synthesized via Bio Basic Inc (Markhamm, ON)] along with a plasmid encoding the bacterial biotin ligase BirA to ensure biotinylation of target GP molecules within cells. ERGIC-53 WT, ΔCRD, Δβ1, ΔHelix were all described previously (Zheng et al., 2010 and Klaus et al., 2013); FLAG-ERGIC-53 WT, ΔCRD, Δβ1, Δβ4, myc-MCFD2 WT, D89A, and D129E were the generous gift of Bin Zhang (Cleveland Clinic, Cleveland, OH) and have been previously described (Zheng et al., 2008) and (Klaus et al., 2013), and were co-transfected into cells with equal μg quantities. Following transfection, cultures were incubated for 48 hours at which point the cells were harvested as previously described (28). Clarified lysates were incubated with streptavidin-coated magnetic beads (Dynabeads MyOne Streptavidin T1, 65602, Invitrogen) at 4°C on a rotating platform for 2.5 hr to allow binding of biotinylated bait-prey protein complexes. The bead fractions were extensively washed with cold lysis buffer to remove unbound proteins, and proteins were eluted via boiling in Lammli buffer supplemented with fresh β-mercaptoethanol to 5%. Captured proteins were then analyzed by SDS PAGE on

Novex Tris-Glycine 4-20% precast gels (Invitrogen) and Western blot by probing for the different bait-prey combinations.

Co-immunoprecipitations in which exogenously added sMCFD2 was used as bait to examine its potential for binding ERGIC-53 released from cells, were carried out by first collecting supernatant from JUNV C#1, or mock, infected HEK cells cultured in Pro293 (protein free) medium (Lonza), and clarifying the supernatant of cellular debris by two centrifugation steps each 15 minutes at 1500 rpm in a refrigerated centrifuge. Following clarification, samples were pre-cleared of immunoglobulin binding proteins by incubation with Protein G beads (Dynabeads Protein G beads, 1004D, Invitrogen). Purified sMCFD2 (10 μg) was added to each condition in a buffer containing PBS supplemented with 0.05% BSA , 2.5 mM calcium chloride, and a Complete Mini EDTA-Free Protease Inhibitor Cocktail tablet (04693159001 Roche Applied Science), buffered with 1% Hepes pH 7.2. The supernatants were incubated for 2.5 hr on a rotating platform in the cold. To immunoprecipitate sMCFD2-ERGIC-53 protein complexes, mouse anti MYC mAb was added to each sample, and incubated for an additional 2 hr. Following the antibody incubation, Protein G magnetic beads were added to each condition and incubated for an additional 2 hr. Following extensive washing with cold wash buffer to remove non-specific bound proteins, the sMCFD2 captured complexes were concentrated on a magnetic column and then eluted by boiling in Lammeli buffer with 5% β-Me. Samples were then analyzed by SDS PAGE and Western blot for myc-MCFD2 (bait) and ERGIC-53 (prey).

3.3.4. SDS PAGE and Immunoblotting

SDS PAGE and Immunoblot analysis was performed as described by Klaus et al., 2013.

3.3.5. Production of sMCFD2

Purification of secreted human MCFD2 was accomplished by transfecting into a T-75 flask of sub-confluent HEKs, a modified PCAGGS plasmid encoding human MCFD2 containing a 6X His tag and MYC tag (sub-cloned from pcDNA3.1 MCFD2 Zhang et al., 2008). Cells were allowed to recover for 2 days, were then trypsinized and re-seeded into 2 T-150 flasks. After 1 day of recovery the medium was removed, cells were washed once with PBS, and then replenished with Pro293 medium (Lonza) and incubated for 2 days prior to harvesting. Following 2 centrifugation steps, to remove any cellular debris (6000 g for 15 min), 5X Qiagen start buffer was added to the collected production medium, containing the secreted MCFD2, to yield a final concentration of 1X Qiagen start buffer (50 mM Tris-HCl, pH 7.5, 300 mM NaCl, 20 mM imidazole, 10% glycerol and 0.05% sodium azide). The His tagged sMCFD2 was then captured by passage over a Qiagen Ni-NTA column (8 mL of resin, 2 mL/min). The column was attached to a BioCad Sprint system (Applied Biosystems) allowing for continuous monitoring of the absorbance at 280 nm, the conductivity, and the pH. Following sample loading, the column was washed with start buffer until the baseline returned to the background level (< 0.1 A_{280} units). The sMCFD2 was eluted with start buffer containing 250 mM imidazole and 3 mL fractions were collected. The absorbance of each fraction at 280 nm was determined on a Cary 100 spectrophotometer. Fractions were

screened via Western blot to identify samples containing myc-MCFD2 which were subsequently pooled. Pooled fractions were then concentrated using 10 kDa MWCO Ultracel microconcentrators to a concentration of 1 mg/mL, stored in Hepes-buffered PBS supplemented with 1 mM calcium chloride, and stored at 4° until use.

3.3.6. Microscopy

2-color confocal microscopy analysis was completed as previously described (28). Briefly, for analysis of intracellular JUNV C#1 GP and MCFD2, HEK293T cells were seeded onto 12 mm glass coverslips (Thermo Scientific), and infected the following day with JUNV C#1 at a multiplicity of infection of 0.1. At 72 hours post-infection cells were washed with PBS, and fixed using 4% paraformaldehyde (PFA) for 30 minutes at room temperature followed by extensive washing with PBS to remove excess PFA. Cells were permeabilized in a buffer containing 0.1% Triton-X 100 and 0.1% bovine serum albumin (BSA). A blocking step was carried out for 30 minutes at room temperature in a buffer containing 1% BSA and 10% normal goat serum (NGS). Mouse anti MCFD2 mAb was used at a dilution of 1:2000, incubated overnight at 4°, and then antibody binding revealed with Alexa Fluor 647-conjugated goat anti-mouse IgG (H+L) (A-21236, Invitrogen) at a dilution of 1:800. JUNV GP was stained using mouse monoclonal anti JUNV GP-1 QC03-BF11 directly conjugated to Alexa Fluor 488 (Invitrogen) at a dilution of 1:50. Nuclei were visualized via 4', 6-diamidino-2-phenylindole hydrochloride (DAPI) (D9542, Sigma Aldrich) staining, and slides were mounted using ProLong Gold Antifade Reagent (P36934, Invitrogen). Cells were imaged using a Zeiss LSM 510 META Laser Scanning Confocal Microscope housed in the UVM Microscopy Imaging Center. Images

were acquired using a 63X lens with a numerical aperature of 1.4 with the optical zoom set to 1.5X. Using the AIM software suite images were captured at 1 airy unit, with gain settings for 488 and 647 signals balanced based on either mock infected controls (GP-488) or secondary only controls (MCFD2-647).

For visualizing JUNV C#1 virions containing three fluorophores using 2-dimensional (2D) and 3-dimernsional (3D) direct stochastic optical reconstruction microscopy (2D and 3D 3dSTORM), clarified supernatant from JUNV C#1 (containing 1.0 x 10^7 PFU/mL virus), or mock infected cells was incubated for 2 hr at 37° in 35 mm glass bottom culture dishes (P356-1.5-10-C, MatTek Corporation, Ashland, MA) pretreated with 0.01% Poly-L-Lysine (3438-100-01, Trevigen, Gaithersburg, MD). Following adsorption, the dishes were fixed using 4% PFA for 30 minutes at room temperature and then washed extensively to remove excess PFA. The virions were then permeabilized in a buffer containing 0.1% Triton-X100 with 0.1% BSA for 10 minutes at room temperature and washed 3x in buffer containing PBS with 0.1% BSA. A blocking step was carried out with PBS containing 1% BSA and 10% NGS for 30 minutes at room temperature.

Staining of virions was accomplished by first bathing the dishes with sMCFD2 (20 ng/μL) in buffer AB, containing PBS supplemented with 0.1% BSA and 1mM $CaCl_2$, for 4 hours at 4° C. Dishes were then washed with buffer AB 3-times, before incubation with a mouse anti myc mAb, recognizing sMCFD2, at 1:50, and a rabbit polyclonal antibody recognizing ERGIC-53, at 1:50 for 2 hours at 4°C. The dishes were then washed 3-times in buffer AB, and incubated with Alexa Fluor 647-conjugated goat anti-rabbit

IgG (H+L) (Invitrogen) to reveal ERGIC-53 staining, and Alexa Fluor 568-conjugated goat anti-mouse IgG (H+L) (Invitrogen) to reveal sMCFD2, at 1:100, respectively for 2 hr 4° C. Following 3 additional washes in Buffer AB, JUNV NP staining was accomplished by incubating dishes with a biotin-conjugated mAb NA05-AG12 recognizing JUNV NP at a dilution of 1:50 for 2 hours at 4 degrees. Dishes were washed 3 additional times in buffer AB before NP was counter-stained with Alexa Fluor 488 conjugated streptavidin (Invitrogen) at a dilution of 1:100 in buffer AB for 2 hr at 4° C. Plates were then washed 3-times with PBS and stored at 4°C prior to imaging.

We have developed a method for the visualization of three fluorophores all using direct STORM (dSTORM) methodology. The Nikon N-STORM super-resolution microscope system consists of a Nikon Eclipse Ti-E TIRF inverted microscope base with laser modules delivering excitation at 405 nm, 488 nm, 561 nm, and 647 nm, and a high sensitivity Andor iXON3 DU897 EMCCD camera. Theoretically, this instrument provides resolution in the fluorescence mode of 20 nm lateral dimension and 50 nm axial dimensions. For the triple dSTORM protocol, the following parameters were chosen: 100X, 1.45 NA objective lens; 64 X 64 pixel frame size; EM gain 10MHz at 14 bit, EM gain multiplier 300, and 1X conversion gain; auto exposure 1 frame, and no binning. TIRF setting of illumination was determined to be 4100 using 647 nm laser excitation. Images were acquired using N-STORM “normal mode” setting with 0 activation cycles and 2 reporter cycles. A STORM quad cube (Nikon part # 260319) was inserted into the microscope turret to separate the three fluorescence signals. Sequential order of activation was 488 nm (62 mWatts), followed by 647 nm (33 mWatts), and finally 561 nm (59

mWatts). Following acquisition of 15,000-30,000 frames, the data were rendered into a super-resolution image using a Gaussian distribution function. For three-dimensional image acquisition, an astigmatic lens was inserted into the microscope beam path. Image processing and display were accomplished with NIS Elements software.

All images were acquired in an oxygen scavenging buffer system containing glucose oxidase (G2133**,** Sigma) and catalase (C30, Sigma) in 50mM Tris-HCl, with 10% glucose, and 0.1M cysteamine (30070, Sigma) that was prepared fresh prior to each imaging session.

3.3.7. Viral challenge assays

Viral challenge assays to assess the role of MCFD2 were conducted as previously described (28). Briefly, to assess the consequences of plasmid over expression of MCFD2 (figure 1), HEK293T cells were seeded in 24 well plates (Fisher) and allowed to adhere for 24 hr at which time they were transfected with a plasmid encoding WT MCFD2, or with an empty plasmid, and incubated overnight. The following day monolayers were infected with JUNV C#1 at a multiplicity of infection of 0.1, or with DANV at a multiplicity of infection of 0.001, and the viruses were allowed to adsorb for 1 hour at 37° C. Following viral adsorption, monolayers were washed extensively with maintenance medium and returned to the incubator. At 48 and 72 hours post-infection, the supernatant was harvested, clarified by centrifugation for 5 minutes at 1500 rpm, transferred to a fresh Eppendorf tube, and stored for determination of PFU by standard

plaque assay on Vero E6 cells. Results were tested for statistical significance using the Student's unpaired t-test where p values < .05 were considered significant.

Viral challenge assays to determine the respective contributions of ERGIC-53's CRD features were carried out as described above with minor modifications. Combinations of plasmids that were transfected were balanced with an equal concentration of an empty vector where indicated (figure 3).

Viral challenge assays to assess the ability of EBV-transformed B cells from a healthy donor (2829D) or 2 MCFD2 null F5F8D patients (CRC-79 and 1258) to produce infectious arenavirus were conducted by infecting equal numbers of cells with JUNV C#1 in a low volume at a multiplicity of infection of 1. Viral adsorption was carried out at 37° C for 2 hours at which time the cells were gently pelleted and inoculums were removed. The cells were then washed 3-times with PBS with each wash being followed by a low speed centrifugation step (1200 rpm for 5 minutes). Infected cells were then plated in a 24 well culture dish in complete RPMI medium, and returned to the incubator. After 72 hours the post infection supernatants were harvested via centrifugation (1200 rpm for minutes), and the clarified supernatants stored at -80° C until determination of PFU content by standard plaque assay on Vero E6 cells.

3.4. Results

3.4.1. MCFD2 is a negative regulator of arenavirus propagation

It is well established that ERGIC-53 plays a critical role in production of infectious arenavirus particles: since it forms a complex, we wanted to explore the role of the macromolecular cargo receptor complex formed between ERGIC-53 and MCFD2. We hypothesized that by increasing MCFD2 expression levels, an enhancement in viral propagation, similar to one observed following ERGIC-53 overexpression, would occur. We transiently overexpressed WT MCFD2 in HEK293T cells, and tested the impact of its expression on a representative New and Old world arenavirus (Junín virus Candid1 (C#1) and Dandenong virus (DANV)). In striking contrast to the effect of overexpressed ERGIC-53, increased expression of MCFD2 led to a potent decrease in the generation of infectious C#1 at 48 and 72 hours post infection (75.22% $p = 0.001$ and 48.7% reduction $p = 0.0116$, respectively) as well as DANV at 48 hpi (83.7% reduction $p = 0.0001$), strongly suggesting a conserved and restrictive effect in both Old and New World arenavirus propagation (Fig 1C-D). Thus, MCFD2 and ERGIC-53 have a divergent contribution to arenavirus propagation.

3.4.2. JUNV C#1 propagation is enhanced in cells from F5F8D patients who are MCFD2 null

We have previously reported that the production of infectious C#1 particles is impaired in B cells derived from ERGIC-53 null F5F8D patients (28). Given the divergent influence of MCFD2 overexpression in arenavirus propagation compared to ERGIC-53's, we next wanted to examine the effect on arenavirus replication in B cells derived from two unrelated F5F8D patients who had WT ERGIC-53, but were null for MCFD2 (1258 and CRC80 – family A21 and A32 (36)). A healthy MCFD2 WT (2829D)

donor served as a neccesary control. Cells from each donor were challenged with C#1 to determine whether loss of MCFD2 would affect the production of infectious virus. Surprisingly, loss of MFD2 in these cells resulted in an increase in the release of infectious virus at 72 hpi (141.2% and 988.3% increase CRC80 and 1258 $p < 0.0001$ and $p = 0.049$, respectively) (figure 1D), thereby adding support to the antiviral role of the molecule.

3.4.3. MCFD2 forms a tripartite complex with ERGIC-53 and viral glycoproteins

We have previously reported the conserved association of ERGIC-53 with envelope GPs encoded by arenaviruses, coronaviruses, filoviruses, hantaviruses, and orthomyxoviruses (28). MCFD2 has likewise been reported to associate with ERGIC-53, and is required for efficient secretion of blood coagulation factors (F)V and FVIII (32, 39, 45). Using a biotin-streptavidin affinity purification technique (46), we therefore wanted to test whether MCFD2 would associate with an arenavirus glycoprotein, or if the viral GP by interacting with ERGIC-53, precluded its binding to MCFD2. HEK 293T cells were co-transfected with plasmids encoding the JUNV C#1 GP and the bacterial biotin ligase BirA to ensure *in-situ* biotinylation of the GP, along with either WT ERGIC-53, WT MCFD2, or CRD mutants of ERGIC-53 (ΔCRD (non GP binding) or Δβ1(non-MCFD2 binding)) and as an internal control ERGIC-53 ΔHelix, and/or mutants of MCFD2 (D89A and D129E) unable to bind ERGIC-53 (37) because of changes in tertiary structure (38), which are sufficient to cause F5F8D (36). Biotinylated C#1 GP efficiently precipitated WT MCFD2 in the presence of WT ERGIC-53, but not ERGIC-53 Δβ1 which lacks the ability to bind MCFD2 (37) (Fig 1F), suggesting that ERGIC-53 links MCFD2 to C#1 GP indirectly.

In validation of the requirement of ERGIC-53 to form the three-part complex, when ERGIC-53 ΔCRD was co-expressed in cells, which is unable to interact with JUNV GP, WT MCFD2 did not precipitate with C#1 GP (Fig 1F). MCFD2 binding was then restored following expression of ERGIC-53 ΔHelix, confirming the minimal requirement of an intact ERGIC CRD (aa 47-60) for the formation of the complex. Conversely, when JUNV GP precipitated WT ERGIC-53 in cells also expressing either of the two inactivating MCFD2 mutants (D89A and D129E), no MCFD2 was detected in the complex. These data indicate that MCFD2 forms an ERGIC-53 dependent complex with C#1 GP that minimally requires MCFD2 EF-hand residues D89 and D129 as well as ERGIC-53 CRD residues 47-60.

3.4.4. MCFD2 trafficking during infection with an arenavirus

To confirm the biochemical data suggesting a multi-protein complex between JUNV C#1 GP and MCFD2, and to visualize the intracellular distribution of these proteins, we performed 2-color confocal microscopy analysis on cells infected, or not, with Candid1 72 hr post-infection (hpi). At 72 hpi, infected cells demonstrated a profound shift in the intracellular concentration and localization of MCFD2 compared to uninfected cells (Figure 1F). The intracellular pool of MCFD2 was found to concentrate with JUNV GP, within the structure we have putatively identified as the ERGIC (figure 1F and data not shown). Compared to the mock-infected control cells, a marked increase in MCFD2 was observed primarily within the ERGIC and punctate transport vesicles. These data demonstrate a virus-specific upregulation of MCFD2 expression and coordinated trafficking of MCFD2 to sites of GP concentration.

3.4.5. ERGIC-53/MCFD2 receptor complex has a conserved interaction with viral GPs

Given the broad extent of ERGIC-53's association with viral envelope glycoproteins, we next examined whether MCFD2 could also form a complex with additional envelope glycoproteins from arenaviruses (JUNV XJ and Lassa Virus (LASV) GP), hantaviruses (ANDV GP), as well as severe acute respiratory syndrome coronavirus (SARS CoV S), orthomyxoviruses (HA proteins from FLUAV WSN and VN (H1 & H5)), filoviruses (Ebola virus and Marburg virus (EBOV & MARV)), and finally a rhabdovirus envelope from vesicular stomatitis virus (VSV G) (figure 2A). All envelope glycoproteins tested, with the exception of VSV G , were found to complex with both ERGIC-53 and MCFD2 clearly showing that the ERGIC-53 : MCFD2 molecular complex has a highly conserved but specific biochemical affinity for viral glycoproteins (Fig 2A).

3.4.6. MCFD2's antiviral action is highly conserved and restricted by the GP

To assess the conservation of MCFD2's regulation of viral propagation, and to determine whether the molecular activity of MCFD2 can be restricted to the envelope glycoprotein : ERGIC-53 complex, we employed a vesicular stomatitis virus (VSV) pseudotyping approach whereby cells overexpressing MCFD2, or not, were transfected with plasmids encoding GPs representing a subset of those able to form a complex with ERGIC-53 and MCFD2 (Figure 2A). Specifically, GPs from JUNV, SARS, ANDV, MARV, EBOV, and as a control VSV. Cells were infected a day later with pre-made VSV pseudo-particles (pp) of VSVΔG GFP + VSV G (47). The resulting pseudotyped particles (VSVΔG + JUNV GP, SARS S, MARV GP, EBOV GP, or ANDV GP) generated from cells overexpressing MCFD2 (75.68 % $p = 0.005$; 71.01% $p = .0152$; 55.26 % $p = 0.0238$; 56.61 % $p = 0.0277$; 68.18% $p = 0.0142$ reduction, respectively), but

not the empty control plasmid, were similarly restricted as with *bona fide* New and Old World arenavirus particles, whereas VSVΔG + VSV G was unaffected by MCFD2 (Figure 2B). The pseudo-particle experiments indicate a highly conserved antiviral mechanism of action of MCFD2 across arenavirus, coronavirus, filovirus, and hantavirus particles that can be restricted to the presence of their respective envelope glycoproteins.

3.4.7. MCFD2 controls ERGIC-53 function in arenavirus propagation

Because MCFD2 associates with arenavirus GPs in an ERGIC-53 dependent fashion (Figure 1F), and ERGIC-53 interacts with the arenavirus GP via its carbohydrate recognition domain (28), we designed a series of challenge experiments to tease apart the relative contributions of the molecular complex. We first wished to assess the role of ERGIC-53's entire CRD, which contains 3 non-overlapping regions: the GP binding region (Figure 1F), the MCFD2 binding site (45), and the sugar binding cleft (48), in arenavirus propagation. We therefore transfected cells with either: (i) a plasmid in which the CRD has been entirely deleted (ΔCRD), or as a control, plasmids encoding either (ii) WT ERGIC-53 (known to enhance C#1 replication), (iii) WT MCFD2, (iv) or an empty plasmid, and infected the cells a day later with JUNV C#1. At 48 hpi, in cells making an ERGIC-53 which can no longer bind to GP, sugar, or MCFD2 (ΔCRD), there was a reduction in the amount of infectious virus produced (61.95% reduction $p = 0.0002$) (Figure 3A). Likewise, when MCFD2 is in excess, there is a net reduction in the release of infectious virus (Figures 1A-C, and Figure 3A).

We next wished to test the individual contributions of ERGIC-53's binding partners (e.g. MCFD2 and carbohydrate) to the ERGIC-53 mechanism of action on arenavirus replication. Given the CRD requirement for binding to GP, MCFD2, and carbohydrates, we designed an experiment in which we infected HEK293T cells that had been co-transfected with either an empty plasmid, or plasmids making WT ERGIC-53, ERGIC-53 Δβ1 (non-MCFD2 binding), ERGIC-53 Δβ4 (non-MCFD2 and non-sugar binding), or N156A (non-sugar binding), in tandem with WT MCFD2 (to ensure the opportunity for the cargo receptor complex to form). Association of MCFD2 with ERGIC-53 is known to increase its ability to bind to N-linked glycans (43). Accordingly, expression of ERGIC-53 ΔCRD, which cannot bind to carbohydrate or MCFD2, diminished the replication of JUNV C#1 (figure 3A). ERGIC-53 lacking MCFD2 (Δβ1) was unable to inhibit viral propagation (28.26% reduction, $p = 0.09$ (ns)), or MCFD2 and carbohydrate binding capabilities (Δβ4) was less efficient at inhibiting viral propagation (61.96% reduction, $p = 0.0067$), respectively. Therefore, these results suggest that an MCFD2-dependent allosteric regulation of ERGIC-53's lectin activity could be contributing to diminished viral propagation. Finally, ERGIC-53 N156A, unable to bind carbohydrate, but able to bind MCFD2, was also able to diminish viral propagation (84.89% reduction, $p = 0.0012$). Collectively these data suggest a potent negative regulatory role for MCFD2 in the propagation of arenaviruses that is exerting its effect via an association with ERGIC-53 (potentially by altering its lectin activities).

3.4.8. Secretory MCFD2 can interact with ERGIC-53 in the extracellular space

It has been suggested that ERGIC-53 plays a role in the attachment of arenavirus particles to the surface of permissive cells. We were then interested in determining whether we could utilize the binding of MCFD2 to secreted ERGIC-53 to alter the entry of an arenavirus. In doing so we could more precisely establish the properties of an ERGIC-53-dependent antiviral mechanism of action by MCFD2 in arenavirus propagation. Specifically, we wanted to first test if a purified recombinant MCFD2 secreted from HEK cells (Fig S1A-B) would interact with ERGIC-53 in the extracellular space. The secreted form of MCFD2 (sMCFD2), in mammalian cells, is heavily O-glycosylated (49). Our purified protein migrated at approximately 28 kDa, consistent with the multiple additions of O-linked glycans in accordance with previous reports. To test whether sMCFD2 was capable of directly binding to ERGIC-53 we utilized a co-immunoprecipitation (Co-IP) technique whereby sMCFD2 was used to co-purify ERGIC-53 secreted from JUNV C#1 infected or mock infected cells (virus and exosome or exosome only). Culture fluid from infected and mock infected cultures was sequentially incubated with soluble recombinant MCFD2 (sMCFD2), followed by an antibody recognizing the C-terminal Myc tag of recombinant protein, and Protein-G coated magnetic beads. Recombinant sMCFD2 was able to co-purify ERGIC-53 from the supernatant under both conditions, indicating that the complex was stable outside of the secretory pathway, and that the post-translational modification of MCFD2 (O-linked glycosylation) did not prevent the formation of the cargo receptor complex (Figure 4A).

3.4.9. MCFD2 neutralizes arenavirus particles

Having demonstrated that sMCFD2 could interact with ERGIC-53 released from cells, and knowing that ERGIC-53 affects the attachment and entry of arenaviruses, we next wanted to determine if sMCFD2 could exert an effect on arenavirus entry via its association with ERGIC-53. To test this we pre-incubated C#1 and or DANV with purified sMCFD2, or a vehicle control, to allow for the formation of protein complexes. Following addition of pre-complexed sMCFD2 – virions to cells, we then tested for an impact on virus production at 72 (C#1) and 48 (DANV) hpi. In both cases there was a potent inhibitory effect on the production of infectious virus; JUNV C#1 (90.32% reduction, $p = 0.0223$) and DANV (94.88% reduction, $p = 0.0038$) (Fig 4 C-D).

To confirm whether sMCFD2 was capable of directly binding to an arenavirus we utilized a 2D and 3D, triple color, direct stochastic optical reconstruction microscopy (2D and 3D 3dSTORM) approach to visualize, at a sub-diffraction level, the spatial arrangement of purified sMCFD2 pre-complexed with arenavirus virions (C#1) adhered to Poly-L-Lysine-treated matTek dishes. The virions, visualized via nucleoprotein (NP) staining, revealed sMCFD2 arranged in clusters of ~ 200-500 nm rings, along with ERGIC-53, that were surrounding the densely packed arenavirus NP core (Fig 4 C-D).

3.5. Discussion

The ERGIC-53-MCFD2 receptor complex consists of equal molar ratios of the type I transmembrane sorting lectin, as well as the soluble EF-hand containing molecule MCFD2 (32, 38). We have previously shown that ERGIC-53's ability to bind to viral glycoproteins occurs in the C-terminus of the carbohydrate recognition domain (CRD)

independently of MCFD2 (28). In the current study, we refined and extended those findings to include the greater macromolecular cargo receptor complex, and found that a tripartite complex was formed between ERGIC-53, MCFD2 and the GPs of arenaviruses, coronaviruses, filoviruses, hantaviruses, and orthomyxoviruses, and that MCFD2's interaction was contingent upon ERGIC-53 binding to the GPs (Figure 1F and 2B). The formation of the complex was also found to require functional EF-hand domains of MCFD2 (Figure 1F), which supports the existing model of ERGIC-53-MCFD2 interactions (37, 38).

The unexpected antiviral activity of MCFD2 was demonstrated to occur via several lines of evidence. First, cells from MCFD2 null F5F8D patients (50) were more adept at producing infectious JUNV (Figure 1D), in contrast to our previous studies on ERGIC-53 null cells (28). Second, plasmid-driven overexpression of MCFD2 was able to inhibit the production of *bonafide* NW and OW arenavirus particles (Figure 1A-C), and we were able to restrict the impact of MCFD2 overexpression on viral propagation to the arenavirus GP independent of the remaining arenavirus core (Figure 2 A-B). VSV pseudoparticles bearing not only arenavirus, but also coronavirus, filovirus, and hantavirus GPs were likewise inhibited by the increased expression of MCFD2 in a GP specific manner which indicates a basic and highly conserved mechanism of action (Figure 2A-B). Third, infection with an arenavirus greatly enhanced the expression of MCFD2, and concentrated it in the structure we and others have identified as the ERGIC (Figure 1F) (51). These data are in agreement with previous studies of an arenavirus infected non-human primate where MCFD2 was shown to be transcriptionally

upregulated nearly 15-fold in the liver (52) which surpasses the transcriptional upregulation of ERGIC-53 in the same study. Lastly, exogenously supplied soluble MCFD2 was able to interact with individual arenavirus particles, visualized at sub-diffraction limited resolution, and pre-complexed virus was deficient in its ability to successfully initiate a new round of propagation (Figure 4A).

How is MCFD2 regulated intracellularly, and how does this affect arenavirus propagation? We and others have observed that MCFD2, following escape from a presumed ERGIC-53 retention system (MCFD2 lacks a known ER retention signal), can become O-glycosylated, and is secreted into the extracellular space (32, 49, 53). In accordance with this, following expression of mutants of ERGIC-53 unable to retain MCFD2 within cells, (Fig1A and data not shown) depletion in the intercellular MCFD2 pool was observed. The increased expression of MCFD2 leads to the efficient secretion of the molecule (Figure S1). Based on this we suggest that an upregulated and secreted MCFD2 may be able to allosterically regulate ERGIC-53's lectin activity, and that changes in ERGIC-53's lectin activity could regulate the infectivity of viral particles (Figure 3A-B and 4A-C). Interestingly, it has been reported that MCFD2 interacts with ERGIC-53 via 2 separate sites (38), which could imply alternative functions of ERGIC-53 based on MCFD2 site usage. However, several other possibilities exist, including MCFD2 regulating a crucial intracellular GP maturation event that requires the ERGIC-53-MCFD2 complex. Alternatively, MCFD2 may be ligating an, as of yet unknown, surface receptor with antiviral potential. The presence and structure of O-linked glycans on sMCFD2 may also contribute to the structure-function relationship of the two

molecules in the complex, however, to date, most biochemical and structural analyses have utilized the de-glycosylated form of MCFD2.

The intracellular regulation thus far reported for MCFD2 is largely dependent upon ERGIC-53 (54), its expression levels, and intracellular location (in terms of binding, the compartment its located in, and calcium levels) (32). The unique upregulation seen during arenavirus infection suggests that the transcriptional or translation regulation for MCFD2 is likely to possess elements distinct from the ER stress response element within ERGIC-53's promoter region (55). In support of this notion, Toda and colleagues noticed an upregulation of MCFD2 (which they refer to as Stem Cell-derived Neural Stem/Progenitor Cell Supporting Factor (SDNSF)) following ischemic treatment and FGF-2 withdrawal of primary rat hippocampal cultures (53). The increased expression of both ERGIC-53 and MCFD2 seen during heat shock (54), also could have implications in protein folding and secretion during the insidious febrile phase of an arenavirus infection (or other viral infections). Additionally, the stimulation of the ATF-6 branch of the unfolded protein response is known to be selectively initiated via LCMV GP (56), and also upregulates both ERGIC-53 and MCFD2 (55). Lastly, during Juinn virus infection, it has been reported that levels of nitric oxide are increased (57) which are also known to upregulate both ERGIC-53 and MCFD2 (58). The consequence of these combined stimuli on MCFD2 transcriptional control, and its regulation of viral propagation, however, remains unsolved.

The binding of an arenavirus GP to a site within the CRD that is distinct from the sugar-binding region, preserves the lectin function of ERGIC-53, presumably to the

benefit of the virus. Accordingly, when the CRD was removed from ERGIC-53 expressed in a viral challenge assay, a concomitant reduction in arenavirus propagation occurred (Figure 3A). Likewise, when the ΔCRD, Δβ4, and N156A mutants were expressed in addition to MCFD2 overexpression, a dampening in the MCFD2-mediated regulation occurred (Figure 3A-B), suggesting MCFD2 acts through the CRD to alter arenavirus propagation. The strategy of utilization of host-machinery, particularly in NW arenavirus entry, by engaging in non-essential areas of the host-molecule, has been elegantly shown for the transferrin receptor 1 (59, 60). NW arenaviruses GPs have evolved to utilize this highly expressed surface receptor at a site distinct from its ligand binding site. The interaction of arenavirus GPs with ERGIC-53 and MCFD2 may follow a similar strategy.

Our findings provide a proof of principle that targeting ERGIC-53's lectin activity, via its known cofactor MCFD2, is an attractive therapeutic approach for treating arenavirus infections (Figure 4A-C). Given the conservation of the MCFD2-dependent antiviral activity with not only arenaviruses, but also coronaviruses, filoviruses, and hantaviruses (Figure 2A-B), the molecule may represent a valuable broad-spectrum antiviral target. Further, the enhanced expression of MCFD2 during arenavirus infection (Figure 1E) (52) may suggest that MCFD2 is acting as an antiviral signaling molecule following its upregulation, if it is indeed secreted under these circumstances. MCFD2, when added to neuron slice cultures, has been recently reported to cause a signaling event contributing to the maintenance of adult neuronal stem ccll populations (53, 61) suggesting it may have inherent signaling capabilities. It is of interest to determine if

sMCFD2 can be detected in the serum of VHF patients during the acute phase of infection, which would support a cytokine-like signaling potential.

The presence of ERGIC-53 in the extracellular space, in the context of both virus (28) and exosomes (62, 63), and MCFD2s ability to engage and interact with ERGIC-53 there (Figure 4A), could alter the activity of the cargo receptor complex via its binding to the blood coagulation factors FV or FVIII. Although this process is poorly understood, FV after it is secreted, is endocytosed and stored within alpha granules in megakaryocytes (64), which is interestingly a site of JUNV replication (65). Our current understanding of the role of ERGIC-53 and MCFD2 in clotting factor biogenesis and activity has been limited to their interactions in the early secretory pathway. One potential role of the ERGIC-53-MCFD2 complex in the extracellular space could be to assist in the targeting or endocytosis of the clotting factors. Accordingly, the C-terminus of ERGIC-53 contains a signal involved in endocytic uptake, as well as targeting (66, 67), and F5F8D patients have been demonstrated with deficiencies not only in circulating levels of FV and FVIII, but in the endocytosed fraction found in platelets (68). Alternatively, during virion biogenesis and budding, disruption of the complex biogenic process of FV and FVIII, by direct GP competition for ERGIC-53/MCFD2, could also contribute to the bleeding abnormalities observed during infection with an arenavirus; a process that is likewise poorly characterized and understood (69, 70).

Last, the paradoxical and diametrically opposed phenotypes driven by loss of ERGIC-53 versus MCFD2 may suggest opposing evolutionary selective pressures from the side of host (MCFD2) versus virus (ERGIC-53). Interestingly, the prevalence of

MCFD2 genetic abnormalities in F5F8D is substantially less than those caused by ERGIC-53 lesions (70% vs 30%) (34, 50). Since loss of MCFD2 could lead to individuals within the human population being more susceptible to infection (Figure 1D), this could select against maintenance of diseased alleles within the human genome. Interestingly, F5F8D caused by disruptions in MCFD2 have also been shown to have a modest, but significant, increase in phenotypic severity (e.g. lower levels of FV and FVIII in the plasma) (68). Epidemiological studies of F5F8D, as well as immunological assessment of the different F5F8D populations will be required, however, before a firm understanding of the evolutionary forces at work on the ERGIC-53 macromolecular receptor complex can be assessed.

3.6. References

1. Buchmeier MJ, de la Torre JC, & Peters CJ (2007) *Arenaviridae*: The Viruses and Their Replication. *Fields Virology*, eds Knipe DM, Howley PM, Griffin DE, Lamb RA, Martin MA, Roizman B, & Straus SE (Wolters Kluwer Health/Lippincott Williams & Wilkins, Philadelphia), 5th Ed Vol 2, pp 1791-1827.
2. Salazar-Bravo J, Ruedas LA, & Yates TL (2002) Mammalian reservoirs of arenaviruses. *Curr Top Microbiol Immunol* 262:25-63.
3. Charrel RN & de Lamballerie X (2010) Zoonotic aspects of arenavirus infections. *Veterinary Microbiology* 140(3–4):213-220.
4. Gire SK*, et al.* (2012) Emerging Disease or Diagnosis? *Science* 338(6108):750-752.
5. Paweska JT*, et al.* (2009) Nosocomial outbreak of novel arenavirus infection, southern Africa. *Emerg Infect Dis* 15(10):1598-1602.
6. Günther S & Lenz O (2004) Lassa Virus. *Critical Reviews in Clinical Laboratory Sciences* 41(4):339-390.
7. Emonet SF, de la Torre JC, Domingo E, & Sevilla N (2009) Arenavirus genetic diversity and its biological implications. *Infect Genet Evol* 9(4):417-429.
8. Frame JD, Baldwin JM, Gocke DJ, & Troup JM (1970) Lassa Fever, a New Virus Disease of Man from West Africa: I. Clinical Description and Pathological Findings. *The American Journal of Tropical Medicine and Hygiene* 19(4):670-676.

9. Bausch DG, *et al.* (2001) Lassa fever in Guinea: I. Epidemiology of human disease and clinical observations. *Vector Borne Zoonotic Dis* 1(4):269-281.
10. Bonthius DJ, *et al.* (2007) Congenital lymphocytic choriomeningitis virus infection: spectrum of disease. *Annals of Neurology* 62(4):347-355.
11. Armstrong C & Lillie RD (1934) Experimental Lymphocytic Choriomeningitis of Monkeys and Mice Produced by a Virus Encountered in Studies of the 1933 St. Louis Encephalitis Epidemic. *Public Health Reports (1896-1970)* 49(35):1019-1027.
12. Palacios G, *et al.* (2008) A new arenavirus in a cluster of fatal transplant-associated diseases. *The New England journal of medicine* 358(10):991-998.
13. Macneil A, *et al.* (2012) Solid organ transplant-associated lymphocytic choriomeningitis, United States, 2011. *Emerging infectious diseases* 18(8):1256-1262.
14. Fischer SA, *et al.* (2006) Transmission of Lymphocytic Choriomeningitis Virus by Organ Transplantation. *New England Journal of Medicine* 354(21):2235-2249.
15. Maiztegui JI, *et al.* (1998) Protective efficacy of a live attenuated vaccine against Argentine hemorrhagic fever. AHF Study Group. *J Infect Dis* 177(2):277-283.
16. Romanowski V, Pidre ML, Ferrel ML, Bender C, & Gomez RM (2013) Argentine Hemorrhagic Fever. *Viral hemorrhagic fevers*, (CRC Press), p 317.
17. Buchmeier MJ (2002) Arenaviruses: protein structure and function. *Curr Top Microbiol Immunol* 262:159-173.
18. Jiang X, *et al.* (2013) Structures of arenaviral nucleoproteins with triphosphate dsRNA reveal a unique mechanism of immune suppression. *J Biol Chem* 288(23):16949-16959.
19. Fan L, Briese T, & Lipkin WI (2010) Z proteins of New World arenaviruses bind RIG-I and interfere with type I interferon induction. *J Virol* 84(4):1785-1791.
20. Froeschke M, Basler M, Groettrup M, & Dobberstein B (2003) Long-lived signal peptide of lymphocytic choriomeningitis virus glycoprotein pGP-C. *J Biol Chem* 278(43):41914-41920.
21. Eichler R, *et al.* (2003) Identification of Lassa virus glycoprotein signal peptide as a trans-acting maturation factor. *EMBO Rep* 4(11):1084-1088.
22. Lenz O (2001) The Lassa virus glycoprotein precursor GP-C is proteolytically processed by subtilase SKI-1/S1P. *Proceedings of the National Academy of Sciences* 98(22):12701-12705.
23. Nunberg JH & York J (2012) The Curious Case of Arenavirus Entry, and Its Inhibition. *Viruses* 4(1):83-101.
24. Cao W, *et al.* (1998) Identification of alpha-dystroglycan as a receptor for lymphocytic choriomeningitis virus and Lassa fever virus. *Science* 282(5396):2079-2081.
25. Radoshitzky SR, *et al.* (2007) Transferrin receptor 1 is a cellular receptor for New World haemorrhagic fever arenaviruses. *Nature* 446(7131):92-96.
26. Shimojima M & Kawaoka Y (2012) Cell surface molecules involved in infection mediated by lymphocytic choriomeningitis virus glycoprotein. *The Journal of veterinary medical science / the Japanese Society of Veterinary Science* 74(10):1363-1366.

27. Urata S & Yasuda J (2012) Molecular mechanism of arenavirus assembly and budding. *Viruses* 4(10):2049-2079.
28. Klaus Joseph P*, et al.* (2013) The Intracellular Cargo Receptor ERGIC-53 Is Required for the Production of Infectious Arenavirus, Coronavirus, and Filovirus Particles. *Cell host & microbe* 14(5):522-534.
29. Ben-Tekaya H, Miura K, Pepperkok R, & Hauri HP (2005) Live imaging of bidirectional traffic from the ERGIC. *J Cell Sci* 118(Pt 2):357-367.
30. Schweizer A, Fransen JA, Bachi T, Ginsel L, & Hauri HP (1988) Identification, by a monoclonal antibody, of a 53-kD protein associated with a tubulo-vesicular compartment at the cis-side of the Golgi apparatus. *J Cell Biol* 107(5):1643-1653.
31. Itin C, Foguet M, Kappeler F, Klumperman J, & Hauri HP (1995) Recycling of the endoplasmic reticulum/Golgi intermediate compartment protein ERGIC-53 in the secretory pathway. *Biochemical Society transactions* 23(3):541-544.
32. Zhang B, Kaufman RJ, & Ginsburg D (2005) LMAN1 and MCFD2 form a cargo receptor complex and interact with coagulation factor VIII in the early secretory pathway. *J Biol Chem* 280(27):25881-25886.
33. Moussalli M*, et al.* (1999) Mannose-dependent endoplasmic reticulum (ER)-Golgi intermediate compartment-53-mediated ER to Golgi trafficking of coagulation factors V and VIII. *J Biol Chem* 274(46):32539-32542.
34. Nichols WC*, et al.* (1998) Mutations in the ER-Golgi intermediate compartment protein ERGIC-53 cause combined deficiency of coagulation factors V and VIII. *Cell* 93(1):61-70.
35. Neerman-Arbez M*, et al.* (1999) Molecular analysis of the ERGIC-53 gene in 35 families with combined factor V-factor VIII deficiency. *Blood* 93(7):2253-2260.
36. Zhang B*, et al.* (2003) Bleeding due to disruption of a cargo-specific ER-to-Golgi transport complex. *Nature genetics* 34(2):220-225.
37. Zheng C, Liu HH, Zhou J, & Zhang B (2010) EF-hand domains of MCFD2 mediate interactions with both LMAN1 and coagulation factor V or VIII. *Blood* 115(5):1081-1087.
38. Nishio M*, et al.* (2010) Structural basis for the cooperative interplay between the two causative gene products of combined factor V and factor VIII deficiency. *Proc Natl Acad Sci U S A* 107(9):4034-4039.
39. Wigren E, Bourhis JM, Kursula I, Guy JE, & Lindqvist Y (2010) Crystal structure of the LMAN1-CRD/MCFD2 transport receptor complex provides insight into combined deficiency of factor V and factor VIII. *FEBS Lett* 584(5):878-882.
40. Appenzeller-Herzog C (2003) pH-induced Conversion of the Transport Lectin ERGIC-53 Triggers Glycoprotein Release. *Journal of Biological Chemistry* 279(13):12943-12950.
41. Appenzeller C, Andersson H, Kappeler F, & Hauri HP (1999) The lectin ERGIC-53 is a cargo transport receptor for glycoproteins. *Nature Cell Biology* 1(6):330-334.
42. Kamiya Y*, et al.* (2008) Molecular basis of sugar recognition by the human L-type lectins ERGIC-53, VIPL, and VIP36. *J Biol Chem* 283(4):1857-1861.
43. Kawasaki N*, et al.* (2008) The sugar-binding ability of ERGIC-53 is enhanced by its interaction with MCFD2. *Blood* 111(4):1972-1979.

44. Zhang B*, et al.* (2003) Bleeding due to disruption of a cargo-specific ER-to-Golgi transport complex. *Nature genetics* 34(2):220-225.
45. Zheng C, Liu HH, Yuan S, Zhou J, & Zhang B (2010) Molecular basis of LMAN1 in coordinating LMAN1-MCFD2 cargo receptor formation and ER-to-Golgi transport of FV/FVIII. *Blood* 116(25):5698-5706.
46. Cornillez-Ty CT, Liao L, Yates JR, Kuhn P, & Buchmeier MJ (2009) Severe Acute Respiratory Syndrome Coronavirus Nonstructural Protein 2 Interacts with a Host Protein Complex Involved in Mitochondrial Biogenesis and Intracellular Signaling. *Journal of Virology* 83(19):10314-10318.
47. Lawson ND, Stillman EA, Whitt MA, & Rose JK (1995) Recombinant vesicular stomatitis viruses from DNA. *Proceedings of the National Academy of Sciences* 92(10):4477-4481.
48. Zheng C*, et al.* (2013) Structural Characterization of Carbohydrate Binding by LMAN1 Protein Provides New Insight into the Endoplasmic Reticulum Export of Factors V (FV) and VIII (FVIII). *Journal of Biological Chemistry* 288(28):20499-20509.
49. Nyfeler B, Zhang B, Ginsburg D, Kaufman RJ, & Hauri H-P (2006) Cargo Selectivity of the ERGIC-53/MCFD2 Transport Receptor Complex. *Traffic* 7(11):1473-1481.
50. Zhang B*, et al.* (2003) Bleeding due to disruption of a cargo-specific ER-to-Golgi transport complex. *Nature genetics* 34(2):220-225.
51. Hauri HP, Kappeler F, Andersson H, & Appenzeller C (2000) ERGIC-53 and traffic in the secretory pathway. *J Cell Sci* 113 (Pt 4):587-596.
52. Djavani M*, et al.* (2009) Gene expression in primate liver during viral hemorrhagic fever. *Virol J* 6:20.
53. Toda H*, et al.* (2003) Stem cell-derived neural stem/progenitor cell supporting factor is an autocrine/paracrine survival factor for adult neural stem/progenitor cells. *The Journal of biological chemistry* 278(37):35491-35500.
54. Spatuzza C*, et al.* (2004) Heat shock induces preferential translation of ERGIC-53 and affects its recycling pathway. *J Biol Chem* 279(41):42535-42544.
55. Nyfeler B, Nufer O, Matsui T, Mori K, & Hauri HP (2003) The cargo receptor ERGIC-53 is a target of the unfolded protein response. *Biochem Biophys Res Commun* 304(4):599-604.
56. Pasqual G, Burri DJ, Pasquato A, de la Torre JC, & Kunz S (2011) Role of the host cell's unfolded protein response in arenavirus infection. *J Virol* 85(4):1662-1670.
57. Gomez RM*, et al.* (2003) Endothelial cell function alteration after Junin virus infection. *Thrombosis and Haemostasis*.
58. Renna M*, et al.* (2006) Nitric oxide-induced endoplasmic reticulum stress activates the expression of cargo receptor proteins and alters the glycoprotein transport to the Golgi complex. *Int J Biochem Cell Biol* 38(12):2040-2048.
59. Demogines A, Abraham J, Choe H, Farzan M, & Sawyer SL (2013) Dual host-virus arms races shape an essential housekeeping protein. *PLoS biology* 11(5):e1001571.

60. Abraham J, Corbett KD, Farzan M, Choe H, & Harrison SC (2010) Structural basis for receptor recognition by New World hemorrhagic fever arenaviruses. *Nat Struct Mol Biol* 17(4):438-444.
61. Liu H*, et al.* (2013) Multiple coagulation factor deficiency protein 2 contains the ability to support stem cell self-renewal. *Faseb J* 27(8):3298-3305.
62. Gonzalez-Begne M*, et al.* (2009) Proteomic analysis of human parotid gland exosomes by multidimensional protein identification technology (MudPIT). *Journal of proteome research* 8(3):1304-1314.
63. Conde-Vancells J*, et al.* (2008) Characterization and comprehensive proteome profiling of exosomes secreted by hepatocytes. *Journal of proteome research* 7(12):5157-5166.
64. Suehiro Y*, et al.* (2005) Endocytosis and storage of plasma factor V by human megakaryocytes. *Thromb Haemost* 94(3):585-592.
65. Pozner RG*, et al.* (2010) Junin virus infection of human hematopoietic progenitors impairs in vitro proplatelet formation and platelet release via a bystander effect involving type I IFN signaling. *PLoS Pathog* 6(4):e1000847.
66. Itin C, Kappeler F, Linstedt AD, & Hauri HP (1995) A novel endocytosis signal related to the KKXX ER-retrieval signal. *EMBO J* 14(10):2250-2256.
67. Kappeler F, Klopfenstein DR, Foguet M, Paccaud JP, & Hauri HP (1997) The recycling of ERGIC-53 in the early secretory pathway. ERGIC-53 carries a cytosolic endoplasmic reticulum-exit determinant interacting with COPII. *J Biol Chem* 272(50):31801-31808.
68. Zhang B*, et al.* (2008) Genotype-phenotype correlation in combined deficiency of factor V and factor VIII. *Blood* 111(12):5592-5600.
69. Schwarz ER*, et al.* (1972) [Coagulation changes in Argentine hemorrhagic fever]. *Medicina* 32(3):247-259.
70. Kunz S (2009) The role of the vascular endothelium in arenavirus haemorrhagic fevers. *Thrombosis and Haemostasis*.

3.7. Figure legends

Figure 3.1 MCFD2 is an arenavirus restriction factor that forms a tripartite complex with ERGIC-53 and JUNV GP:

(A-C) Overexpression of WT MCFD2 leads to impairment in production of infectious JUNV C#1 and DANV. HEK293T cells were transfected with a plasmid encoding MCFD2 or an empty plasmid. 24 hr. following transfection, cells were infected with JUNV C#1 at an MOI of 0.1, or DANV at an MOI of 0.001, and after 48 or 72 hour post-

infection (hpi) supernatants were screened for number of plaque forming units (PFU) by a standard plaque assay on Vero E6 cells. Data are from replicate experiments (n=6, 48 hpi C#1 and n= 3 DANV, n=6 72 hpi C#1) and are presented as mean PFU ± SEM relative to the cells receiving the empty vector.

(D) Production of infectious JUNV C#1 is enhanced in MCFD2 null cells. EBV transformed lymphoblastoid cells from a healthy MCFD2 $^{+/+}$ donor (2829D) and MCFD2 $^{-/-}$ individuals with F5F8D (CRC-80 and 1258) were challenged with JUNV C#1 at an MOI of 1.0 and 72 hpi supernatants were screened for PFU via plaque assay. Data are presented as mean PFU ± SEM relative to the MCFD2 $^{+/+}$ cells. Data are representative of two independent experiments (n=6 per condition per experiment).

(E) MCFD2 expression and trafficking during infection with an arenavirus. HEK293T infected cells infected with JUNV C#1 were fixed 72 hpi and stained internally for JUNV GP (green) and MCFD2 (red) and visualized by confocal microscopy. The image is representative of a minimum of 10 fields of view. Background signal was subtracted via gain reduction based on values obtained from secondary antibody alone (MCFD2) or mock infected cells (GP).

(F). MCFD2 forms an ERGIC-53 dependent tripartite complex with JUNV C#1 GP that requires MCFD2 EF-hand residues 89 and 129. HEK293T cells were co-transfected with a modified PCAGGS vector (pCC384) encoding JUNV C#1 GP with a carboxy-terminal biotin acceptor peptide (BAP), for efficient streptavidin based purification, and an HA epitope used for detection of GPC and GP2 by Western blot; a bacterial biotin ligase, BirA, to ensure in-situ biotinylation, and plasmids encoding the indicated versions of ERGIC-53 and MCFD2. Biotinylated proteins were isolated using streptavidin coated

beads, and purified complexes were eluted and analyzed by SDS PAGE and Western blot detection of GPC/GP2 (bait), FLAG-ERGIC-53 (prey), MYC-MCFD2 (prey), and CRT as a control.

Figure 3.2 MCFD2 antiviral action is conserved across multiple pathogenic RNA viruses and is specific to the viral GP.

(A) MCFD2 forms a tripartite complex with arenavirus, coronavirus, filovirus, hantavirus, and orthomyxovirus envelope glycoproteins. HEK293T cells were co-transfected with modified PCAGSS vectors (pCC384) with carboxy terminal BAP and HA features for purification and detection procedures encoding the respective viral GPs: LASV GP, JUNV XJ GP, ANDV GP, EBOV GP, MARV GP, SARS S, VN HA (H5), WSN HA (H1), and VSV G, along with WT ERGIC-53 and MCFD2, as well as BirA to ensure in-situ biotinylation. Streptavidin precipitated GP-cellular protein complexes were analyzed via SDS PAGE and Western blot for GP (bait) content, ERGIC-53, and MCFD2 (prey) content along with CRT as a control.(B) MCFD2 has a highly conserved antiviral function that can be restricted to the viral glycoprotein. HEK293T cells were first transfected with either an empty plasmid, or one encoding WT MCFD2. The following day cells were transfected with each of the respective viral glycoproteins: VSV G, JUNV XJ GP, SARS S, MARV GP, EBOV GP, and ANDV GP. 24 hr following the final transfection, monolayers were infected with VSVΔG-GFP pseudoparticles decorated with VSV G. Supernatants were harvested 24 hpi to assay for focus forming units (FFU) on fresh Vero monolayers. Data are presented as mean FFU ± SEM relative to the cells

receiving an empty vector. Data are representative of two independent experiments (n=3 per condition per experiment).

Figure 3.3 MCFD2 regulates ERGIC-53's lectin activity to inhibit arenavirus replication.

(A) ERGIC-53's CRD is critical for production of infectious JUNV C#1. HEK 293T cells were transfected with either an empty plasmid, or one containing WT ERGIC-53, ERGIC-53 ΔCRD, or WT MCFD2. Monolayers were infected 24 hpi with JUNV C#1 at an MOI or 0.1, virus containing supernatants were harvested at 48 hpi and assayed for PFU content via standard plaque assay. Data are represented as mean PFU ± SEM relative to the cells receiving an empty vector.

(B) Interactions of ERGIC-53's CRD regulate arenavirus production. HEK 293T cells were co-transfected with either an empty plasmid, or one containing WT MCFD2 in tandem with WT and functional mutants of ERGIC-53 to test for their relative contributions to the ERGIC-53 dependent phenotype; ΔCRD (unable to bind GP, MCFD2, or sugar), Δβ1 (unable to bind MCFD2), Δβ4 (unable to bind MCFD2 or sugar), N156A (unable to bind sugar). Monolayers were infected 24 hpi with JUNV C#1 at an MOI or 0.1, virus containing supernatants were harvested at 72 hpi and assayed for PFU content via standard plaque assay. Data are represented as PFU ± SEM relative to the cells receiving equal μg amounts of the empty vector.

Figure 3.4 sMCFD2 interacts with extracellular ERGIC-53 and arenaviruses to inhibit infectivity.

(A) Purified MCFD2 interacts with ERGIC-53 secreted from infected and mock infected cells. MCFD2 purified from HEK293T cells (see methods section for details on purification) was added to clarified supernatant from JUNV C#1 and mock infected cultures. Recombinant MCFD2 in complex with ERGIC-53 was immunoprecipitated using an anti-myc antibody that recognizes the recombinant MCFD2 molecule. Precipitated fractions were separated via SDS PAGE and analyzed by Western blot for the presence of myc-MCFD2 (bait) and endogenous ERGIC-53 (prey).

(B) Purified MCFD2 is able to inhibit the entry of Old and New World arenaviruses. Purified MCFD2 or vehicle was added to supernatant containing 200 PFU of JUNV C#1 or DANV derived from Vero E6 cells. The supernatant was incubated with purified protein for 2 hr at 4° C before being overlaid onto monolayers of HEK293T cells. Following a 2 hr adsorption at 37° C the cells were washed extensively and fresh medium was added. At 48 (DANV) and (72) hpi, supernatants were harvested and assayed for PFU content by standard plaque assay. Data are represented as mean PFU ± SEM relative to the supernatant treated with vehicle.

(C-D) 2D and 3D 3dSTORM imaging reveals organization of sMCFD2 and ERGIC-53 on arenavirus particles. JUNV C#1 containing particles generated in Vero E6 cells were fixed onto poly-L-Lysine treated MatTek dishes. Following fixation with PFA, adsorbed virions were permeablized and incubated with purified sMCFD2 from HEK293T cells prior to staining for myc-MCFD2(blue), JUNV NP (green), and endogenous ERGIC-53 (red). Images are representative from a minimum of 10 acquisitions of 15,000 to 30,000 frames. Scale bars are indicated for each image. Signal versus noise values were assessed by imaging single fluorophores in their respective channels, as well as in all 3 channels to

ensure localizations from each respective fluorophore were distinct. The 2 panels in (C) are of a 1,000 nm view of a series of JUNV C#1 particles, and then a single particle magnified. The image in panel (D) is a 3D rendering of an individual JUNV C#1 virion identified via NP staining (green) containing a ring of ERGIC-53 (red) and MCFD2 (blue). The model presented in panel (E) illustrates the arenavirus lifecycle and specific stages where MCFD2 can exert an effect. The bottom WT cell (red shaded) represents a scenario where MCFD2 is present in abundance. The interaction between ERGIC-53/MCFD2 and GP is likely to occur early during synthesis in the ER/ERGIC (1) where the proteins are concentrated. Binding of MCFD2 to the complex may alter an intracellular maturation event leading up (folding, proteolysis, glycan maturation) to budding and release (2). MCFD2 interacts with ERGIC-53 in the context of viral particles (3) when added exogenously, and presumably during endogenous secretion, where it interferes with steps of arenavirus entry. MCFD2 binding may act at the level of receptor binding (4) either through blocking of arenavirus receptors, by changing ERGIC-53's sugar preference, or by ligation of an unknown MCFD2-specific receptor. If the entry defect is post-attachment, the targeting and trafficking (5), and fusion cascade (6) may also be disrupted.

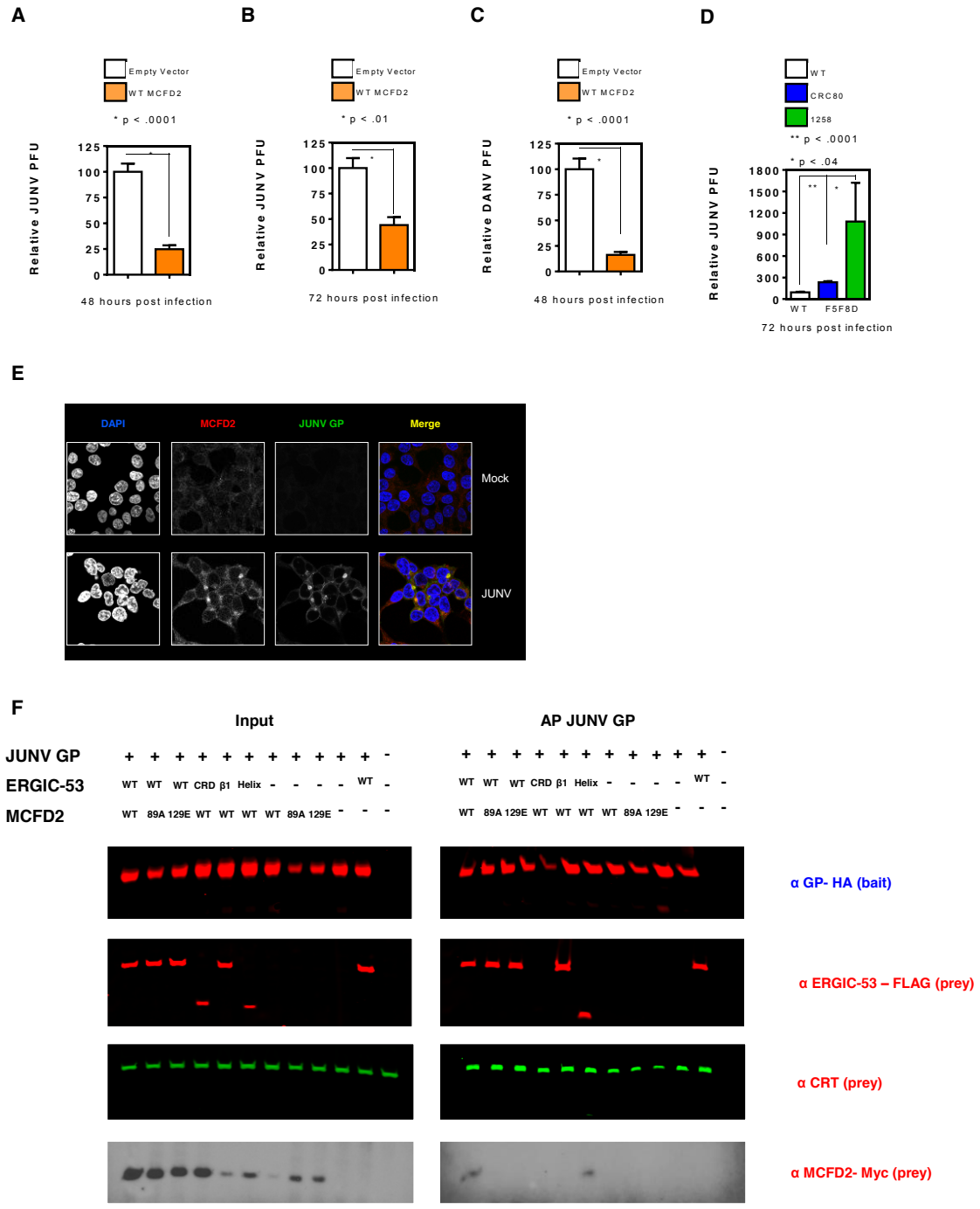

Figure 3.1 MCFD2 is an arenavirus restriction factor that forms a tripartite complex with ERGIC-53 and JUNV GP

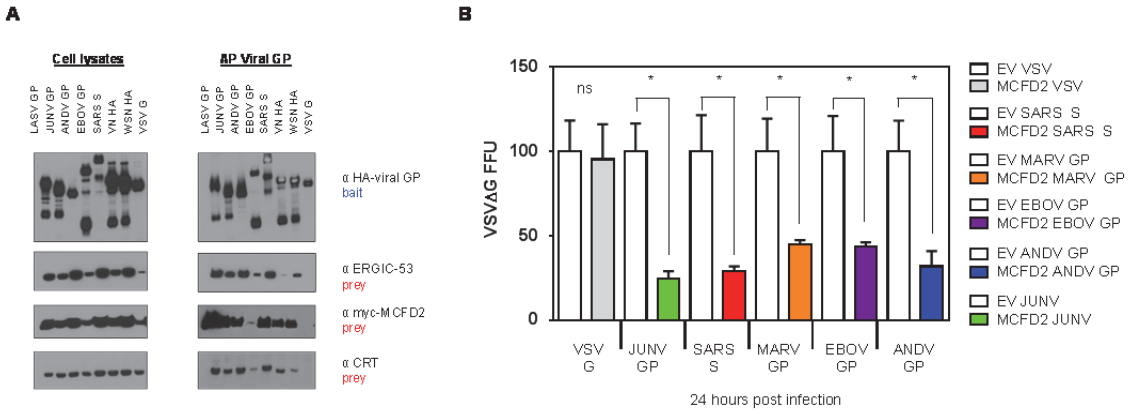

Figure 3.2 MCFD2 antiviral action is conserved across multiple pathogenic RNA viruses and is specific the viral GP.

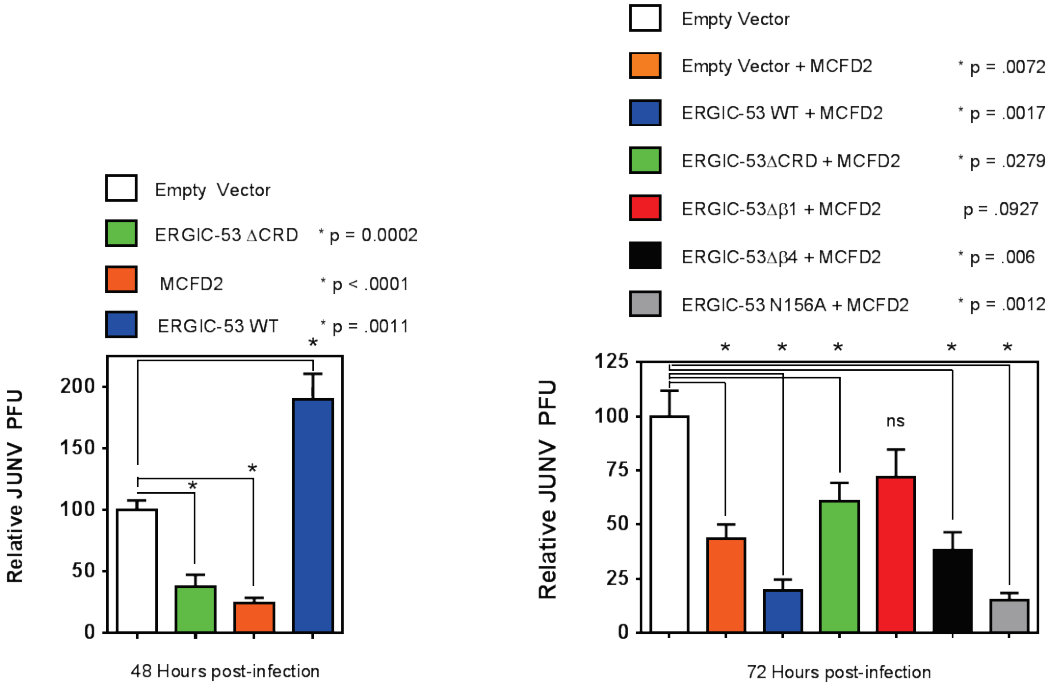

Figure 3.3 MCFD2 regulates ERGIC-53's lectin activity to inhibit arenavirus replication.

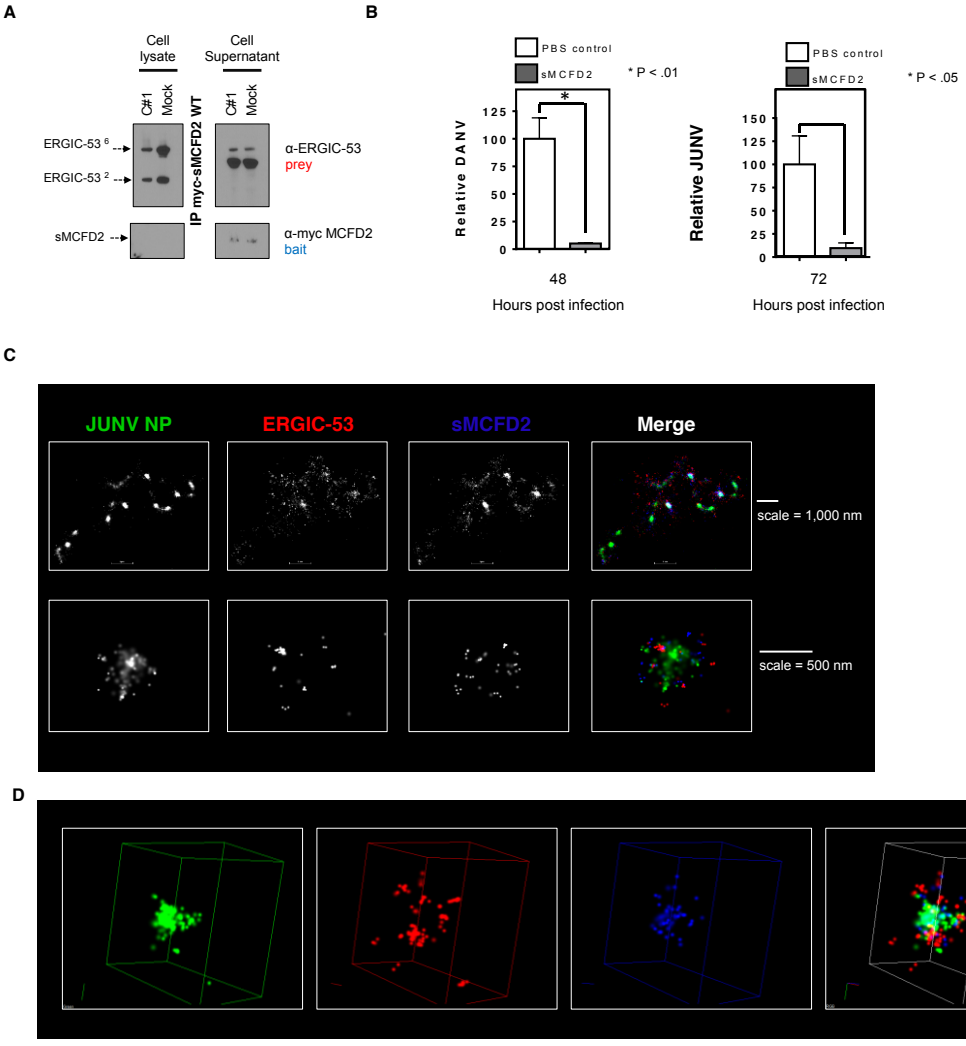
A
Cell lysate
Cell Supernatant
C#1
Mock
C#1
Mock
IP myc-sMCFD2 WT
ERGIC-53 6
ERGIC-53 2
sMCFD2
α-ERGIC-53
prey
α-myc MCFD2
bait
B
PBS control
sMCFD2
* P < .01
Relative DANV
125
100
75
50
25
0
48
Hours post infection
PBS control
sMCFD2
* P < .05
Relative JUNV
150
125
100
75
50
25
0
72
Hours post infection
C
JUNV NP
ERGIC-53
sMCFD2
Merge
scale = 1,000 nm
scale = 500 nm
D

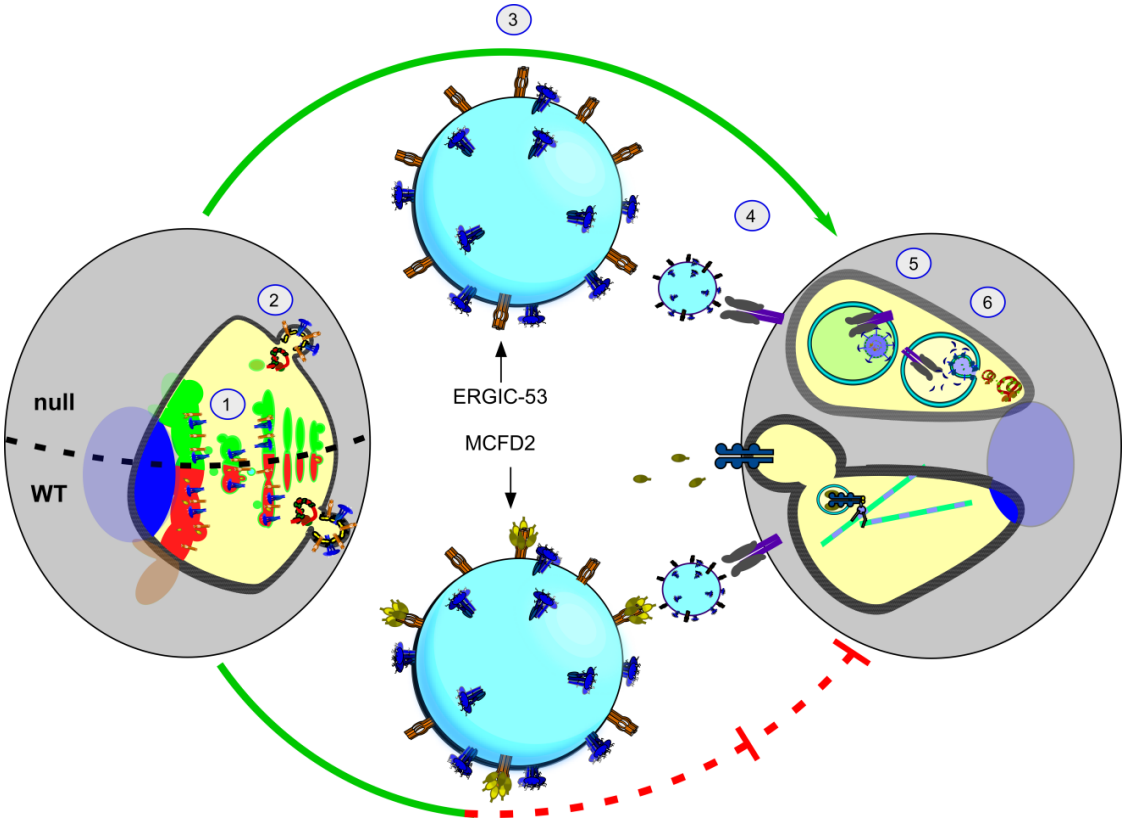

Figure 3.4 sMCFD2 interacts with extracellular ERGIC-53 and arenaviruses to inhibit infectivity.

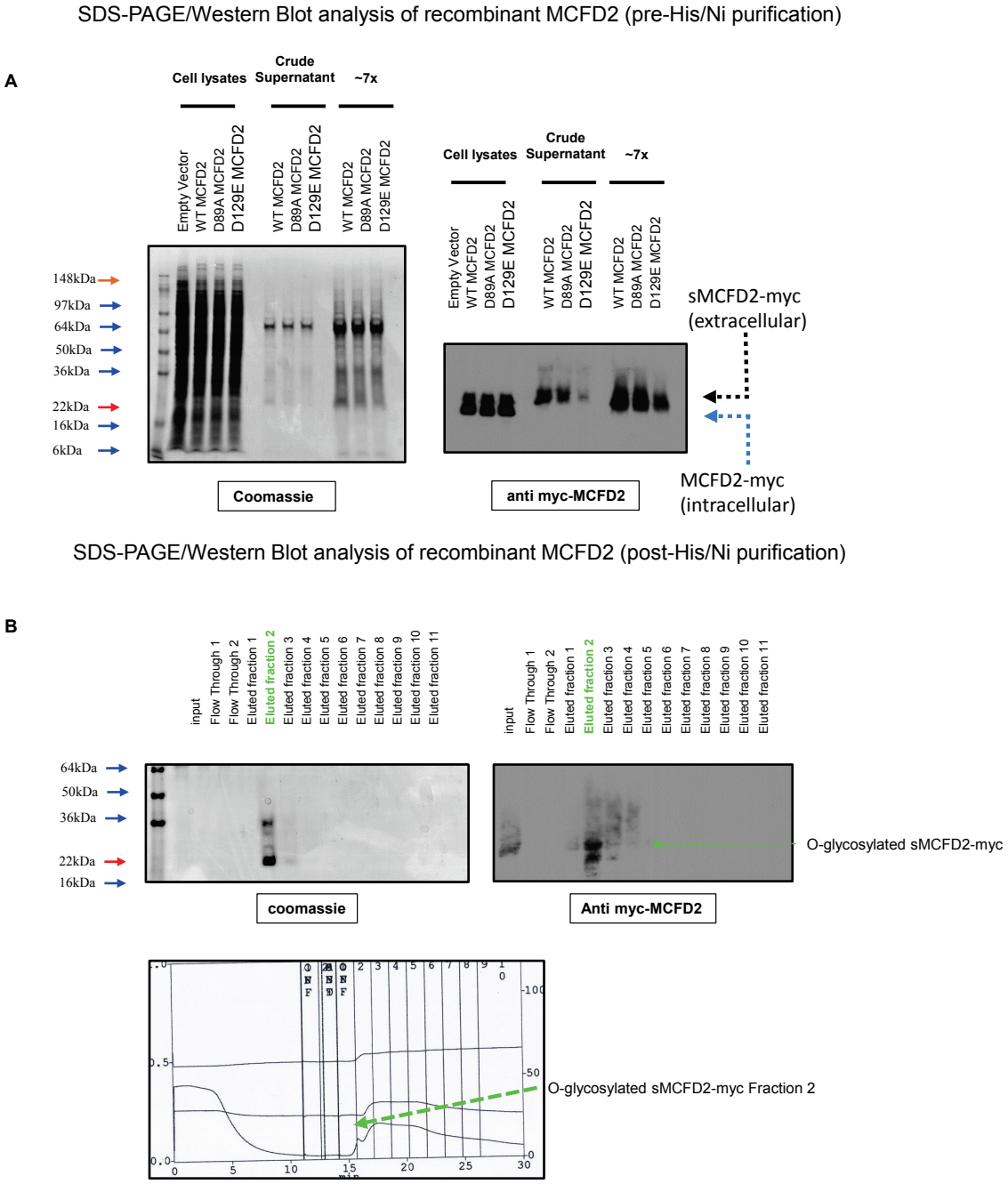

Figure 3.5 Supplemental Figure 1. Analysis of sMCFD2 production

4. SUMMARY OF RESULTS, DISCUSSION, AND FUTURE DIRECTIONS

Summary of aims

The body of this dissertation has been put forth to discuss, at length, four specific aims that, following their completion, would advance the field's current understanding of the cellular biological framework of arenavirus biogenesis and pathogenesis. The focus of the dissertation was directed primarily on the arenavirus envelope glycoprotein complex, but also incorporated hantavirus GPs. The first aim was to establish a comprehensive interactome of an arenavirus GP with the human proteome. The inclusion of a prototypic hantavirus GP served both as a control for this venture, as well as a scientific advancement in its own right. The hantavirus glycoproteins, much like their arenavirus counterparts, have a dearth of information regarding their interactions (and subsequent biological consequences) with human cellular proteins. Following the characterization of these interactomes, the second aim of these studies was to identify cellular targets from the interactomes that were biologically relevant to either the propagation of viruses, or the progression of disease caused by each virus. This aim focused on two specific host proteins; ERGIC-53 and MCFD2. The third aim, which became the bulk of the studies, was to identify and characterize the mechanism of action of the biologically relevant cellular targets identified in aim 2 (ERGIC-53 and MCFD2). The fourth aim was to characterize the molecular nature of the interaction between the viral and host molecules (e.g. map domains and residues supporting the interaction). These four aims will be summarized and explored individually where possible; however given the interesting and occasionally circuitous route the data led us on, some sections are not mutually exclusive.

4.1. Summary of GP interactome studies and future directions (aim 1)

The first aim of this dissertation was to generate an arenavirus and hantavirus GP – human protein interactome. Accordingly, data presented here provides a primary and comprehensive identification of human proteins involved in the biogenesis of arenavirus and hantavirus glycoproteins. Our collective understanding of specific proteins involved in their biogenesis has been limited thus far to the proteases involved in maturation cleavage of the arenavirus (SPase and S1P) and hantavirus GPs (SPase). The new collection of interacting proteins identified here will be of use to researchers interested in dissecting the molecular machinery involved in the chaperone-assisted folding, glycosylation, isomerization, and transport of the glycoprotein complex. The proteomics screen revealed molecules with associated functions in each of these categories. It should be noted, however, that there was a caveat to the approach detailed in chapter 2 in the use of HEK293T cells to generate the interactomes. The cells were selected based on both the ability of these viruses to productively infect them, as well as for their permissiveness to transfection for the production of recombinant proteins. Future studies to confirm these interactions within tissue relevant cell types will likely provide additional interactions, some of which may be tissue specific.

Chapter 1 summarizes the different approaches to understanding the imperative nature of the N-linked glycosylation additions to arenavirus glycoprotein structure and function. It will be of particular interest to investigate more fully the glycosylation machinery involved. Despite several elegant studies, the exact make-up of the glycan additions remain unknown and the enzymes involved in shaping them are likewise

murky. We identified several sugar processing (adding and trimming) enzymes as well as lectins and lectin binding proteins in this study including ERGIC-53, calreticulin, calnexin, Golgi apparatus protein 1, LMAN2, and LMAN2L. Given the importance of ERGIC-53 and its lectin function in the production of infectious virus, characterizing the role of each of these lectins may also shed insight into the intracellular trafficking and glycosylation content of the GP, as well as reveal other unknown lectin-mediated activities for both virus and cell.

Chapter 2 describes the cluster analysis of the individual versus the conserved GP interactomes. While this type of primary analysis is insightful, a more thorough investigation will be required to cross-reference the interactomes with existing databases for human viral pathogens (i.e. influenza and HIV) for which similar proteomics or RNAi based studies have been carried out. In addition to an in-depth bioinformatics analysis, functional studies carried out via forward or reverse genetics approaches (genetic deletion vs over expression) will be needed to characterize the significance of the remainder of the interactome. Since there are several enzymes also listed, specifically those involved in the proteasome function, small molecules targeting their enzymatic activity should also be utilized where feasible. This type of approach has gained traction recently. Specifically, treatment of cells with Bortezomib, a clinically approved proteasome inhibitor, as well as MG12, has been demonstrated to result in the impaired propagation of orthomyxoviruses and paramyxoviruses, respectively (Dudek, Luig, Pauli, Schubert, & Ludwig, 2010; Watanabe et al., 2005). During the preparation of this dissertation, Jager et al. identified ERGIC-53 as an interacting protein of HIV-1 GP in a proteomics screen characterizing

the HIV-interactome (Jager et al., 2012), however it has not yet been revealed whether ERGIC-53 will likewise be important for retrovirus propagation. Given the phenotypes presented thus far for the arenavirus, coronavirus, filoviruses, and hantaviruses, and ERGIC-53's interaction with them, it is plausible that HIV may also utilize ERGIC-53's pro-viral function.

While these studies were underway, Panda et al. performed a genome-wide siRNA screen searching for proteins involved in rhabdovirus (VSV), arenavirus (LCMV), and human parainfluenza virus (HPIV) replication (D. Panda et al., 2011). Several GP partners identified in our studies were found to be deleterious to viral replication when silenced. Specifically coatomer (COPA), archain 1 (ARCN), stromal cell derived factor 4 (SDF4), and Renin Receptor (ATP6AP2), when silenced, restricted replication. In light of our findings, it is likely that the mechanism by which these proteins restrict replication occurs via their interaction with the arenavirus glycoprotein. A recent study by Iwasaki and colleagues, after mining the Panda data set, extended their findings for sodium hydrogen exchanging 3 (NHE3), by demonstrating that loss of NHE3 resulted in an entry defect involving the macropinocytosis pathway that was conserved across OW and NW arenaviruses. Further, the authors were able to utilize zoniporide, a drug used in clinical trials for preventing myocardial ischemia, to inhibit arenavirus entry (Iwasaki, Ngo, & de la Torre, 2014). This study is an excellent example of how the sharing of large data sets encourages cooperation amongst labs in the field to understand more in detail the cellular biology of these viruses, and how therapeutic targets can be identified through basic science.

In addition to the study by Panda and colleagues, an arenavirus entry screen into human cells has recently been carried out using a gene-trap viral vector, bearing LASV GP, as a platform to select for genes allowing survival in a population of virally disrupted haploid cells (L. T. Jae et al., 2013). Disruption of both ERGIC-53 and MCFD2 genes showed signs of inactivating insertions within the genes, but were below the threshold of statistical significance, suggesting that there may be either tissue specificity in the ERGIC-53/MCFD2 phenotype, or different sensitivities between screening techniques. Further, a recent genome-wide siRNA screen was also carried out using VSV decorated with JUNV C#1 GP, which yielded little to no overlap amongst the validated protein targets with the data presented in this dissertation (M. Lavanya, C. D. Cuevas, M. Thomas, S. Cherry, & S. R. Ross, 2013). A thorough pathway analysis may provide clues as to the incongruence of overlap amongst the varying screens which has thus far been minimal. Specifically, it will be important to determine if the conserved protein complexes, rather than specific proteins, are similarly impacted. This criterion may then re-connect the disparate data sets. However, similar discrepancies in host-protein significance have been reported in the HIV literature, and so does not come as a surprise that following genome-scale screens specific proteins are not found to be functionally relevant across studies (Brass et al., 2008; Zhou et al., 2008). In summary, the proteomics data generated in these studies provide a starting point for a more detailed and comprehensive testing of the cellular mechanisms involved with individual proteins, and may be carried out by the arenavirus and hantavirus community at large. The remainder of the discussion will emphasize the results obtained regarding ERGIC-53, MCFD2, and the ERGIC-53-MCFD2 receptor complex.

4.1.1. ERGIC-53 interacting proteins and future directions

Several interesting hypotheses can be made regarding the GP proteomics data presented in these studies, that though not specifically tested, may provide additional insight into the mechanisms at play regarding ERGIC-53's presence and purpose in a multi-protein complex with the GPs. Accordingly, multiple ERGIC-53 interacting proteins were also identified in the GP interactome data sets including several COP proteins (including alpha and gamma) (Haines et al., 2012; Itin, Foguet, et al., 1995; Itin, Schindler, et al., 1995a; Kappeler et al., 1994b), and several tubulin proteins (Haines et al., 2012) (TUBB), ERP44 (Margherita Cortini & Roberto Sitia, 2010), valosin-containing protein (VCP) (Haines et al., 2012), nicastrin (NCSTN) (Morais et al., 2006), and sulfatase modifying factor 1 (SUMF1) (Fraldi et al., 2008) which binds indirectly through SUMF2 heterodimer formation (Zito et al., 2005). Interrogating the contribution of these proteins, individually and synergistically, to viral propagation may greatly increase our understanding of ERGIC-53's regulation and function in the secretory pathway and beyond. Several of these proteins have a variety of documented roles involved in viral replication including coatomer protein's pro-viral role with VSV, LCMV, HPIV (D. Panda et al., 2011), as well as FLUAV (Sun, He, & Zhuang, 2013)). VCP/p97 has also been shown to be critical for entry of an alphavirus, Sinbis virus (SINV), (Panda et al., 2013) and is involved in a human adenovirus (AdV) TRIM21-mediated neutralization process (Hauler, Mallery, McEwan, Bidgood, & James, 2012), as well as an enterovirus (polio virus (PV)) RNA replication (Arita, Wakita, & Shimizu, 2012). Examining how ERGIC-53 associates with its other known interacting proteins

may reveal additional functionality to the molecule and/or molecular complex, as well as illustrate the exact role it is playing during the production of infectious virus.

It is interesting to note that despite the large complex of ERGIC-53 interacting proteins identified in our proteomics screen, several of its known interacting partners were not found (α-1 antitrypsin (Nyfeler, Reiterer, et al., 2008a), fibroblast growth factor receptor 3 (Lievens et al., 2008), as well as the cathepsins C and Z (Christian Appenzeller et al., 1999; Vollenweider et al., 1998a)). This may suggest that there are separate pools of ERGIC-53 within the early secretory pathway, each with their own repertoire of regulatory proteins purposed to unique tasks. Alternatively, binding of ERGIC-53/MCFD2 to the viral GPs may impair its ability to interact with the remaining proteins mentioned above. In addition, the sensitivity of our assay may be insufficient to isolate macromolecular complexes past the second layer of proteins involved (e.g. GP to ERGIC-53 (1^{st}) and GP-ERGIC-53 to COP (2^{nd})). The lack of MCFD2 identification within the interactomes suggests that the sensitivity may indeed be insufficient to detect low abundance proteins, or protein complexes that may only be formed transiently. However, the exact ordering of the interactions is not currently known based on our biochemical interrogations. There may in fact be additional proteins bridging the GPs to ERGIC-53. Given the discovery of ERGIC-53 outside of the confines of the cell (e.g. within exosomes and virions), it will be important to extend the search for its cargo/ligands to the extracellular milieu (i.e. exosomes), cell surface proteins, as well as within the endocytic pathway.

4.1.2. Summary of the ERGIC-53-GP interaction

In chapters 2 and 3 we demonstrated ERGIC-53's conserved binding to several viral GPs. The structural significance of the conservation of ERGIC-53's interaction with GPs encoded by arenaviruses, coronaviruses, filoviruses, hantaviruses, orthomyxoviruses, and retroviruses remains to be determined. However, these data strongly suggest that these viral envelopes share some structural homology to an ancestral viral GP. The conservation of the cargo-receptor complex formed with MCFD2 and the listed GPs reinforces this idea. The large degree of primary amino acid separation amongst the GPs further suggests that the specific recruitment is based on a conserved fold or domain, rather than a specific amino acid sequence (or the presence of glycans). High-resolution structural data exist for several of the viral GPs listed including SARS S1 (receptor binding domain) and S2 (fusion subunit) (Deng, Liu, Zheng, Yong, & Lu, 2006; Li, Li, Farzan, & Harrison, 2005), EBOV GP1/GP2 (J. E. Lee et al., 2008; Weissenhorn, Carfi, Lee, Skehel, & Wiley, 1998), HIV Env (reviewed in (Merk & Subramaniam, 2013), as well as both OW and NW arenavirus GP-1/GP-2 (Abraham et al., 2010; Igonet et al., 2011; Parsy et al., 2013) . Comparisons of the individual subunits, and their respective domains, may yield vital information regarding how ERGIC-53 recognizes and binds to a viral GP. The ERGIC-53 CRD and MCFD2 complex, likewise, has been crystallized (Nishio et al., 2010). Fitting of the known GP subunits with the reported structures may reveal how the overall complex is formed. It has been reported that upon binding to MCFD2, carbohydrate, or calcium, that some refolding occurs amongst the ERGIC-53 - MCFD2 complex (Guy, Wigren, Svard, Hard, & Lindqvist, 2008; Nishio et al., 2010;

Wigren et al., 2010). It will therefore be imperative to analyze these proteins as a complex. The envelope glycoproteins have, however, produced several barriers to crystallization in a native state as glycosylated, full length, or intact GPs are notoriously challenging to crystallize (Lee et al., 2009).

The biochemical studies presented in chapters 2 and 3 demonstrate that GP's are all recognized by ERGIC-53 early in the secretory pathway based on its selective binding to full-length GPs (with the exception of hantavirus GPs). This was further supported by the finding that intracellular C#1 GP, ERGIC-53 (Chapter 2) and MCFD2 (Chapter 3), all selectively concentrate within the ERGIC during infection. Also, the ERGIC-53 domain mapping experiments in chapter 2, which demonstrated that the ER-restricted ERGIC-53 (KKAA) binds to GP, confirms a pre-ERGIC association. The consequence, if any, of the intracellular concentration, and how it relates to the proteolytic and/or maturation status of the glycoproteins also remains to be determined. One potential explanation is that a conserved glycan array on the viral GPs could be selectively modified within the ERGIC. In support of this notion, a specific endomannosidase has been reported to colocalize with ERGIC-53 and the intermediate compartment (Zuber, Spiro, Guhl, Spiro, & Roth, 2000). This glycan modification could in turn target the GPs to a specific subdomain or compartment, much like the mannose-6-phospate receptor (a P-type lectin) lysosomal targeting mechanism (reviewed in (Kim, Olson, & Dahms, 2009)), for later modification or secretion. However, in our studies, we were unable to detect changes in the release of GP, or in their migration via SDS PAGE in cells lacking ERGIC-53 that would be indicative of changes in glycosylation. The limit of resolution in our SDS-PAGE –

Western blot assay, may however, be insufficient to detect minor alterations in glycan composition. A mass spectroscopy-based approach to analyze the glycan composition with substantially greater mass-resolution would answer this question, much like what has been proposed by Krudysz-Amblo and colleagues for human tissue factor (Krudysz-Amblo, Jennings, Matthews, Mann, & Butenas, 2011).

4.2. Summary of findings for ERGIC-53 and MCFD2 functional studies and future directions (aim 2)

4.2.1. Summary of findings for ERGIC-53 functional studies and future directions (aim 2)

The discovery of an important role for ERGIC-53 in the propagation of arenaviruses fulfilled the goal of aim 2, and in doing so, catalyzed several additional important biological findings for not only ERGIC-53, but also for its soluble cofactor MCFD2. This significance was extended to several additional families of enveloped RNA viruses, all of which represent human pathogens in need of antiviral treatments. Briefly, following the biochemical identification of a novel class of pathogen-derived ligands for ERGIC-53, we used several complimentary techniques to determine that ERGIC-53 plays a critical role in the generation of infectious virions. First, RNAi knockdown of ERGIC-53 in cells resulted in JUNV C#1 propagation being reduced. Second, overexpression of ERGIC-53 in cells resulted in an enhancement in production of JUNV C#1. Third, human B cells naturally lacking ERGIC-53 were defective in their ability to produce infectious arenavirus particles. Lastly, expression of an ER-restricted mutant of ERGIC-53 potently inhibited the production of infectious C#1 and DANV particles, as well as

pseudoparticles of VSV decorated with SARS S and EBOV GP. This last piece of data suggested specifically that either the post-ER trafficking of ERGIC-53 was important for the production of infectious virus, or that its C-terminal targeting domain was required for viral propagation. These two concepts are not mutually exclusive, and so can be challenging to separate. Creating an ERGIC-53 tail chimera on a related lectin (VIP-36) could assist in discriminating between these two potential contributors.

ERGIC-53 expression has also been found to be upregulated in several types of mouse-derived cells (ANA-1 macrophages, MEFs, or embryonic endothelial progenitor cells) following infection with murine gammaherpes virus 68 (MHV68). Following ERGIC-53 siRNA knockdown there was a reduction in virus yield (Mages et al., 2008). Interestingly, the authors also pre-treated NIH3T3 cells with a phospholipase A_2 inhibitor (ONO-RS-082), known to inhibit retrograde trafficking of ERGIC-53 (de Figueiredo et al., 2000), and found that treatment also inhibited viral yield. These data, together with ours, indicates that the intact recycling pathway of ERGIC-53 is of critical importance for the generation of infectious virions, and is important in the propagation of multiple families of enveloped RNA viruses, and at least one DNA virus. Screening for an ERGIC-53 - dependent phenotype for additional pathogenic viruses including OW and NW hantaviruses, flaviviruses, and paramyxoviruses will be of interest to the virology community at large.

4.2.2. Summary of findings for MCFD2 functional studies and future directions (aim 2)

The investigation into the role of MCFD2 in viral propagation was initiated (unlike ERGIC-53, which began from an unbiased screen) as an interesting control because of its known role in forming a complex with ERGIC-53. The protective role of overexpressed MCFD2 during JUNV C#1 and DANV propagation (chapter 3) led us to hypothesize that MCFD2 may be acting as a viral restriction factor. The unexpected discovery of its antiviral role following overexpression, led us to investigate whether cells from MCFD2 null F5F8D patients would support infectious virus production. The enhanced production of infectious virus from MCFD2 null cells further supports the notion that this protein is acting as a restriction factor for arenaviruses. Overexpression of MCFD2 was also shown to inhibit the propagation of VSV bearing coronavirus, filovirus, and hantavirus GPs suggesting that, like ERGIC-53, its impact is highly conserved, and can be restricted to the presence of the respective viral GPs. The difference, however, was in the respective direction of regulation (i.e ERGIC-53 is pro-viral and MCFD2 is anti-viral).

4.3. Summary of findings for ERGIC-53's mechanism of action and future directions (aim 3)

Using several techniques we tested how ERGIC-53 and MCFD2 were impacting the production of infectious arenavirus particles. In chapter 2 we relied upon the DN ERGIC-53 to show that trafficking of ERGIC-53, despite being critical for generating infectious virus, was not required for the proteolytic processing, trafficking of GP, or its assembly and release in viral particles. During these studies we also discovered that ERGIC-53 would traffic to the plasma membrane along with the GP, and be packaged

into viral particles. Further, we were able to minimally map the stage of the defect in viral propagation to cell surface attachment. Specifically, virus from ERGIC-53 null cells was defective, in part, in its ability to attach to a permissive cell. These data are supported by the fact that DN ERGIC-53 cannot traffic beyond the ER (Andersson et al., 1999; Felix Kappeler & Hauri, 1997), and so would be prevented from entering into viral particles and thus influencing attachment. Collectively, these data suggest that ERGIC-53 may be acting as a host-derived attachment factor that is incorporated into virions.

The presence of ERGIC-53 in the extracellular space in both infected and uninfected preparations suggested that it was also found in cellular exosomes. This finding was corroborated by 2 additional studies which identified ERGIC-53 in human and rat derived exosomes (Conde-Vancells et al., 2008; Gonzalez-Begne et al., 2009). Moreover, it has been demonstrated that d,l-threo-1-phenyl-2-decanoylamino-3-morpholino-1-propanol (PDMP), a sphingolipid synthesis inhibitor known to interfere with the production of glycosylceramide and sphingomyelin, ER calcium homeostasis, and interfere with ERGIC-53's recycling (Maceyka & Machamer, 1997; Sprocati, Ronchi, Raimondi, Francolini, & Borgese, 2006), causes a reduction in the uptake of HIV-1 particles, produced in PDMP treated cells, by dendritic cells (Hatch, Archer, & Gummuluru, 2009). Further, this mechanism was later refined to include the requirement of CD169 (a SigLec) on the surface of dendritic cells recognizing the glycosphingolipid GM3 (for capture and trans-infection of HIV (Puryear et al., 2013). The same surface receptor (CD169) has been recently shown to mediate exosome capture via α2,3 sialic acid, specifically within the marginal zone of the spleen (Saunderson, Dunn, Crocker, &

McLellan, 2014), a prominent site involved in LCMV infection (Macal et al., 2012). If ERGIC-53, or its recycling, is required for biosynthesis of this class of specialized lipid, restriction of ERGIC-53 to the ER could disrupt the lipid content of viruses, as well as exosomes, and could therefore be expected to interfere with both capture of virus, as well as exosomes. Given our findings on the presence of ERGIC-53 in both virus and exosomes, we can further postulate that ERGIC-53 is involved directly in targeting or maintaining of the GPs in specific microdomains enriched in these lipids. Interestingly, equine influenza virus (EIV), also known to utilize α2,3 sialic acid, is inhibited via addition of PDMP (Stuart & Brown, 2007). We provide evidence in chapters 2 and 3 that additional FLUAV HA's from WSN and VN (H1 and H5) also interact with ERGIC-53. The effect of PDMP and ERGIC-53 on the uptake of these respective HA-bearing viruses will be important to determine experimentally. Further, dissecting a potential role of ERGIC-53 in the cellular biology of CD169 as well as glycosphingolipid biogenesis may shed light on the exact nature of this otherwise complicated interaction.

Another potential connection to lipid metabolism can be inferred by the interaction of both LCMV and ANDV GPs with molecules associated with sphingolipid biosynthesis; serine palmitoyltransferase long chain base subunit 1 and 2 (SPTLC1 and 2) which are involved in ER synthesis of sphingolipids (Gault, Obeid, & Hannun, 2010), and UDP-glucose ceramide glucosyltransferase-like 1 and 2 (UGCGL1 and UGCGL2). Given the number of other ERGIC-53 interacting proteins found within the proteomics list, some of these enzymes may have been found in complex with the glycoproteins via their association with ERGIC-53. In support of this notion, Haines and colleagues, while

mapping binding partners of UBDX1 and ERGIC-53, identified UGCGL1 (Haines et al., 2012).

Several additional hypotheses can be made regarding the role that ERGIC-53 is asserting during its control of arenavirus particle infectivity. Chapter 2 describes the mapping of the interaction between C#1 GP and ERGIC-53, minimally, to the C-terminal portion of ERGIC-53's CRD (in completion of aim 4). Further, chapter 3 demonstrates that expression of ERGIC-53ΔCRD restricts the propagation of JUNV C#1. The requirement of ERGIC-53's CRD both for binding to the GP and coordinating its function in the production of infectious virus could indicate that ERGIC-53 (without its CRD) is not packaged in virions due to lack of GP binding and/or that the CRD is controlling the infectivity of the particles directly. The major biological role of the CRD is binding to N-linked sugars (and the proteins to which they are attached) (Appenzeller-Herzog et al., 2004; Christian Appenzeller et al., 1999; Kawasaki et al., 2008; Moussalli et al., 1999b). ERGIC-53 ΔCRD, therefore, would be unable to carry out this function, which could indicate that ERGIC-53 controls viral infectivity, in part, via binding of its CRD to N-linked glycans on the surface of cells. This idea is supported by data illustrating that infection by an arenavirus could be blocked via addition of mannan (Goncalves et al., 2013; Martinez et al., 2013). The authors in these studies were investigating C-type lectin attachment factors (DC-SIGN and L-Sign) which are also known to bind mannosylated glycoproteins. Collectively these data may suggest a cooperative lectin-mediated attachment mechanism between virion associated ERGIC-53 and host cell-displayed DC-SIGN.

Alternatively, Velloso and colleagues, while examining the structure of ERGIC-53's CRD, reported on the structural similarity between the CRD and neurexins (Velloso, Svensson, Schneider, Pettersson, & Lindqvist, 2002). Neurexins are also known ligands of α-DG, and occupy a similar site on the receptor as OW arenavirus GPs (Rojek, Campbell, et al., 2007). These data could indicate that ERGIC-53, contained in OW arenavirus virions, is interacting with α-DG along with the GP to increase binding avidity of virions to cells. Furthermore, ERGIC-53 has also been reported to show structural homology to galectins (Arar et al., 1995). Galectin-3 has been demonstrated to be upregulated following infection with JUNV C#1 (Giusti et al., 2011), and has been shown also to bind to Mac-2BP (Inohara, Akahani, Koths, & Raz, 1996). Mac-2BP which also interacts with ERGIC-53's CRD (Chen et al., 2013), in a carbohydrate-dependent fashion. Therefore, Mac-2BP could bridge ERGIC-53 embedded in virions to Galectin-3 on the surface of cells. In addition, Mac-2BP has also been demonstrated to be upregulated during hantavirus infection, and binds to Tula virus, an OW hantavirus (Vaheri et al., 2013), suggesting a similar mechanism could be involved in hantavirus entry.

The presence of ERGIC-53 within arenavirus virions was an unexpected finding. The mechanism(s) involved in its recruitment to sites of arenavirus assembly and budding are currently unclear. Of relevance, ERGIC-53's expression levels are upregulated 2.5 fold during LCMV WE infection in primate liver cells (Djavani et al., 2009). Therefore it could be postulated that this upregulation allows ERGIC-53 to saturate its COPI retention (Kappeler et al., 1997b; Ellen J. Tisdale, Helen Plutner, Jeanne Matteson, & William E.

Balch, 1997) and traffic to the surface of cells. LCMV GP has also been reported to selectively induce the ATF6 branch of the unfolded protein response (Pasqual, Burri, et al., 2011b), which has been shown to upregulate ERGIC-53 (Nyfeler et al., 2003a), further supporting the hypothesis of its role in causing post-ERGIC movement of ERGIC-53. Heat-shock (Spatuzza et al., 2004) as well as the presence of NO (Renna et al., 2006) also upregulate ERGIC-53, and are known consequences of arenavirus infection (Brocato & Voss, 2009) and would likewise support this proposed mechanism of viral GP induced alterations in ERGIC-53's trafficking.

4.3.1. Summary of findings for the mechanism of action of ERGIC-53 and MCFD2 in viral propagation and future directions

An outstanding question remains: how does MCFD2 regulate viral propagation? Several lines of evidence support its role as a restriction factor. First, MCFD2 following arenavirus infection, is highly upregulated (Chapter 3) and (Djavani et al., 2009)). Second, plasmid overexpression inhibits propagation of multiple enveloped RNA viruses in a GP-restricted fashion. Third, cells lacking MCFD2 are more susceptible to infection. Importantly, VSV is neither impacted by MCFD2, nor is its GP able to form a complex with ERGIC-53 and MCFD2. This evidence indicates that the MCFD2 contains specificity in its antiviral action, and that its action is restricted by specific viral GPs. The data presented in Chapter 3 also indicate that MCFD2 may be acting as a restriction factor through its interaction with ERGIC-53 by regulating ERGIC-53's ability to control viral infectivity. We have not, however, conclusively ruled out the possibility that the two

proteins may be acting independently of one another. MCFD2 may bind to a separate receptor on the surface of cells that, following binding, initiates an antiviral cascade. In order to test for this possibility, several methodologies could be employed. To identify a cell surface receptor of MCFD2, cell surface proteins could be biotinylated and isolated via streptavidin beads, and the captured proteins subjected to a Far-Western blot analysis where soluble MCFD2 was used as a probe. MCFD2 positive proteins bands could then be excised and identified via mass spectroscopy. Alternatively, cell membrane preparations could be isolated via gradient ultracentrifugation, and incubated with immobilized MCFD2. Captured proteins could then be eluted, and identified via mass spectroscopy. These two approaches would require additional studies targeting the expression and function of the putative receptor to then formally test its sufficiency for antiviral signaling.

The triple dSTORM analysis of sMCFD2, ERGIC-53, and C#1 NP, as well as the pre-complexed sMCFD2-virus addition assays lend support to a model where the antiviral activity of MCFD2 is taking place directly via neutralization of the virus. Using the highly sensitive qPCR-based attachment assay outlined in chapter 2, it could be tested whether the defect is taking place solely at the level of attachment, or if MCFD2, when pre-complexed to virions, is impeding its intracellular trafficking, disrupting the fusion capabilities of the GP, or interfering with the transcription or replication of the RNA through an unknown mechanism. In order to examine potential alterations in either fusion potential or trafficking of the pre-complexed virions, Alexa Fluor 647 conjugated virus (highly concentrated) could be used to study the trafficking of virus through the

endosomal system (Lozach et al., 2011; Pasqual, Rojek, et al., 2011). A similar approach, but with dual fluorescently labeled virus (DioC and R18) has been successfully used to quantitate influenza virus fusion in real-time based on fluorescent shifts following fusion of virus within endosomes (Sakai et al., 2006). A similar approach would be feasible with arenaviruses, and would facilitate the quantitative assessment of fusion alterations following addition of MCFD2, if that is indeed the case. A pitfall to both of these approaches is the high multiplicity of infection required to gain adequate signal to noise ratios. However, the ERGIC-53 dependent phenotype could likewise be altered during these steps of the viral life cycle, and thus could benefit from a quantitative assessment.

Collectively, the identification of a proviral and antiviral role for the ERGIC-53/MCFD2 cargo receptor complex strongly suggests that this cellular machinery is of critical importance to the outcome of infection with multiple viruses that are pathogenic for humans. Selectively targeting the CRD of ERGIC-53 via a library of small molecules would likely yield valuable lead compounds for drug development, based on the critical role demonstrated in chapter 2 for binding to GP, and chapter 3 for controlling viral infectivity. Interestingly, in support of this notion, a recent study by Lu and colleagues demonstrated that a small molecule interfering with the interaction of JUNV C#1 Z and TSG101 resulted in a pronounced reduction in viral release (Lu et al., 2014). Further, given the small size and solubility of MCFD2, its potent role in the neutralization of viral infectivity, and the advanced structural data on the molecule, a small molecule could be rationally designed to mimic MCFD2's ERGIC-53 interacting residues.

4.4. Summary of findings for the molecular arrangement of the ERGIC-53/MCFD2 complex binding to glycoproteins.

The details of the domain residues required for ERGIC-53 to interact with JUNV C#1 GP were discussed in chapter 2, and have been mentioned in section 4.2.2. Briefly, we tested a comprehensive panel of plasmids encoding deletions and mutations in each of the known functional regions of ERGIC-53 (excluding the transmembrane domain) and found that the CRD alone was responsible for binding to an arenavirus GP. This finding was in agreement with our original hypothesis, as the glycoproteins are heavily mannosylated (Buchmeier et al., 2007; Wright et al., 1990a) and ERGIC-53 is a mannose-specific lectin (C. Appenzeller et al., 1999b; Kamiya et al., 2008; Moussalli et al., 1999b). Interestingly, the sugar, calcium, and MCFD2 binding properties of ERGIC-53 along with its oligomerization, and forward trafficking, were all found to be unrelated to the interaction with C#1 GP. These data demonstrate a novel lectin-independent mechanism of cargo binding. As has been discussed above, there is a plausible benefit to the virus to maintain its interaction with ERGIC-53 from a site distinct from its normal ligand binding: maintenance of ERGIC-53's normal cellular functions. This strategy has also been employed by New World arenaviruses interacting with TfR1 and may then represent a common mechanism by which the viruses engage passively with a host molecule (Abraham et al., 2010; Radoshitzky et al., 2007).

4.5. Summary of findings, biological and evolutionary significance, and closing remarks

It is feasible that the interaction of viral GPs with the ERGIC-53/MCFD2 cargo receptor complex is not entirely harmless to the host. While loss of ERGIC-53 and MCFD2 is well tolerated by humans (Khoriaty et al., 2012), it does, however, result in a specific deficiency in FV and FVIII (F5F8D) (Nichols et al., 1998; Bin Zhang et al., 2003). Accordingly, deficiencies in circulating FV and FVIII cause bleeding abnormalities following trauma such as surgery or child birth (Spreafico & Peyvandi, 2008; Zhang, 2009). Loss of ERGIC-53 or MCFD2, though able to cause disease, is a manageable syndrome with little to no long term consequences. Loss of ERGIC-53 or MCFD2 allows the cellular architecture to remain intact and the host secretome is largely unmodified (Mitrovic et al., 2008; Vollenweider et al., 1998a; Zhang et al., 2011). This information was the primary impetus for this in-depth study of ERGIC-53 and specifically its selection as an antiviral target. Arenaviruses, hantaviruses, and notably the filoviruses, each can cause a hemorrhagic fever syndrome, where specific deficiencies in clotting factors have been reported (Lee, 1987; Lee et al., 1989; Felisa C. Molinas et al., 1981; Schwarz et al., 1972). However, given the logistical problems involved in obtaining and testing serum samples from infected patients, much of what is currently understood about coagulation abnormalities caused by these viruses is the result of animal models of infection (Molinas et al., 1978; Xiao, Zhang, Yang, & Tesh, 2001). We provide several lines of evidence that support the notion that the ERGIC-53/MCFD2 cargo receptor may no longer be able to support the secretion of coagulation factors during an infection. First, the binding of the trimeric GP complex to the ERGIC-53/MCFD2 complex, specifically within the CRD, may impede the binding of the large FV and FVIII molecules. Second, the re-routing of ERGIC-53, along with the viral GP, to

the plasma membrane, as well as to the surface of virions, removes the potential for those ERGIC-53 molecules to shuttle FV and FVIII forward. Given the recycling nature of the ERGIC-53/MCFD2 complex, removal of a fraction of the pool is likely to have a compounding effect over time.

The first explanation mentioned in the preceding paragraph, inhibition of FV/FVIII binding caused by GP-mediated steric hindrance, can be experimentally tested using a well-established co-immunoprecipitation technique (Cunningham et al., 2003; Zheng, Liu, Yuan, et al., 2010; Zheng, Liu, Zhou, et al., 2010). Expression of the glycoprotein in cells also expressing the clotting factors should, if this hypothesis is correct, show a reduced co-immunoprecipitation of each factor with ERGIC-53 and MCFD2. There are notable caveats to this approach, however, first in the cost reagents to identify FV and FVIII directly, and secondly, the need to express the clotting factors *in trans*. To date, most biochemical evaluations of the ERGIC-53/MCFD2 complex and FV/FVIII binding have relied upon transient transfections to express FV and FVIII. The second proposed mechanism, inefficient secretion due to lack of available ERGIC-53/MCFD2, can be tested indirectly through a coagulation activity assay (Tilley, Levit, & Samis, 2012; Zhang et al., 2008). Similar caveats exist for this approach as well.

A thorough understanding the molecular mechanisms behind the bleeding abnormalities observed during infection with VHFs will likely reveal a multifactorial cause. Platelet abnormalities, specific factor deficiencies, as well as endothelial barrier dysfunction may all contribute to the hemorrhaging. However, removal of either ERGIC-53 or MCFD2 is sufficient to cause a coagulopathy. Through the biochemical interaction

and the trafficking alterations, it would seem that the arenavirus GPs are likely sufficient to disrupt the efficient secretion of these molecules, and therefore provide a direct molecular mechanism explaining the bleeding abnormalities that have mystified scientists and clinicians for half of a century.

Last, and perhaps most importantly, given the potent role of ERGIC-53 and MCFD2 in dictating the infectivity of arenavirus, coronavirus, filovirus, and hantavirus particles, there may be sufficient selective pressure to preserve (ERGIC-53) or discourage (MCFD2) the maintenance of diseased alleles in the human population. Several lines of evidence support of this idea. Firstly, genetic lesions in the MCFD2 gene occur much less frequently in the human population relative to ERGIC-53 (30% vs 70 %). The disease caused by loss of MCFD2 is also somewhat more profound in the impairment of FV and FVIII secretion (Zhang et al., 2008). We demonstrate that cells from people lacking ERGIC-53 produce less infectious virus, whereas cells from people lacking MCFD2 produce more infectious virus. People lacking MCFD2, if this cellular phenotype holds true, would produce more virus. Viral titer is a strong predictor of disease severity (Richmond & Baglole, 2003). Further, in areas of Africa where Lassa virus is endemic, it has been hypothesized that the virus may provide a selective pressure on certain SNPs that were found in genes regulating the biosynthesis of its receptor, α-DG (Oldstone & Campbell, 2011; Sabeti et al., 2007). The receptor for pathogenic NW arenaviruses has also been hypothesized to be under positive selection (Demogines et al., 2013). Inherent human disease providing protection from acquired disease has been proposed for a number of circumstances. The earliest, and perhaps, most well-known example of this

would be the proposal of Allison in 1954, who, based on Raper and Lehman's 1949 observations of high frequencies of sickle cell anemia in Ugandans (Lehmann & Raper, 1949), suggested that the abundance of the disease could be a result of the protection it afforded from malaria (Allison, 1954), the disease cause by the plasmodium falciparum parasite. Therefore, in our studies, exposure to rodents and the viruses they harbored may have provided a similar protection to an archetype arenavirus.

In conclusion, the identification of conserved biosynthetic machinery utilized by multiple families of enveloped RNA viruses has revealed a wealth of information about not only the evolution of these viruses, but also the co-evolution of virus and host. From these studies, a clearer picture of the underlying cellular biology and cause of arenavirus propagation and disease has been obtained, a novel molecular machine to interfere with therapeutically has been identified, and insight into the selective pressures that have shaped the modern human have been gained.

5. Comprehensive Bibliography

Abraham, J., Corbett, K. D., Farzan, M., Choe, H., & Harrison, S. C. (2010). Structural basis for receptor recognition by New World hemorrhagic fever arenaviruses. *Nat Struct Mol Biol, 17*(4), 438-444. doi: 10.1038/nsmb.1772

Abraham, J., Kwong, J. A., Albarino, C. G., Lu, J. G., Radoshitzky, S. R., Salazar-Bravo, J., . . . Choe, H. (2009). Host-species transferrin receptor 1 orthologs are cellular receptors for nonpathogenic new world clade B arenaviruses. *PLoS Pathog, 5*(4), e1000358. doi: 10.1371/journal.ppat.1000358

Agnihothram, S. S., Dancho, B., Grant, K. W., Grimes, M. L., Lyles, D. S., & Nunberg, J. H. (2009). Assembly of Arenavirus Envelope Glycoprotein GPC in Detergent-Soluble Membrane Microdomains. *Journal of Virology, 83*(19), 9890-9900. doi: 10.1128/jvi.00837-09

Agnihothram, S. S., York, J., & Nunberg, J. H. (2006). Role of the stable signal peptide and cytoplasmic domain of G2 in regulating intracellular transport of the Junin virus envelope glycoprotein complex. *J Virol, 80*(11), 5189-5198. doi: 80/11/5189 [pii] 10.1128/JVI.00208-06

Agnihothram, S. S., York, J., Trahey, M., & Nunberg, J. H. (2007). Bitopic membrane topology of the stable signal peptide in the tripartite Junin virus GP-C envelope glycoprotein complex. *J Virol, 81*(8), 4331-4337. doi: JVI.02779-06 [pii] 10.1128/JVI.02779-06

Ahmed, R., & Oldstone, M. B. (1988). Organ-specific selection of viral variants during chronic infection. *J Exp Med, 167*(5), 1719-1724.

Ahmed, R., Salmi, A., Butler, L. D., Chiller, J. M., & Oldstone, M. B. (1984). Selection of genetic variants of lymphocytic choriomeningitis virus in spleens of persistently infected mice. Role in suppression of cytotoxic T lymphocyte response and viral persistence. *J Exp Med, 160*(2), 521-540.

Albarino, C. G. (2010). High Diversity and Ancient Common Ancestry of Lymphocytic Choriomeningitis Virus. *Emerging Infectious Diseases, 16*(7). doi: 10.3201/eid1607.091902

Albarino, C. G., Bird, B. H., Chakrabarti, A. K., Dodd, K. A., Flint, M., Bergeron, E., . . . Nichol, S. T. (2011). The major determinant of attenuation in mice of the Candid1 vaccine for Argentine hemorrhagic fever is located in the G2 glycoprotein transmembrane domain. *J Virol, 85*(19), 10404-10408. doi: JVI.00856-11 [pii] 10.1128/JVI.00856-11

Albarino, C. G., Bird, B. H., Chakrabarti, A. K., Dodd, K. A., White, D. M., Bergeron, E., . . . Nichol, S. T. (2011). Reverse genetics generation of chimeric infectious Junin/Lassa virus is dependent on interaction of homologous glycoprotein stable signal peptide and G2 cytoplasmic domains. *J Virol, 85*(1), 112-122. doi: JVI.01837-10 [pii] 10.1128/JVI.01837-10

Albarino, C. G., Ghiringhelli, P. D., Posik, D. M., Lozano, M. E., Ambrosio, A. M., Sanchez, A., & Romanowski, V. (1997). Molecular characterization of attenuated Junin virus strains. *J Gen Virol, 78 (Pt 7)*, 1605-1610.

Allison, A. C. (1954). Protection afforded by sickle-cell trait against subtertian malareal infection. *Br Med J, 1*(4857), 290-294.

Amman, B. R., Pavlin, B. I., Albarino, C. G., Comer, J. A., Erickson, B. R., Oliver, J. B., . . . Ksiazek, T. G. (2007). Pet rodents and fatal lymphocytic choriomeningitis in transplant patients. *Emerg Infect Dis, 13*(5), 719-725. doi: 10.3201/eid1305.061269

Amorosa, V., MacNeil, A., McConnell, R., Patel, A., Dillon, K. E., Hamilton, K., . . . Nichol, S. T. (2010). Imported Lassa fever, Pennsylvania, USA, 2010. *Emerg Infect Dis, 16*(10), 1598-1600.

Andersson, H., Kappeler, F., & Hauri, H. P. (1999). Protein targeting to endoplasmic reticulum by dilysine signals involves direct retention in addition to retrieval. *J Biol Chem, 274*(21), 15080-15084.

Anelli, T., Ceppi, S., Bergamelli, L., Cortini, M., Masciarelli, S., Valetti, C., & Sitia, R. (2007). Sequential steps and checkpoints in the early exocytic compartment during secretory IgM biogenesis. *EMBO J, 26*(19), 4177-4188. doi: 10.1038/sj.emboj.7601844

Appenzeller-Herzog, C. (2003). pH-induced Conversion of the Transport Lectin ERGIC-53 Triggers Glycoprotein Release. *Journal of Biological Chemistry, 279*(13), 12943-12950. doi: 10.1074/jbc.M313245200

Appenzeller-Herzog, C., Roche, A. C., Nufer, O., & Hauri, H. P. (2004). pH-induced conversion of the transport lectin ERGIC-53 triggers glycoprotein release. *Journal of Biological Chemistry, 279*(13), 12943-12950. doi: 10.1074/jbc.M313245200 M313245200 [pii]

Appenzeller, C., Andersson, H., Kappeler, F., & Hauri, H. P. (1999a). The lectin ERGIC-53 is a cargo transport receptor for glycoproteins. *Nature Cell Biology, 1*(6), 330-334.

Arar, C., Carpentier, V., Le Caer, J. P., Monsigny, M., Legrand, A., & Roche, A. C. (1995). ERGIC-53, a membrane protein of the endoplasmic reticulum-Golgi

intermediate compartment, is identical to MR60, an intracellular mannose-specific lectin of myelomonocytic cells. *J Biol Chem, 270*(8), 3551-3553.

Aridor, M., Bannykh, S. I., Rowe, T., & Balch, W. E. (1995). Sequential coupling between COPII and COPI vesicle coats in endoplasmic reticulum to Golgi transport. *The Journal of Cell Biology, 131*(4), 875-893. doi: 10.1083/jcb.131.4.875

Arita, M., Wakita, T., & Shimizu, H. (2012). Valosin-containing protein (VCP/p97) is required for poliovirus replication and is involved in cellular protein secretion pathway in poliovirus infection. *J Virol, 86*(10), 5541-5553. doi: 10.1128/JVI.00114-12

Armstrong, C., & Lillie, R. D. (1934). Experimental Lymphocytic Choriomeningitis of Monkeys and Mice Produced by a Virus Encountered in Studies of the 1933 St. Louis Encephalitis Epidemic. *Public Health Reports (1896-1970), 49*(35), 1019-1027. doi: 10.2307/4581290

Arribalzaga, R. A. (1955). [New epidemic disease due to unidentified germ: nephrotoxic, leukopenic and enanthematous hyperthermia]. *Dia Med, 27*(40), 1204-1210.

Auperin, D. D., Romanowski, V., Galinski, M., & Bishop, D. H. (1984). Sequencing studies of pichinde arenavirus S RNA indicate a novel coding strategy, an ambisense viral S RNA. *Journal of Virology, 52*(3), 897-904.

Ballif, B. A., Cao, Z., Schwartz, D., Carraway, K. L., 3rd, & Gygi, S. P. (2006). Identification of 14-3-3epsilon substrates from embryonic murine brain. *J Proteome Res, 5*(9), 2372-2379. doi: 10.1021/pr060206k

Barresi, R., & Campbell, K. P. (2006). Dystroglycan: from biosynthesis to pathogenesis of human disease. *Journal of Cell Science, 119*(2), 199-207. doi: 10.1242/jcs.02814

Barton, L. L., & Hyndman, N. J. (2000). Lymphocytic Choriomeningitis Virus: Reemerging Central Nervous System Pathogen. *Pediatrics, 105*(3), e35.

Baum, S. G., Lewis, A. M., Rowe, W. P., & Huebner, R. J. (1966). Epidemic Nonmeningitic Lymphocytic-Choriomeningitis-Virus Infection. *New England Journal of Medicine, 274*(17), 934-936. doi: doi:10.1056/NEJM196604282741704

Bausch, D. G., Demby, A. H., Coulibaly, M., Kanu, J., Goba, A., Bah, A., . . . Rollin, P. E. (2001). Lassa fever in Guinea: I. Epidemiology of human disease and clinical observations. *Vector Borne Zoonotic Dis, 1*(4), 269-281.

Bausch, D. G., Rollin, P. E., Demby, A. H., Coulibaly, M., Kanu, J., Conteh, A. S., . . . Ksiazek, T. G. (2000). Diagnosis and clinical virology of Lassa fever as evaluated by enzyme-linked immunosorbent assay, indirect fluorescent-antibody test, and virus isolation. *J Clin Microbiol, 38*(7), 2670-2677.

Ben-Tekaya, H., Kahn, R. A., & Hauri, H.-P. (2010). ADP Ribosylation Factors 1 and 4 and Group VIA Phospholipase A2 Regulate Morphology and Intraorganellar Traffic in the Endoplasmic Reticulum–Golgi Intermediate Compartment. *Molecular Biology of the Cell, 21*(23), 4130-4140. doi: 10.1091/mbc.E10-01-0022

Ben-Tekaya, H., Miura, K., Pepperkok, R., & Hauri, H. P. (2005). Live imaging of bidirectional traffic from the ERGIC. *Journal of Cell Science, 118*(Pt 2), 357-367. doi: jcs.01615 [pii] 10.1242/jcs.01615

Bergthaler, A., Flatz, L., Hegazy, A. N., Johnson, S., Horvath, E., Lohning, M., & Pinschewer, D. D. (2010). Viral replicative capacity is the primary determinant of lymphocytic choriomeningitis virus persistence and immunosuppression. *Proc Natl Acad Sci U S A, 107*(50), 21641-21646. doi: 10.1073/pnas.1011998107

Bergthaler, A., Merkler, D., Horvath, E., Bestmann, L., & Pinschewer, D. D. (2007). Contributions of the lymphocytic choriomeningitis virus glycoprotein and polymerase to strain-specific differences in murine liver pathogenicity. *J Gen Virol, 88*(Pt 2), 592-603. doi: 88/2/592 [pii] 10.1099/vir.0.82428-0

Beyer, W. R., Popplau, D., Garten, W., von Laer, D., & Lenz, O. (2003). Endoproteolytic Processing of the Lymphocytic Choriomeningitis Virus Glycoprotein by the Subtilase SKI-1/S1P. *Journal of Virology, 77*(5), 2866-2872. doi: 10.1128/jvi.77.5.2866-2872.2003

Bolken, T. C., Laquerre, S., Zhang, Y., Bailey, T. R., Pevear, D. C., Kickner, S. S., . . . Hruby, D. E. (2006). Identification and characterization of potent small molecule inhibitor of hemorrhagic fever New World arenaviruses. *Antiviral Res, 69*(2), 86-97. doi: 10.1016/j.antiviral.2005.10.008

Bond, N., Schieffelin, J. S., Moses, L. M., Bennett, A. J., & Bausch, D. G. (2012). A Historical Look at the First Reported Cases of Lassa Fever: IgG Antibodies 40 Years After Acute Infection. *Am J Trop Med Hyg*. doi: 10.4269/ajtmh.12-0466

Bonhomme, C. J., Capul, A. A., Lauron, E. J., Bederka, L. H., Knopp, K. A., & Buchmeier, M. J. (2011). Glycosylation modulates arenavirus glycoprotein expression and function. *Virology, 409*(2), 223-233. doi: S0042-6822(10)00647-1 [pii] 10.1016/j.virol.2010.10.011

Bonhomme, C. J., Knopp, K. A., Bederka, L. H., Angelini, M. M., & Buchmeier, M. J. (2013). LCMV Glycosylation Modulates Viral Fitness and Cell Tropism. *PLoS One, 8*(1), e53273. doi: 10.1371/journal.pone.0053273

Bonilla, W. V., Pinschewer, D. D., Klenerman, P., Rousson, V., Gaboli, M., Pandolfi, P. P., . . . Hengartner, H. (2002). Effects of Promyelocytic Leukemia Protein on Virus-Host Balance. *Journal of Virology, 76*(8), 3810-3818. doi: 10.1128/jvi.76.8.3810-3818.2002

Bonthius, D. J. (2012). Lymphocytic Choriomeningitis Virus: An Underrecognized Cause of Neurologic Disease in the Fetus, Child, and Adult. *Seminars in Pediatric Neurology, 19*(3), 89-95. doi: http://dx.doi.org/10.1016/j.spen.2012.02.002

Bonthius, D. J., Mahoney, J., Buchmeier, M. J., Karacay, B., & Taggard, D. (2002). Critical role for glial cells in the propagation and spread of lymphocytic choriomeningitis virus in the developing rat brain. *J Virol, 76*(13), 6618-6635.

Bonthius, D. J., Wright, R., Tseng, B., Barton, L., Marco, E., Karacay, B., & Larsen, P. D. (2007). Congenital lymphocytic choriomeningitis virus infection: spectrum of disease. *Annals of Neurology, 62*(4), 347-355. doi: 10.1002/ana.21161

Borden, K. L., Campbell Dwyer, E. J., & Salvato, M. S. (1998). An arenavirus RING (zinc-binding) protein binds the oncoprotein promyelocyte leukemia protein (PML) and relocates PML nuclear bodies to the cytoplasm. *J Virol, 72*(1), 758-766.

Borden, K. L. B., CampbellDwyer, E. J., Carlile, G. W., Djavani, M., & Salvato, M. S. (1998). Two RING Finger Proteins, the Oncoprotein PML and the Arenavirus Z Protein, Colocalize with the Nuclear Fraction of the Ribosomal P Proteins. *Journal of Virology, 72*(5), 3819-3826.

Borrow, P., Evans, C. F., & Oldstone, M. B. (1995). Virus-induced immunosuppression: immune system-mediated destruction of virus-infected dendritic cells results in generalized immune suppression. *J Virol, 69*(2), 1059-1070.

Borrow, P., Martínez-Sobrido, L., & De la Torre, J. (2010). Inhibition of the Type I Interferon Antiviral Response During Arenavirus Infection. *Viruses, 2*(11), 2443-2480.

Borrow, P., & Oldstone, M. B. (1994). Mechanism of lymphocytic choriomeningitis virus entry into cells. *Virology, 198*(1), 1-9. doi: 10.1006/viro.1994.1001

Botten, J., King, B., Klaus, Joseph P., & Zeigler, C. (2013). Pathogenic Old World Arenaviruses *Viral hemorrhagic fevers* (pp. 233-260): CRC Press.

Botten, J., Whitton, J. L., Barrowman, P., Sidney, J., Whitmire, J. K., Alexander, J., . . . Buchmeier, M. J. (2007). HLA-A2-restricted protection against lethal lymphocytic choriomeningitis. *J Virol, 81*(5), 2307-2317. doi: JVI.02063-06 [pii] 10.1128/JVI.02063-06

Bowden, T. A., Crispin, M., Graham, S. C., Harvey, D. J., Grimes, J. M., Jones, E. Y., & Stuart, D. I. (2009). Unusual Molecular Architecture of the Machupo Virus Attachment Glycoprotein. *Journal of Virology, 83*(16), 8259-8265. doi: 10.1128/jvi.00761-09

Bowen, M. D., Peters, C. J., & Nichol, S. T. (1996). The phylogeny of New World (Tacaribe complex) arenaviruses. *Virology, 219*(1), 285-290. doi: 10.1006/viro.1996.0248

Bowen, M. D., Peters, C. J., & Nichol, S. T. (1997). Phylogenetic analysis of the Arenaviridae: patterns of virus evolution and evidence for cospeciation between arenaviruses and their rodent hosts. *Molecular Phylogenetics and Evolution, 8*(3), 301-316. doi: 10.1006/mpev.1997.0436

Bowen, M. D., Rollin, P. E., Ksiazek, T. G., Hustad, H. L., Bausch, D. G., Demby, A. H., . . . Nichol, S. T. (2000). Genetic Diversity among Lassa Virus Strains. *Journal of Virology, 74*(15), 6992-7004. doi: 10.1128/jvi.74.15.6992-7004.2000

Branco, L. M., & Garry, R. F. (2009). Characterization of the Lassa virus GP1 ectodomain shedding: implications for improved diagnostic platforms. *Virology Journal, 6*(1), 147. doi: 10.1186/1743-422x-6-147

Branco, L. M., Grove, J. N., Geske, F. J., Boisen, M. L., Muncy, I. J., Magliato, S. A., . . . Garry, R. F. (2010). Lassa virus-like particles displaying all major immunological determinants as a vaccine candidate for Lassa hemorrhagic fever. *Virology Journal, 7*(1), 279. doi: 10.1186/1743-422x-7-279

Branco, L. M., Grove, J. N., Moses, L. M., Goba, A., Fullah, M., Momoh, M., . . . Garry, R. F. (2010). Shedding of soluble glycoprotein 1 detected during acute Lassa virus infection in human subjects. *Virol J, 7*, 306. doi: 10.1186/1743-422X-7-306

Brass, A. L., Dykxhoorn, D. M., Benita, Y., Yan, N., Engelman, A., Xavier, R. J., . . . Elledge, S. J. (2008). Identification of host proteins required for HIV infection through a functional genomic screen. *Science, 319*(5865), 921-926. doi: 10.1126/science.1152725

Breuza, L., Halbeisen, R., Jenö, P., Otte, S., Barlowe, C., Hong, W., & Hauri, H.-P. (2004). Proteomics of Endoplasmic Reticulum-Golgi Intermediate Compartment (ERGIC) Membranes from Brefeldin A-treated HepG2 Cells Identifies ERGIC-32, a New Cycling Protein That Interacts with Human Erv46. *Journal of Biological Chemistry, 279*(45), 47242-47253. doi: 10.1074/jbc.M406644200

Briese, T., Paweska, J. T., McMullan, L. K., Hutchison, S. K., Street, C., Palacios, G., . . . Lipkin, W. I. (2009). Genetic detection and characterization of Lujo virus, a new hemorrhagic fever-associated arenavirus from southern Africa. *PLoS Pathog, 5*(5), e1000455. doi: 10.1371/journal.ppat.1000455

Briknarova, K., Thomas, C. J., York, J., & Nunberg, J. H. (2011). Structure of a zinc-binding domain in the Junin virus envelope glycoprotein. *J Biol Chem, 286*(2), 1528-1536. doi: M110.166025 [pii] 10.1074/jbc.M110.166025

Brocato, R. L., & Voss, T. G. (2009). Pichinde virus induces microvascular endothelial cell permeability through the production of nitric oxide. *Virol J, 6*, 162. doi: 10.1186/1743-422X-6-162

Brunotte, L., Kerber, R., Shang, W., Hauer, F., Hass, M., Gabriel, M., . . . Günther, S. (2011). Structure of the Lassa Virus Nucleoprotein Revealed by X-ray Crystallography, Small-angle X-ray Scattering, and Electron Microscopy. *Journal of Biological Chemistry, 286*(44), 38748-38756. doi: 10.1074/jbc.M111.278838

Brunotte, L., Lelke, M., Hass, M., Kleinsteuber, K., Becker-Ziaja, B., & Gunther, S. (2011). Domain structure of Lassa virus L protein. *J Virol, 85*(1), 324-333. doi: 10.1128/JVI.00721-10

Buchmeier, M., & Zajac, A. (1999). Lymphocytic choriomeningitis virus. *Persistent viral infections, 575*.

Buchmeier, M. J. (2002). Arenaviruses: protein structure and function. *Curr Top Microbiol Immunol, 262*, 159-173.

Buchmeier, M. J., de la Torre, J. C., & Peters, C. J. (2007). *Arenaviridae*: The Viruses and Their Replication. In D. M. Knipe, P. M. Howley, D. E. Griffin, R. A. Lamb, M. A. Martin, B. Roizman & S. E. Straus (Eds.), *Fields Virology* (5th ed., Vol. 2, pp. 1791-1827). Philadelphia: Wolters Kluwer Health/Lippincott Williams & Wilkins.

Buchmeier, M. J., Elder, J. H., & Oldstone, M. B. (1978). Protein structure of lymphocytic choriomeningitis virus: identification of the virus structural and cell associated polypeptides. *Virology, 89*(1), 133-145.

Buchmeier, M. J., & Oldstone, M. B. (1979). Protein structure of lymphocytic choriomeningitis virus: evidence for a cell-associated precursor of the virion glycopeptides. *Virology, 99*(1), 111-120.

Buchmeier, M. J., Southern, P. J., Parekh, B. S., Wooddell, M. K., & Oldstone, M. B. (1987). Site-specific antibodies define a cleavage site conserved among arenavirus GP-C glycoproteins. *J Virol, 61*(4), 982-985.

Buckley, S. M., & Casals, J. (1970). Lassa Fever, a New Virus Disease of Man from West Africa: III. Isolation and Characterization of the Virus. *The American Journal of Tropical Medicine and Hygiene, 19*(4), 680-691.

Burns, J., & Buchmeier, M. (1993). Glycoproteins of the Arenaviruses. In M. Salvato (Ed.), *The Arenaviridae* (pp. 17-35): Springer US.

Burns, J. W., and M. J. Buchmeier. (1993). *Glycoproteins of the arenaviruses*. New York: Plenum Press.

Burns, J. W., & Buchmeier, M. J. (1991). Protein-protein interactions in lymphocytic choriomeningitis virus. *Virology, 183*(2), 620-629. doi: 0042-6822(91)90991-J [pii]

Burri, D. J., Pasquato, A., da Palma, J. R., Igonet, S., Oldstone, M. B., & Kunz, S. (2013). The role of proteolytic processing and the stable signal peptide in expression of the Old World arenavirus envelope glycoprotein ectodomain. *Virology, 436*(1), 127-133. doi: 10.1016/j.virol.2012.10.038

Byrd, R. G., Cone, L. A., Commess, B. C., Williams-Herman, D., Rowland, J. M., Lee, B., . . . Charrel, R. N. (2000). Fatal illnesses associated with a New World arenavirus - California, 1999-2000 (Reprinted from MMWR, vol 49, pg 709-711, 2000). *Jama-Journal of the American Medical Association, 284*(10), 1237-1238.

Cajimat, M. N., Milazzo, M. L., Borchert, J. N., Abbott, K. D., Bradley, R. D., & Fulhorst, C. F. (2008). Diversity among Tacaribe serocomplex viruses (family Arenaviridae) naturally associated with the Mexican woodrat (Neotoma mexicana). *Virus Res, 133*(2), 211-217. doi: S0168-1702(08)00028-2 [pii] 10.1016/j.virusres.2008.01.005

Cajimat, M. N., Milazzo, M. L., Bradley, R. D., & Fulhorst, C. F. (2007). Catarina virus, an arenaviral species principally associated with Neotoma micropus (southern plains woodrat) in Texas. *Am J Trop Med Hyg, 77*(4), 732-736. doi: 77/4/732 [pii]

Camire, R. M., & Bos, M. H. (2009). The molecular basis of factor V and VIII procofactor activation. *J Thromb Haemost, 7*(12), 1951-1961. doi: 10.1111/j.1538-7836.2009.03622.x

Candurra, N. A., & Damonte, E. B. (1997). Effect of inhibitors of the intracellular exocytic pathway on glycoprotein processing and maturation of Junin virus. *Archives of Virology, 142*(11), 2179-2193. doi: 10.1007/s007050050234

Cao, W., Henry, M. D., Borrow, P., Yamada, H., Elder, J. H., Ravkov, E. V., . . . Oldstone, M. B. (1998). Identification of alpha-dystroglycan as a receptor for lymphocytic choriomeningitis virus and Lassa fever virus. *Science, 282*(5396), 2079-2081.

Capul, A. A., Perez, M., Burke, E., Kunz, S., Buchmeier, M. J., & de la Torre, J. C. (2007). Arenavirus Z-glycoprotein association requires Z myristoylation but not functional RING or late domains. *J Virol, 81*(17), 9451-9460. doi: JVI.00499-07 [pii] 10.1128/JVI.00499-07

Carrière, V., Piller, V., Legrand, A., Monsigny, M., & Roche, A.-C. (1999). The sugar binding activity of MR60, a mannose-specific shuttling lectin, requires a dimeric state. *Glycobiology, 9*(10), 995-1002.

Casabona, J. C., Levingston Macleod, J. M., Loureiro, M. E., Gomez, G. A., & Lopez, N. (2009). The RING domain and the L79 residue of Z protein are involved in both the rescue of nucleocapsids and the incorporation of glycoproteins into infectious chimeric arenavirus-like particles. *J Virol, 83*(14), 7029-7039. doi: JVI.00329-09 [pii] 10.1128/JVI.00329-09

Casals, J., Buckley, S. M., & Cedeno, R. (1975). Antigenic properties of the arenaviruses. *Bull World Health Organ, 52*(4-6), 421-427.

Castilla, V. (1996). Low-pH-induced fusion of Vero cells infected with Junin virus. *Arch Virol, 141*(7).

Castilla, V., Mersich, S. E., Candurra, N. A., & Damonte, E. B. (1994). The entry of Junin virus into Vero cells. *Arch Virol, 136*(3-4), 363-374.

Castilla, V., Mersich, S. E., & Damonte, E. B. (1991). [Lysosomotropic compounds inhibiting the multiplication of Junin virus]. *Rev Argent Microbiol, 23*(2), 86-89.

Centers for Disease, C., & Prevention. (2012). Notes from the field: lymphocytic choriomeningitis virus infections in employees of a rodent breeding facility--Indiana, May-June 2012. *MMWR Morb Mortal Wkly Rep, 61*(32), 622-623.

Chakrabarti, A., Chen, A. W., & Varner, J. D. (2011). A review of the mammalian unfolded protein response. *Biotechnol Bioeng, 108*(12), 2777-2793. doi: 10.1002/bit.23282

Chang, J., Warren, T. K., Zhao, X., Gill, T., Guo, F., Wang, L., . . . Block, T. M. (2013). Small molecule inhibitors of ER alpha-glucosidases are active against multiple hemorrhagic fever viruses. *Antiviral Res, 98*(3), 432-440. doi: 10.1016/j.antiviral.2013.03.023

Charrel, R. N., & de Lamballerie, X. (2010). Zoonotic aspects of arenavirus infections. *Veterinary Microbiology, 140*(3–4), 213-220. doi: http://dx.doi.org/10.1016/j.vetmic.2009.08.027

Charrel, R. N., de Lamballerie, X., & Emonet, S. (2008). Phylogeny of the genus Arenavirus. *Curr Opin Microbiol, 11*(4), 362-368. doi: 10.1016/j.mib.2008.06.001

Charrel, R. N., Feldmann, H., Fulhorst, C. F., Khelifa, R., de Chesse, R., & de Lamballerie, X. (2002). Phylogeny of New World arenaviruses based on the complete coding sequences of the small genomic segment identified an evolutionary lineage produced by intrasegmental recombination. *Biochem Biophys Res Commun, 296*(5), 1118-1124.

Charrel, R. N., Lemasson, J.-J., Garbutt, M., Khelifa, R., Micco, P. D., Feldmann, H., & Lamballerie, X. d. (2003). New insights into the evolutionary relationships between arenaviruses provided by comparative analysis of small and large segment sequences. *Virology, 317*(2), 191-196. doi: http://dx.doi.org/10.1016/j.virol.2003.08.016

Chen, Y., Hojo, S., Matsumoto, N., & Yamamoto, K. (2013). Regulation of Mac-2BP secretion is mediated by its N-glycan binding to ERGIC-53. *Glycobiology, 23*(7), 904-916. doi: 10.1093/glycob/cwt027

Childs, J., & Peters, C. (1993). Ecology and Epidemiology of Arenaviruses and Their Hosts. In M. Salvato (Ed.), *The Arenaviridae* (pp. 331-384): Springer US.

Childs, J. E., Glass, G. E., Korch, G. W., Ksiazek, T. G., & Leduc, J. W. (1992). Lymphocytic choriomeningitis virus infection and house mouse (Mus musculus) distribution in urban Baltimore. *Am J Trop Med Hyg, 47*(1), 27-34.

Childs, J. E., Glass, G. E., Ksiazek, T. G., Rossi, C. A., Oro, J. G., & Leduc, J. W. (1991). Human-rodent contact and infection with lymphocytic choriomeningitis and Seoul viruses in an inner-city population. *Am J Trop Med Hyg, 44*(2), 117-121.

Choe, H., Jemielity, S., Abraham, J., Radoshitzky, S. R., & Farzan, M. (2011). Transferrin receptor 1 in the zoonosis and pathogenesis of New World hemorrhagic fever arenaviruses. *Curr Opin Microbiol, 14*(4), 476-482. doi: S1369-5274(11)00098-1 [pii] 10.1016/j.mib.2011.07.014

Chosewood, L. C., Wilson, D. E., Centers for Disease Control and Prevention (U.S.), & National Institutes of Health (U.S.). (2009). *Biosafety in microbiological and biomedical laboratories* (5th ed.). Washington, D.C.: U.S. Dept. of Health and Human Services, Public Health Service, Centers for Disease Control and Prevention, National Institutes of Health.

Clegg, J. C. (1982). Glycoprotein detection in nitrocellulose transfers of electrophoretically separated protein mixtures using concanavalin A and

peroxidase: application to arenavirus and flavivirus proteins. *Anal Biochem, 127*(2), 389-394.

Clegg, J. C., & Lloyd, G. (1983). Structural and cell-associated proteins of Lassa virus. *J Gen Virol, 64*(Pt 5), 1127-1136.

Cole, N. B., Sciaky, N., Marotta, A., Song, J., & Lippincott-Schwartz, J. (1996). Golgi dispersal during microtubule disruption: regeneration of Golgi stacks at peripheral endoplasmic reticulum exit sites. *Mol Biol Cell, 7*(4), 631-650.

Conde-Vancells, J., Rodriguez-Suarez, E., Embade, N., Gil, D., Matthiesen, R., Valle, M., . . . Falcon-Perez, J. M. (2008). Characterization and comprehensive proteome profiling of exosomes secreted by hepatocytes. *J Proteome Res, 7*(12), 5157-5166.

Contigiani, M., Medeot, S., & Diaz, G. (1993). Heterogeneity and stability characteristics of Candid 1 attenuated strain of Junin virus. *Acta Virol, 37*(1), 41-46.

Cordo, S. M., Cesio y Acuna, M., & Candurra, N. A. (2005). Polarized entry and release of Junin virus, a New World arenavirus. *J Gen Virol, 86*(Pt 5), 1475-1479. doi: 86/5/1475 [pii] 10.1099/vir.0.80473-0

Cordo, S. M., Valko, A., Martinez, G. M., & Candurra, N. A. (2013). Membrane localization of Junín virus glycoproteins requires cholesterol and cholesterol rich membranes. *Biochemical and Biophysical Research Communications, 430*(3), 912-917. doi: http://dx.doi.org/10.1016/j.bbrc.2012.12.053

Cornillez-Ty, C. T., Liao, L., Yates, J. R., 3rd, Kuhn, P., & Buchmeier, M. J. (2009). Severe acute respiratory syndrome coronavirus nonstructural protein 2 interacts with a host protein complex involved in mitochondrial biogenesis and intracellular signaling. *Journal of Virology, 83*(19), 10314-10318. doi: JVI.00842-09 [pii] 10.1128/JVI.00842-09

Cortini, M., & Sitia, R. (2010). ERp44 and ERGIC-53 Synergize in Coupling Efficiency and Fidelity of IgM Polymerization and Secretion. *Traffic, 11*(5), 651-659. doi: 10.1111/j.1600-0854.2010.01043.x

Cresta, B., Padula, P., & de Martinez Segovia, M. (1980). Biological properties of Junin virus proteins. I. Identification of the immunogenic glycoprotein. *Intervirology, 13*(5), 284-288.

Cuevas, C. D., Lavanya, M., Wang, E., & Ross, S. R. (2011). Junin virus infects mouse cells and induces innate immune responses. *J Virol, 85*(21), 11058-11068. doi: 10.1128/JVI.05304-11

Cummings, R. D., & Liu, F. T. (2009). Galectins. In A. Varki, R. D. Cummings, J. D. Esko, H. H. Freeze, P. Stanley, C. R. Bertozzi, G. W. Hart & M. E. Etzler (Eds.), *Essentials of Glycobiology* (2nd ed.). Cold Spring Harbor (NY).

Cummins, D., Fisher-Hoch, S. P., Walshe, K. J., Mackie, I. J., McCormick, J. B., Bennett, D., . . . Machin, S. J. (1989). A plasma inhibitor of platelet aggregation in patients with Lassa fever. *Br J Haematol, 72*(4), 543-548.

Cummins, D., McCormick, J. B., Bennett, D., & et al. (1990). Acute sensorineural deafness in lassa fever. *JAMA, 264*(16), 2093-2096. doi: 10.1001/jama.1990.03450160063030

Cummins, D., Molinas, F. C., Lerer, G., Maiztegui, J. I., Faint, R., & Machin, S. J. (1990). A plasma inhibitor of platelet aggregation in patients with Argentine hemorrhagic fever. *Am J Trop Med Hyg, 42*(5), 470-475.

Cunningham, M. A., Pipe, S. W., Zhang, B., Hauri, H. P., Ginsburg, D., & Kaufman, R. J. (2003). LMAN1 is a molecular chaperone for the secretion of coagulation factor VIII. *J Thromb Haemost, 1*(11), 2360-2367.

da Rosa Elkhoury, M., da Silva Mendes, W., Waldman, E. A., Dias, J. P., Carmo, E. H., & Fernando da Costa Vasconcelos, P. (2012). Hantavirus pulmonary syndrome: prognostic factors for death in reported cases in Brazil. *Transactions of the Royal Society of Tropical Medicine and Hygiene, 106*(5), 298-302. doi: S0035-9203(12)00003-X [pii] 10.1016/j.trstmh.2012.01.002

Damonte, E. B., Mersich, S. E., & Candurra, N. A. (1994). Intracellular processing and transport of Junin virus glycoproteins influences virion infectivity. *Virus Res, 34*(3), 317-326.

de Figueiredo, P., Drecktrah, D., Polizotto, R. S., Cole, N. B., Lippincott-Schwatrz, J., & Brown, W. J. (2000). Phospholipase A2 Antagonists Inhibit Constitutive Retrograde Membrane Traffic to the Endoplasmic Reticulum. *Traffic, 1*(6), 504-511. doi: 10.1034/j.1600-0854.2000.010608.x

Delgado, S., Erickson, B. R., Agudo, R., Blair, P. J., Vallejo, E., Albariño, C. G., . . . Nichol, S. T. (2008). Chapare Virus, a Newly Discovered Arenavirus Isolated from a Fatal Hemorrhagic Fever Case in Bolivia. *PLoS Pathog, 4*(4), e1000047. doi: 10.1371/journal.ppat.1000047

Demogines, A., Abraham, J., Choe, H., Farzan, M., & Sawyer, S. L. (2013). Dual host-virus arms races shape an essential housekeeping protein. *PLoS Biol, 11*(5), e1001571. doi: 10.1371/journal.pbio.1001571

Deng, Y., Liu, J., Zheng, Q., Yong, W., & Lu, M. (2006). Structures and polymorphic interactions of two heptad-repeat regions of the SARS virus S2 protein. *Structure, 14*(5), 889-899. doi: 10.1016/j.str.2006.03.007

Di Simone, C., & Buchmeier, M. J. (1995). Kinetics and pH dependence of acid-induced structural changes in the lymphocytic choriomeningitis virus glycoprotein complex. *Virology, 209*(1), 3-9. doi: S0042-6822(85)71225-1 [pii] 10.1006/viro.1995.1225

Di Simone, C., Zandonatti, M. A., & Buchmeier, M. J. (1994). Acidic pH triggers LCMV membrane fusion activity and conformational change in the glycoprotein spike. *Virology, 198*(2), 455-465. doi: S0042-6822(84)71057-9 [pii] 10.1006/viro.1994.1057

Disimone, C., & Buchmeier, M. J. (1993). The Fusion Activity and Related Conformational-Changes in the Arenavirus Lcmv Glycoprotein Spike. *Biophysical Journal, 64*(2), A234-A234.

Djavani, M., Crasta, O. R., Zhang, Y., Zapata, J. C., Sobral, B., Lechner, M. G., . . . Salvato, M. S. (2009). Gene expression in primate liver during viral hemorrhagic fever. *Virol J, 6*, 20. doi: 1743-422X-6-20 [pii] 10.1186/1743-422X-6-20

Djavani, M., Rodas, J., Lukashevich, I. S., Horejsh, D., Pandolfi, P. P., Borden, K. L. B., & Salvato, M. S. (2001). Role of the Promyelocytic Leukemia Protein PML in the Interferon Sensitivity of Lymphocytic Choriomeningitis Virus. *Journal of Virology, 75*(13), 6204-6208. doi: 10.1128/jvi.75.13.6204-6208.2001

Dodd, R. B., & Drickamer, K. (2001). Lectin-like proteins in model organisms: implications for evolution of carbohydrate-binding activity. *Glycobiology, 11*(5), 71R-79R. doi: 10.1093/glycob/11.5.71R

Downs, W. G., Anderson, C. R., Spence, L., Aitken, T. H. G., & Greenhall, A. H. (1963). Tacaribe Virus, a New Agent Isolated from Artibeus Bats and Mosquitoes in Trinidad, West Indies. *The American Journal of Tropical Medicine and Hygiene, 12*(4), 640-646.

Droniou-Bonzom, M. E., Reignier, T., Oldenburg, J. E., Cox, A. U., Exline, C. M., Rathbun, J. Y., & Cannon, P. M. (2011). Substitutions in the glycoprotein (GP) of the Candid#1 vaccine strain of junin virus increase dependence on human transferrin receptor 1 for entry and destabilize the metastable conformation of GP. *J Virol, 85*(24), 13457-13462. doi: JVI.05616-11 [pii] 10.1128/JVI.05616-11

Dudek, S. E., Luig, C., Pauli, E.-K., Schubert, U., & Ludwig, S. (2010). The Clinically Approved Proteasome Inhibitor PS-341 Efficiently Blocks Influenza A Virus and Vesicular Stomatitis Virus Propagation by Establishing an Antiviral State. *Journal of Virology, 84*(18), 9439-9451. doi: 10.1128/jvi.00533-10

Dykewicz, C. A., Dato, V. M., Fisher-Hoch, S. P., & et al. (1992). LYmphocytic choriomeningitis outbreak associated with nude mice in a research institute. *JAMA, 267*(10), 1349-1353. doi: 10.1001/jama.1992.03480100055030

Dylla, D. E., Michele, D. E., Campbell, K. P., & McCray, P. B. (2008). Basolateral Entry and Release of New and Old World Arenaviruses from Human Airway Epithelia. *Journal of Virology, 82*(12), 6034-6038. doi: 10.1128/jvi.00100-08

Eckenroth, B. E., Steere, A. N., Chasteen, N. D., Everse, S. J., & Mason, A. B. (2011). How the binding of human transferrin primes the transferrin receptor potentiating iron release at endosomal pH. *Proc Natl Acad Sci U S A, 108*(32), 13089-13094. doi: 10.1073/pnas.1105786108

Edington, G. M., & White, H. A. (1972). The pathology of Lassa fever. *Trans R Soc Trop Med Hyg, 66*(3), 381-389.

Eichler, R., Lenz, O., Garten, W., & Strecker, T. (2006). The role of single N-glycans in proteolytic processing and cell surface transport of the Lassa virus glycoprotein GP-C. *Virology Journal, 3*(1), 41. doi: 10.1186/1743-422x-3-41

Eichler, R., Lenz, O., Strecker, T., Eickmann, M., Klenk, H. D., & Garten, W. (2003). Identification of Lassa virus glycoprotein signal peptide as a trans-acting maturation factor. *EMBO Rep, 4*(11), 1084-1088. doi: 10.1038/sj.embor.embor7400002 embor7400002 [pii]

Eichler, R., Lenz, O., Strecker, T., Eickmann, M., Klenk, H. D., & Garten, W. (2004). Lassa virus glycoprotein signal peptide displays a novel topology with an extended endoplasmic reticulum luminal region. *J Biol Chem, 279*(13), 12293-12299. doi: 10.1074/jbc.M312975200 M312975200 [pii]

Eichler, R., Lenz, O., Strecker, T., & Garten, W. (2003). Signal peptide of Lassa virus glycoprotein GP-C exhibits an unusual length. *FEBS Lett, 538*(1-3), 203-206. doi: S0014579303001601 [pii]

Elsner, B., Schwarz, E., Mando, O. G., Maiztegui, J., & Vilches, A. (1973). Pathology of 12 fatal cases of Argentine hemorrhagic fever. *Am J Trop Med Hyg, 22*(2), 229-236.

Emonet, S., Lemasson, J. J., Gonzalez, J. P., de Lamballerie, X., & Charrel, R. N. (2006). Phylogeny and evolution of old world arenaviruses. *Virology, 350*(2), 251-257. doi: 10.1016/j.virol.2006.01.026

Emonet, S. F., de la Torre, J. C., Domingo, E., & Sevilla, N. (2009). Arenavirus genetic diversity and its biological implications. *Infect Genet Evol, 9*(4), 417-429. doi: S1567-1348(09)00050-1 [pii] 10.1016/j.meegid.2009.03.005

Enders, G., Varho-Gobel, M., Lohler, J., Terletskaia-Ladwig, E., & Eggers, M. (1999). Congenital lymphocytic choriomeningitis virus infection: an underdiagnosed disease. *Pediatr Infect Dis J, 18*(7), 652-655.

Enria, D. A., Ambrosio, A. M., Briggiler, A. M., Feuillade, M. R., & Crivelli, E. (2010). [Candid#1 vaccine against Argentine hemorrhagic fever produced in Argentina. Immunogenicity and safety]. *Medicina (B Aires), 70*(3), 215-222.

Eschli, B., Quirin, K., Wepf, A., Weber, J., Zinkernagel, R., & Hengartner, H. (2006). Identification of an N-Terminal Trimeric Coiled-Coil Core within Arenavirus Glycoprotein 2 Permits Assignment to Class I Viral Fusion Proteins. *Journal of Virology, 80*(12), 5897-5907. doi: 10.1128/jvi.00008-06

Etzler, M. E., Surolia, A., & Cummings, R. D. (2009). L-type Lectins. In A. Varki, R. D. Cummings, J. D. Esko, H. H. Freeze, P. Stanley, C. R. Bertozzi, G. W. Hart & M. E. Etzler (Eds.), *Essentials of Glycobiology* (2nd ed.). Cold Spring Harbor (NY).

Fan, L., Briese, T., & Lipkin, W. I. (2010). Z proteins of New World arenaviruses bind RIG-I and interfere with type I interferon induction. *J Virol, 84*(4), 1785-1791. doi: 10.1128/JVI.01362-09

Farah, R. A., de Moerloose, P., Bouchardy, I., Morris, M. A., Barakat, W., Sayad, A. E., & Neerman-Arbez, M. (2006). Combined factor V - factor VIII deficiency (F5F8D): compound heterozygosity for two novel truncating mutations in LMAN1 in a consanguineous patient. *Thromb Haemost, 95*(5), 893-895.

Fehling, S. K., Lennartz, F., & Strecker, T. (2012). Multifunctional nature of the arenavirus RING finger protein Z. *Viruses, 4*(11), 2973-3011. doi: 10.3390/v4112973

Feldmann, H., & Geisbert, T. W. (2011). Ebola haemorrhagic fever. *Lancet, 377*(9768), 849-862. doi: S0140-6736(10)60667-8 [pii] 10.1016/S0140-6736(10)60667-8

Felix Kappeler , D. R. C. K., Montserrat Foguet§, Jean-Pierre Paccaudi, and, & Hauri, H.-P. (1997). The recycling of ERGIC-53 in the Early secretory *The Journal of Biological Chemistry, 272*

Fiedler, K., & Simons, K. (1994). A putative novel class of animal lectins in the secretory pathway homologous to leguminous lectins. *Cell, 77*(5), 625-626.

Fiedler, K., & Simons, K. (1995). The role of N-glycans in the secretory pathway. *Cell, 81*(3), 309-312.

Fields, B. N., Knipe, D. M., & Howley, P. M. (2007). *Fields' virology* (5th ed.). Philadelphia: Wolters Kluwer Health/Lippincott Williams & Wilkins.

Fischer, S. A., Graham, M. B., Kuehnert, M. J., Kotton, C. N., Srinivasan, A., Marty, F. M., . . . Zaki, S. R. (2006). Transmission of Lymphocytic Choriomeningitis Virus by Organ Transplantation. *New England Journal of Medicine, 354*(21), 2235-2249. doi: doi:10.1056/NEJMoa053240

Fisher-Hoch, S., McCormick, J. B., Sasso, D., & Craven, R. B. (1988). Hematologic dysfunction in Lassa fever. *J Med Virol, 26*(2), 127-135.

Flanagan, M. L., Oldenburg, J., Reignier, T., Holt, N., Hamilton, G. A., Martin, V. K., & Cannon, P. M. (2008). New world clade B arenaviruses can use transferrin receptor 1 (TfR1)-dependent and -independent entry pathways, and glycoproteins from human pathogenic strains are associated with the use of TfR1. *J Virol, 82*(2), 938-948. doi: JVI.01397-07 [pii] 10.1128/JVI.01397-07

Fraldi, A., Zito, E., Annunziata, F., Lombardi, A., Cozzolino, M., Monti, M., . . . Cosma, M. P. (2008). Multistep, sequential control of the trafficking and function of the multiple sulfatase deficiency gene product, SUMF1 by PDI, ERGIC-53 and ERp44. *Hum Mol Genet, 17*(17), 2610-2621. doi: 10.1093/hmg/ddn161

Frame, J. D., Baldwin, J. M., Gocke, D. J., & Troup, J. M. (1970). Lassa Fever, a New Virus Disease of Man from West Africa: I. Clinical Description and Pathological Findings. *The American Journal of Tropical Medicine and Hygiene, 19*(4), 670-676.

Franze-Fernandez, M. T., Zetina, C., Iapalucci, S., Lucero, M. A., Bouissou, C., Lopez, R., . . . Zakin, M. M. (1987). Molecular structure and early events in the replication of Tacaribe arenavirus S RNA. *Virus Res, 7*(4), 309-324.

Froeschke, M., Basler, M., Groettrup, M., & Dobberstein, B. (2003). Long-lived signal peptide of lymphocytic choriomeningitis virus glycoprotein pGP-C. *J Biol Chem, 278*(43), 41914-41920. doi: 10.1074/jbc.M302343200 M302343200 [pii]

Fulhorst, C. F., Bowen, M. D., Ksiazek, T. G., Rollin, P. E., Nichol, S. T., Kosoy, M. Y., & Peters, C. J. (1996). Isolation and Characterization of Whitewater Arroyo Virus, a Novel North American Arenavirus. *Virology, 224*(1), 114-120. doi: http://dx.doi.org/10.1006/viro.1996.0512

Fulhorst, C. F., Bowen, M. D., Salas, R. A., Duno, G., Utrera, A., Ksiazek, T. G., . . . Tesh, R. B. (1999). Natural rodent host associations of Guanarito and pirital viruses (Family Arenaviridae) in central Venezuela. *Am J Trop Med Hyg, 61*(2), 325-330.

Gallaher, W. R., DiSimone, C., & Buchmeier, M. J. (2001). The viral transmembrane superfamily: possible divergence of Arenavirus and Filovirus glycoproteins from a common RNA virus ancestor. *BMC Microbiol, 1*, 1.

Gangemi, J. D., Rosato, R. R., Connell, E. V., Johnson, E. M., & Eddy, G. A. (1978). Structural Polypeptides of Machupo Virus. *Journal of General Virology, 41*(1), 183-188. doi: 10.1099/0022-1317-41-1-183

Gault, C. R., Obeid, L. M., & Hannun, Y. A. (2010). An overview of sphingolipid metabolism: from synthesis to breakdown. *Adv Exp Med Biol, 688*, 1-23.

Ge, J., Xue, F., Gu, D. S., Du, W. T., Zhao, H. F., Sui, T., . . . Yang, R. C. (2010). [Combined deficiency of factors V and VIII caused by a novel compound heterozygous mutation of gene Lman1]. *Zhongguo Shi Yan Xue Ye Xue Za Zhi, 18*(1), 185-190.

Ghiringhelli, P. D., Riverapomar, R. V., Lozano, M. E., Grau, O., & Romanowski, V. (1991). Molecular-Organization of Junin Virus-S Rna - Complete Nucleotide-Sequence, Relationship with Other Members of the Arenaviridae and Unusual Secondary Structures. *Journal of General Virology, 72*, 2129-2141.

Gire, S. K., Stremlau, M., Andersen, K. G., Schaffner, S. F., Bjornson, Z., Rubins, K., . . . Sabeti, P. C. (2012). Emerging Disease or Diagnosis? *Science, 338*(6108), 750-752. doi: 10.1126/science.1225893

Giusti, C. J. D., Alberdi, L., Frik, J., Ferrer, M. F., Scharrig, E., Schattner, M., & Gomez, R. M. (2011). Galectin-3 is upregulated in activated glia during Junin virus-induced murine encephalitis. *Neuroscience Letters, 501*(3), 163-166. doi: http://dx.doi.org/10.1016/j.neulet.2011.07.007

Glushakova, S. E., Lukashevich, I. S., & Baratova, L. A. (1990). Prediction of arenavirus fusion peptides on the basis of computer analysis of envelope protein sequences. *FEBS Lett, 269*(1), 145-147.

Glushakova, S. E., Omelyanenko, V. G., Lukashevitch, I. S., Bogdanov, A. A., Jr., Moshnikova, A. B., Kozytch, A. T., & Torchilin, V. P. (1992). The fusion of artificial lipid membranes induced by the synthetic arenavirus 'fusion peptide'. *Biochim Biophys Acta, 1110*(2), 202-208.

Gómez, R. M., Jaquenod de Giusti, C., Sanchez Vallduvi, M. M., Frik, J., Ferrer, M. F., & Schattner, M. (2011). Junín virus. A XXI century update. *Microbes and Infection, 13*(4), 303-311. doi: http://dx.doi.org/10.1016/j.micinf.2010.12.006

Gomez, R. M., Pozner, R. G., Lazzari, M. A., D'Atri, L. P., Negrotto, S., Chudzinski-Tavassi, A. M., . . . Schattner, M. (2003). Endothelial cell function alteration after Junin virus infection. *Thrombosis and Haemostasis*. doi: 10.1160/th02-09-0043

Goncalves, A.-R., Moraz, M.-L., Pasquato, A., Helenius, A., Lozach, P.-Y., & Kunz, S. (2013). Role of DC-SIGN in Lassa Virus Entry into Human Dendritic Cells. *Journal of Virology, 87*(21), 11504-11515. doi: 10.1128/jvi.01893-13

Goni, S. E., Borio, C. S., Romano, F. B., Rota, R. P., Pilloff, M. G., Iserte, J. A., . . . Lozano, M. E. (2010). Expression and purification of Z protein from Junin virus. *J Biomed Biotechnol, 2010*, 970491. doi: 10.1155/2010/970491

Goni, S. E., Iserte, J. A., Ambrosio, A. M., Romanowski, V., Ghiringhelli, P. D., & Lozano, M. E. (2006). Genomic features of attenuated Junin virus vaccine strain candidate. *Virus Genes, 32*(1), 37-41. doi: 10.1007/s11262-005-5843-2

Gonzalez-Begne, M., Lu, B., Han, X., Hagen, F. K., Hand, A. R., Melvin, J. E., & Yates, J. R. (2009). Proteomic analysis of human parotid gland exosomes by multidimensional protein identification technology (MudPIT). *J Proteome Res, 8*(3), 1304-1314. doi: 10.1021/pr800658c

Gonzalez, P. H., Cossio, P. M., Arana, R., Maiztegui, J. I., & Laguens, R. P. (1980). Lymphatic tissue in Argentine hemorrhagic fever. Pathologic features. *Arch Pathol Lab Med, 104*(5), 250-254.

Grant, A., Seregin, A., Huang, C., Kolokoltsova, O., Brasier, A., Peters, C., & Paessler, S. (2012). Junín Virus Pathogenesis and Virus Replication. *Viruses, 4*(10), 2317-2339.

Gregg, M. B. (1975). Recent outbreaks of lymphocytic choriomeningitis in the United States of America. *Bull World Health Organ, 52*(4-6), 549-553.

Günther, S., & Lenz, O. (2004). Lassa Virus. *Critical Reviews in Clinical Laboratory Sciences, 41*(4), 339-390. doi: 10.1016/0035-9203(72)90269-6. Find this article online

Gunther, S., Weisner, B., Roth, A., Grewing, T., Asper, M., Drosten, C., . . . Schmitz, H. (2001). Lassa fever encephalopathy: Lassa virus in cerebrospinal fluid but not in serum. *Journal of Infectious Diseases, 184*(3), 345-349. doi: 10.1086/322033

Guy, J. E., Wigren, E., Svard, M., Hard, T., & Lindqvist, Y. (2008). New insights into multiple coagulation factor deficiency from the solution structure of human MCFD2. *J Mol Biol, 381*(4), 941-955. doi: 10.1016/j.jmb.2008.06.042

Haas, W. H., Breuer, T., Pfaff, G., Schmitz, H., Kohler, P., Asper, M., . . . Gunther, S. (2003). Imported Lassa fever in Germany: surveillance and management of contact persons. *Clin Infect Dis, 36*(10), 1254-1258. doi: 10.1086/374853

Haines, D. S., Lee, J. E., Beauparlant, S. L., Kyle, D. B., den Besten, W., Sweredoski, M. J., . . . Deshaies, R. J. (2012). Protein Interaction Profiling of the p97 Adaptor UBXD1 Points to a Role for the Complex in Modulating ERGIC-53 Trafficking. *Molecular & Cellular Proteomics, 11*(6). doi: 10.1074/mcp.M111.016444

Hammond, C., Braakman, I., & Helenius, A. (1994). Role of N-linked oligosaccharide recognition, glucose trimming, and calnexin in glycoprotein folding and quality control. *Proc Natl Acad Sci U S A, 91*(3), 913-917.

Hamza, A., Wei, N. N., Johnson-Scalise, T., Naftolin, F., Cho, H., & Zhan, C. G. (2012). Unveiling the Unfolding Pathway of F5F8D Disorder-Associated D81H/V100D Mutant of MCFD2 via Multiple Molecular Dynamics Simulations. *J Biomol Struct Dyn, 29*(4), 699-714.

Han, D. P., Lohani, M., & Cho, M. W. (2007). Specific asparagine-linked glycosylation sites are critical for DC-SIGN- and L-SIGN-mediated severe acute respiratory syndrome coronavirus entry. *J Virol, 81*(21), 12029-12039. doi: 10.1128/JVI.00315-07

Hara-Kuge, S., Ohkura, T., Seko, A., & Yamashita, K. (1999). Vesicular-integral membrane protein, VIP36, recognizes high-mannose type glycans containing α1→2 mannosyl residues in MDCK cells. *Glycobiology, 9*(8), 833-839.

Hara, Y., Kanagawa, M., Kunz, S., Yoshida-Moriguchi, T., Satz, J. S., Kobayashi, Y. M., . . . Campbell, K. P. (2011). Like-acetylglucosaminyltransferase (LARGE)-dependent modification of dystroglycan at Thr-317/319 is required for laminin binding and arenavirus infection. *Proc Natl Acad Sci U S A, 108*(42), 17426-17431. doi: 1114836108 [pii] 10.1073/pnas.1114836108

Harnish, D. G., Dimock, K., Bishop, D. H., & Rawls, W. E. (1983). Gene mapping in Pichinde virus: assignment of viral polypeptides to genomic L and S RNAs. *Journal of Virology, 46*(2), 638-641.

Harnish, D. G., Leung, W. C., & Rawls, W. E. (1981). Characterization of polypeptides immunoprecipitable from Pichinde virus-infected BHK-21 cells. *Journal of Virology, 38*(3), 840-848.

Hastie, K. M., Kimberlin, C. R., Zandonatti, M. A., MacRae, I. J., & Saphire, E. O. (2011). Structure of the Lassa virus nucleoprotein reveals a dsRNA-specific 3' to 5' exonuclease activity essential for immune suppression. *Proc Natl Acad Sci U S A, 108*(6), 2396-2401. doi: 10.1073/pnas.1016404108

Hastie, K. M., King, L. B., Zandonatti, M. A., & Saphire, E. O. (2012). Structural basis for the dsRNA specificity of the Lassa virus NP exonuclease. *PLoS One, 7*(8), e44211. doi: 10.1371/journal.pone.0044211

Hatch, S. C., Archer, J., & Gummuluru, S. (2009). Glycosphingolipid composition of human immunodeficiency virus type 1 (HIV-1) particles is a crucial determinant for dendritic cell-mediated HIV-1 trans-infection. *J Virol, 83*(8), 3496-3506. doi: 10.1128/JVI.02249-08

Hauler, F., Mallery, D. L., McEwan, W. A., Bidgood, S. R., & James, L. C. (2012). AAA ATPase p97/VCP is essential for TRIM21-mediated virus neutralization. *Proc Natl Acad Sci U S A, 109*(48), 19733-19738. doi: 10.1073/pnas.1210659109

Hauri, H. P., Kappeler, F., Andersson, H., & Appenzeller, C. (2000b). ERGIC-53 and traffic in the secretory pathway. *Journal of Cell Science, 113 (Pt 4)*, 587-596.

Helenius, A., & Aebi, M. (2001). Intracellular functions of N-linked glycans. *Science, 291*(5512), 2364-2369.

Heller, M. V., Marta, R. F., Sturk, A., Maiztegui, J. I., Hack, C. E., Cate, J. W., & Molinas, F. C. (1995). Early markers of blood coagulation and fibrinolysis activation in Argentine hemorrhagic fever. *Thromb Haemost, 73*(3), 368-373.

Heller, M. V., Saavedra, M. C., Falcoff, R., Maiztegui, J. I., & Molinas, F. C. (1992). Increased Tumor Necrosis Factor-α Levels in Argentine Hemorrhagic Fever. *Journal of Infectious Diseases, 166*(5), 1203-1204. doi: 10.1093/infdis/166.5.1203

Hirabayashi, Y., Oka, S., Goto, H., Shimada, K., Kurata, T., Fisher-Hoch, S. P., & McCormick, J. B. (1989). [The first imported case of Lassa fever in Japan]. *Nihon Rinsho, 47*(1), 71-75.

Hombach, J., Pircher, H., Tonegawa, S., & Zinkernagel, R. M. (1995). Strictly transporter of antigen presentation (TAP)-dependent presentation of an immunodominant cytotoxic T lymphocyte epitope in the signal sequence of a virus protein. *J Exp Med, 182*(5), 1615-1619.

Hudrisier, D., Oldstone, M. B., & Gairin, J. E. (1997). The signal sequence of lymphocytic choriomeningitis virus contains an immunodominant cytotoxic T cell epitope that is restricted by both H-2D(b) and H-2K(b) molecules. *Virology, 234*(1), 62-73. doi: S0042-6822(97)98627-X [pii] 10.1006/viro.1997.8627

Hugot, J. P., Gonzalez, J. P., & Denys, C. (2001). Evolution of the Old World Arenaviridae and their rodent hosts: generalized host-transfer or association by descent? *Infect Genet Evol, 1*(1), 13-20.

Igonet, S., Vaney, M. C., Vonhrein, C., Bricogne, G., Stura, E. A., Hengartner, H., . . . Rey, F. A. (2011). X-ray structure of the arenavirus glycoprotein GP2 in its postfusion hairpin conformation. *Proc Natl Acad Sci U S A, 108*(50), 19967-19972. doi: 1108910108 [pii] 10.1073/pnas.1108910108

Illick, M. M., Branco, L. M., Fair, J. N., Illick, K. A., Matschiner, A., Schoepp, R., . . . Guttieri, M. C. (2008). Uncoupling GP1 and GP2 expression in the Lassa virus glycoprotein complex: implications for GP1 ectodomain shedding. *Virology Journal, 5*(1), 161. doi: 10.1186/1743-422x-5-161

Imperiali, M., Spörri, R., Hewitt, J., & Oxenius, A. (2008). Post-translational modification of α-dystroglycan is not critical for lymphocytic choriomeningitis virus receptor function in vivo. *Journal of General Virology, 89*(11), 2713-2722. doi: 10.1099/vir.0.2008/004721-0

Imperiali, M., Thoma, C., Pavoni, E., Brancaccio, A., Callewaert, N., & Oxenius, A. (2005). O Mannosylation of alpha-dystroglycan is essential for lymphocytic choriomeningitis virus receptor function. *J Virol, 79*(22), 14297-14308. doi: 79/22/14297 [pii] 10.1128/JVI.79.22.14297-14308.2005

Inohara, H., Akahani, S., Koths, K., & Raz, A. (1996). Interactions between Galectin-3 and Mac-2-Binding Protein Mediate Cell-Cell Adhesion. *Cancer Research, 56*(19), 4530-4534.

Itin, C., Foguet, M., Kappeler, F., Klumperman, J., & Hauri, H. P. (1995). Recycling of the endoplasmic reticulum/Golgi intermediate compartment protein ERGIC-53 in the secretory pathway. *Biochem Soc Trans, 23*(3), 541-544.

Itin, C., Kappeler, F., Linstedt, A. D., & Hauri, H. P. (1995a). A novel endocytosis signal related to the KKXX ER-retrieval signal. *EMBO J, 14*(10), 2250-2256.

Itin, C., Roche, A. C., Monsigny, M., & Hauri, H. P. (1996). ERGIC-53 is a functional mannose-selective and calcium-dependent human homologue of leguminous lectins. *Molecular Biology of the Cell, 7*(3), 483-493.

Itin, C., Schindler, R., & Hauri, H. P. (1995b). Targeting of protein ERGIC-53 to the ER/ERGIC/cis-Golgi recycling pathway. *Journal of Cell Biology, 131*(1), 57-67.

Iwasaki, M., Ngo, N., & de la Torre, J. C. (2014). Sodium Hydrogen Exchangers Contribute to Arenavirus Cell Entry. *Journal of Virology, 88*(1), 643-654. doi: 10.1128/jvi.02110-13

Jacamo, R., Lopez, N., Wilda, M., & Franze-Fernandez, M. T. (2003). Tacaribe virus Z protein interacts with the L polymerase protein to inhibit viral RNA synthesis. *J Virol, 77*(19), 10383-10393.

Jae, L. T., Raaben, M., Riemersma, M., van Beusekom, E., Blomen, V. A., Velds, A., . . . Brummelkamp, T. R. (2013). Deciphering the Glycosylome of Dystroglycanopathies Using Haploid Screens for Lassa Virus Entry. *Science, 340*(6131), 479-483. doi: 10.1126/science.1233675

Jager, S., Cimermancic, P., Gulbahce, N., Johnson, J. R., McGovern, K. E., Clarke, S. C., . . . Krogan, N. J. (2012). Global landscape of HIV-human protein complexes. *Nature, 481*(7381), 365-370. doi: 10.1038/nature10719

Jemielity, S., Wang, J. J., Chan, Y. K., Ahmed, A. A., Li, W., Monahan, S., . . . Choe, H. (2013). TIM-family proteins promote infection of multiple enveloped viruses through virion-associated phosphatidylserine. *PLoS Pathog, 9*(3), e1003232. doi: 10.1371/journal.ppat.1003232

Jiang, X., Huang, Q., Wang, W., Dong, H., Ly, H., Liang, Y., & Dong, C. (2013). Structures of arenaviral nucleoproteins with triphosphate dsRNA reveal a unique mechanism of immune suppression. *J Biol Chem, 288*(23), 16949-16959. doi: 10.1074/jbc.M112.420521

Johnson, K. M. (1965). Epidemiology of Machupo Virus Infection: III. Significance of Virological Observations in Man and Animals. *The American Journal of Tropical Medicine and Hygiene, 14*(5), 816-818.

Johnson, K. M., McCormick, J. B., Webb, P. A., Smith, E. S., Elliott, L. H., & King, I. J. (1987). Clinical virology of Lassa fever in hospitalized patients. *Journal of Infectious Diseases, 155*(3), 456-464.

Kamiya, Y., Kamiya, D., Yamamoto, K., Nyfeler, B., Hauri, H. P., & Kato, K. (2008). Molecular basis of sugar recognition by the human L-type lectins ERGIC-53, VIPL, and VIP36. *J Biol Chem, 283*(4), 1857-1861. doi: 10.1074/jbc.M709384200

Kappeler, F., Itin, C., Schindler, R., & Hauri, H. P. (1994b). A dual role for COOH-terminal lysine residues in pre-Golgi retention and endocytosis of ERGIC-53. *Journal of Biological Chemistry, 269*(9), 6279-6281.

Kappeler, F., Klopfenstein, D. R., Foguet, M., Paccaud, J. P., & Hauri, H. P. (1997a). The recycling of ERGIC-53 in the early secretory pathway. ERGIC-53 carries a cytosolic endoplasmic reticulum-exit determinant interacting with COPII. *Journal of Biological Chemistry, 272*(50), 31801-31808.

Kawasaki, N., Ichikawa, Y., Matsuo, I., Totani, K., Matsumoto, N., Ito, Y., & Yamamoto, K. (2008). The sugar-binding ability of ERGIC-53 is enhanced by its interaction with MCFD2. *Blood, 111*(4), 1972-1979. doi: 10.1182/blood-2007-06-097022

Keenlyside, R. A., McCormick, J. B., Webb, P. A., Smith, E., Elliott, L., & Johnson, K. M. (1983). Case-Control Study of Mastomys Natalensis and Humans in Lassa Virus-Infected Households in Sierra Leone. *The American Journal of Tropical Medicine and Hygiene, 32*(4), 829-837.

Kelly, R. B. (1985). Pathways of protein secretion in eukaryotes. *Science, 230*(4721), 25-32.

Kentsis, A., Dwyer, E. C., Perez, J. M., Sharma, M., Chen, A., Pan, Z. Q., & Borden, K. L. (2001). The RING domains of the promyelocytic leukemia protein PML and the arenaviral protein Z repress translation by directly inhibiting translation initiation factor eIF4E. *J Mol Biol, 312*(4), 609-623. doi: 10.1006/jmbi.2001.5003

Khoriaty, R., Vasievich, M. P., & Ginsburg, D. (2012). The COPII pathway and hematologic disease. *Blood, 120*(1), 31-38. doi: blood-2012-01-292086 [pii] 10.1182/blood-2012-01-292086

Kim, J.-J. P., Olson, L. J., & Dahms, N. M. (2009). Carbohydrate recognition by the mannose-6-phosphate receptors. *Current Opinion in Structural Biology, 19*(5), 534-542. doi: http://dx.doi.org/10.1016/j.sbi.2009.09.002

Klaus, Joseph P., Eisenhauer, P., Russo, J., Mason, A. B., Do, D., King, B., . . . Botten, Jason W. (2013). The Intracellular Cargo Receptor ERGIC-53 Is Required for the Production of Infectious Arenavirus, Coronavirus, and Filovirus Particles. *Cell Host & Microbe, 14*(5), 522-534.

Klewitz, C., Klenk, H.-D., & ter Meulen, J. (2007). Amino acids from both N-terminal hydrophobic regions of the Lassa virus envelope glycoprotein GP-2 are critical for pH-dependent membrane fusion and infectivity. *Journal of General Virology, 88*(8), 2320-2328. doi: 10.1099/vir.0.82950-0

Klumperman, J., Schweizer, A., Clausen, H., Tang, B. L., Hong, W., Oorschot, V., & Hauri, H. P. (1998a). The recycling pathway of protein ERGIC-53 and dynamics of the ER-Golgi intermediate compartment. *Journal of Cell Science, 111*(22), 3411-3425.

Knust, B., Stroher, U., Edison, L., Albarino, C. G., Lovejoy, J., Armeanu, E., . . . Rollin, P. E. (2014). Lymphocytic choriomeningitis virus in employees and mice at multipremises feeder-rodent operation, United States, 2012. *Emerg Infect Dis, 20*(2), 240-247. doi: 10.3201/eid2002.130860

Kranzusch, P. J., & Whelan, S. P. (2011). Arenavirus Z protein controls viral RNA synthesis by locking a polymerase-promoter complex. *Proc Natl Acad Sci U S A, 108*(49), 19743-19748. doi: 10.1073/pnas.1112742108

Krudysz-Amblo, J., Jennings, M. E., 2nd, Matthews, D. E., Mann, K. G., & Butenas, S. (2011). Differences in the fractional abundances of carbohydrates of natural and recombinant human tissue factor. *Biochim Biophys Acta, 1810*(4), 398-405. doi: 10.1016/j.bbagen.2010.12.003

Kuns, M. L. (1965). Epidemiology of Machupo virus infection. II. Ecological and control studies of hemorrhagic fever. *Am J Trop Med Hyg, 14*(5), 813-816.

Kunz, S. (2009). The role of the vascular endothelium in arenavirus haemorrhagic fevers. *Thrombosis and Haemostasis*. doi: 10.1160/th09-06-0357

Kunz, S., Campbell, K. P., & Oldstone, M. B. (2003). Alpha-dystroglycan can mediate arenavirus infection in the absence of beta-dystroglycan. *Virology, 316*(2), 213-220. doi: S0042682203005920 [pii]

Kunz, S., Edelmann, K. H., de la Torre, J.-C., Gorney, R., & Oldstone, M. B. A. (2003). Mechanisms for lymphocytic choriomeningitis virus glycoprotein cleavage, transport, and incorporation into virions. *Virology, 314*(1), 168-178. doi: 10.1016/s0042-6822(03)00421-5

Kunz, S., Rojek, J. M., Kanagawa, M., Spiropoulou, C. F., Barresi, R., Campbell, K. P., & Oldstone, M. B. A. (2005). Posttranslational Modification of α-Dystroglycan, the Cellular Receptor for Arenaviruses, by the Glycosyltransferase LARGE Is Critical for Virus Binding. *Journal of Virology, 79*(22), 14282-14296. doi: 10.1128/jvi.79.22.14282-14296.2005

Kunz, S., Sevilla, N., McGavern, D. B., Campbell, K. P., & Oldstone, M. B. A. (2001). Molecular analysis of the interaction of LCMV with its cellular receptor α-dystroglycan. *The Journal of Cell Biology, 155*(2), 301-310. doi: 10.1083/jcb.200104103

Kunz, S., Sevilla, N., Rojek, J. M., & Oldstone, M. B. A. (2004). Use of alternative receptors different than α-dystroglycan by selected isolates of lymphocytic choriomeningitis virus. *Virology, 325*(2), 432-445. doi: 10.1016/j.virol.2004.05.009

Lahtinen, U., Hellman, U., Wernstedt, C., Saraste, J., & Pettersson, R. F. (1996). Molecular cloning and expression of a 58-kDa cis-Golgi and intermediate compartment protein. *J Biol Chem, 271*(8), 4031-4037.

Lahtinen, U., Svensson, K., & Pettersson, R. F. (1999). Mapping of structural determinants for the oligomerization of p58, a lectin-like protein of the intermediate compartment and cis-Golgi. *European Journal of Biochemistry, 260*(2), 392-397. doi: 10.1046/j.1432-1327.1999.00158.x

Lalis, A., Leblois, R., Lecompte, E., Denys, C., Ter Meulen, J., & Wirth, T. (2012). The impact of human conflict on the genetics of Mastomys natalensis and Lassa virus in West Africa. *PLoS One, 7*(5), e37068. doi: 10.1371/journal.pone.0037068

Lan, S., McLay, L., Aronson, J., Ly, H., & Liang, Y. (2008). Genome comparison of virulent and avirulent strains of the Pichinde arenavirus. *Arch Virol, 153*(7), 1241-1250. doi: 10.1007/s00705-008-0101-2

Lander, E. S., & Botstein, D. (1987). Homozygosity mapping: a way to map human recessive traits with the DNA of inbred children. *Science, 236*(4808), 1567-1570.

Lavanya, M., Cuevas, C. D., Thomas, M., Cherry, S., & Ross, S. R. (2013). siRNA Screen for Genes That Affect Junín Virus Entry Uncovers Voltage-Gated Calcium Channels as a Therapeutic Target. *Science Translational Medicine, 5*(204), 204ra131. doi: 10.1126/scitranslmed.3006827

Lawson, N. D., Stillman, E. A., Whitt, M. A., & Rose, J. K. (1995). Recombinant vesicular stomatitis viruses from DNA. *Proceedings of the National Academy of Sciences, 92*(10), 4477-4481.

Ledesma, J., Fedele, C. G., Carro, F., Lledo, L., Sanchez-Seco, M. P., Tenorio, A., . . . Gegundez, M. I. (2009). Independent lineage of lymphocytic choriomeningitis virus in wood mice (Apodemus sylvaticus), Spain. *Emerg Infect Dis, 15*(10), 1677-1680. doi: 10.3201/eid1510.090563

Lee, A. M., Rojek, J. M., Spiropoulou, C. F., Gundersen, A. T., Jin, W., Shaginian, A., . . . Kunz, S. (2008). Unique Small Molecule Entry Inhibitors of Hemorrhagic Fever Arenaviruses. *Journal of Biological Chemistry, 283*(27), 18734-18742. doi: 10.1074/jbc.M802089200

Lee, J. E., Fusco, M. L., Abelson, D. M., Hessell, A. J., Burton, D. R., & Saphire, E. O. (2009). Techniques and tactics used in determining the structure of the trimeric ebolavirus glycoprotein. *Acta Crystallogr D Biol Crystallogr, 65*(Pt 11), 1162-1180. doi: 10.1107/S0907444909032314

Lee, J. E., Fusco, M. L., Hessell, A. J., Oswald, W. B., Burton, D. R., & Saphire, E. O. (2008). Structure of the Ebola virus glycoprotein bound to an antibody from a human survivor. *Nature, 454*(7201), 177-182. doi: 10.1038/nature07082

Lee, K. J., Perez, M., Pinschewer, D. D., & de la Torre, J. C. (2002). Identification of the lymphocytic choriomeningitis virus (LCMV) proteins required to rescue LCMV RNA analogs into LCMV-like particles. *J Virol, 76*(12), 6393-6397.

Lee, M. (1987). Coagulopathy in patients with hemorrhagic fever with renal syndrome. *J.Korean Med.Sci., 2*(4), 201-211.

Lee, M., Kim, B. K., Kim, S., Park, S., Han, J. S., Kim, S. T., & Lee, J. S. (1989). Coagulopathy in hemorrhagic fever with renal syndrome (Korean hemorrhagic fever). *Reviews of Infectious Diseases, 11 Suppl 4*, S877-883.

Lehmann-Grube, F. (1989). Diseases of the nervous system caused by lymphocytic choriomeningitis virus and other arenaviruses. *Handbook of Clinical Neurology, 56*, 355-381.

Lehmann-Grube, F., Slenczka, W., & Tees, R. (1969). A Persistent and Inapparent Infection of L Cells with the Virus of Lymphocytic Choriomeningitis. *Journal of General Virology, 5*(1), 63-68,NP,69-81. doi: 10.1099/0022-1317-5-1-63

Lehmann, H., & Raper, A. B. (1949). Distribution of the sickle-cell trait in Uganda, and its ethnological significance. *Nature, 164*(4168), 494.

Leifer, E., Gocke, D. J., & Bourne, H. (1970). Lassa Fever, a New Virus Disease of Man from West Africa: II. Report of a Laboratory-Acquired Infection Treated with Plasma from a Person Recently Recovered from the Disease. *The American Journal of Tropical Medicine and Hygiene, 19*(4), 677-679.

Lenting PJ, v. M. J., Mertens K. (1998). The Life Cycle of Coagulation Factor VIII in View of Its Structure and Function. *Blood*, 3983-3996.

Lenz, O., ter Meulen, J., Feldmann, H., Klenk, H.-D., & Garten, W. (2000). Identification of a Novel Consensus Sequence at the Cleavage Site of the Lassa Virus Glycoprotein. *Journal of Virology, 74*(23), 11418-11421. doi: 10.1128/jvi.74.23.11418-11421.2000

Lenz, O., ter Meulen, J., Klenk, H. D., Seidah, N. G., & Garten, W. (2001). The Lassa virus glycoprotein precursor GP-C is proteolytically processed by subtilase SKI-1/S1P. *Proc. Natl. Acad. Sci. U. S. A., 98*(22), 12701-12705.

Leung, W. C., Ghosh, H. P., & Rawls, W. E. (1977). Strandedness of Pichinde virus RNA. *J Virol, 22*(1), 235-237.

Lewis, J. M., & Utz, J. P. (1961). Orchitis, Parotitis and Meningoencephalitis Due to Lymphocytic-Choriomeningitis Virus. *New England Journal of Medicine, 265*(16), 776-780. doi: doi:10.1056/NEJM196110192651604

Li, F., Li, W., Farzan, M., & Harrison, S. C. (2005). Structure of SARS coronavirus spike receptor-binding domain complexed with receptor. *Science, 309*(5742), 1864-1868. doi: 10.1126/science.1116480

Lievens, P. M. J., De Servi, B., Garofalo, S., Lunstrum, G. P., Horton, W. A., & Liboi, E. (2008). Transient dimerization and interaction with ERGIC-53 occur in the fibroblast growth factor receptor 3 early secretory pathway. *The International Journal of Biochemistry & Cell Biology, 40*(11), 2649-2659. doi: 10.1016/j.biocel.2008.05.017

Lin, G., Simmons, G., Pöhlmann, S., Baribaud, F., Ni, H., Leslie, G. J., . . . Doms, R. W. (2003). Differential N-Linked Glycosylation of Human Immunodeficiency Virus and Ebola Virus Envelope Glycoproteins Modulates Interactions with DC-SIGN and DC-SIGNR. *Journal of Virology, 77*(2), 1337-1346. doi: 10.1128/jvi.77.2.1337-1346.2003

Lippincott-Schwartz, J., Donaldson, J. G., Schweizer, A., Berger, E. G., Hauri, H. P., Yuan, L. C., & Klausner, R. D. (1990). Microtubule-dependent retrograde transport of proteins into the ER in the presence of brefeldin A suggests an ER recycling pathway. *Cell, 60*(5), 821-836.

Lis, H., & Sharon, N. (2007). *Lectins*: Springer.

Lisieux, T., Coimbra, M., Nassar, E. S., Burattini, M. N., de Souza, L. T., Ferreira, I., . . . et al. (1994). New arenavirus isolated in Brazil. *Lancet, 343*(8894), 391-392.

Liu, H., Zhao, B., Chen, Y., You, D., Liu, R., Rong, M., . . . Lai, R. (2013). Multiple coagulation factor deficiency protein 2 contains the ability to support stem cell self-renewal. *Federation Proceedings, 27*(8), 3298-3305. doi: 10.1096/fj.13-228825

Lober, C., Anheier, B., Lindow, S., Klenk, H. D., & Feldmann, H. (2001). The Hantaan virus glycoprotein precursor is cleaved at the conserved pentapeptide WAASA. *Virology, 289*(2), 224-229.

López, N., Jácamo, R., & Franze-Fernández, M. a. T. (2001). Transcription and RNA Replication of Tacaribe Virus Genome and Antigenome Analogs Require N and L Proteins: Z Protein Is an Inhibitor of These Processes. *Journal of Virology, 75*(24), 12241-12251. doi: 10.1128/jvi.75.24.12241-12251.2001

Lozach, P.-Y., Kühbacher, A., Meier, R., Mancini, R., Bitto, D., Bouloy, M., & Helenius, A. (2011). DC-SIGN as a Receptor for Phleboviruses. *Cell Host & Microbe, 10*(1), 75-88. doi: 10.1016/j.chom.2011.06.007

Lu, J., Han, Z., Liu, Y., Liu, W., Lee, M. S., Olson, M. A., . . . Harty, R. N. (2014). A Host-Oriented Inhibitor of Junin Argentine Hemorrhagic Fever Virus Egress. *J Virol*. doi: 10.1128/JVI.03757-13

Lukashevich, I. S., Djavani, M., Shapiro, K., Sanchez, A., Ravkov, E., Nichol, S. T., & Salvato, M. S. (1997). The Lassa fever virus L gene: nucleotide sequence, comparison, and precipitation of a predicted 250 kDa protein with monospecific antiserum. *J Gen Virol, 78 (Pt 3)*, 547-551.

Lukashevich, S. E. G. a. I. S. (1989). Early events in arenavirus replication are sensitive to lysosomotropic compounds. *Archives of Virology*, 157-161.

Macal, M., Lewis, G. M., Kunz, S., Flavell, R., Harker, J. A., & Zuniga, E. I. (2012). Plasmacytoid dendritic cells are productively infected and activated through TLR-7 early after arenavirus infection. *Cell Host Microbe, 11*(6), 617-630. doi: 10.1016/j.chom.2012.04.017

Maceyka, M., & Machamer, C. E. (1997). Ceramide Accumulation Uncovers a Cycling Pathway for the cis-Golgi Network Marker, Infectious Bronchitis Virus M Protein. *The Journal of Cell Biology, 139*(6), 1411-1418. doi: 10.1083/jcb.139.6.1411

Mackenzie, R. B. (1965). Epidemiology of Machupo Virus Infection: I. Pattern of Human Infection, San Joaquín, Bolivia, 1962–1964. *The American Journal of Tropical Medicine and Hygiene, 14*(5), 808-813.

MacNeil, A., Ksiazek, T. G., & Rollin, P. E. (2011). Hantavirus pulmonary syndrome, United States, 1993-2009. *Emerging Infectious Diseases, 17*(7), 1195-1201. doi: 10.3201/eid1707.101306

Macneil, A., Stroher, U., Farnon, E., Campbell, S., Cannon, D., Paddock, C. D., . . . Team, L. T. I. (2012). Solid organ transplant-associated lymphocytic choriomeningitis, United States, 2011. *Emerg Infect Dis, 18*(8), 1256-1262. doi: 10.3201/eid1808.120212

Mages, J., Freimuller, K., Lang, R., Hatzopoulos, A. K., Guggemoos, S., Koszinowski, U. H., & Adler, H. (2008). Proteins of the secretory pathway govern virus productivity during lytic gammaherpesvirus infection. *J Cell Mol Med, 12*(5B), 1974-1989. doi: 10.1111/j.1582-4934.2008.00235.x

Mahanty, S., Hutchinson, K., Agarwal, S., McRae, M., Rollin, P. E., & Pulendran, B. (2003). Cutting edge: impairment of dendritic cells and adaptive immunity by Ebola and Lassa viruses. *J Immunol, 170*(6), 2797-2801.

Maisa, A., Stroher, U., Klenk, H. D., Garten, W., & Strecker, T. (2009). Inhibition of Lassa virus glycoprotein cleavage and multicycle replication by site 1 protease-adapted alpha(1)-antitrypsin variants. *PLoS Negl Trop Dis, 3*(6), e446. doi: 10.1371/journal.pntd.0000446

Maiztegui, J. I. (1975). Clinical and epidemiological patterns of Argentine haemorrhagic fever. *Bull World Health Organ, 52*(4-6), 567-575.

Maiztegui, J. I., Fernandez, N. J., & de Damilano, A. J. (1979). Efficacy of immune plasma in treatment of Argentine haemorrhagic fever and association between treatment and a late neurological syndrome. *Lancet, 2*(8154), 1216-1217.

Maiztegui, J. I., McKee, K. T., Jr., Barrera Oro, J. G., Harrison, L. H., Gibbs, P. H., Feuillade, M. R., . . . Peters, C. J. (1998). Protective efficacy of a live attenuated vaccine against Argentine hemorrhagic fever. AHF Study Group. *Journal of Infectious Diseases, 177*(2), 277-283.

Marta, R. F., Montero, V. S., Hack, C. E., Sturk, A., Maiztegui, J. I., & Molinas, F. C. (1999). Proinflammatory cytokines and elastase-alpha-1-antitrypsin in Argentine hemorrhagic fever. *Am J Trop Med Hyg, 60*(1), 85-89.

Martin, V. K., Droniou-Bonzom, M. E., Reignier, T., Oldenburg, J. E., Cox, A. U., & Cannon, P. M. (2009). Investigation of Clade B New World Arenavirus Tropism by Using Chimeric GP1 Proteins. *Journal of Virology, 84*(2), 1176-1182. doi: 10.1128/jvi.01625-09

Martínez-Sobrido , L., Emonet, S., Giannakas, P., Cubitt, B., García-Sastre, A., & de la Torre, J. C. (2009). Identification of Amino Acid Residues Critical for the Anti-Interferon Activity of the Nucleoprotein of the Prototypic Arenavirus Lymphocytic Choriomeningitis Virus. *Journal of Virology, 83*(21), 11330-11340. doi: 10.1128/jvi.00763-09

Martínez-Sobrido, L., Giannakas, P., Cubitt, B., García-Sastre, A., & de la Torre, J. C. (2007). Differential Inhibition of Type I Interferon Induction by Arenavirus Nucleoproteins. *Journal of Virology, 81*(22), 12696-12703. doi: 10.1128/jvi.00882-07

Martinez, M. G., Bialecki, M. A., Belouzard, S., Cordo, S. M., Candurra, N. A., & Whittaker, G. R. (2013). Utilization of human DC-SIGN and L-SIGN for entry and infection of host cells by the New World arenavirus, Junin virus. *Biochem Biophys Res Commun, 441*(3), 612-617. doi: 10.1016/j.bbrc.2013.10.106

Martinez, M. G., Cordo, S. M., & Candurra, N. A. (2007). Characterization of Junin arenavirus cell entry. *J Gen Virol, 88*(Pt 6), 1776-1784. doi: 88/6/1776 [pii] 10.1099/vir.0.82808-0

Martinez Peralta, L. A., Leon, M. E., Coto, C. E., & Laguens, R. P. (1979). Effect of glucosamine on the replication of the arenavirus Junin in Vero cells. *Intervirology, 11*(3), 188-190.

McCormick, J. B., Webb, P. A., Krebs, J. W., Johnson, K. M., & Smith, E. S. (1987). A Prospective Study of the Epidemiology and Ecology of Lassa Fever. *Journal of Infectious Diseases, 155*(3), 437-444. doi: 10.1093/infdis/155.3.437

McLay, L., Liang, Y., & Ly, H. (2014). Comparative analysis of disease pathogenesis and molecular mechanisms of New World and Old World arenavirus infections. *Journal of General Virology, 95*(Pt 1), 1-15. doi: 10.1099/vir.0.057000-0

Merk, A., & Subramaniam, S. (2013). HIV-1 envelope glycoprotein structure. *Current Opinion in Structural Biology, 23*(2), 268-276. doi: http://dx.doi.org/10.1016/j.sbi.2013.03.007

Mersich, S. E., Castilla, V., & Damonte, E. B. (1988). Lectin affinity of Junin virus glycoproteins. *Ann Inst Pasteur Virol, 139*(3), 277-283.

Messina, E. L., York, J., & Nunberg, J. H. (2012). Dissection of the Role of the Stable Signal Peptide of the Arenavirus Envelope Glycoprotein in Membrane Fusion. *Journal of Virology, 86*(11), 6138-6145. doi: 10.1128/jvi.07241-11

Meulen, J. T., Lukashevich, I., Sidibe, K., Inapogui, A., Marx, M., Dorlemann, A., . . . Schmitz, H. (1996). Hunting of Peridomestic Rodents and Consumption of Their Meat as Possible Risk Factors for Rodent-to-Human Transmission of Lassa Virus in the Republic of Guinea. *The American Journal of Tropical Medicine and Hygiene, 55*(6), 661-666.

Meyer, B. J., de la Torre, J. C., & Southern, P. J. (2002). Arenaviruses: genomic RNAs, transcription, and replication. *Curr Top Microbiol Immunol, 262*, 139-157.

Milazzo, M. L., Barragan-Gomez, A., Hanson, J. D., Estrada-Franco, J. G., Arellano, E., Gonzalez-Cozatl, F. X., . . . Fulhorst, C. F. (2010). Antibodies to Tacaribe serocomplex viruses (family Arenaviridae, genus Arenavirus) in cricetid rodents from New Mexico, Texas, and Mexico. *Vector Borne Zoonotic Dis, 10*(6), 629-637. doi: 10.1089/vbz.2009.0206

Milazzo, M. L., Cajimat, M. N., Duno, G., Duno, F., Utrera, A., & Fulhorst, C. F. (2011). Transmission of Guanarito and Pirital viruses among wild rodents, Venezuela. *Emerg Infect Dis, 17*(12), 2209-2215. doi: 10.3201/eid1712.110393

Milazzo, M. L., Campbell, G. L., & Fulhorst, C. F. (2011). Novel arenavirus infection in humans, United States. *Emerg Infect Dis, 17*(8), 1417-1420. doi: 10.3201/eid1708.110285

Mills, J. N., Ellis, B. A., Childs, J. E., McKee, K. T., Jr., Maiztegui, J. I., Peters, C. J., . . . Jahrling, P. B. (1994). Prevalence of infection with Junin virus in rodent populations in the epidemic area of Argentine hemorrhagic fever. *Am J Trop Med Hyg, 51*(5), 554-562.

Mills, J. N., Ellis, B. A., McKee, K. T., Jr., Calderon, G. E., Maiztegui, J. I., Nelson, G. O., . . . Childs, J. E. (1992). A longitudinal study of Junin virus activity in the rodent reservoir of Argentine hemorrhagic fever. *Am J Trop Med Hyg, 47*(6), 749-763.

Mitchell, K. J., Pinson, K. I., Kelly, O. G., Brennan, J., Zupicich, J., Scherz, P., . . . Skarnes, W. C. (2001). Functional analysis of secreted and transmembrane proteins critical to mouse development. *Nat Genet, 28*(3), 241-249. doi: 10.1038/90074

Mitrovic, S., Ben-Tekaya, H., Koegler, E., Gruenberg, J., & Hauri, H. P. (2008). The cargo receptors Surf4, endoplasmic reticulum-Golgi intermediate compartment (ERGIC)-53, and p25 are required to maintain the architecture of ERGIC and Golgi. *Molecular Biology of the Cell, 19*(5), 1976-1990. doi: E07-10-0989 [pii] 10.1091/mbc.E07-10-0989

Molinas, F. C., Bracco, M. M. E. d., & Maiztegui, J. I. (1981). Coagulation Studies in Argentine Hemorrhagic Fever. *The Journal of Infectious Diseases, 143*(1), 1-6.

Molinas, F. C., Paz, R. A., Rimoldi, M. T., & de Bracco, M. M. (1978). Studies of blood coagulation and pathology in experimental infection of guinea pigs with Junin virus. *Journal of Infectious Diseases, 137*(6), 740-746.

Monath, T. P., Maher, M., Casals, J., Kissling, R. E., & Cacciapuoti, A. (1974). Lassa Fever in the Eastern Province of Sierra Leone, 1970–1972: II. Clinical Observations and Virological Studies on Selected Hospital Cases. *The American Journal of Tropical Medicine and Hygiene, 23*(6), 1140-1149.

Monath, T. P., Newhouse, V. F., Kemp, G. E., Setzer, H. W., & Cacciapuoti, A. (1974). Lassa virus isolation from Mastomys natalensis rodents during an epidemic in Sierra Leone. *Science, 185*(4147), 263-265.

Monson, M. H., Cole, A. K., Frame, J. D., Serwint, J. R., Alexander, S., & Jahrling, P. B. (1987). Pediatric Lassa Fever: A Review of 33 Liberian Cases. *The American Journal of Tropical Medicine and Hygiene, 36*(2), 408-415.

Monson, M. H., Frame, J. D., Jahrling, P. B., & Alexander, K. (1984). Endemic Lassa fever in Liberia. I. Clinical and epidemiological aspects at Curran Lutheran Hospital, Zorzor, Liberia. *Transactions of the Royal Society of Tropical Medicine and Hygiene, 78*(4), 549-553. doi: http://dx.doi.org/10.1016/0035-9203(84)90082-8

Morais, V. A., Brito, C., Pijak, D. S., Crystal, A. S., Fortna, R. R., Li, T., . . . Costa, J. (2006). N-glycosylation of human nicastrin is required for interaction with the lectins from the secretory pathway calnexin and ERGIC-53. *Biochimica et Biophysica Acta (BBA) - Molecular Basis of Disease, 1762*(9), 802-810. doi: 10.1016/j.bbadis.2006.06.018

Morin, B., Coutard, B., Lelke, M., Ferron, F., Kerber, R., Jamal, S., . . . Canard, B. (2010). The N-Terminal Domain of the Arenavirus L Protein Is an RNA Endonuclease Essential in mRNA Transcription. *PLoS Pathog, 6*(9), e1001038. doi: 10.1371/journal.ppat.1001038

Moussalli, M., Pipe, S. W., Hauri, H. P., Nichols, W. C., Ginsburg, D., & Kaufman, R. J. (1999b). Mannose-dependent endoplasmic reticulum (ER)-Golgi intermediate

compartment-53-mediated ER to Golgi trafficking of coagulation factors V and VIII. *Journal of Biological Chemistry, 274*(46), 32539-32542.

Munro, S., & Pelham, H. R. (1987). A C-terminal signal prevents secretion of luminal ER proteins. *Cell, 48*(5), 899-907.

Murphy, F. A., Webb, P. A., Johnson, K. M., Whitfield, S. G., & Chappell, W. A. (1970). Arenoviruses in Vero cells: ultrastructural studies. *J Virol, 6*(4), 507-518.

Neerman-Arbez, M., Antonarakis, S. E., Blouin, J. L., Zeinali, S., Akhtari, M., Afshar, Y., & Tuddenham, E. G. (1997). The locus for combined factor V-factor VIII deficiency (F5F8D) maps to 18q21, between D18S849 and D18S1103. *Am J Hum Genet, 61*(1), 143-150. doi: 10.1086/513897

Neerman-Arbez, M., Johnson, K. M., Morris, M. A., McVey, J. H., Peyvandi, F., Nichols, W. C., . . . Tuddenham, E. G. (1999). Molecular analysis of the ERGIC-53 gene in 35 families with combined factor V-factor VIII deficiency. *Blood, 93*(7), 2253-2260.

Neuman, B. W., Adair, B. D., Burns, J. W., Milligan, R. A., Buchmeier, M. J., & Yeager, M. (2005). Complementarity in the supramolecular design of arenaviruses and retroviruses revealed by electron cryomicroscopy and image analysis. *J Virol, 79*(6), 3822-3830. doi: 79/6/3822 [pii] 10.1128/JVI.79.6.3822-3830.2005

Neuman, B. W., Adair, B. D., Yeager, M., & Buchmeier, M. J. (2008). Purification and electron cryomicroscopy of coronavirus particles. *Methods in Molecular Biology, 454*, 129-136. doi: 10.1007/978-1-59745-181-9_12

Neve, E. P., Lahtinen, U., & Pettersson, R. F. (2005). Oligomerization and interacellular localization of the glycoprotein receptor ERGIC-53 is independent of disulfide bonds. *Journal of Molecular Biology, 354*(3), 556-568. doi: S0022-2836(05)01181-2 [pii] 10.1016/j.jmb.2005.09.077

Nichols, W. C., Seligsohn, U., Zivelin, A., Terry, V. H., Arnold, N. D., Siemieniak, D. R., . . . Ginsburg, D. (1997). Linkage of combined factors V and VIII deficiency to chromosome 18q by homozygosity mapping. *J Clin Invest, 99*(4), 596-601. doi: 10.1172/JCI119201

Nichols, W. C., Seligsohn, U., Zivelin, A., Terry, V. H., Hertel, C. E., Wheatley, M. A., . . . Ginsburg, D. (1998). Mutations in the ER-Golgi intermediate compartment protein ERGIC-53 cause combined deficiency of coagulation factors V and VIII. *Cell, 93*(1), 61-70. doi: S0092-8674(00)81146-0 [pii]

Nickel, W., & Brügger, B. (1999). COPI-mediated protein and lipid sorting in the early secretory pathway. *Protoplasma, 207*(3-4), 115-124. doi: 10.1007/BF01282990

Nishio, M., Kamiya, Y., Mizushima, T., Wakatsuki, S., Sasakawa, H., Yamamoto, K., . . . Kato, K. (2010). Structural basis for the cooperative interplay between the two causative gene products of combined factor V and factor VIII deficiency. *Proc Natl Acad Sci U S A, 107*(9), 4034-4039. doi: 10.1073/pnas.0908526107

Nufer, O., Kappeler, F., Guldbrandsen, S., & Hauri, H. P. (2003). ER export of ERGIC-53 is controlled by cooperation of targeting determinants in all three of its domains. *Journal of Cell Science, 116*(Pt 21), 4429-4440. doi: 10.1242/jcs.00759 jcs.00759 [pii]

Nunberg, J. H., & York, J. (2012). The Curious Case of Arenavirus Entry, and Its Inhibition. *Viruses, 4*(1), 83-101.

Nyfeler, B., Kamiya, Y., Boehlen, F., Yamamoto, K., Kato, K., de Moerloose, P., . . . Neerman-Arbez, M. (2008). Deletion of 3 residues from the C-terminus of MCFD2 affects binding to ERGIC-53 and causes combined factor V and factor VIII deficiency. *Blood, 111*(3), 1299-1301. doi: 10.1182/blood-2007-09-112854

Nyfeler, B., Michnick, S. W., & Hauri, H.-P. (2005). Capturing protein interactions in the secretory pathway of living cells. *Proceedings of the National Academy of Sciences of the United States of America, 102*(18), 6350-6355. doi: 10.1073/pnas.0501976102

Nyfeler, B., Nufer, O., Matsui, T., Mori, K., & Hauri, H. P. (2003a). The cargo receptor ERGIC-53 is a target of the unfolded protein response. *Biochemical and Biophysical Research Communications, 304*(4), 599-604. doi: S0006291X0300634X [pii]

Nyfeler, B., Reiterer, V., Wendeler, M. W., Stefan, E., Zhang, B., Michnick, S. W., & Hauri, H. P. (2008a). Identification of ERGIC-53 as an intracellular transport receptor of alpha1-antitrypsin. *J Cell Biol, 180*(4), 705-712. doi: 10.1083/jcb.200709100

Nyfeler, B., Zhang, B., Ginsburg, D., Kaufman, R. J., & Hauri, H.-P. (2006). Cargo Selectivity of the ERGIC-53/MCFD2 Transport Receptor Complex. *Traffic, 7*(11), 1473-1481. doi: 10.1111/j.1600-0854.2006.00483.x

Oeri, J., Matter, M., Isenschmid, H., Hauser, F., & Koller, F. (1954). [Congenital factor V deficiency (parahemophilia) with true hemophilia in two brothers]. *Bibl Paediatr, 58*, 575-588.

Okokhere, P. O., Ibekwe, T. S., & Akpede, G. O. (2009). Sensorineural hearing loss in Lassa fever: two case reports. *J Med Case Rep, 3*, 36. doi: 10.1186/1752-1947-3-36

Oldenburg, J., Reignier, T., Flanagan, M. L., Hamilton, G. A., & Cannon, P. M. (2007). Differences in tropism and pH dependence for glycoproteins from the Clade B1 arenaviruses: Implications for receptor usage and pathogenicity. *Virology, 364*(1), 132-139. doi: 10.1016/j.virol.2007.03.003

Oldstone, M. B., & Buchmeier, M. J. (1982). Restricted expression of viral glycoprotein in cells of persistently infected mice. *Nature, 300*(5890), 360-362.

Oldstone, M. B., & Campbell, K. P. (2011). Decoding arenavirus pathogenesis: essential roles for alpha-dystroglycan-virus interactions and the immune response. *Virology, 411*(2), 170-179. doi: S0042-6822(10)00741-5 [pii] 10.1016/j.virol.2010.11.023

Oldstone, M. B., Sinha, Y. N., Blount, P., Tishon, A., Rodriguez, M., von Wedel, R., & Lampert, P. W. (1982). Virus-induced alterations in homeostasis: alteration in differentiated functions of infected cells in vivo. *Science, 218*(4577), 1125-1127.

Oldstone, P. B. a. M. B. A. (1992). Characterization of Lymphocytic Choriomeningitis Virus-Binding Protein(s): a Candidate Cellular Receptor for the Virus. *Journal of Virology ,, 66,*(12), 7270-7281.

Ortiz-Riano, E., Cheng, B. Y., de la Torre, J. C., & Martinez-Sobrido, L. (2011). The C-terminal region of lymphocytic choriomeningitis virus nucleoprotein contains distinct and segregable functional domains involved in NP-Z interaction and counteraction of the type I interferon response. *J Virol, 85*(24), 13038-13048. doi: 10.1128/JVI.05834-11

Pablo Daniel Ghiringhelli, C. G. A., Mariel Piboul, and Victor Romanowski. (1997). The Glycoprotein Precursor Gene of the Attenuated Junin Virus Vaccine Strain (CANDID #1). *The American Society of Tropical Medicine and Hygiene, 56*(2), 216-225.

Padula, P. J., & Segovia, Z. M. D. (1984). Replication of Junin Virus in The Presence of Tunicamycin. *Intervirology, 22*(4), 227-231. doi: 10.1159/000149555

Palacios, G., Druce, J., Du, L., Tran, T., Birch, C., Briese, T., . . . Lipkin, W. I. (2008a). A new arenavirus in a cluster of fatal transplant-associated diseases. *New England Journal of Medicine, 358*(10), 991-998. doi: NEJMoa073785 [pii] 10.1056/NEJMoa073785

Palade, G. (1975). Intracellular aspects of the process of protein synthesis. *Science, 189*(4200), 347-358.

Panda, D., Das, A., Dinh, P. X., Subramaniam, S., Nayak, D., Barrows, N. J., . . . Pattnaik, A. K. (2011). RNAi screening reveals requirement for host cell secretory pathway in infection by diverse families of negative-strand RNA viruses.

Proceedings of the National Academy of Sciences of the United States of America, 108(47), 19036-19041. doi: 1113643108 [pii] 10.1073/pnas.1113643108

Panda, D., Rose, P. P., Hanna, S. L., Gold, B., Hopkins, K. C., Lyde, R. B., . . . Cherry, S. (2013). Genome-wide RNAi screen identifies SEC61A and VCP as conserved regulators of Sindbis virus entry. *Cell Rep, 5*(6), 1737-1748. doi: 10.1016/j.celrep.2013.11.028

Parekh, B. S., & Buchmeier, M. J. (1986). Proteins of lymphocytic choriomeningitis virus: antigenic topography of the viral glycoproteins. *Virology, 153*(2), 168-178.

Parodi, A. S., Greenway, D. J., Rugiero, H. R., Frigerio, M., De La Barrera, J. M., Mettler, N., . . . Nota, N. (1958). [Concerning the epidemic outbreak in Junin]. *Dia Med, 30*(62), 2300-2301.

Paroutis, P., Touret, N., & Grinstein, S. (2004). The pH of the Secretory Pathway: Measurement, Determinants, and Regulation. *Physiology, 19*(4), 207-215. doi: 10.1152/physiol.00005.2004

Parsy, M.-L., Harlos, K., Huiskonen, J. T., & Bowden, T. A. (2013). Crystal Structure of Venezuelan Hemorrhagic Fever Virus Fusion Glycoprotein Reveals a Class 1 Postfusion Architecture with Extensive Glycosylation. *Journal of Virology, 87*(23), 13070-13075. doi: 10.1128/jvi.02298-13

Pasqual, G., Burri, D. J., Pasquato, A., de la Torre, J. C., & Kunz, S. (2011a). Role of the host cell's unfolded protein response in arenavirus infection. *Journal of Virology, 85*(4), 1662-1670. doi: JVI.01782-10 [pii] 10.1128/JVI.01782-10

Pasqual, G., Rojek, J. M., Masin, M., Chatton, J. Y., & Kunz, S. (2011). Old world arenaviruses enter the host cell via the multivesicular body and depend on the endosomal sorting complex required for transport. *PLoS Pathog, 7*(9), e1002232. doi: 10.1371/journal.ppat.1002232 10-PLPA-RA-4139 [pii]

Pasquato, A. (2006). The Proprotein Convertase SKI-1/S1P: In vitro analysis of Lassa virus glycoprotein-derived substrates and ex vivo validation of irreversible peptide inhibitors. *Journal of Biological Chemistry, 281*(33), 23471-23481. doi: 10.1074/jbc.M513675200

Pasquato, A., Burri, D. J., Traba, E. G., Hanna-El-Daher, L., Seidah, N. G., & Kunz, S. (2011). Arenavirus envelope glycoproteins mimic autoprocessing sites of the cellular proprotein convertase subtilisin kexin isozyme-1/site-1 protease. *Virology, 417*(1), 18-26. doi: S0042-6822(11)00201-7 [pii] 10.1016/j.virol.2011.04.021

Patel, A. J., Liu, H. H., Lager, R. A., Malkovska, V., & Zhang, B. (2013). Successful percutaneous coronary intervention in a patient with combined deficiency of FV

and FVIII due to novel compound heterozygous mutations in LMAN1. *Haemophilia, 19*(4), 607-610. doi: 10.1111/hae.12128

Patterson, M., Grant, A., & Paessler, S. (2014). Epidemiology and pathogenesis of Bolivian hemorrhagic fever. *Current Opinion in Virology, 5*(0), 82-90. doi: http://dx.doi.org/10.1016/j.coviro.2014.02.007

Paweska, J. T., Sewlall, N. H., Ksiazek, T. G., Blumberg, L. H., Hale, M. J., Lipkin, W. I., . . . Investigation, T. (2009). Nosocomial outbreak of novel arenavirus infection, southern Africa. *Emerg Infect Dis, 15*(10), 1598-1602. doi: 10.3201/eid1510.090211

Pelham, H. R. (1988). Evidence that luminal ER proteins are sorted from secreted proteins in a post-ER compartment. *EMBO J, 7*(4), 913-918.

Perez, M., Craven, R. C., & de la Torre, J. C. (2003). The small RING finger protein Z drives arenavirus budding: implications for antiviral strategies. *Proc Natl Acad Sci U S A, 100*(22), 12978-12983. doi: 10.1073/pnas.2133782100

Perez, M., Greenwald, D. L., & de la Torre, J. C. (2004). Myristoylation of the RING finger Z protein is essential for arenavirus budding. *J Virol, 78*(20), 11443-11448. doi: 10.1128/JVI.78.20.11443-11448.2004

Peters, C. J. (2002). Human Infection with Arenaviruses in the Americas. In M. A. Oldstone (Ed.), *Arenaviruses I* (Vol. 262, pp. 65-74): Springer Berlin Heidelberg.

Peters, C. J., & Zaki, S. R. (2002). Role of the endothelium in viral hemorrhagic fevers. *Crit Care Med, 30*(5 Suppl), S268-273.

Pezzati, R., Bossi, M., Podini, P., Meldolesi, J., & Grohovaz, F. (1997). High-resolution calcium mapping of the endoplasmic reticulum-Golgi-exocytic membrane system. Electron energy loss imaging analysis of quick frozen-freeze dried PC12 cells. *Molecular Biology of the Cell, 8*(8), 1501-1512. doi: 10.1091/mbc.8.8.1501

Pfeffer, S. R., & Rothman, J. E. (1987). Biosynthetic protein transport and sorting by the endoplasmic reticulum and Golgi. *Annu Rev Biochem, 56*, 829-852. doi: 10.1146/annurev.bi.56.070187.004145

Pimpaneau, V., Midoux, P., Monsigny, M., & Roche, A. C. (1991). Characterization and isolation of an intracellular d-mannose-specific receptor from human promyelocytic HL60 cells. *Carbohydr Res, 213*(0), 95-108. doi: http://dx.doi.org/10.1016/S0008-6215(00)90601-3

Pinschewer, D. D., Perez, M., & de la Torre, J. C. (2003). Role of the virus nucleoprotein in the regulation of lymphocytic choriomeningitis virus transcription and RNA replication. *J Virol, 77*(6), 3882-3887.

Pircher, H., Moskophidis, D., Rohrer, U., Burki, K., Hengartner, H., & Zinkernagel, R. M. (1990). Viral escape by selection of cytotoxic T cell-resistant virus variants in vivo. *Nature, 346*(6285), 629-633.

Popkin, D. L., Teijaro, J. R., Sullivan, B. M., Urata, S., Rutschmann, S., de la Torre, J. C., . . . Oldstone, M. (2011). Hypomorphic mutation in the site-1 protease Mbtps1 endows resistance to persistent viral infection in a cell-specific manner. *Cell Host Microbe, 9*(3), 212-222. doi: S1931-3128(11)00062-X [pii] 10.1016/j.chom.2011.02.006

Pozner, R. G., Ure, A. E., Jaquenod de Giusti, C., D'Atri, L. P., Italiano, J. E., Torres, O., . . . Gomez, R. M. (2010). Junin virus infection of human hematopoietic progenitors impairs in vitro proplatelet formation and platelet release via a bystander effect involving type I IFN signaling. *PLoS Pathog, 6*(4), e1000847. doi: 10.1371/journal.ppat.1000847

Price, M. E., Fisher-Hoch, S. P., Craven, R. B., & McCormick, J. B. (1988). A prospective study of maternal and fetal outcome in acute Lassa fever infection during pregnancy. *BMJ, 297*(6648), 584-587.

Puryear, W. B., Akiyama, H., Geer, S. D., Ramirez, N. P., Yu, X., Reinhard, B. M., & Gummuluru, S. (2013). Interferon-Inducible Mechanism of Dendritic Cell-Mediated HIV-1 Dissemination Is Dependent on Siglec-1/CD169. *PLoS Pathog, 9*(4), e1003291. doi: 10.1371/journal.ppat.1003291

Pythoud, C., Rodrigo, W. W., Pasqual, G., Rothenberger, S., Martinez-Sobrido, L., de la Torre, J. C., & Kunz, S. (2012). Arenavirus nucleoprotein targets interferon regulatory factor-activating kinase IKKepsilon. *J Virol, 86*(15), 7728-7738. doi: 10.1128/JVI.00187-12

Qi, X., Lan, S., Wang, W., Schelde, L. M., Dong, H., Wallat, G. D., . . . Dong, C. (2010). Cap binding and immune evasion revealed by Lassa nucleoprotein structure. *Nature, 468*(7325), 779-783. doi: 10.1038/nature09605

Qin, S.-Y., Kawasaki, N., Hu, D., Tozawa, H., Matsumoto, N., & Yamamoto, K. (2012). Subcellular localization of ERGIC-53 under endoplasmic reticulum stress condition. *Glycobiology, 22*(12), 1709-1720. doi: 10.1093/glycob/cws114

Quirin, K., Eschli, B., Scheu, I., Poort, L., Kartenbeck, J., & Helenius, A. (2008). Lymphocytic choriomeningitis virus uses a novel endocytic pathway for infectious entry via late endosomes. *Virology, 378*(1), 21-33. doi: http://dx.doi.org/10.1016/j.virol.2008.04.046

Radoshitzky, S. R., Abraham, J., Spiropoulou, C. F., Kuhn, J. H., Nguyen, D., Li, W., . . . Choe, H. (2007). Transferrin receptor 1 is a cellular receptor for New World

haemorrhagic fever arenaviruses. *Nature, 446*(7131), 92-96. doi: nature05539 [pii] 10.1038/nature05539

Radoshitzky, S. R., Kuhn, J. H., Spiropoulou, C. F., Albarino, C. G., Nguyen, D. P., Salazar-Bravo, J., . . . Farzan, M. (2008). Receptor determinants of zoonotic transmission of New World hemorrhagic fever arenaviruses. *Proc Natl Acad Sci U S A, 105*(7), 2664-2669. doi: 0709254105 [pii] 10.1073/pnas.0709254105

Raiger Iustman, L. J., Candurra, N., & Mersich, S. E. (1995). [Influence] of enzymatic treatment on Junin virus--Vero cells interaction]. *Rev Argent Microbiol, 27*(1), 28-32.

Raiger Iustman, L. J., Castilla, V., Meich, V., & Mersich, S. E. (1998). Effects of reducing, oxidizing and alkylating agents on early steps of Junin virus multiplication. *Arch Virol, 143*(7), 1425-1432.

Rawls, W. E., Chan, M. A., & Gee, S. R. (1981). Mechanisms of persistence in arenavirus infections: a brief review. *Can J Microbiol, 27*(6), 568-574.

Reignier, T., Oldenburg, J., Flanagan, M. L., Hamilton, G. A., Martin, V. K., & Cannon, P. M. (2008). Receptor use by the Whitewater Arroyo virus glycoprotein. *Virology, 371*(2), 439-446. doi: S0042-6822(07)00660-5 [pii] 10.1016/j.virol.2007.10.004

Reignier, T., Oldenburg, J., Noble, B., Lamb, E., Romanowski, V., Buchmeier, M. J., & Cannon, P. M. (2006). Receptor use by pathogenic arenaviruses. *Virology, 353*(1), 111-120. doi: S0042-6822(06)00337-0 [pii] 10.1016/j.virol.2006.05.018

Renna, M., Caporaso, M. G., Bonatti, S., Kaufman, R. J., & Remondelli, P. (2007). Regulation of ERGIC-53 gene transcription in response to endoplasmic reticulum stress. *J Biol Chem, 282*(31), 22499-22512. doi: 10.1074/jbc.M703778200

Renna, M., Faraonio, R., Bonatti, S., De Stefano, D., Carnuccio, R., Tajana, G., & Remondelli, P. (2006). Nitric oxide-induced endoplasmic reticulum stress activates the expression of cargo receptor proteins and alters the glycoprotein transport to the Golgi complex. *Int J Biochem Cell Biol, 38*(12), 2040-2048. doi: 10.1016/j.biocel.2006.05.016

Reuter, G., & Gabius, H. J. (1999). Eukaryotic glycosylation: whim of nature or multipurpose tool? *Cell Mol Life Sci, 55*(3), 368-422.

Richmond, J. K., & Baglole, D. J. (2003). Lassa fever: epidemiology, clinical features, and social consequences. *BMJ, 327*(7426), 1271-1275. doi: 10.1136/bmj.327.7426.1271

Riviere, Y., Ahmed, R., Southern, P. J., Buchmeier, M. J., Dutko, F. J., & Oldstone, M. B. (1985). The S RNA segment of lymphocytic choriomeningitis virus codes for the nucleoprotein and glycoproteins 1 and 2. *J Virol, 53*(3), 966-968.

Rodrigo, W. W., Ortiz-Riano, E., Pythoud, C., Kunz, S., de la Torre, J. C., & Martinez-Sobrido, L. (2012). Arenavirus nucleoproteins prevent activation of nuclear factor kappa B. *J Virol, 86*(15), 8185-8197. doi: 10.1128/JVI.07240-11

Rojek, J. M., Campbell, K. P., Oldstone, M. B., & Kunz, S. (2007). Old World arenavirus infection interferes with the expression of functional alpha-dystroglycan in the host cell. *Mol Biol Cell, 18*(11), 4493-4507. doi: E07-04-0374 [pii] 10.1091/mbc.E07-04-0374

Rojek, J. M., & Kunz, S. (2008). Cell entry by human pathogenic arenaviruses. *Cell Microbiol, 10*(4), 828-835. doi: 10.1111/j.1462-5822.2007.01113.x

Rojek, J. M., Lee, A. M., Nguyen, N., Spiropoulou, C. F., & Kunz, S. (2008). Site 1 protease is required for proteolytic processing of the glycoproteins of the South American hemorrhagic fever viruses Junin, Machupo, and Guanarito. *J Virol, 82*(12), 6045-6051. doi: 10.1128/JVI.02392-07

Rojek, J. M., Pasqual, G., Sanchez, A. B., Nguyen, N. T., de la Torre, J. C., & Kunz, S. (2010). Targeting the proteolytic processing of the viral glycoprotein precursor is a promising novel antiviral strategy against arenaviruses. *J Virol, 84*(1), 573-584. doi: 10.1128/JVI.01697-09

Rojek, J. M., Perez, M., & Kunz, S. (2008). Cellular entry of lymphocytic choriomeningitis virus. *J Virol, 82*(3), 1505-1517. doi: 10.1128/JVI.01331-07

Rojek, J. M., Sanchez, A. B., Nguyen, N. T., de la Torre, J. C., & Kunz, S. (2008). Different mechanisms of cell entry by human-pathogenic Old World and New World arenaviruses. *J Virol, 82*(15), 7677-7687. doi: 10.1128/JVI.00560-08

Rojek, J. M., Spiropoulou, C. F., Campbell, K. P., & Kunz, S. (2007). Old World and clade C New World arenaviruses mimic the molecular mechanism of receptor recognition used by alpha-dystroglycan's host-derived ligands. *J Virol, 81*(11), 5685-5695. doi: JVI.02574-06 [pii] 10.1128/JVI.02574-06

Rojek, J. M., Spiropoulou, C. F., & Kunz, S. (2006). Characterization of the cellular receptors for the South American hemorrhagic fever viruses Junin, Guanarito, and Machupo. *Virology, 349*(2), 476-491. doi: 10.1016/j.virol.2006.02.033

Romanowski, V., Pidre, M. L., Ferrel, M. L., Bender, C., & Gomez, R. M. (2013). Argentine Hemorrhagic Fever *Viral hemorrhagic fevers* (pp. 317): CRC Press.

Rousseau, M. C., Saron, M. F., Brouqui, P., & Bourgeade, A. (1997). Lymphocytic choriomeningitis virus in southern France: four case reports and a review of the literature. *Eur J Epidemiol, 13*(7), 817-823.

Rowe, W. P., Murphy, F. A., Bergold, G. H., Casals, J., Hotchin, J., Johnson, K. M., . . . Webb, P. A. (1970). Arenoviruses: proposed name for a newly defined virus group. *J Virol, 5*(5), 651-652.

Ruggiero, H. A., Perez Isquierdo, F., Milani, H. A., Barri, A., Val, A., Maglio, F., . . . Tallone, J. C. (1986). [Treatment of Argentine hemorrhagic fever with convalescent's plasma. 4433 cases]. *Presse Med, 15*(45), 2239-2242.

Russier, M., Pannetier, D., & Baize, S. (2012). Immune responses and Lassa virus infection. *Viruses, 4*(11), 2766-2785. doi: 10.3390/v4112766

Sabeti, P. C., Varilly, P., Fry, B., Lohmueller, J., Hostetter, E., Cotsapas, C., . . . Lander, E. S. (2007). Genome-wide detection and characterization of positive selection in human populations. *Nature, 449*(7164), 913-918. doi: http://www.nature.com/nature/journal/v449/n7164/suppinfo/nature06250_S1.html

Sakai, T., Ohuchi, M., Imai, M., Mizuno, T., Kawasaki, K., Kuroda, K., & Yamashina, S. (2006). Dual wavelength imaging allows analysis of membrane fusion of influenza virus inside cells. *J Virol, 80*(4), 2013-2018. doi: 10.1128/JVI.80.4.2013-2018.2006

Salas, R., de Manzione, N., Tesh, R. B., Rico-Hesse, R., Shope, R. E., Betancourt, A., . . . et al. (1991). Venezuelan haemorrhagic fever. *Lancet, 338*(8774), 1033-1036.

Salazar-Bravo, J., Ruedas, L. A., & Yates, T. L. (2002). Mammalian reservoirs of arenaviruses. *Curr Top Microbiol Immunol, 262*, 25-63.

Salvato, M., Borrow, P., Shimomaye, E., & Oldstone, M. B. (1991). Molecular basis of viral persistence: a single amino acid change in the glycoprotein of lymphocytic choriomeningitis virus is associated with suppression of the antiviral cytotoxic T-lymphocyte response and establishment of persistence. *J Virol, 65*(4), 1863-1869.

Salvato, M. S., Schweighofer, K. J., Burns, J., & Shimomaye, E. M. (1992). Biochemical and immunological evidence that the 11 kDa zinc-binding protein of lymphocytic choriomeningitis virus is a structural component of the virus. *Virus Res, 22*(3), 185-198.

Salvato, M. S., & Shimomaye, E. M. (1989). The completed sequence of lymphocytic choriomeningitis virus reveals a unique RNA structure and a gene for a zinc finger protein. *Virology, 173*(1), 1-10.

Sanchez, A., Pifat, D. Y., Kenyon, R. H., Peters, C. J., McCormick, J. B., & Kiley, M. P. (1989). Junin virus monoclonal antibodies: characterization and cross-reactivity with other arenaviruses. *J Gen Virol, 70 (Pt 5)*, 1125-1132.

Saraste, J., Palade, G. E., & Farquhar, M. G. (1987). Antibodies to rat pancreas Golgi subfractions: identification of a 58-kD cis-Golgi protein. *J Cell Biol, 105*(5), 2021-2029.

Satoh, T., Cowieson, N. P., Hakamata, W., Ideo, H., Fukushima, K., Kurihara, M., . . . Wakatsuki, S. (2007). Structural basis for recognition of high mannose type glycoproteins by mammalian transport lectin VIP36. *J Biol Chem, 282*(38), 28246-28255. doi: 10.1074/jbc.M703064200

Saunders, A. A., Ting, J. P., Meisner, J., Neuman, B. W., Perez, M., de la Torre, J. C., & Buchmeier, M. J. (2007). Mapping the landscape of the lymphocytic choriomeningitis virus stable signal peptide reveals novel functional domains. *J Virol, 81*(11), 5649-5657. doi: JVI.02759-06 [pii] 10.1128/JVI.02759-06

Saunderson, S. C., Dunn, A. C., Crocker, P. R., & McLellan, A. D. (2014). CD169 mediates the capture of exosomes in spleen and lymph node. *Blood, 123*(2), 208-216. doi: 10.1182/blood-2013-03-489732

Scales, S. J., Pepperkok, R., & Kreis, T. E. (1997). Visualization of ER-to-Golgi transport in living cells reveals a sequential mode of action for COPII and COPI. *Cell, 90*(6), 1137-1148.

Schattner, M., Rivadeneyra, L., Pozner, R., & Gómez, R. (2013). Pathogenic Mechanisms Involved in the Hematological Alterations of Arenavirus-induced Hemorrhagic Fevers. *Viruses, 5*(1), 340-351.

Schindler, R., Itin, C., Zerial, M., Lottspeich, F., & Hauri, H. P. (1993). ERGIC-53, a membrane protein of the ER-Golgi intermediate compartment, carries an ER retention motif. *Eur J Cell Biol, 61*(1), 1-9.

Schlie, K., Maisa, A., Freiberg, F., Groseth, A., Strecker, T., & Garten, W. (2010). Viral Protein Determinants of Lassa Virus Entry and Release from Polarized Epithelial Cells. *Journal of Virology, 84*(7), 3178-3188. doi: 10.1128/jvi.02240-09

Schlie, K., Maisa, A., Lennartz, F., Stroher, U., Garten, W., & Strecker, T. (2009). Characterization of Lassa Virus Glycoprotein Oligomerization and Influence of Cholesterol on Virus Replication. *Journal of Virology, 84*(2), 983-992. doi: 10.1128/jvi.02039-09

Schlie, K., Strecker, T., & Garten, W. (2010). Maturation cleavage within the ectodomain of Lassa virus glycoprotein relies on stabilization by the cytoplasmic tail. *FEBS Lett, 584*(21), 4379-4382. doi: 10.1016/j.febslet.2010.09.032

Schmaljohn, C. S., Hasty, S. E., Rasmussen, L., & Dalrymple, J. M. (1986). Hantaan virus replication: effects of monensin, tunicamycin and endoglycosidases on the structural glycoproteins. *J.Gen.Virol., 67 (Pt 4)*, 707-717.

Schmaljohn, C. S., & Nichol, S. T. (2007). Bunyaviridae. In D. M. Knipe, P. M. Howley, D. E. Griffin, R. A. Lamb, M. A. Martin, B. Roizman & S. E. Straus (Eds.), *Field's Virology* (5th ed., Vol. 2, pp. 1741-1789). Philadelphia: Wolters Kluwer Health/Lippincott Williams & Wilkins.

Schrempf, S., Froeschke, M., Giroglou, T., von Laer, D., & Dobberstein, B. (2007). Signal Peptide Requirements for Lymphocytic Choriomeningitis Virus Glycoprotein C Maturation and Virus Infectivity. *Journal of Virology, 81*(22), 12515-12524. doi: 10.1128/jvi.01481-07

Schwarz, E. R., Mando, O. G., Maiztegui, J. I., Vilches, A. M., Otero, E. R., & Berrutti, Z. C. (1972). [Coagulation changes in Argentine hemorrhagic fever]. *Medicina (B Aires), 32*(3), 247-259.

Schweizer, A., Fransen, J. A., Bachi, T., Ginsel, L., & Hauri, H. P. (1988). Identification, by a monoclonal antibody, of a 53-kD protein associated with a tubulo-vesicular compartment at the cis-side of the Golgi apparatus. *J Cell Biol, 107*(5), 1643-1653.

Schweizer, A., Matter, K., Ketcham, C. M., & Hauri, H. P. (1991). The isolated ER-Golgi intermediate compartment exhibits properties that are different from ER and cis-Golgi. *J Cell Biol, 113*(1), 45-54.

Scolaro, L. A., Mersich, S. E., & Damonte, E. B. (1990). A mouse attenuated mutant of Junin virus with an altered envelope glycoprotein. *Arch Virol, 111*(3-4), 257-262.

Scott, T. F., & Rivers, T. M. (1936). Meningitis in Man Caused by a Filterable Virus : I. Two Cases and the Method of Obtaining a Virus from Their Spinal Fluids. *J Exp Med, 63*(3), 397-414.

Seidah, N. G., Mowla, S. J., Hamelin, J., Mamarbachi, A. M., Benjannet, S., Toure, B. B., . . . Marcinkiewicz, M. (1999). Mammalian Subtilisin/Kexin Isozyme SKI-1: A Widely Expressed Proprotein Convertase with a Unique Cleavage Specificity and Cellular Localization. *Proceedings of the National Academy of Sciences of the United States of America, 96*(4), 1321-1326.

Sergio Grutadauria a, Viviana Castilla b, Marta Zapata a, Susana Mersich. (1999). Analysis of viral glycoproteins by glycosidic digestion inside a polyacrylamide gel. *Journal of Virological Methods, 80*, 217–221.

Sevilla, N., Kunz, S., Holz, A., Lewicki, H., Homann, D., Yamada, H., . . . Oldstone, M. B. (2000). Immunosuppression and resultant viral persistence by specific viral targeting of dendritic cells. *J Exp Med, 192*(9), 1249-1260.

Sevilla, N., Kunz, S., McGavern, D., & Oldstone, M. B. (2003). Infection of dendritic cells by lymphocytic choriomeningitis virus. *Curr Top Microbiol Immunol, 276*, 125-144.

Shah, W. A., Peng, H., & Carbonetto, S. (2006). Role of non-raft cholesterol in lymphocytic choriomeningitis virus infection via α-dystroglycan. *Journal of General Virology, 87*(3), 673-678. doi: 10.1099/vir.0.81444-0

Sheftel, A. D., Mason, A. B., & Ponka, P. The long history of iron in the Universe and in health and disease. *Biochimica et Biophysica Acta (BBA) - General Subjects*(0). doi: 10.1016/j.bbagen.2011.08.002

Shimojima, M., & Kawaoka, Y. (2012). Cell surface molecules involved in infection mediated by lymphocytic choriomeningitis virus glycoprotein. *J Vet Med Sci, 74*(10), 1363-1366.

Shimojima, M., Ströher, U., Ebihara, H., Feldmann, H., & Kawaoka, Y. (2011). Identification of cell surface molecules involved in dystroglycan-independent Lassa virus cell entry. *Journal of Virology*. doi: 10.1128/jvi.06451-11

Shtanko, O., Watanabe, S., Jasenosky, L. D., Watanabe, T., & Kawaoka, Y. (2011). ALIX/AIP1 is required for NP incorporation into Mopeia virus Z-induced virus-like particles. *J Virol, 85*(7), 3631-3641. doi: 10.1128/JVI.01984-10

Silber, A. M., Candurra, N. A., & Damonte, E. B. (1993). The effects of oligosaccharide trimming inhibitors on glycoprotein expression and infectivity of Junin virus. *FEMS Microbiol Lett, 109*(1), 39-43.

Sirachainan, N., Zhang, B., Chuansumrit, A., Pipe, S., Sasanakul, W., & Ginsburg, D. (2005). Combined factor V and factor VIII deficiency in a Thai patient: a case report of genotype and phenotype characteristics. *Haemophilia, 11*(3), 280-284. doi: 10.1111/j.1365-2516.2005.01092.x

Smelt, S. C., Borrow, P., Kunz, S., Cao, W., Tishon, A., Lewicki, H., . . . Oldstone, M. B. (2001). Differences in affinity of binding of lymphocytic choriomeningitis virus strains to the cellular receptor alpha-dystroglycan correlate with viral tropism and disease kinetics. *J Virol, 75*(1), 448-457. doi: 10.1128/JVI.75.1.448-457.2001

Soares, M. M., King, S. W., & Thorpe, P. E. (2008). Targeting inside-out phosphatidylserine as a therapeutic strategy for viral diseases. *Nat Med, 14*(12), 1357-1362. doi: 10.1038/nm.1885

Spatuzza, C., Renna, M., Faraonio, R., Cardinali, G., Martire, G., Bonatti, S., & Remondelli, P. (2004). Heat shock induces preferential translation of ERGIC-53 and affects its recycling pathway. *J Biol Chem, 279*(41), 42535-42544. doi: 10.1074/jbc.M401860200

Speir, R. W., Wood, O., Liebhaber, H., & Buckley, S. M. (1970). Lassa Fever, a New Virus Disease of Man from West Africa: IV. Electron Microscopy of Vero Cell Cultures Infected with Lassa Virus. *The American Journal of Tropical Medicine and Hygiene, 19*(4), 692-694.

Spiropoulou, C. F., Kunz, S., Rollin, P. E., Campbell, K. P., & Oldstone, M. B. (2002). New World arenavirus clade C, but not clade A and B viruses, utilizes alpha-dystroglycan as its major receptor. *J Virol, 76*(10), 5140-5146.

Spreafico, M., & Peyvandi, F. (2008). Combined FV and FVIII deficiency. *Haemophilia, 14*(6), 1201-1208. doi: 10.1111/j.1365-2516.2008.01845.x

Sprocati, T., Ronchi, P., Raimondi, A., Francolini, M., & Borgese, N. (2006). Dynamic and reversible restructuring of the ER induced by PDMP in cultured cells. *Journal of Cell Science, 119*(15), 3249-3260. doi: 10.1242/jcs.03058

Stenglein, M. D., Sanders, C., Kistler, A. L., Ruby, J. G., Franco, J. Y., Reavill, D. R., . . . DeRisi, J. L. (2012). Identification, Characterization, and In Vitro Culture of Highly Divergent Arenaviruses from Boa Constrictors and Annulated Tree Boas: Candidate Etiological Agents for Snake Inclusion Body Disease. *mBio, 3*(4). doi: 10.1128/mBio.00180-12

Strausbaugh, L. J., Barton, L. L., & Mets, M. B. (2001). Congenital Lymphocytic Choriomeningitis Virus Infection: Decade of Rediscovery. *Clinical Infectious Diseases, 33*(3), 370-374. doi: 10.1086/321897

Stuart, A. D., & Brown, T. D. K. (2007). α2,6-Linked sialic acid acts as a receptor for Feline calicivirus. *Journal of General Virology, 88*(1), 177-186. doi: 10.1099/vir.0.82158-0

Suehiro, Y., Veljkovic, D. K., Fuller, N., Motomura, Y., Masse, J. M., Cramer, E. M., & Hayward, C. P. (2005). Endocytosis and storage of plasma factor V by human megakaryocytes. *Thromb Haemost, 94*(3), 585-592.

Sullivan, B. M., Emonet, S. F., Welch, M. J., Lee, A. M., Campbell, K. P., de la Torre, J. C., & Oldstone, M. B. (2011). Point mutation in the glycoprotein of lymphocytic choriomeningitis virus is necessary for receptor binding, dendritic cell infection, and long-term persistence. *Proc Natl Acad Sci U S A, 108*(7), 2969-2974. doi: 1019304108 [pii] 10.1073/pnas.1019304108

Sullivan, B. M., Welch, M. J., Lemke, G., & Oldstone, M. B. (2013). Is the TAM receptor Axl a receptor for lymphocytic choriomeningitis virus? *J Virol, 87*(7), 4071-4074. doi: 10.1128/JVI.03268-12

Sun, E., He, J., & Zhuang, X. (2013). Dissecting the role of COPI complexes in influenza virus infection. *J Virol, 87*(5), 2673-2685. doi: 10.1128/JVI.02277-12

Takada, A., Robison, C., Goto, H., Sanchez, A., Murti, K. G., Whitt, M. A., & Kawaoka, Y. (1997). A system for functional analysis of Ebola virus glycoprotein. *Proceedings of the National Academy of Sciences of the United States of America, 94*(26), 14764-14769.

Tassaneetrithep, B., Burgess, T. H., Granelli-Piperno, A., Trumpfheller, C., Finke, J., Sun, W., . . . Marovich, M. A. (2003). DC-SIGN (CD209) mediates dengue virus infection of human dendritic cells. *J Exp Med, 197*(7), 823-829. doi: 10.1084/jem.20021840

Tayeh, A., Tatard, C., Kako-Ouraga, S., Duplantier, J. M., & Dobigny, G. (2010). Rodent host cell/Lassa virus interactions: evolution and expression of alpha-Dystroglycan, LARGE-1 and LARGE-2 genes, with special emphasis on the Mastomys genus. *Infect Genet Evol, 10*(8), 1262-1270. doi: 10.1016/j.meegid.2010.07.018

Teijaro, J. R., Ng, C., Lee, A. M., Sullivan, B. M., Sheehan, K. C., Welch, M., . . . Oldstone, M. B. (2013). Persistent LCMV infection is controlled by blockade of type I interferon signaling. *Science, 340*(6129), 207-211. doi: 10.1126/science.1235214

Tellez-Sanz, R., Garcia-Fuentes, L., & Vargas-Berenguel, A. (2013). Human galectin-3 selective and high affinity inhibitors. Present state and future perspectives. *Curr Med Chem, 20*(24), 2979-2990.

Teng, M. N., Borrow, P., Oldstone, M. B., & de la Torre, J. C. (1996). A single amino acid change in the glycoprotein of lymphocytic choriomeningitis virus is associated with the ability to cause growth hormone deficiency syndrome. *Journal of Virology, 70*(12), 8438-8443.

Tesh, R. B., Wilson, M. L., Salas, R., De Manzione, N. M. C., Tovar, D., Ksiazek, T. G., & Peters, C. J. (1993). Field Studies on the Epidemiology of Venezuelan Hemorrhagic Fever: Implication of the Cotton Rat Sigmodon alstoni as the Probable Rodent Reservoir. *The American Journal of Tropical Medicine and Hygiene, 49*(2), 227-235.

Thomas, C. J., Casquilho-Gray, H. E., York, J., DeCamp, D. L., Dai, D., Petrilli, E. B., . . . Nunberg, J. H. (2011). A specific interaction of small molecule entry inhibitors with the envelope glycoprotein complex of the Junin hemorrhagic fever

arenavirus. *J Biol Chem, 286*(8), 6192-6200. doi: M110.196428 [pii] 10.1074/jbc.M110.196428

Tilley, D., Levit, I., & Samis, J. A. (2012). Measurement of factor v activity in human plasma using a microplate coagulation assay. *J Vis Exp*(67). doi: 10.3791/3822

Tisdale, E. J., Plutner, H., Matteson, J., & Balch, W. E. (1997). p53/58 Binds COPI and Is Required for Selective Transport through the Early Secretory Pathway. *The Journal of Cell Biology, 137*(3), 581-593. doi: 10.1083/jcb.137.3.581

Toda, H., Tsuji, M., Nakano, I., Kobuke, K., Hayashi, T., Kasahara, H., . . . Tashiro, K. (2003). Stem cell-derived neural stem/progenitor cell supporting factor is an autocrine/paracrine survival factor for adult neural stem/progenitor cells. *J Biol Chem, 278*(37), 35491-35500. doi: 10.1074/jbc.M305342200

Tortorici, M. A., Albarino, C. G., Posik, D. M., Ghiringhelli, P. D., Lozano, M. E., Rivera Pomar, R., & Romanowski, V. (2001). Arenavirus nucleocapsid protein displays a transcriptional antitermination activity in vivo. *Virus Res, 73*(1), 41-55.

Traub, E. (1936). Persistence of Lymphocytic Choriomeningitis Virus in Immune Animals and Its Relation to Immunity. *J Exp Med, 63*(6), 847-861.

Trombley, A. R., Wachter, L., Garrison, J., Buckley-Beason, V. A., Jahrling, J., Hensley, L. E., . . . Kulesh, D. A. (2010). Comprehensive panel of real-time TaqMan polymerase chain reaction assays for detection and absolute quantification of filoviruses, arenaviruses, and New World hantaviruses. *American Journal of Tropical Medicine and Hygiene, 82*(5), 954-960. doi: 82/5/954 [pii] 10.4269/ajtmh.2010.09-0636

Urata, S., & Yasuda, J. (2012). Molecular mechanism of arenavirus assembly and budding. *Viruses, 4*(10), 2049-2079. doi: 10.3390/v4102049

Vaheri, A., Henttonen, H., Voutilainen, L., Mustonen, J., Sironen, T., & Vapalahti, O. (2013). Hantavirus infections in Europe and their impact on public health. *Rev Med Virol, 23*(1), 35-49. doi: 10.1002/rmv.1722

Valsamakis, V., Southern, P., Blount, P., Ahmed, R., Buchmeier, M. J., & Oldstone, M. B. (1986). Dissecting the molecular anatomy of persistent infection with lymphocytic choriomeningitis virus. *Med Microbiol Immunol, 175*(2-3), 97-99.

Van Damme, E. J. M., Allen, A. K., & Peumans, W. J. (1987). Isolation and characterization of a lectin with exclusive specificity towards mannose from snowdrop (Galanthus nivalis) bulbs. *FEBS Letters, 215*(1), 140-144. doi: http://dx.doi.org/10.1016/0014-5793(87)80129-1

Varki, A., Etzler, M. E., Cummings, R. D., & Esko, J. D. (2009). Discovery and Classification of Glycan-Binding Proteins. In A. Varki, R. D. Cummings, J. D. Esko, H. H. Freeze, P. Stanley, C. R. Bertozzi, G. W. Hart & M. E. Etzler (Eds.), *Essentials of Glycobiology* (2nd ed.). Cold Spring Harbor (NY).

Vasconcelos, P. F., Travassos da Rosa, A. P., Rodrigues, S. G., Tesh, R., Travassos da Rosa, J. F., & Travassos da Rosa, E. S. (1993). [Laboratory-acquired human infection with SP H 114202 virus (Arenavirus: Arenaviridae family): clinical and laboratory aspects]. *Rev Inst Med Trop Sao Paulo, 35*(6), 521-525.

Vela, E. (2012). Animal Models, Prophylaxis, and Therapeutics for Arenavirus Infections. *Viruses, 4*(9), 1802-1829.

Vela, E. M., Zhang, L., Colpitts, T. M., Davey, R. A., & Aronson, J. F. (2007). Arenavirus entry occurs through a cholesterol-dependent, non-caveolar, clathrin-mediated endocytic mechanism. *Virology, 369*(1), 1-11. doi: S0042-6822(07)00479-5 [pii] 10.1016/j.virol.2007.07.014

Velloso, L. M., Svensson, K., Pettersson, R. F., & Lindqvist, Y. (2003a). The crystal structure of the carbohydrate-recognition domain of the glycoprotein sorting receptor p58/ERGIC-53 reveals an unpredicted metal-binding site and conformational changes associated with calcium ion binding. *Journal of Molecular Biology, 334*(5), 845-851. doi: S0022283603012932 [pii]

Velloso, L. M., Svensson, K., Schneider, G., Pettersson, R. F., & Lindqvist, Y. (2002). Crystal structure of the carbohydrate recognition domain of p58/ERGIC-53, a protein involved in glycoprotein export from the endoplasmic reticulum. *J Biol Chem, 277*(18), 15979-15984. doi: 10.1074/jbc.M112098200

Vitullo, A. D., Hodara, V. L., & Merani, M. S. (1987). Effect of persistent infection with Junin virus on growth and reproduction of its natural reservoir, Calomys musculinus. *The American Journal of Tropical Medicine and Hygiene, 37*(3), 663-669.

Vitullo, A. D., & Merani, M. S. (1990). Vertical transmission of Junin virus in experimentally infected adult Calomys musculinus. *Intervirology, 31*(6), 339-344.

Vollenweider, F., Kappeler, F., Itin, C., & Hauri, H. P. (1998b). Mistargeting of the lectin ERGIC-53 to the endoplasmic reticulum of HeLa cells impairs the secretion of a lysosomal enzyme. *Journal of Cell Biology, 142*(2), 377-389.

Volpon, L., Osborne, M. J., Capul, A. A., de la Torre, J. C., & Borden, K. L. (2010). Structural characterization of the Z RING-eIF4E complex reveals a distinct mode of control for eIF4E. *Proc Natl Acad Sci U S A, 107*(12), 5441-5446. doi: 10.1073/pnas.0909877107

Walker, D. H., McCormick, J. B., Johnson, K. M., Webb, P. A., Komba-Kono, G., Elliott, L. H., & Gardner, J. J. (1982). Pathologic and virologic study of fatal Lassa fever in man. *Am J Pathol, 107*(3), 349-356.

Watanabe, H., Tanaka, Y., Shimazu, Y., Sugahara, F., Kuwayama, M., Hiramatsu, A., . . . Sakaguchi, T. (2005). Cell-Specific Inhibition of Paramyxovirus Maturation by Proteasome Inhibitors. *Microbiology and Immunology, 49*(9), 835-844. doi: 10.1111/j.1348-0421.2005.tb03672.x

Webb, P. A., McCormick, J. B., King, I. J., Bosman, I., Johnson, K. M., Elliott, L. H., . . . O'Sullivan, R. (1986). Lassa fever in children in Sierra Leone, West Africa. *Transactions of the Royal Society of Tropical Medicine and Hygiene, 80*(4), 577-582. doi: 10.1016/0035-9203(86)90147-1

Weissenhorn, W., Carfi, A., Lee, K. H., Skehel, J. J., & Wiley, D. C. (1998). Crystal structure of the Ebola virus membrane fusion subunit, GP2, from the envelope glycoprotein ectodomain. *Mol Cell, 2*(5), 605-616.

Welsh, R. M., Jr., & Buchmeier, M. J. (1979). Protein analysis of defective interfering lymphocytic choriomeningitis virus and persistently infected cells. *Virology, 96*(2), 503-515.

Wherry, E. J., Ha, S. J., Kaech, S. M., Haining, W. N., Sarkar, S., Kalia, V., . . . Ahmed, R. (2007). Molecular signature of CD8+ T cell exhaustion during chronic viral infection. *Immunity, 27*(4), 670-684. doi: 10.1016/j.immuni.2007.09.006

Whitt, M. A. (2010). Generation of VSV pseudotypes using recombinant DeltaG-VSV for studies on virus entry, identification of entry inhibitors, and immune responses to vaccines. *Journal of Virological Methods, 169*(2), 365-374. doi: S0166-0934(10)00288-0 [pii] 10.1016/j.jviromet.2010.08.006

Wieland, F. T., Gleason, M. L., Serafini, T. A., & Rothman, J. E. (1987). The rate of bulk flow from the endoplasmic reticulum to the cell surface. *Cell, 50*(2), 289-300. doi: http://dx.doi.org/10.1016/0092-8674(87)90224-8

Wiertz, E. J., Tortorella, D., Bogyo, M., Yu, J., Mothes, W., Jones, T. R., . . . Ploegh, H. L. (1996). Sec61-mediated transfer of a membrane protein from the endoplasmic reticulum to the proteasome for destruction. *Nature, 384*(6608), 432-438. doi: 10.1038/384432a0

Wigren, E., Bourhis, J. M., Kursula, I., Guy, J. E., & Lindqvist, Y. (2010). Crystal structure of the LMAN1-CRD/MCFD2 transport receptor complex provides insight into combined deficiency of factor V and factor VIII. *FEBS Lett, 584*(5), 878-882. doi: 10.1016/j.febslet.2010.02.009

Wolff, S., Becker, S., & Groseth, A. (2013). Cleavage of the Junin Virus Nucleoprotein Serves a Decoy Function To Inhibit the Induction of Apoptosis during Infection. *Journal of Virology, 87*(1), 224-233. doi: 10.1128/jvi.01929-12

Wright, K. E., Salvato, M. S., & Buchmeier, M. J. (1989). Neutralizing epitopes of lymphocytic choriomeningitis virus are conformational and require both glycosylation and disulfide bonds for expression. *Virology, 171*(2), 417-426.

Wright, K. E., Spiro, R. C., Burns, J. W., & Buchmeier, M. J. (1990a). Post-translational processing of the glycoproteins of lymphocytic choriomeningitis virus. *Virol., 177*(1), 175-183.

Wright, R., Johnson, D., Neumann, M., Ksiazek, T. G., Rollin, P., Keech, R. V., . . . Bale, J. F., Jr. (1997). Congenital lymphocytic choriomeningitis virus syndrome: a disease that mimics congenital toxoplasmosis or Cytomegalovirus infection. *Pediatrics, 100*(1), E9.

Xiao, S. Y., Zhang, H., Yang, Y., & Tesh, R. B. (2001). Pirital virus (arenaviridae) infection in the Syrian golden hamster, Mesocricetus auratus: A new animal model for arenaviral hemorrhagic fever. *American Journal of Tropical Medicine and Hygiene, 64*(3-4), 111-118.

York, J., Agnihothram, S. S., Romanowski, V., & Nunberg, J. H. (2005). Genetic analysis of heptad-repeat regions in the G2 fusion subunit of the Junin arenavirus envelope glycoprotein. *Virology, 343*(2), 267-274. doi: S0042-6822(05)00520-9 [pii] 10.1016/j.virol.2005.08.030

York, J., Berry, J. D., Stroher, U., Li, Q., Feldmann, H., Lu, M., . . . Nunberg, J. H. (2010). An Antibody Directed against the Fusion Peptide of Junin Virus Envelope Glycoprotein GPC Inhibits pH-Induced Membrane Fusion. *Journal of Virology, 84*(12), 6119-6129. doi: 10.1128/jvi.02700-09

York, J., Dai, D., Amberg, S. M., & Nunberg, J. H. (2008). pH-induced activation of arenavirus membrane fusion is antagonized by small-molecule inhibitors. *J Virol, 82*(21), 10932-10939. doi: JVI.01140-08 [pii] 10.1128/JVI.01140-08

York, J., & Nunberg, J. H. (2006). Role of the stable signal peptide of Junin arenavirus envelope glycoprotein in pH-dependent membrane fusion. *J Virol, 80*(15), 7775-7780. doi: 80/15/7775 [pii] 10.1128/JVI.00642-06

York, J., & Nunberg, J. H. (2007a). Distinct requirements for signal peptidase processing and function in the stable signal peptide subunit of the Junin virus envelope glycoprotein. *Virology, 359*(1), 72-81. doi: S0042-6822(06)00620-9 [pii] 10.1016/j.virol.2006.08.048

York, J., & Nunberg, J. H. (2007b). A novel zinc-binding domain is essential for formation of the functional Junin virus envelope glycoprotein complex. *J Virol, 81*(24), 13385-13391. doi: JVI.01785-07 [pii] 10.1128/JVI.01785-07

York, J., & Nunberg, J. H. (2009). Intersubunit Interactions Modulate pH-Induced Activation of Membrane Fusion by the Junin Virus Envelope Glycoprotein GPC. *Journal of Virology, 83*(9), 4121-4126. doi: 10.1128/jvi.02410-08

York, J., Romanowski, V., Lu, M., & Nunberg, J. H. (2004). The Signal Peptide of the Junin Arenavirus Envelope Glycoprotein Is Myristoylated and Forms an Essential Subunit of the Mature G1-G2 Complex. *Journal of Virology, 78*(19), 10783-10792. doi: 10.1128/jvi.78.19.10783-10792.2004

Yun, N. E., & Walker, D. H. (2012). Pathogenesis of Lassa Fever. *Viruses, 4*(10), 2031-2048.

Zajac, A. J., Blattman, J. N., Murali-Krishna, K., Sourdive, D. J., Suresh, M., Altman, J. D., & Ahmed, R. (1998). Viral immune evasion due to persistence of activated T cells without effector function. *J Exp Med, 188*(12), 2205-2213.

Zapata, J., & Salvato, M. (2013). Arenavirus Variations Due to Host-Specific Adaptation. *Viruses, 5*(1), 241-278.

Zeuschner, D., Geerts, W. J. C., van Donselaar, E., Humbel, B. M., Slot, J. W., Koster, A. J., & Klumperman, J. (2006). Immuno-electron tomography of ER exit sites reveals the existence of free COPII-coated transport carriers. *Nat Cell Biol, 8*(4), 377-383. doi: http://www.nature.com/ncb/journal/v8/n4/suppinfo/ncb1371_S1.html

Zhang, B. (2009). Recent developments in the understanding of the combined deficiency of FV and FVIII. *Br J Haematol, 145*(1), 15-23. doi: 10.1111/j.1365-2141.2008.07559.x

Zhang, B., Cunningham, M. A., Nichols, W. C., Bernat, J. A., Seligsohn, U., Pipe, S. W., . . . Ginsburg, D. (2003a). Bleeding due to disruption of a cargo-specific ER-to-Golgi transport complex. *Nat Genet, 34*(2), 220-225. doi: 10.1038/ng1153 ng1153 [pii]

Zhang, B., Cunningham, M. A., Nichols, W. C., Bernat, J. A., Seligsohn, U., Pipe, S. W., . . . Ginsburg, D. (2003). Bleeding due to disruption of a cargo-specific ER-to-Golgi transport complex. *Nat Genet, 34*(2), 220-225. doi: http://www.nature.com/ng/journal/v34/n2/suppinfo/ng1153_S1.html

Zhang, B., Kaufman, R. J., & Ginsburg, D. (2005a). LMAN1 and MCFD2 form a cargo receptor complex and interact with coagulation factor VIII in the early secretory

pathway. *Journal of Biological Chemistry, 280*(27), 25881-25886. doi: M502160200 [pii] 10.1074/jbc.M502160200

Zhang, B., McGee, B., Yamaoka, J. S., Guglielmone, H., Downes, K. A., Minoldo, S., . . . Ginsburg, D. (2006). Combined deficiency of factor V and factor VIII is due to mutations in either LMAN1 or MCFD2. *Blood, 107*(5), 1903-1907. doi: 10.1182/blood-2005-09-3620

Zhang, B., Spreafico, M., Zheng, C., Yang, A., Platzer, P., Callaghan, M. U., . . . Ginsburg, D. (2008). Genotype-phenotype correlation in combined deficiency of factor V and factor VIII. *Blood, 111*(12), 5592-5600. doi: 10.1182/blood-2007-10-113951

Zhang, B., Zheng, C., Zhu, M., Tao, J., Vasievich, M. P., Baines, A., . . . Ginsburg, D. (2011). Mice deficient in LMAN1 exhibit FV and FVIII deficiencies and liver accumulation of alpha1-antitrypsin. *Blood, 118*(12), 3384-3391. doi: 10.1182/blood-2011-05-352815

Zhang, L., Marriott, K., & Aronson, J. F. (1999). Sequence analysis of the small RNA segment of guinea pig-passaged Pichinde virus variants. *Am J Trop Med Hyg, 61*(2), 220-225.

Zhang, Y. C., Zhou, Y., Yang, C. Z., & Xiong, D. S. (2009). A review of ERGIC-53: its structure, functions, regulation and relations with diseases. *Histol Histopathol, 24*(9), 1193-1204.

Zheng, C., Liu, H. H., Yuan, S., Zhou, J., & Zhang, B. (2010). Molecular basis of LMAN1 in coordinating LMAN1-MCFD2 cargo receptor formation and ER-to-Golgi transport of FV/FVIII. *Blood, 116*(25), 5698-5706. doi: blood-2010-04-278325 [pii] 10.1182/blood-2010-04-278325

Zheng, C., Liu, H. H., Zhou, J., & Zhang, B. (2010). EF-hand domains of MCFD2 mediate interactions with both LMAN1 and coagulation factor V or VIII. *Blood, 115*(5), 1081-1087. doi: 10.1182/blood-2009-09-241877

Zheng, C., Page, R. C., Das, V., Nix, J. C., Wigren, E., Misra, S., & Zhang, B. (2013). Structural Characterization of Carbohydrate Binding by LMAN1 Protein Provides New Insight into the Endoplasmic Reticulum Export of Factors V (FV) and VIII (FVIII). *Journal of Biological Chemistry, 288*(28), 20499-20509. doi: 10.1074/jbc.M113.461434

Zhou, H., Xu, M., Huang, Q., Gates, A. T., Zhang, X. D., Castle, J. C., . . . Espeseth, A. S. (2008). Genome-scale RNAi screen for host factors required for HIV replication. *Cell Host Microbe, 4*(5), 495-504. doi: 10.1016/j.chom.2008.10.004

Zhou, S., Cerny, A. M., Zacharia, A., Fitzgerald, K. A., Kurt-Jones, E. A., & Finberg, R. W. (2010). Induction and Inhibition of Type I Interferon Responses by Distinct Components of Lymphocytic Choriomeningitis Virus. *Journal of Virology, 84*(18), 9452-9462. doi: 10.1128/jvi.00155-10

Zinselmeyer, B. H., Heydari, S., Sacristan, C., Nayak, D., Cammer, M., Herz, J., . . . McGavern, D. B. (2013). PD-1 promotes immune exhaustion by inducing antiviral T cell motility paralysis. *J Exp Med, 210*(4), 757-774. doi: 10.1084/jem.20121416

Zito, E., Fraldi, A., Pepe, S., Annunziata, I., Kobinger, G., Di Natale, P., . . . Cosma, M. P. (2005). Sulphatase activities are regulated by the interaction of sulphatase-modifying factor 1 with SUMF2. *EMBO Rep, 6*(7), 655-660. doi: 10.1038/sj.embor.7400454

Zuber, C., Spiro, M. J., Guhl, B., Spiro, R. G., & Roth, J. (2000). Golgi apparatus immunolocalization of endomannosidase suggests post-endoplasmic reticulum glucose trimming: implications for quality control. *Mol Biol Cell, 11*(12), 4227-4240.

6. Appendix

Table S1A, Related to Figures 1A-1C. Intersect of Identified Proteins Interacting with GP Proteins of ANDV and LCMV. The number of total peptides identified is listed. *Indicates non-GP control contained peptides from this protein but at levels at least five times less.

Proteins Identified Interacting with GP proteins of both ANDV and LCMV			**ANDV**	**LCMV**
Gene symbol	**Description**	**IPI id**	**# Peptides**	**# Peptides**
B3GALT6	UDP-Gal:betaGal beta 1,3-galactosyltransferase polypeptide 6	IPI00064848	2	2
BAG2	BCL2-associated athanogene 2	IPI00000643	3	16*
CALR	calreticulin	IPI00020599	9	24
CALU	calumenin	IPI00045396	8	36
CANX	calnexin	IPI00020984	53*	75
CPNE3	copine III	IPI00024403	2	3
DDOST	dolichyl-diphosphooligosaccharide-protein glycosyltransferase	IPI00297084	6	10*
DHX30	DEAH (Asp-Glu-Ala-His) box polypeptide 30	IPI00164906	29*	2
DNAJA1	DnaJ (Hsp40) homolog, subfamily A, member 1	IPI00012535	2	7*
DNAJB11	DnaJ (Hsp40) homolog, subfamily B, member 11	IPI00008454	5	11
DNAJC10	DnaJ (Hsp40) homolog, subfamily C, member 10	IPI00293260	4	4
DNAJC7	DnaJ (Hsp40) homolog, subfamily C, member 7	IPI00329629	6	12
EMD	emerin (Emery-Dreifuss muscular dystrophy)	IPI00032003	6	20*
ERLIN1	SPFH domain family, member 1	IPI00007940	2	15
ERLIN2	SPFH domain family, member 2	IPI00026942	6*	19
G3BP1	Ras-GTPase-activating protein SH3-domain-binding protein	IPI00012442	8	4
GANAB	glucosidase, alpha; neutral AB	IPI00011454	19*	16
GPX8	similar to RIKEN cDNA 2310016C16	IPI00291695	2	4
HSP90B1	heat shock protein 90kDa beta (Grp94), member 1	IPI00027230	18*	22*
HSPA5	heat shock 70kDa protein 5 (glucose-regulated protein, 78kDa)	IPI00003362	481*	144*
KPNA2;LOC728860	karyopherin alpha 2 (RAG cohort 1, importin alpha 1)	IPI00002214	2	4

LMAN1 (ERGIC53)	lectin, mannose-binding, 1 (ERGIC53)	IPI00026530	12	15
LYAR	hypothetical protein FLJ20425	IPI00015838	3	6
MYBBP1A	MYB binding protein (P160) 1a	IPI00005024	9	18*
MYO1B	myosin IB	IPI00376344	3	2
MYO1C	myosin IC	IPI00010418	10	9*
MYO6	myosin VI	IPI00008455	21	2
P4HB	procollagen-proline, 2-oxoglutarate 4-dioxygenase (proline 4-hydroxylase), beta polypeptide	IPI00010796	14	10
PDIA6	protein disulfide isomerase family A, member 6	IPI00299571	27*	17*
PSMB6	proteasome (prosome, macropain) subunit, beta type, 6	IPI00000811	3	4
PSMD2	proteasome (prosome, macropain) 26S subunit, non-ATPase, 2	IPI00012268	3	6
RCN1	reticulocalbin 1, EF-hand calcium binding domain	IPI00015842	9	50
RPL22	ribosomal protein L22	IPI00219153	2	5*
RPL28	ribosomal protein L28	IPI00182533	7	10*
RPLP2	ribosomal protein, large, P2	IPI00008529	7	3
RPN1	ribophorin I	IPI00025874	9	13
RPS24	ribosomal protein S24	IPI00029750	3	3
RPS9	ribosomal protein S9	IPI00221088	11	10*
RRBP1	ribosome binding protein 1 homolog 180kDa (dog)	IPI00215743	11	3
RRP1	DNA segment on chromosome 21 (unique) 2056 expressed sequence	IPI00550766	2	3
SDF2L1	stromal cell-derived factor 2-like 1	IPI00106642	2	3
SDF4	stromal cell derived factor 4	IPI00009794	2	12
SEP15	15 kDa selenoprotein	IPI00030877	4	3
SIL1	SIL1 homolog, endoplasmic reticulum chaperone (S. cerevisiae)	IPI00296197	3	5
SLC25A13	solute carrier family 25, member 13 (citrin)	IPI00007084	2	8
SMC2	SMC2 structural maintenance of chromosomes 2-like 1 (yeast)	IPI00007927	2	9
TOR3A	torsin family 3, member A	IPI00301631	3	5
TUBB2A	tubulin, beta 2A	IPI00013475	5	27*
UBC;RPS27A;UBB	ribosomal protein S27a	IPI00179330	50*	88*
UGCGL1	UDP-glucose ceramide glucosyltransferase-like 1	IPI00024466	51	58
VCP	valosin-containing protein	IPI00022774	15	21

Table S1B, Related to Figures 1A-1C. Proteins Identified Interacting with LCMV GP and Not ANDV GP. The number of total peptides identified is listed. *Indicates non-GP control contained peptides from this protein but at levels at least five times less.

Gene symbol	Description	IPI id	# Peptides
ABCD3	ATP-binding cassette, sub-family D (ALD), member 3	IPI00002372	2
ACAD9	acyl-Coenzyme A dehydrogenase family, member 9	IPI00152981	2
ACOT8	acyl-CoA thioesterase 8	IPI00298202	3
ACP1	acid phosphatase 1, soluble	IPI00218847	3
AIFM1	programmed cell death 8 (apoptosis-inducing factor)	IPI00000690	12
AKAP8L	A kinase (PRKA) anchor protein 8-like	IPI00297455	2
ALDH1B1	aldehyde dehydrogenase 1 family, member B1	IPI00103467	3
ARCN1	archain 1	IPI00298520	5
ARF1	ADP-ribosylation factor 1	IPI00215914	2
ARF4	ADP-ribosylation factor 4	IPI00215918	5*
ARMCX3	armadillo repeat containing, X-linked 3	IPI00009906	2
ATAD3B	ATPase family, AAA domain containing 3B	IPI00045921; IPI00178879	40*
ATP2A1	ATPase, Ca++ transporting, cardiac muscle, fast twitch 1	IPI00024804	5
ATP2A2	ATPase, Ca++ transporting, cardiac muscle, slow twitch 2	IPI00177817	8
ATP5A1	ATP synthase, H+ transporting, mitochondrial F1 complex, alpha subunit 1	IPI00440493	19*
ATP6AP2	ATPase, H+ transporting, lysosomal accessory protein 2	IPI00168884	4
ATXN10	ataxin 10	IPI00001636	7
AURKB	aurora kinase B	IPI00176642	2
BCAP31	B-cell receptor-associated protein 31	IPI00218200	8
BZW2	basic leucine zipper and W2 domains 2	IPI00022305	3
C14orf21	chromosome 14 open reading frame 21	IPI00216999	8
C19orf10	chromosome 19 open reading frame 10	IPI00056357	2
C22orf28	hypothetical protein HSPC117	IPI00550689	2
C8orf41	chromosome 8 open reading frame 41	IPI00306207	2
C8orf55	chromosome 8 open reading frame 55	IPI00171421	2
C9orf89	chromosome 9 open reading frame 89	IPI00177808	2
CAND1	cullin-associated and neddylation-dissociated 1	IPI00100160	8
CAND2	cullin-associated and neddylation-dissociated	IPI00374208	4

	2		
CCDC3	coiled-coil domain-containing protein 3	IPI00385079	2
CCDC47	coiled-coil domain containing 47	IPI00024642	2
CDC2	cell division cycle 2, G1 to S and G2 to M	IPI00026689	2
CDKN2A	cyclin-dependent kinase inhibitor 2A (melanoma, p16, inhibits CDK4)	IPI00001560	3
CHST14	dermatan 4 sulfotransferase 1	IPI00044326	2
CLTC	clathrin, heavy polypeptide (Hc)	IPI00024067	2
CNPY2	transmembrane protein 4	IPI00443909	3
COPA	coatomer protein complex, subunit alpha	IPI00295857	2
COPG2	coatomer protein complex, subunit gamma 2	IPI00002557	2
CPE	carboxypeptidase E	IPI00031121	2
CSE1L	CSE1 chromosome segregation 1-like (yeast)	IPI00022744	6
CYC1	cytochrome c-1	IPI00029264	2
DHCR24	24-dehydrocholesterol reductase	IPI00016703	3
DHCR7	7-dehydrocholesterol reductase	IPI00294501	2
DHRS7B	dehydrogenase/reductase (SDR family) member 7B	IPI00550165	2
DNAJA2	DnaJ (Hsp40) homolog, subfamily A, member 2	IPI00032406	9
DNAJB1	DnaJ (Hsp40) homolog, subfamily B, member 1	IPI00015947	3
DNAJB4	DnaJ (Hsp40) homolog, subfamily B, member 4	IPI00003848	3
DNAJB6	DnaJ (Hsp40) homolog, subfamily B, member 6	IPI00024523	6*
DNAJC11	DnaJ (Hsp40) homolog, subfamily C, member 11	IPI00333016	3
DSG2	desmoglein 2	IPI00028931	3
EARS2	KIAA1970 protein	IPI00384503	4
EIF2B1	eukaryotic translation initiation factor 2B, subunit 1 alpha, 26kDa	IPI00221300	2
EIF2B2	eukaryotic translation initiation factor 2B, subunit 2 beta, 39kDa	IPI00028083	6
EIF2B4	eukaryotic translation initiation factor 2B, subunit 4 delta, 67kDa	IPI00005979	6
ERP44	thioredoxin domain containing 4 (endoplasmic reticulum)	IPI00401264	5
FAF2	UBX domain containing 8	IPI00172656	6
FAM3C	family with sequence similarity 3, member C	IPI00334282	3
FANCD2	Fanconi anemia, complementation group D2	IPI00075081	4
FANCI	KIAA1794	IPI00019447	5
FAR1	male sterility domain containing 2	IPI00386139	7
FSTL1	follistatin-like 1	IPI00029723	2
FUCA2	fucosidase, alpha-L- 2, plasma	IPI00012440	2
GALK1	galactokinase 1	IPI00019383	3
GALNT2	UDP-N-acetyl-alpha-D-galactosamine:polypeptide N-	IPI00004669	3

	acetylgalactosaminyltransferase 2		
GBAS	glioblastoma amplified sequence	IPI00016077	5
GCN1L1	GCN1 general control of amino-acid synthesis 1-like 1 (yeast)	IPI00001159	20
GEMIN4	gem (nuclear organelle) associated protein 4	IPI00027717	4
GEMIN6	gem (nuclear organelle) associated protein 6	IPI00103087	3
GLA	galactosidase, alpha	IPI00025869	2
GLG1	golgi apparatus protein 1	IPI00414717	2
GLMN	glomulin, FKBP associated protein	IPI00074604	3
GLT8D1	glycosyltransferase 8 domain containing 1	IPI00020470	2
GPC4	glypican 4	IPI00232571	2
HADHA	hydroxyacyl-Coenzyme A dehydrogenase alpha subunit	IPI00031522	8*
HAX1	HCLS1 associated protein X-1	IPI00010440	8
HEATR2	hypothetical protein FLJ20397	IPI00242630	2
HEATR3	hypothetical protein FLJ20718	IPI00100984	4
HEXA	hexosaminidase A (alpha polypeptide)	IPI00027851	2
HLA-A	major histocompatibility complex, class I, A	IPI00472013	3
HLA-B;HLA-C	major histocompatibility complex, class I, B	IPI00004657	3
HS2ST1	heparan sulfate 2-O-sulfotransferase 1	IPI00040900	7
HSD17B12	hydroxysteroid (17-beta) dehydrogenase 12	IPI00007676	3
HSPB1	heat shock 27kDa protein 1	IPI00025512	2
HSPBP1	hsp70-interacting protein	IPI00100748	7
HSPD1	heat shock 60kD protein 1	IPI00784154	9
IARS2	isoleucine-tRNA synthetase 2, mitochondrial	IPI00017283	2
IDH3A	isocitrate dehydrogenase 3 (NAD+) alpha	IPI00030702	2
IKIP	IKK interacting protein	IPI00043598	2
ILK-2;CCT4	chaperonin containing TCP1, subunit 4 (delta)	IPI00302927	5
IMMT	inner membrane protein, mitochondrial (mitofilin)	IPI00009960	16
IPO11	importin 11	IPI00301107	2
IPO4	importin 4	IPI00156374	6
IPO5	importin 5	IPI00793443; IPI00514205; IPI00639960	41
IPO7	importin 7	IPI00007402	15
IPO8	importin 8	IPI00007401	4
IPO9	importin 9	IPI00185146	10
IQGAP2	IQ motif containing GTPase activating protein 2	IPI00299048	2
KIAA0368	proteasome-associated protein ECM29 homolog	IPI00157790	2
KIAA0913	zinc finger SWIM domain-containing protein KIAA0913	IPI00166606	2
KIAA1524	cancerous inhibitor of PP2A	IPI00154283	2

KPNB1	karyopherin (importin) beta 1	IPI00001639	15*
LAP3	leucine aminopeptidase 3	IPI00419237	6
LEPRE1	leucine proline-enriched proteoglycan (leprecan) 1	IPI00045839	4
LMAN2	lectin, mannose-binding 2	IPI00009950	3
LMNB1	lamin B1	IPI00217975	2
LOC442497;SLC3A2	solute carrier family 3 (activators of dibasic and neutral amino acid transport), member 2	IPI00027493	6
LPCAT1	acyltransferase like 2	IPI00171626	4
LRPAP1	low density lipoprotein receptor-related protein associated protein 1	IPI00026848	5
LRRC59	leucine rich repeat containing 59	IPI00396321	3
MAGED1	melanoma antigen family D, 1	IPI00328354	3
MAGT1	implantation-associated protein	IPI00301202	4
MARS	methionine-tRNA synthetase	IPI00008240	6*
MCM3AP	MCM3 minichromosome maintenance deficient 3 (S. cerevisiae) associated protein	IPI00028954	2
MDN1	MDN1, midasin homolog (yeast)	IPI00167941	11
MIA3	melanoma inhibitory activity family, member 3	IPI00455473	17
MLF2	myeloid leukemia factor 2	IPI00023095	3
MSH6	mutS homolog 6 (E. coli)	IPI00106847	2
MTCH1	mitochondrial carrier homolog 1 (C. elegans)	IPI00386258	3
MTCH2	mitochondrial carrier homolog 2 (C. elegans)	IPI00003833	3
MTHFD1	methylenetetrahydrofolate dehydrogenase (NADP+ dependent) 1	IPI00218342	2
MTX2	metaxin 2	IPI00025717	4
MYH15	myosin, heavy chain 15	IPI00180408	2
NCLN	nicalin homolog (zebrafish)	IPI00470649	3
NCSTN	nicastrin	IPI00021983	2
NDUFS1	NADH dehydrogenase (ubiquinone) Fe-S protein 1, 75kDa (NADH-coenzyme Q reductase)	IPI00604664	6
NDUFS3	NADH dehydrogenase (ubiquinone) Fe-S protein 3, 30kDa (NADH-coenzyme Q reductase)	IPI00025796	2
NDUFS7	NADH dehydrogenase (ubiquinone) Fe-S protein 7, 20kDa (NADH-coenzyme Q reductase)	IPI00307749	2
NDUFV1	NADH dehydrogenase (ubiquinone) flavoprotein 1, 51kDa	IPI00028520	4
NDUFV2	NADH dehydrogenase (ubiquinone) flavoprotein 2, 24kDa	IPI00291328	4
NGDN	neuroguidin, EIF4E binding protein	IPI00000162	2
NOMO1;NOMO3	NODAL modulator 1	IPI00329352	4
NRM	nurim (nuclear envelope membrane protein)	IPI00217557	3
NUCB1	nucleobindin 1	IPI00295542	9
NUCB2	nucleobindin 2	IPI00009123	5

NUP205	nucleoporin 205kDa	IPI00783781	19
NUP210	nucleoporin 210kDa	IPI00291755	3
NUP93	nucleoporin 93kDa	IPI00397904	9*
ORC4L	origin recognition complex, subunit 4-like	IPI00015164	2
OS9	amplified in osteosarcoma	IPI00186581	3
OXA1L	oxidase (cytochrome c) assembly 1-like	IPI00014301	2
P4HA1	procollagen-proline, 2-oxoglutarate 4-dioxygenase (proline 4-hydroxylase), alpha polypeptide I	IPI00009923	3
P4HA2	procollagen-proline, 2-oxoglutarate 4-dioxygenase (proline 4-hydroxylase), alpha polypeptide II	IPI00003128	2
PCYT1A	phosphate cytidylyltransferase 1, choline, alpha	IPI00329338	8
PCYT1B	phosphate cytidylyltransferase 1, choline, beta	IPI00001562	3
PDIA3	protein disulfide isomerase family A, member 3	IPI00025252	25
PEX11B	peroxisomal biogenesis factor 11B	IPI00021978	6
PHB	prohibitin	IPI00017334	5
PHB2	prohibitin 2	IPI00027252	8
PHGDH	phosphoglycerate dehydrogenase	IPI00011200	7*
PIGK	phosphatidylinositol glycan, class K	IPI00022543	2
PIGS	phosphatidylinositol glycan, class S	IPI00465308	2
PIK3CG	phosphoinositide-3-kinase, catalytic, gamma polypeptide	IPI00292690	2
PLOD1	procollagen-lysine 1, 2-oxoglutarate 5-dioxygenase 1	IPI00027192	3
PPFIBP1	PTPRF interacting protein, binding protein 1 (liprin beta 1)	IPI00179172	17
PPP2R1A	protein phosphatase 2 (formerly 2A), regulatory subunit A (PR 65), alpha isoform	IPI00168184	3
PREB	prolactin regulatory element binding	IPI00033349	2
PRKDC	protein kinase, DNA-activated, catalytic polypeptide	IPI00296337	135*
PSMA1	proteasome (prosome, macropain) subunit, alpha type, 1	IPI00016832	8
PSMA3	proteasome (prosome, macropain) subunit, alpha type, 3	IPI00171199	4
PSMA4	proteasome (prosome, macropain) subunit, alpha type, 4	IPI00299155	3
PSMA5	proteasome (prosome, macropain) subunit, alpha type, 5	IPI00291922	7
PSMA6	proteasome (prosome, macropain) subunit, alpha type, 6	IPI00029623	4
PSMA7	proteasome (prosome, macropain) subunit, alpha type, 7	IPI00024175	6
PSMB1	proteasome (prosome, macropain) subunit, beta type, 1	IPI00025019	4
PSMB2	proteasome (prosome, macropain) subunit,	IPI00028006	3

	beta type, 2		
PSMB4	proteasome (prosome, macropain) subunit, beta type, 4	IPI00555956	4
PSMB5	proteasome (prosome, macropain) subunit, beta type, 5	IPI00383971; IPI00479306	9*
PSMB7	proteasome (prosome, macropain) subunit, beta type, 7	IPI00003217	6
PSMC1	proteasome (prosome, macropain) 26S subunit, ATPase, 1	IPI00011126	5
PSMC2	proteasome (prosome, macropain) 26S subunit, ATPase, 2	IPI00021435	18*
PSMC3	proteasome (prosome, macropain) 26S subunit, ATPase, 3	IPI00018398	18*
PSMC4	proteasome (prosome, macropain) 26S subunit, ATPase, 4	IPI00020042	10
PSMC5	proteasome (prosome, macropain) 26S subunit, ATPase, 5	IPI00023919	16
PSMC6	proteasome (prosome, macropain) 26S subunit, ATPase, 6	IPI00021926	12
PSMD1	proteasome (prosome, macropain) 26S subunit, non-ATPase, 1	IPI00299608	5*
PSMD11	proteasome (prosome, macropain) 26S subunit, non-ATPase, 11	IPI00105598	17
PSMD12	proteasome (prosome, macropain) 26S subunit, non-ATPase, 12	IPI00185374	9
PSMD13	proteasome (prosome, macropain) 26S subunit, non-ATPase, 13	IPI00375380	10
PSMD14	proteasome (prosome, macropain) 26S subunit, non-ATPase, 14	IPI00024821	2
PSMD3	proteasome (prosome, macropain) 26S subunit, non-ATPase, 3	IPI00011603	11
PSMD4	proteasome (prosome, macropain) 26S subunit, non-ATPase, 4	IPI00022694	4
PSMD6	proteasome (prosome, macropain) 26S subunit, non-ATPase, 6	IPI00014151	7
PSMD7	proteasome (prosome, macropain) 26S subunit, non-ATPase, 7 (Mov34 homolog)	IPI00019927	4
PSMD8	proteasome (prosome, macropain) 26S subunit, non-ATPase, 8	IPI00010201	2
PTPLAD1	protein tyrosine phosphatase-like A domain containing 1	IPI00008998	3
RAD23B	RAD23 homolog B (S. cerevisiae)	IPI00008223	2
RCN2	reticulocalbin 2, EF-hand calcium binding domain	IPI00029628	19
RPL35	ribosomal protein L35	IPI00412607	5*
RPL36	ribosomal protein L36	IPI00216237	3
RPN2	ribophorin II	IPI00028635	4*
RPS10	ribosomal protein S10	IPI00008438	7*
RPS13	ribosomal protein S13	IPI00221089	14
RPS15	ribosomal protein S15	IPI00479058	2
RPS17	ribosomal protein S17	IPI00221093	6*

SAAL1	serum amyloid A-like 1	IPI00304935	5
SAPS3	SAPS domain family, member 3	IPI00019540	2
SDF4	stromal cell derived factor 4	IPI00106646	2
SEC11A	SEC11-like 1 (S. cerevisiae)	IPI00104128	4
SEC16A	SEC16-like 1 (S. cerevisiae)	IPI00031242	2
SEC22B	SEC22 vesicle trafficking protein-like 1 (S. cerevisiae)	IPI00006865	2
SFXN4	sideroflexin 4	IPI00412741	2
SGPL1	sphingosine-1-phosphate lyase 1	IPI00099463	4
SIRT1	sirtuin (silent mating type information regulation 2 homolog) 1 (S. cerevisiae)	IPI00016802	5
SLC16A1	solute carrier family 16 (monocarboxylic acid transporters), member 1	IPI00024650	4
SLC25A12	solute carrier family 25 (mitochondrial carrier, Aralar), member 12	IPI00386271	2
SLC25A22	solute carrier family 25 (mitochondrial carrier: glutamate), member 22	IPI00003004	4
SLC25A24	solute carrier family 25 (mitochondrial carrier; phosphate carrier), member 24	IPI00337494	6*
SLC25A3	solute carrier family 25 (mitochondrial carrier; phosphate carrier), member 3	IPI00022202	8*
SLC25A5	solute carrier family 25 (mitochondrial carrier; adenine nucleotide translocator), member 5	IPI00007188	94*
SMC4	SMC4 structural maintenance of chromosomes 4-like 1 (yeast)	IPI00328298	7
SMPD4	sphingomyelin phosphodiesterase 4, neutral membrane (neutral sphingomyelinase-3)	IPI00743121	2
SNX3	sorting nexin 3	IPI00216508	3
SPTLC1	serine palmitoyltransferase, long chain base subunit 1	IPI00005745	7
SPTLC2	serine palmitoyltransferase, long chain base subunit 2	IPI00005751	3
SRPRB	signal recognition particle receptor, B subunit	IPI00295098	2
SSR4	signal sequence receptor, delta (translocon-associated protein delta)	IPI00019385	11*
STT3B	STT3, subunit of the oligosaccharyltransferase complex, homolog B (S. cerevisiae)	IPI00152377	5
STUB1	STIP1 homology and U-box containing protein 1	IPI00025156	5
SUMF2	sulfatase modifying factor 2	IPI00171412	4
TBRG4	transforming growth factor beta regulator 4	IPI00329625	3
TELO2	KIAA0683 gene product	IPI00016868	2
TFB2M	transcription factor B2, mitochondrial	IPI00034069	2
TIMELESS	timeless homolog (Drosophila)	IPI00335541	2
TMED1	transmembrane emp24 protein transport domain containing 1	IPI00009976	3
TMED10	transmembrane emp24-like trafficking	IPI00028055	8

	protein 10 (yeast)		
TMED2	transmembrane emp24 domain trafficking protein 2	IPI00016608	7
TMED4	transmembrane emp24 protein transport domain containing 4	IPI00296259	3
TMED9	transmembrane emp24 protein transport domain containing 9	IPI00023542	6
TMEM109	transmembrane protein 109	IPI00031697	2
TMEM33	transmembrane protein 33	IPI00299084	21*
TMEM43	transmembrane protein 43	IPI00301280	10
TMEM59	transmembrane protein 59	IPI00399320	6
TMX1	thioredoxin domain containing	IPI00395887	2
TNPO1	transportin 1	IPI00024364	9
TOMM40	translocase of outer mitochondrial membrane 40 homolog (yeast)	IPI00014053	2
TOR1AIP2	torsin A interacting protein 2	IPI00168878	7
TROVE2	TROVE domain family, member 2	IPI00019450	2
TTC13	tetratricopeptide repeat domain 13	IPI00301227	2
TUBA4A	tubulin, alpha 1 (testis specific)	IPI00007750	45*
TUBB	tubulin, beta	IPI00011654	40*
TUBB2C	tubulin, beta 2C	IPI00007752	150*
TUBB3	tubulin, beta 3	IPI00013683	3
TUBB4	tubulin, beta 4	IPI00023598	3
TUBB6	tubulin, beta 6	IPI00646779	4
TUBG1	tubulin, gamma 1	IPI00295081	2
UBAC2	phosphoglycerate dehydrogenase like 1	IPI00007034	3
UBE3C	ubiquitin protein ligase E3C	IPI00472810; IPI00604464	7
UFD1L	ubiquitin fusion degradation 1 like (yeast)	IPI00218292	4
UGCGL2	UDP-glucose ceramide glucosyltransferase-like 2	IPI00024467	3
UNC45A	unc-45 homolog A (C. elegans)	IPI00072534	4
UQCRC2	ubiquinol-cytochrome c reductase core protein II	IPI00305383	16*
USP9X	ubiquitin specific peptidase 9, X-linked	IPI00003964	5*
VDAC3	voltage-dependent anion channel 3	IPI00031804	2
XPO1	exportin 1 (CRM1 homolog, yeast)	IPI00298961	27
XPO5	exportin 5	IPI00549861; IPI00640703	10
XPO6	exportin 6	IPI00465296	2
XPOT	exportin, tRNA (nuclear export receptor for tRNAs)	IPI00306290	7
YME1L1	YME1-like 1 (S. cerevisiae)	IPI00045946	3
YWHAH	tyrosine 3-monooxygenase/tryptophan 5-monooxygenase activation protein, eta polypeptide	IPI00216319	2

Table S1C, Related to Figures 1A-1C. Proteins Identified Interacting with ANDV GP and Not LCMV GP. The number of total peptides identified is listed. *Indicates non-GP control contained peptides from this protein but at levels at least five times less.

Gene symbol	Description	IPI id	# Peptides
AMOT	angiomotin	IPI00163085	5
ANXA6	annexin A6	IPI00002459	5
ATAD3A	ATPase family, AAA domain containing 3A	IPI00295992	6
CAPRIN1	cell cycle associated protein 1	IPI00783872	12
CHMP4B	chromatin modifying protein 4B	IPI00025974	2
CLGN	calmegin	IPI00024776	3
CSDA	cold shock domain protein A	IPI00031801	4
DARS	aspartyl-tRNA synthetase	IPI00216951	2
DDX21	DEAD (Asp-Glu-Ala-Asp) box polypeptide 21	IPI00015953	7
DHX29	DEAH (Asp-Glu-Ala-His) box polypeptide 29	IPI00217413	3
DIMT1L	dimethyladenosine transferase	IPI00004459	4
DNAJB12	DnaJ (Hsp40) homolog, subfamily B, member 12	IPI00014400	2
DNAJC3	DnaJ (Hsp40) homolog, subfamily C, member 3	IPI00006713	8
ERGIC1	endoplasmic reticulum-golgi intermediate compartment (ERGIC) 1	IPI00003635	2
EXT2	exostoses (multiple) 2	IPI00004047	2
FLOT2	flotillin 2	IPI00789008	2
FMR1	fragile X mental retardation 1	IPI00215720	2
G3BP2	Ras-GTPase activating protein SH3 domain-binding protein 2	IPI00009057	6
GNB2	guanine nucleotide binding protein (G protein), beta polypeptide 2	IPI00003348	2
HSPA7	heat shock 70kDa protein 7 (HSP70B)	IPI00011134	13*
IGF2BP3	insulin-like growth factor 2 mRNA binding protein 3	IPI00165467	4
LACTB	lactamase, beta	IPI00294186	2
LARS	leucyl-tRNA synthetase	IPI00103994	3

LIMA1	LIM domain and actin binding 1	IPI00008918	4
LMAN2L	lectin, mannose-binding 2-like	IPI00218337	2
MOGS	glucosidase I	IPI00328170	3
MYO1D	myosin ID	IPI00329719	2
NACA	nascent-polypeptide-associated complex alpha polypeptide	IPI00023748	3
NCL	nucleolin	IPI00183526	4
NDUFA9	NADH dehydrogenase (ubiquinone) 1 alpha subcomplex, 9, 39kDa	IPI00003968	2
NOP2	nucleolar protein 1, 120kDa	IPI00294891	2
NPM1	anaplastic lymphoma kinase (Ki-1)	IPI00220740	11*
NUFIP2	nuclear fragile X mental retardation protein interacting protein 2	IPI00002349	2
PABPC4	poly(A) binding protein, cytoplasmic 4 (inducible form)	IPI00012726	3
PCBP2	poly(rC) binding protein 2	IPI00012066	3
PCNA	proliferating cell nuclear antigen	IPI00021700	2
PLOD2	procollagen-lysine, 2-oxoglutarate 5-dioxygenase 2	IPI00337495	2
PURA	purine-rich element binding protein A	IPI00023591	3
PXDN	peroxidasin homolog (Drosophila)	IPI00016112	2
QARS	glutaminyl-tRNA synthetase	IPI00026665	2
RAB11B	RAB11B, member RAS oncogene family	IPI00020436	2
RARS	arginyl-tRNA synthetase	IPI00004860	2
RFC2	replication factor C (activator 1) 2, 40kDa	IPI00017412	2
RFC3	replication factor C (activator 1) 3, 38kDa	IPI00031521	3
ROD1	ROD1 regulator of differentiation 1 (S. pombe)	IPI00159072	3
RPL11	ribosomal protein L11	IPI00376798	7*
RPL13A	ribosomal protein L13a	IPI00304612	11*
RPL14	ribosomal protein L14 variant	IPI00069693	7*
RPL17	ribosomal protein L17	IPI00413324	2
RPL18	ribosomal protein L18	IPI00215719	20*
RPL18A	ribosomal protein L18a	IPI00026202	5
RPL19	ribosomal protein L19	IPI00025329	5*
RPL23A	ribosomal protein L23a	IPI00021266	6
RPL24	ribosomal protein L24	IPI00306332	8*
RPL26	ribosomal protein L26	IPI00027270	3
RPL26L1	ribosomal protein L26-like 1	IPI00007144	5
RPL3	ribosomal protein L3	IPI00550021	6
RPL30	ribosomal protein L30	IPI00219156	5
RPL35A	ribosomal protein L35a	IPI00029731	5
RPL37A	ribosomal protein L37a	IPI00414860	3
RPL5	ribosomal protein L5	IPI00000494	17*
RPL6	ribosomal protein L6	IPI00329389	3
RPL7;	ribosomal protein L7; ribosomal protein L7 pseudogene	IPI00796861	2

RPL7P32	32		
RPL7A	ribosomal protein L7a	IPI00299573	9
RPL7A; RPL7AP27	ribosomal protein L7; ribosomal protein L7a pseudogene 27	IPI00075558	11*
RPLP0	ribosomal protein, large, P0	IPI00008530	22*
RPS12	ribosomal protein S12	IPI00013917	3
RPS16	ribosomal protein S16	IPI00221092	7*
RPS19	ribosomal protein S19	IPI00215780	21*
RPS27	ribosomal protein S27	IPI00397358	2
RPS3A	ribosomal protein S3A	IPI00419880	16*
RPS5	ribosomal protein S5	IPI00008433	9*
RPS6	ribosomal protein S6	IPI00021840	9*
RPS8	ribosomal protein S8	IPI00216587	2
RRP1B	ribosomal RNA processing 1 homolog B (S. cerevisiae)	IPI00032374	2
SND1	staphylococcal nuclease domain containing 1	IPI00140420	4
STAU1	staufen, RNA binding protein, homolog 1 (Drosophila)	IPI00000001	2
TEX10	testis expressed sequence 10	IPI00549664	2
TMPO	thymopoietin	IPI00030131	2
TP53	tumor protein p53 (Li-Fraumeni syndrome)	IPI00025087	2
USP10	ubiquitin specific peptidase 10	IPI00291946	5
WRNIP1	Werner helicase interacting protein 1	IPI00102997	3
XRN2	5'-3' exoribonuclease 2	IPI00100151	2

Table S1D, Related to Figures 1A-1C, S1D, and Tables S1-S3. NIH DAVID Functional Annotation Clustering of Proteomic Data. Gene symbols from proteins identified interacting with LCMV GPC, ANDV GPC, or those interacting with both (intersect) were analyzed by NIH DAVID using medium stringency and with *Homo sapiens* as background. Data for the clusters below all show enrichments of four-fold over background. Sub-categories are provided and the numbers of proteins identified in each sub-category and their corresponding P value and percent of total proteins. These data are tabulated at the end of this table and were used to generate Figure S1D.

LCMV and ANDV Intersect				
Annotation Cluster 1	Sub-category	Count	P Value	Percent
(Endoplasmic Reticulum A)	endoplasmic reticulum lumen	12	4.20E-15	24

Enrichment Score: 8.9	intracellular organelle lumen	23	5.70E-08	46
	organelle lumen	23	8.60E-08	46
	membrane-enclosed lumen	23	1.20E-07	46
	Average	20		41
Annotation Cluster 2 (Endoplasmic Reticulum B)	Sub-category	Count	P Value	Percent
	endoplasmic reticulum	21	1.80E-16	42
Enrichment Score: 8.49	endoplasmic reticulum part	18	2.10E-15	36
	endoplasmic reticulum lumen	12	4.20E-15	24
	endoplasmic reticulum	23	3.50E-13	46
	short sequence motif:Prevents secretion from ER	9	2.10E-12	18
	signal	19	6.80E-04	38
	signal peptide	19	7.30E-04	38
	glycosylation site:N-linked (GlcNAc...)	14	2.50E-01	28
	glycoprotein	14	3.00E-01	28
	Average	17		33
Annotation Cluster 3 (Protein Folding)	Sub-category	Count	P Value	Percent
	protein folding	13	1.40E-13	26
Enrichment Score: 7.44	unfolded protein binding	9	2.70E-09	18
	Chaperone	9	5.90E-09	18
	disulfide bond	7	7.80E-01	14
	Average	10		19
Annotation Cluster 4 (Vesicles)	Sub-category	Count	P Value	Percent
	melanosome	8	3.10E-08	16
Enrichment Score: 4.39	pigment granule	8	3.10E-08	16
	cytoplasmic membrane-bounded vesicle	9	8.00E-04	18
	membrane-bounded vesicle	9	9.80E-04	18
	cytoplasmic vesicle	9	2.10E-03	18
	vesicle	9	2.80E-03	18
	Average	9		17
LCMV_NOT_ANDV				
Annotation Cluster 5	Sub-category	Count	P Value	Percent

(Proteasome A)	proteasome	30	3.30E-40	12
Enrichment Score: 19.93	proteasome complex	31	1.20E-36	12
	Proteasome	27	4.30E-32	10
	negative regulation of ubiquitin-protein ligase activity	28	1.00E-31	11
	negative regulation of ligase activity	28	1.00E-31	11
	negative regulation of ubiquitin-protein ligase activity during mitotic cell cycle	27	1.80E-30	10
	anaphase-promoting complex-dependent proteasomal ubiquitin-dependent protein catabolic process	27	1.80E-30	10
	proteasomal protein catabolic process	31	2.50E-30	12
	proteasomal ubiquitin-dependent protein catabolic process	31	2.50E-30	12
	negative regulation of protein ubiquitination	28	2.70E-30	11
	positive regulation of ubiquitin-protein ligase activity during mitotic cell cycle	27	7.70E-30	10
	regulation of ubiquitin-protein ligase activity	28	1.50E-29	11
	positive regulation of ubiquitin-protein ligase activity	27	1.90E-29	10
	regulation of ubiquitin-protein ligase activity during mitotic cell cycle	27	3.00E-29	10
	regulation of ligase activity	28	4.80E-29	11
	positive regulation of ligase activity	27	7.00E-29	10
	positive regulation of protein ubiquitination	28	1.50E-28	11
	regulation of protein ubiquitination	29	1.10E-27	11
	negative regulation of protein modification process	29	2.30E-25	11
	negative regulation of cellular protein metabolic process	31	1.90E-22	12
	negative regulation of protein metabolic process	31	6.10E-22	12
	negative regulation of catalytic activity	35	6.50E-21	14
	ubiquitin-dependent protein catabolic process	33	1.00E-20	13
	negative regulation of molecular function	36	3.00E-19	14
	positive regulation of protein modification process	28	1.30E-18	11
	mitotic cell cycle	35	5.90E-17	14
	regulation of protein modification process	31	3.00E-16	12
	positive regulation of cellular protein	28	3.90E-16	11

	metabolic process			
	positive regulation of protein metabolic process	28	1.20E-15	11
	regulation of cellular protein metabolic process	37	3.30E-15	14
	cell cycle process	40	4.70E-15	16
	threonine protease	11	2.20E-14	4
	Proteasome, subunit alpha/beta	11	2.70E-14	4
	threonine-type peptidase activity	11	6.10E-14	4
	threonine-type endopeptidase activity	11	6.10E-14	4
	proteasome core complex	11	5.00E-13	4
	protein catabolic process	38	2.40E-12	15
	proteolysis involved in cellular protein catabolic process	37	3.90E-12	14
	cellular protein catabolic process	37	4.50E-12	14
	modification-dependent macromolecule catabolic process	36	5.10E-12	14
	modification-dependent protein catabolic process	36	5.10E-12	14
	cell cycle	41	2.50E-11	16
	macromolecule catabolic process	41	3.00E-11	16
	positive regulation of catalytic activity	33	3.70E-11	13
	cellular macromolecule catabolic process	39	5.20E-11	15
	negative regulation of macromolecule metabolic process	39	7.50E-11	15
	positive regulation of molecular function	33	7.80E-10	13
	proteolysis	45	1.90E-09	17
	positive regulation of macromolecule metabolic process	33	4.80E-06	13
	Average	30		12
Annotation Cluster 2 (Ednoplasmic Reticulum B)	Sub-category	Count	P Value	Percent
	endoplasmic reticulum	50	8.30E-22	19
Enrichment Score: 11.87	endoplasmic reticulum	55	3.20E-14	21
	endoplasmic reticulum part	28	1.70E-10	11
	nuclear envelope-endoplasmic reticulum network	23	1.00E-08	9
	endoplasmic reticulum membrane	21	9.60E-08	8
	Average	35		14
Annotation Cluster 6	Sub-category	Count	P Value	Percent

(Nuclear Import A)	Armadillo-like helical	25	3.40E-20	10
Enrichment Score: 9.36	protein import into nucleus, docking	12	1.40E-16	5
	domain:Importin N-terminal	11	1.40E-16	4
	Importin-beta, N-terminal	11	9.30E-16	4
	cellular protein complex assembly	22	1.00E-13	9
	protein transport	31	2.20E-12	12
	pore complex	17	1.30E-11	7
	nuclear pore	15	1.20E-10	6
	nuclear envelope	22	1.40E-10	9
	cellular macromolecular complex assembly	25	2.20E-10	10
	transport	55	4.90E-10	21
	protein import into nucleus	14	8.50E-10	5
	nuclear import	14	1.10E-09	5
	protein import	16	2.30E-09	6
	cellular macromolecular complex subunit organization	25	2.30E-09	10
	protein localization in nucleus	14	2.60E-09	5
	nucleocytoplasmic transport	17	3.30E-09	7
	protein localization	40	3.90E-09	16
	nuclear transport	17	4.00E-09	7
	protein transporter activity	13	4.90E-09	5
	cellular protein localization	26	7.90E-09	10
	cellular macromolecule localization	26	9.10E-09	10
	protein localization in organelle	16	1.00E-08	6
	protein transport	36	1.10E-08	14
	intracellular transport	33	1.30E-08	13
	establishment of protein localization	36	1.40E-08	14
	intracellular protein transport	24	2.70E-08	9
	protein targeting	17	3.10E-07	7
	protein complex biogenesis	24	5.20E-06	9
	protein complex assembly	24	5.20E-06	9
	macromolecular complex assembly	27	1.90E-05	10
	macromolecular complex subunit organization	27	5.60E-05	10
	Average	23		9
Annotation Cluster 7	Sub-category	Count	P Value	Percent
(Protease)	threonine protease	11	2.20E-14	4
Enrichment Score: 8.44	Proteasome, subunit alpha/beta	11	2.70E-14	4
	threonine-type peptidase activity	11	6.10E-14	4

	threonine-type endopeptidase activity	11	6.10E-14	4
	proteinase	10	2.30E-13	4
	proteasome core complex	11	5.00E-13	4
	Proteasome, alpha and beta subunits	8	3.80E-10	3
	Proteasome, alpha-subunit, conserved site	6	3.30E-08	2
	Proteasome, beta-type subunit, conserved site	6	4.40E-07	2
	peptidase activity	22	1.10E-04	9
	peptidase activity, acting on L-amino acid peptides	21	1.70E-04	8
	Protease	18	2.60E-04	7
	endopeptidase activity	16	4.30E-04	6
	hydrolase	31	2.30E-02	12
	Average	14		5
Annotation Cluster 8 (Heat Repeat)	Sub-category	Count	P Value	Percent
Enrichment Score: 8.09	repeat:HEAT 6	13	1.60E-15	5
	repeat:HEAT 5	13	1.50E-14	5
	repeat:HEAT 2	15	2.30E-14	6
	repeat:HEAT 1	15	2.30E-14	6
	repeat:HEAT 4	13	2.50E-13	5
	repeat:HEAT 8	10	9.20E-13	4
	repeat:HEAT 3	13	1.80E-12	5
	repeat:HEAT 7	10	1.20E-11	4
	repeat:HEAT 10	8	4.00E-10	3
	repeat:HEAT 9	8	4.00E-10	3
	HEAT	11	5.50E-09	4
	repeat:HEAT 15	6	8.20E-09	2
	repeat:HEAT 14	6	4.80E-08	2
	repeat:HEAT 13	6	9.50E-08	2
	repeat:HEAT 12	6	9.50E-08	2
	repeat:HEAT 11	6	1.70E-07	2
	repeat:HEAT 24	4	9.20E-06	2
	repeat:HEAT 20	4	9.20E-06	2
	repeat:HEAT 21	4	9.20E-06	2
	repeat:HEAT 22	4	9.20E-06	2
	repeat:HEAT 23	4	9.20E-06	2
	repeat:HEAT 17	4	9.20E-06	2
	repeat:HEAT 18	4	9.20E-06	2
	repeat:HEAT 19	4	9.20E-06	2
	repeat:HEAT 16	4	9.20E-06	2

	repeat:HEAT 25	3	5.20E-04	1
	repeat:HEAT 26	3	5.20E-04	1
	Average	7		3
Annotation Cluster 9 (Mitochondria) Enrichment Score: 6.78	Sub-category	Count	P Value	Percent
	organelle envelope	48	2.30E-17	19
	envelope	48	2.60E-17	19
	mitochondrion inner membrane	18	8.10E-10	7
	mitochondrion	34	1.70E-08	13
	organelle inner membrane	24	3.20E-08	9
	mitochondrial inner membrane	23	3.90E-08	9
	mitochondrion	47	4.20E-08	18
	mitochondrial part	32	1.10E-07	12
	mitochondrial envelope	26	1.70E-07	10
	mitochondrial membrane	25	2.10E-07	10
	oxidoreductase	23	6.00E-06	9
	oxidation reduction	26	2.70E-05	10
	transit peptide:Mitochondrion	19	5.70E-05	7
	transit peptide	19	6.70E-05	7
	mitochondrial membrane part	10	4.50E-04	4
	generation of precursor metabolites and energy	14	1.50E-03	5
	Parkinson's disease	10	2.00E-03	4
	Huntington's disease	11	6.30E-03	4
	Average	25		10
Annotation Cluster 10 (Nuclear Import B) Enrichment Score: 5.28	Sub-category	Count	P Value	Percent
	domain:Importin N-terminal	11	1.40E-16	4
	Importin-beta, N-terminal	11	9.30E-16	4
	Ran GTPase binding	4	6.30E-04	2
	Ras GTPase binding	4	1.50E-01	2
	small GTPase binding	4	1.90E-01	2
	GTPase binding	4	2.20E-01	2
	enzyme binding	11	2.40E-01	4
	Average	7		3
Annotation Cluster 11 (GOLD Domain) Enrichment Score:	Sub-category	Count	P Value	Percent
	emp24/gp25L/p24	5	5.10E-06	2
	domain:GOLD	5	6.30E-05	2

4.48				
	GOLD	5	1.10E-04	2
	Average	5		2
Annotation Cluster 12 (Proteasome B)	Sub-category	Count	P Value	Percent
	PINT	5	9.90E-06	2
Enrichment Score: 4.35	Proteasome component region PCI	5	8.80E-05	2
	domain:PCI	5	1.00E-04	2
	Average	5		2
ANDV_NOT_LCMV				
Annotation Cluster 13 (Protein Translation)	Sub-category	Count	P Value	Percent
	ribosome	25	2.30E-40	30
Enrichment Score: 28.79	translational elongation	28	7.60E-40	34
	Ribosome	28	1.80E-37	34
	translation	36	4.30E-37	43
	protein biosynthesis	29	1.80E-36	35
	ribosome	31	6.60E-35	37
	ribosomal protein	28	1.10E-34	34
	ribosomal subunit	27	1.30E-34	33
	structural constituent of ribosome	28	8.30E-33	34
	cytosolic ribosome	23	2.70E-32	28
	ribonucleoprotein	29	1.80E-31	35
	ribonucleoprotein complex	37	2.00E-31	45
	large ribosomal subunit	19	2.50E-26	23
	cytosolic part	23	1.00E-25	28
	cytosolic large ribosomal subunit	15	7.30E-23	18
	RNA binding	33	2.70E-21	40
	structural molecule activity	29	2.30E-18	35
	intracellular non-membrane-bounded organelle	49	1.50E-17	59
	non-membrane-bounded organelle	49	1.50E-17	59
	cytosol	37	2.50E-17	45
	Average	30		36
Annotation Cluster 14 (Ribosome Biogenesis)	Sub-category	Count	P Value	Percent
	ribosome biogenesis	16	9.90E-17	19

Enrichment Score: 11.65	ribosomal large subunit biogenesis	8	1.30E-14	10
	ribonucleoprotein complex biogenesis	16	3.70E-14	19
	ncRNA metabolic process	16	1.40E-12	19
	rRNA processing	12	2.30E-12	14
	rRNA metabolic process	12	3.70E-12	14
	ncRNA processing	12	5.10E-09	14
	RNA processing	16	2.10E-07	19
	Average	14		16

Cluster	Average Percent of Total	Sample
1. Endoplasmic Reticulum (A)	41	Intersect
2. Endoplasmic Reticulum (B)	33	Intersect
2. Endoplasmic Reticulum (B)	14	LCMV Only
3. Protein Folding	19	Intersect
4. Vesicles	17	Intersect
5. Proteasome (A)	12	LCMV Only
6. Nuclear Import (A)	9	LCMV Only
7. Protease	5	LCMV Only
8. HEAT Repeat	3	LCMV Only
9. Mitochondria	10	LCMV Only
10. Nuclear Import (B)	3	LCMV Only
11. GOLD Domain	2	LCMV Only
12. Proteasome (B)	2	LCMV Only
13. Protein Translation	36	ANDV Only
14. Ribosome Biogenesis	16	ANDV Only